PARAMETER OPTIMIZATION OF STEEL FIBER REINFORCED HIGH STRENGTH CONCRETE BY STATISTICAL DESIGN AND ANALYSIS OF EXPERIMENTS

A THESIS SUBMITTED TO
THE GRADUATE SCHOOL OF NATURAL AND APPLIED SCIENCES
OF
THE MIDDLE EAST TECHNICAL UNIVERSITY

BY
ELİF AYAN

IN PARTIAL FULFILMENT OF THE REQUIREMENTS FOR THE DEGREE OF
MASTER OF SCIENCE
IN
THE DEPARTMENT OF INDUSTRIAL ENGINEERING

JANUARY 2004

Approval of the Graduate School of Natural and Applied Sciences

_____
Prof. Dr. Canan Özgen
Director

I certify that this thesis satisfies all the requirements as a thesis for the degree of Master of Science.

_____
Prof. Dr. Çağlar Güven
Head of Department

This is to certify that we have read this thesis and that in our opinion it is fully adequate, in scope and quality, as a thesis for the degree of Master of Science.

_____
Dr. Lütfullah Turanlı
Co-Supervisor

_____
Prof. Dr. Ömer Saatçioğlu
Supervisor

Examining Committee Members

Prof. Dr. Mustafa Tokyay _____

Prof. Dr. Ömer Saatçioğlu _____

Dr. Lütfullah Turanlı _____

Doç. Dr. Refik Güllü _____

Doç. Dr. Gülser Köksal _____

ABSTRACT

PARAMETER OPTIMIZATION OF STEEL FIBER REINFORCED HIGH STRENGTH CONCRETE BY STATISTICAL DESIGN AND ANALYSIS OF EXPERIMENTS

Ayan, Elif

M.S., Department of Industrial Engineering

Supervisor: Prof. Dr. Ömer Saatçioğlu

Co-Supervisor: Dr. Lütfullah Turanlı

January 2004, 351 pages

This thesis illustrates parameter optimization of compressive strength, flexural strength and impact resistance of steel fiber reinforced high strength concrete (SFRHSC) by statistical design and analysis of experiments. Among several factors affecting the compressive strength, flexural strength and impact resistance of SFRHSC, five parameters that maximize all of the responses have been chosen as the most important ones as age of testing, binder type, binder amount, curing type and steel fiber volume fraction. Taguchi and regression analysis techniques have been used to evaluate $L_{27}(3^{13})$ Taguchi's orthogonal array and $3^4 2^1$ full factorial experimental design results. Signal to noise ratio transformation and ANOVA have been applied to the results of experiments in Taguchi analysis. Response surface methodology has been employed to optimize the best regression model selected for all the three responses. In this study Charpy Impact Test, which is a different kind of impact test, have been applied to SFRHSC for the first time. The mean of compressive strength, flexural strength and impact resistance have been observed as around 125 MPa,

14.5 MPa and 9.5 kgf.m respectively which are very close to the desired values. Moreover, this study is unique in the sense that the derived models enable the identification of underlying primary factors and their interactions that influence the modeled responses of steel fiber reinforced high strength concrete.

Keywords: Process Parameter Optimization, Statistical Design of Experiments, Taguchi Method, Regression Analysis, Response Surface Methodology, Steel Fiber, High Strength Concrete, Compressive Strength, Flexural Strength, Impact Resistance

ÖZ

YÜKSEK DAYANIMLI ÇELİK LİFLİ BETONLARIN İSTATİSTİKSEL DENEY TASARIMI VE ÇÖZÜMLEME YÖNTEMLERİYLE PARAMETRE OPTİMİZASYONU

Ayan, Elif

Yüksek Lisans, Endüstri Mühendisliği

Tez Yöneticisi: Prof. Dr. Ömer Saatçioğlu

Ortak Tez Yöneticisi : Dr. Lütfullah Turanlı

Ocak 2004, 351 sayfa

Bu tez çalışması yüksek dayanımlı çelik lifli betonların (YDÇLB) basınç dayanımı, eğilme dayanımı ve darbe dayanımlarının istatistiksel deney tasarımı ve çözümlemesi yöntemleriyle parametre optimizasyonunu içermektedir. YDÇLB'nun basınç dayanımı, eğilme dayanımı ve darbe dayanımını etkileyen çeşitli faktörler arasından bütün cevapları yükseltecek en önemli beş tanesi, test etme yaşı, bağlayıcı çeşidi, bağlayıcı miktarı, kür yöntemi ve çelik fiber oranı olarak seçilmiştir. $L_{27}(3^{13})$ Taguchi'nin dikeysel tasarımı ve $3^4 2^1$ tam faktörel deney tasarımlarının değerlendirilmesi için Taguchi ve regresyon analiz yöntemleri kullanılmıştır. Taguchi analiz metodunda sinyal / gürültü oranı değişimi ve ANOVA deney sonuçları üzerinde uygulanmıştır. Her üç cevap için seçilen en iyi regresyon modelini optimize etmek amacı ile cevap yüzeyi metodu kullanılmıştır. Bu çalışmada, diğerlerinden değişik bir darbe testi olan Charpy Darbe Testi YDÇLB'lara ilk defa uygulanmıştır. Ortalama basınç dayanımı, eğilme dayanımı ve darbe dayanımı arzulanan değerlere oldukça yakın bulunarak sırası ile 125 MPa, 14.5 MPa ve 9.5 kgf.m olarak gözlenmiştir.

Bunlara ek olarak bu çalışma, elde edilen modellerin YDÇLB'ların modellenen cevaplarını etkileyen esas faktörlerin ve bunların etkileşimlerinin belirlenmesini sağlaması açısından tektir.

Anahtar kelimeler: Yöntem Parametre Optimizasyonu, İstatistiksel Deney Tasarımı, Taguchi Metodu, Regresyon Analizi, Cevap Yüzeyi Metodolojisi, Çelik Lif, Yüksek Dayanımlı Beton, Basınç Dayanımı, Eğilme Dayanımı, Darbe Dayanımı

To Mehmet and Zeynep Ayan

ACKNOWLEDGEMENTS

I would like to express sincere appreciation to Prof. Dr. Ömer Saatçioğlu and Dr. Lütfullah Turanlı for their suggestions, continuous supervision, guidance and insight throughout the thesis. I am grateful to METU Civil Engineering Department for letting me such a research in the Materials and Construction Laboratory. I also acknowledge all laboratory personnel, Harun Koralay, Cuma Yıldırım, Ali Sünbüle and Ali Yıldırım for their assistance in carrying out the experiments. I am thankful to Eray Mustafa Günel for his continuous helps throughout his trainship in the laboratory. Finally, to my parents, Zeynep and Mehmet Ayan, they did their best to encourage me to continue, I offer sincere thanks for their unshakable faith in me and their willingness to understand me.

TABLE OF CONTENTS

LIST OF TABLES

LIST OF FIGURES

CHAPTER 1

INTRODUCTION

The aim of this study is to use different statistical design of experiments and analysis techniques for maximizing the compressive strength, flexural strength and impact resistance of steel fiber reinforced high strength concrete. Taguchi's L_{27} (3^{13}) orthogonal array and $3^4 2^1$ full factorial designs are the evaluated statistical design of experiments. Taguchi and regression analysis are the investigated analysis techniques. Signal-to-Noise (S/N) ratio and Analysis of Variance (ANOVA) have been used for Taguchi analysis in both designs. Three replicates of each experiment have been performed because when sample mean is used to estimate the effect of a factor in the experiment, then replication permits to obtain a more precise estimate of this effect, and if noise factors vary, then repeating trials may reveal their influence. Since the results of the experiments involve three runs, S/N ratio analysis can be applied because it provides guidance to a selection of the optimum level based on least variation around the target and also on the average value closest to the target. In other words it analyzes both the variability and main effects at the same time. Response Surface Methodology have been applied separately to both experimental designs in order to maximize the compressive strength, flexural strength and impact resistance of steel fiber reinforced high strength concrete by using the regression models obtained for each response.

Steel fiber reinforced concrete is a composite material made of hydraulic cements, fine and coarse aggregate, and a dispersion of discontinuous, small

steel fibers [1]. Fiber reinforced concrete has found many applications in tunnels, hydraulic structures, airport and highway paving and overlays, industrial floors, refractory concrete, bridge decks, shotcrete linings and coverings, and thin-shell structures. It can also be used as a repair material for rehabilitation and strengthening of existing concrete structures [2]. The addition of steel fibers significantly improves many of the engineering properties of concrete such as flexural strength, direct tensile strength, impact strength and toughness. In addition to static loads, many concrete structures are subjected to short duration dynamic loads. These loads originate from sources such as impact from missiles and projectiles, wind gusts, earthquakes and machine dynamics [1]. Many investigators have shown that the addition of steel fibers greatly improves the energy absorption and cracking resistance of concrete.

The term high strength concrete is used for concrete with a compressive strength in excess of 41 MPa, as defined by the ACI Committee 363 [3]. Use of high strength concrete leads to smaller cross sections and hence, reduced dead load of a structure. This helps engineers to build high-rise buildings and long-span bridges. High strength is made possible by reducing porosity, inhomogeneity and microcracks in concrete. This can be achieved by using superplasticizers and supplementary cementing materials such as fly ash, silica fume, granulated blast furnace slag and natural pozzolan. Fortunately, most of these materials are industrial by products and help in reducing the amount of cement required to make concrete less costly, more environmental friendly and less energy intensive [4].

Although there are some full factorial and one factor at a time process parameter optimization studies of steel fiber reinforced high strength concrete (SFRHSC), there is no comprehensive study involving Taguchi statistical design and many different analysis of experiments to fully investigate the compressive strength, flexural strength and impact resistance of SFRHSC. Also in this study, a different approach for impact resistance measurement is applied to SFRHSC specimens. This approach, which is called Charpy Impact Test, employs an

experimentation method used for testing metals and alloys. The studies in literature have not used this method before.

The most important parameters affecting the compressive strength, flexural strength and impact resistance of SFRHSC are: age of testing, binder type, binder amount, curing type and steel fiber volume fraction. Three levels for age of testing, binder type, binder amount and steel fiber volume fraction and two levels for curing type have been used in the conducted experiments. Taguchi's L_{27} (3^{13}) orthogonal array is chosen in order to estimate the main effects and three two-way interaction effects. $3^4 2^1$ full factorial design is employed to estimate the main effects and all possible factor level interaction effects on each response. For both designs ANOVA has been performed for the mean and S/N values of all three responses separately. Then, the regression analysis has been conducted and the best model has been chosen for the mean of each response variable for the two designs. Finally, in order to achieve the maximum compressive strength, flexural strength and impact resistance, response surface methodology has been used.

This study shows that type of statistical experimental design and analysis techniques are important for maximizing all three responses of SFRHSC. The type of statistical experimental design determines which factor effects can be analyzed separately and type of statistical analysis technique determines the way the process parameters are optimized. The results of both design methodologies and analysis techniques are in consistent and led to nearly the same optimal results for each response. The same main factor level combination is found to be optimal in order to maximize the compressive strength and flexural strength of SFRHSC, whereas a different combination maximizes the impact resistance.

CHAPTER 2

BACKGROUND INFORMATION

2.1 Background on Concrete Technology

Concrete is a composite material composed of coarse granular material (the aggregate or filler) embedded in a hard matrix of material (the cement or binder) that fills the space between the aggregate particles and glues them together [5]. Besides some disadvantages, concrete competes directly with all major construction materials such as timber, steel, rock and so on. The ability of concrete to be cast to any desired shape and configuration is an important characteristic.

2.1.1 Concrete

Good quality concrete is a very durable material and should remain maintenance-free for many years when it has been properly designed for the service conditions and properly placed. Unlike structural steel, it does not require protective coatings except in very corrosive environments. It is also an excellent material for fire resistance. However, concrete has weaknesses which may limit its use in certain applications. Concrete is a brittle material with very low tensile strength. Thus, concrete should generally not be loaded in tension and reinforcing steel bars must be used to carry the tensile loads. The low ductility of concrete also means that concrete lacks impact strength and toughness compared to metals. Even in compression concrete has a relatively

low strength to weight ratio, and high load capacity requires comparatively large masses of concrete, but, since concrete is low in cost this is economically possible. Concrete undergoes considerable irreversible shrinkage due to moisture loss at ambient temperatures, and also creeps significantly under an applied load even under conditions of normal service. A great deal of research effort has been devoted to overcome these problems and has led to the development of new types of concrete, such as fiber reinforcement concrete [5].

2.1.2 Structure of Cement

Cement is the binding aggregate in concrete. Normally about 250 to 350 kg is added to 1 m^3 of concrete, which is sufficient to bind all aggregates together to form a solid material. Cement, as it is currently used has been known under the name of portland cement since 1824 when it was first used by Joseph Aspdin in England. It consists of mainly calcareous (lime) and argillaceous materials and contains other silica, alumina and iron oxide bearing materials [6].

In principle, the manufacture of portland cement is very simple. An intimate mixture, usually limestone and clay, is heated in a kiln to 1400 to 1600^{o}C, which is the temperature range in which the two materials interact chemically to form the calcium silicates [5]. The particle size of cement is around 1μm to 100μm with a surface area of around 3 m^2/g [6].

Other than the ordinary portland cement, there are some modified cements consisting mainly of portland cement and other materials such as blast furnace slag, natural pozzolan or fly ash. Blast furnace slag is a by-product from the production of iron, natural pozzolan is a volcanic ash and fly ash is a rest product from coal burning power plants. Both the blast furnace slag and fly ash are residues from industrial processes, and in this way cement production helps to limit the amount of waste.

2.1.3 Water-Cement Ratio and Porosity

When water is added to the portland cement, several chemical reactions occur and the end product is the hardened cement paste. The reaction with water is usually called as the hydration process. The amount of water added is usually expressed as the water/cement ratio (abbreviated to w/c ratio). The w/c ratio is important as it affects the porosity of the cement paste, and thus, has a direct influence on the mechanical behavior of the concrete.

For the hydration to proceed smoothly, a certain amount of water is needed. For full hydration of cement, water is added 25% of the weight of cement. This amount of water is chemically bound to the cement gel. Since the size of the cement particles are very fine, quite a bit of water is absorbed by the cement particles and as a result 25% is not available for hydration. The physically absorbed water is about 15% of the cement weight. Thus, in order to hydrate all the cement, 40% of the cement weight must be added as water. In reality a 0.4 w/c ratio does not guarantee full hydration because the water will not always reach the core of all cement particles. In that case, pockets of unhydrated cement remain in the hardened cement paste structure, which however are not affecting the strength of the material [6]. Therefore the w/c ratio used in practice deviates from 0.4. In order to obtain a good workability (plasticity) of the fresh concrete, higher values are used. However, when special additives like superplasticizers are added, the amount of water is reduced to values as low as 18 to 20%. Superplasticizers reduce the surface tension of the particles. The trend in the low w/c ratio is in the development of new very high strength concretes.

The major effect of excess water on the structure of hardened cement paste is on the porosity. If more water is added, the surplus is not used in the chemical reactions and remains as free water in the cement structure to form capillary pores (Figure 2.1). On the other hand, when the amount of water is decreased, not enough water is available for cement to hydrate. The cores of the cement

particles do not react. However, no free water remains in the cement structure, and the total porosity decreases substantially. But due to chemical shrinkage, an increase of porosity will occur since, the volume of the reaction products is smaller than the volume of the water and solid cement particles [6]. The porosity of the cement paste is a very important factor. Both strength and durability of the cement are directly affected by the pore structure. Pores of different size are found in hardened cement paste. Very small pores (in the nanometer range) exist in the cement gel itself, whereas larger pores (of micrometer size) develop as capillary pores between the particles. Even larger air voids may occur during mixing. Because of a poor compaction of the cement paste or concrete these larger air voids (of millimeter size) will become an integral part of the material structure (Figure 2.2).

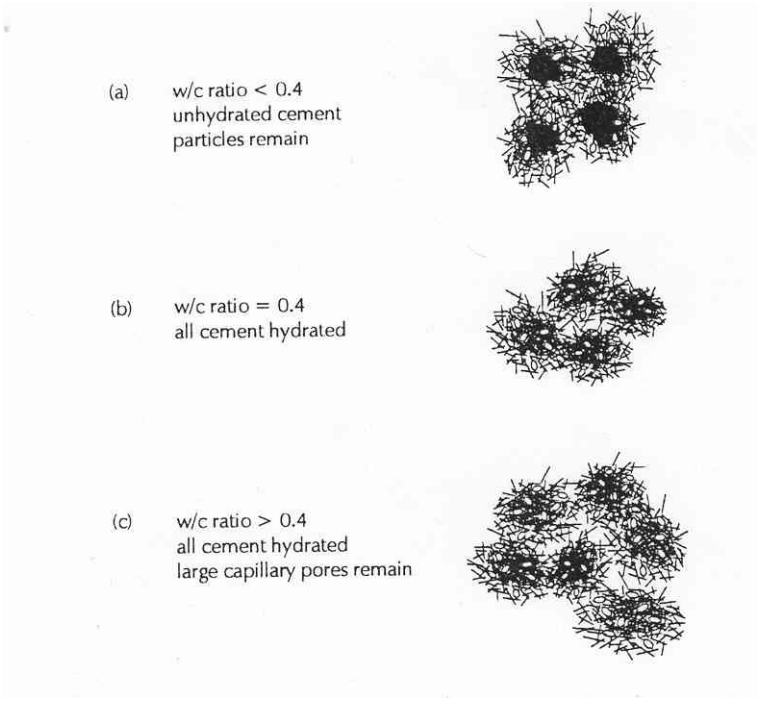

Figure 2.1 Effect of water/cement ratio on the structure of hardened cement

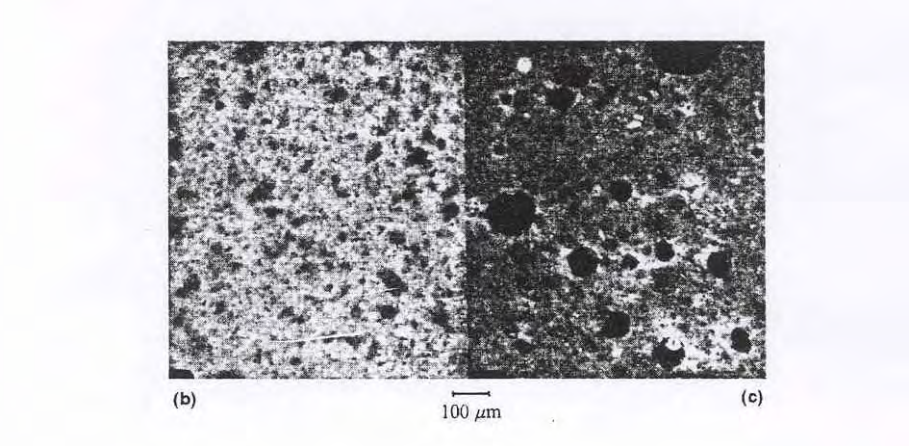

Figure 2.2 Effect of porosity on the flexural strength of ordinary Portland cement

2.1.4 Aggregates

Aggregates are normally about 75% of the total volume of concrete. Because of this large volume fraction much of the properties of concrete depend on the type of aggregate used. In addition to their use as economical filler, aggregates generally provide concrete with better dimensional stability and wear resistance [5]. They are granular materials, derived for the most part from natural rocks such as basalt, diabase, granite, quartz, magnetite and limestone. Aggregates should be hard and strong and free of undesirable impurities. Soft, porous rock can limit strength and wear resistance; it may also break down during mixing and adversely affect workability by increasing the amount of fines. Rocks that tend to fracture easily along specific planes can also limit strength and wear resistance. Aggregates should also be free of impurities such as silt, clay, dirt or organic matter. If these materials coat the surfaces of the aggregate, they will interfere with the cement-aggregate bond [5]. For high strength concrete strong aggregates such as basalt and granite are recommended.

2.1.4.1 Shape and Texture of Aggregates

Aggregate shape and texture affect the workability of fresh concrete through their influence on cement paste requirements. Sufficient paste is required to coat the aggregates and to provide lubrication to decrease interactions between aggregate particles during mixing [5]. The aggregate particles that are close to spherical in shape, well rounded and compact, with a relatively smooth surface (Figure 2.3) will generally give an improved workability [6]. The full role of shape and texture of aggregate in the development of concrete strength is not known, but possibly a rougher texture results in a greater adhesive force between the particles and cement matrix. Likewise, the larger surface area of angular aggregate means that a larger adhesive force can be developed [7].

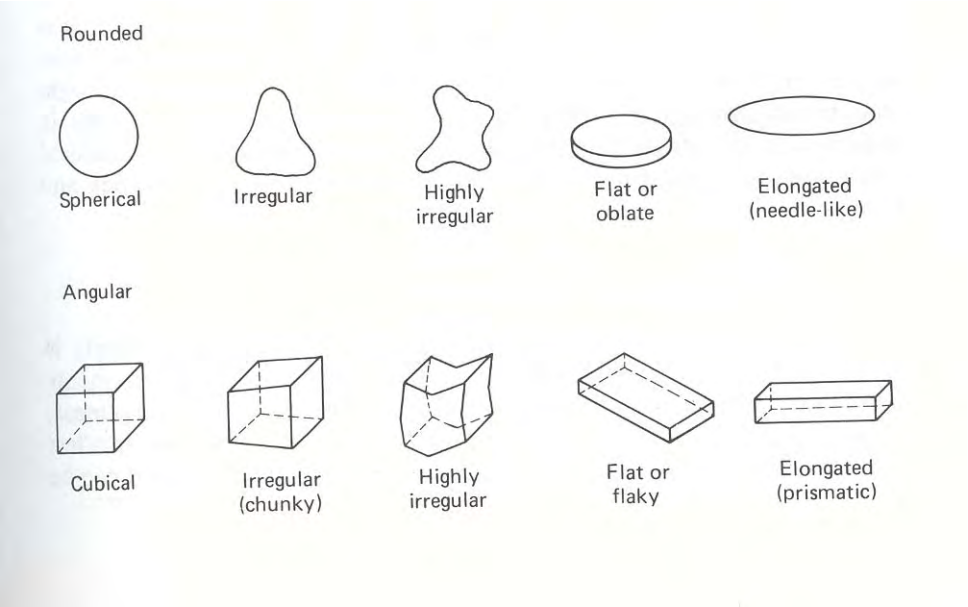

Figure 2.3 Classification of aggregate shapes

2.1.4.2 Size Gradation of Aggregates

Grading of an aggregate is an important characteristic because it determines the paste requirements for a workable concrete. Since cement is the most expensive component, it is desirable to minimize the cost of concrete by using the smallest amount of paste consistent with the production of a concrete that can be handled, compacted, and finished and provide the necessary strength and durability. The significance of aggregate gradation is best understood by considering concrete as a slightly compacted assembly of aggregate particles bonded together with cement paste, with the voids between particles completely filled with paste [5]. Thus, the amount of paste depends on the amount of void space that must be filled and the total surface area of the aggregate that must be coated with paste. The volume of the voids between roughly spherical aggregate particles is greatest when the particles are of uniform size (Figure 2.4a). When a range of sizes is used, the smaller particles can pack between the larger (Figure 2.4b), thereby decreasing the void space and lowering paste requirements. Using a larger maximum aggregate size (Figure 2.4c) can also reduce the void space [5].

Aggregate strength is not the only measure that has to be considered. In order to limit the porosity of the concrete, aggregate grading must be balanced. Grading is an important factor, since it not only affects the total porosity, but also it influences the amount of water that must be mixed into the concrete to obtain certain workability. More water will be absorbed to the surface of small sized aggregates [6].

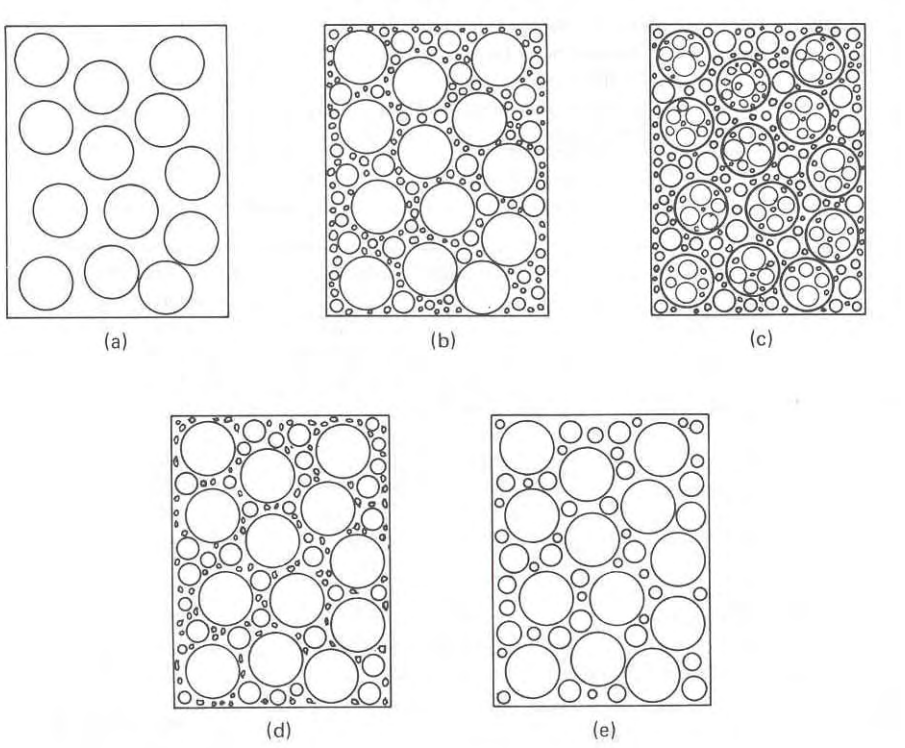

Figure 2.4 Schematic representations of aggregate gradations in an assembly of aggregate particles: (a) uniform size; (b) continuous grading; (c) replacement of small sizes by large sizes

The grading of an aggregate supply is determined by a sieve analysis. A representative sample of the aggregate is passed through a stack of sieves arranged in order of decreasing size of the openings of the sieve. The aggregates are divided in two size groups, namely fine (often called sand) and coarse. This division is made at No.4 ASTM sieve, which is 4.75 mm in size [7]. The coarse aggregates comprises materials that are retained on the No.4 sieve, that is the particle size is at least 4.75 mm and fine aggregates comprises the materials that are passing the No.4 sieve meaning the maximum particle size is limited to 4.75 mm. In the coarse range the sieves are designated by the size of the openings, but in the fine range the sieves are assigned a number that represents the number of openings per inch.

2.1.5 Admixtures

The official definition of an admixture set out in ASTM C125 is "a material other than water, aggregates and hydraulic cement that is used as an ingredient of concrete or mortar and is added to the batch immediately before or during mixing."

2.1.5.1 Water Reducing Admixtures

Superplasticizers are a modern type of water-reducing admixture, which can achieve water reductions of 15 to 30%. Superplasticizers are used for:

- to create flowing concretes with very high slumps in the range of 175 to 225 mm [5]
- to produce high-strength concretes at w/c ratios in the range 0.28 to 0.40 [5, 7]

Flowing concrete can be used in difficult placements or in placements where adequate consolidation by vibration can not be readily achieved. When w/c ratios can be lowered below 0.40, very high strengths can be achieved. By decreasing w/c ratio, superplasticizers can increase the 24 hour strength by 50 to 75% [7]. Also the fine porosity in the cement matrix can be reduced by using superplasticizers (Figure 2.5b) [6].

The effectiveness of superplasticizers is that the undesirable side effects, air entrainment and set retardation are absent or at least very much reduced. Thus, they can be used at high rates of addition, in amounts exceeding 1% of active ingredient by weight of cement, whereas conventional water reducers can not be used in such large quantities [5].

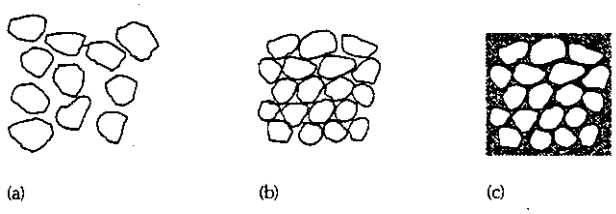

Figure 2.5 Effect of superplasticizer and silica fume on the density of cement paste: (a) cement without additives, (b) with superplasticizer, (c) with silica fume

2.1.5.2 Mineral Admixtures

Supplementary cementing materials, also called mineral admixtures, contribute to the properties of hardened concrete through hydraulic or pozzolanic activity. Typical examples are natural pozzolans, fly ash, ground granulated blast-furnace slag, and silica fume, which can be used individually with portland or blended cement or in different combinations. These materials react chemically with calcium hydroxide released from the hydration of portland cement to form cement compounds. These materials are often added to concrete to make concrete mixtures more economical, reduce permeability, increase strength, or influence other concrete properties.

2.1.5.2.1 Silica Fume

Silica fume, a co-product of the silicon and ferrosilicon metal industry, is an amorphous silicon dioxide (SiO_2) which is generated as a gas in submerged electrical arc furnaces during the reduction of very pure quartz. This gas vapor is condensed in bag house collectors as very fine gray to off-white powder of spherical particles that average 0.1 to 0.3 microns in diameter with a surface area of 17 to 30 m^2/g [8]. The specific gravity of silica fume is about 2.2 - 2.3 and the unit weight is between 2.4 – 3.0 g/cm^3 [9].

When added to concrete, silica fume acts as both a filler, improving the physical structure by occupying the spaces between the cement particles and as a pozzolan, reacting chemically to impart far greater strength and durability to concrete. Another advantage of silica fume is that it is latently hydraulic, causing a very dense material structure (Figure 2.5c) with very good strength properties [6]. In the case of fiber reinforced concretes, the addition of silica fume improves the bond between fibers and matrix (Figure 2.6) [10].

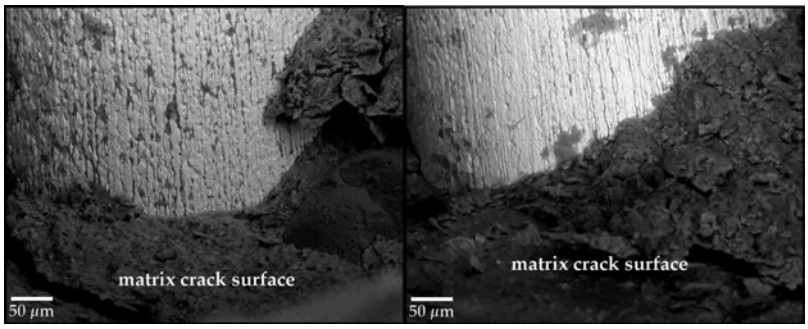

Figure 2.6 Electron microscope images showing a single steel fiber interface in a mortar. On the left is a mortar with no silica fume and on the right is a mortar with silica fume at 15% replacement of cement

The use of silica fume has different effects on the strength of concrete. First of all, due to its small particle size it will reduce the pore space, which has a positive effect on the strength of concrete. Second, with increasing the amount of silica fume, the amount of mixing water must increase because the specific surface of silica fume is very high [6]. The increased water demand increases the w/c ratio, which has a negative effect on the strength of concrete and also the increased water demand results in more plastic shrinkage cracks in the hardened concrete. Third, the hydraulic properties of silica fume will have a positive effect on the strength since it gives sufficient time to hydrate. When the three effects are combined, an optimum amount of silica fume will be found. In

practice, 10 to 20% of silica fume is added to obtain a high strength concrete [6]. Also silica fume concrete made with superplasticizer, has very good viscous properties.

2.1.5.2.2 Fly Ash

Fly ash is an artificial pozzolan produced when pulverized coal is burned in electric power plants. It is formed from the non-combustible minerals found in coal. The powdered coal is conveyed by air to a furnace where the carbon is ignited in an atmosphere of 1900 to 2100^{o}F. The non-combustible minerals become molten as they are carried through the firing zone by the air stream. The molten minerals solidify in this moving air stream which gives approximately 60% of the fly ash particles a spherical shape. Similar to the fact that Portland cement is manufactured by firing raw materials at 2700^{o}F, the non-combustible minerals in the coal become reactive due to the formation of amorphous silica in the coal-fired furnace [11].

Fly ash particle size ranges from 1 to 150 μm (Figure 2.7) with a surface area of 4 – 7 m^2/g. Normally, the unit weight is between 2.1 – 2.7 g/cm^3 [9]. The cement replacement level of fly ash in concrete differs from 15 to 50 % leading to more economical concrete mixes since they are relatively cheap waste products [9].

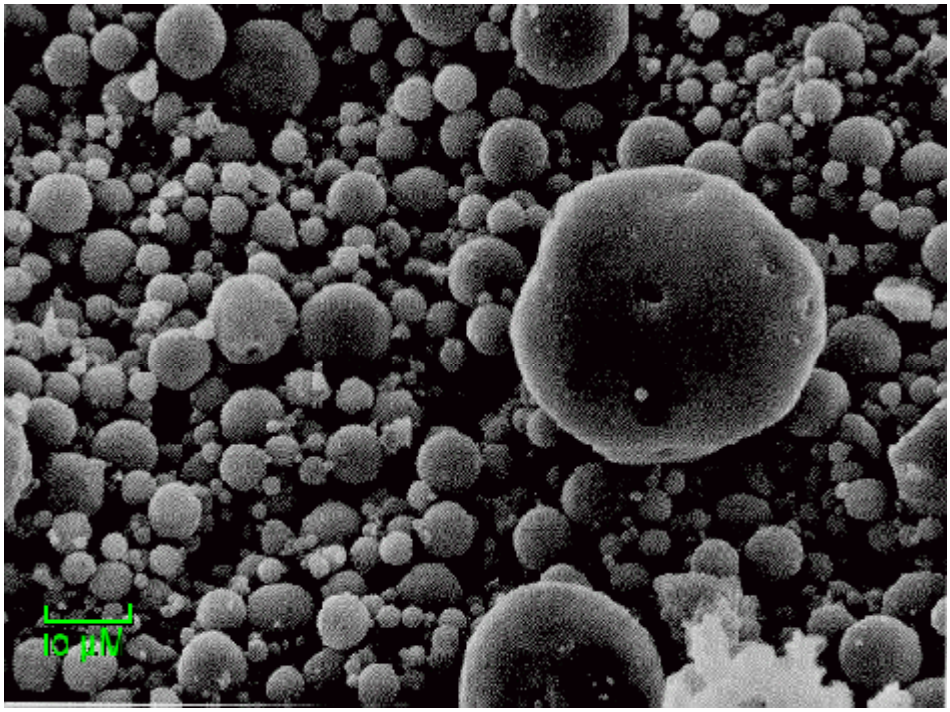

Figure 2.7 An electron microscope image of fly ash with green scale showing 10 µm

When added to concrete, fly ash fills in voids and reduces the total area covered with cement. Since its particle shape is spherical, the spheres act like ball bearings increasing workability. It decreases the heat of hydration which is important for large masses of concrete pours such as dams. Because the fly ash chemically combines and stabilizes the water soluble calcium hydroxide in concrete, the fly ash concrete is from 5 to 13 times more impermeable to the passage of water than a comparable Portland cement mix. Water and Portland cement are the two main contributors to drying shrinkage of ready mixed concrete. By lowering the water demand of concrete-making material and by the removal of Portland cement, drying shrinkage of fly ash concrete is less than a comparable Portland cement mix [11]. It creates stronger concrete, but strength develops more slowly than all Portland cement concretes. Another disadvantage is that since fly ash retards the setting time of concrete, the curing time should be longer than Portland cement mixes.

2.1.5.2.3 Ground Granulated Blast Furnace Slag

Granulated blast furnace slag, which has an amorphous structure containing highly SiO_2 and Al_2O_3, is obtained during the manufacturing process of pig iron in blast furnace. When the molten slag at 1400-1500°C is tapped and subjected to a special process of quenching it forms granules, which is called granulated slag [12]. This slag when ground to very high fineness is called Ground Granulated Blast Furnace Slag (GGBFS) and acts similarly as fly ash. GGBFS when used along with ordinary Portland cement (OPC) in concrete or mortar mix imparts unique properties to obtain very strong and durable concrete and mortar mix.

Use of GGBFS in concrete usually improves workability and decreases the water demand due to the increase in paste volume caused by the lower relative density of slag. Setting times of concretes containing slag increases as the slag content increases. An increase of slag content from 35 to 65% by mass can extend the setting time by as much as 60 minutes. This delay can be beneficial, particularly in large pours and in hot weather conditions. The compressive strength development of slag concrete depends primarily upon the type, fineness, and the proportions of slag used in concrete mixtures. In general, the strength development of concrete incorporating slags is slow at 1-5 days compared with that of the OPC concrete. Between 7 and 28 days, the strength approaches that of the OPC concrete; beyond this period, the strength of the slag concrete exceeds the strength of OPC concrete. Flexural strength is usually improved by the use of slag cement, which makes it beneficial to concrete paving application where flexural strengths are important. It is believed that the increased flexural strength is the result of the stronger bonds in the cement-slag-aggregate system because of the shape and surface texture of the slag particles. Incorporation of granulated slags in cement paste helps in the transformation of large pores in the paste into smaller pores, resulting in decreased permeability of the matrix and of the concrete. The reduced heat of hydration and reduced rate of strength gain at early ages exhibited by ground granulated blast furnace slag

modified concretes reinforces the need for proper curing of these mixes. With an increased time of set and a reduced rate of strength gain, concretes containing ground granulated blast furnace slag may be more susceptible to cracking caused by drying shrinkage [13].

2.1.6 High Strength Concrete

There is a trend toward the use of higher-strength concrete in conventional structures, with 28 day compressive strengths in excess of 55 MPa. The use of high-strength concrete (HSC) has advantages in the precast and prestressed concrete industries, where it can result in a more rapid output of components and less product loss during handling. In high-rise construction, advantage can be taken of reduced dead loads, which allow thinner concrete sections and longer beam spans. A disadvantage of high-strength concrete is that it behaves in a more brittle fashion because the paste aggregate bond is also strengthened [5]. The amount of additional paste content depends on shape, texture, grading and dust content of the aggregates. For HSC, the strength of the mortar and bond at the interface may be similar to the coarse aggregate. Thus, using a coarse aggregate of higher strength and lower brittleness, proper texture and mineralogical characteristics may improve the mechanical properties of concrete [14].

Crushed stones are mostly used as aggregates in high-strength concretes since it has a rougher surface texture than gravel and gives a better paste aggregate bond and, therefore, better strength. Also, crushed stone has a greater surface to volume ratio than does rounded gravel. To increase the total surface area and thereby improve the total bond contribution, the maximum aggregate size is generally held below 19 mm [5]. This means that the paste content has to be increased to provide sufficient workability. The combination of low w/c ratio and small maximum aggregate size means that cement contents will be quite high, generally in the range 400 to 600 kg/m^3 [5].

High-strength concrete has undergone many developments based on the studies of influence of cement type, type and proportions of mineral admixtures, type of superplasticizer and the mineralogical composition of coarse aggregates [15].

2.1.7 Steel Fiber Reinforced Concrete

Fiber reinforced concrete (FRC) may be defined as concrete made from portland cement with various aggregates and incorporating discrete fibers. A number of different types of fibers have been found suitable for use in concrete: steel, glass, polymers (acrylic, aramid, nylon, polypropylene etc.), ceramics, asbestos, carbon and naturally occurring fibers (bamboo, coconut, wood etc.) are the most common. These fibers vary considerably in both cost and effectiveness [5, 10].

Steel fibers may be produced either by cutting wire, sheering sheets, or from a hot melt extract. They may be smooth, or deformed in a variety of ways to improve the bond (Figure 2.8). The fiber cross section may be circular, square, crescent shape or irregular. The length of the fibers is normally less than 75 mm and the length-diameter ratio (aspect ratio) typically ranges from 30 to 100 [10]. They will rust at the surface of the concrete, but appear to be very durable within the concrete mass.

For the fiber reinforced concrete, the mechanical behavior depends not only on the properties of the fiber and the concrete, but also on the bonding between them. Most FRC failures occur due to bond failure (fiber pull out). It is possible to increase the bond strength substantially by deforming the fibers so as to increase the end anchorage. A very good bond may increase the tensile strength, while a poor bond may increase the energy absorption. Large changes in the bond strength are not reflected by similar changes in the concrete strength. Since fibers tend to have relatively large surface areas, they have a large water requirement, as well as exhibiting a tendency to interlock or ball. The workability is decreased as the fiber content increases, as the aspect ratio of the fibers increases, or as the coarse aggregate content increases. Apart from

difficulties in the workability, it is also harder to compact FRC [5]. When they are used in high strength concretes, fiber reinforcement decreases the brittleness.

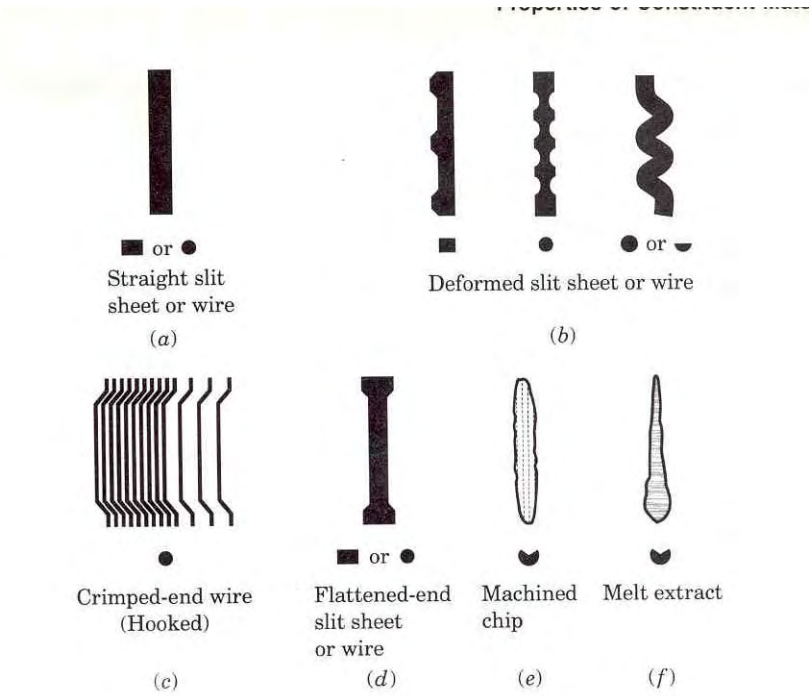

Figure 2.8 Various shapes of steel fibers used in FRC. (a) straight silt sheet or wire (b) deformed silt sheet or wire (c) crimped-end wire (d) flattened-end silt sheet or wire (e) machined chip (f) melt extract

Fiber reinforced cement and concrete materials have been developed progressively since the early work by Romualdi and Batson [16] in the 1960s. The use of steel fiber reinforced concrete has steadily increased during the last 25 years. Considerable developments have taken place in the field of steel fiber reinforced concrete as reported by Bentur and Mindess [17].

Plain, unreinforced cementitious materials are characterized by low tensile strengths, and low tensile strain capacities; that is they are brittle materials. They thus require reinforcement before they can be used as construction materials.

Historically, this reinforcement has been in the form of continuous reinforcing bars, which could be placed in the structure at the appropriate locations to withstand the imposed tensile and shear stresses. Fibers, on the other hand, are discontinuous, and are randomly distributed throughout the cementitious matrix. Therefore, they are not as efficient in withstanding the tensile stresses. On the other hand, since they are more closely spaced than the conventional reinforcing bars, they are better at controlling the cracking. Due to these differences, there are certain applications in which fiber reinforcement is better than conventional reinforcing bars [17]:

1. Thin sheet materials, in which conventional reinforcing bars cannot be used, and in which the fibers constitute the primary reinforcement. In thin sheet materials, fiber concentrations are high, typically exceeding 5% by volume. In these applications, the fibers act to increase both the strength and the toughness of the composite.

2. Components which must withstand locally high loads or deformations, such as tunnel linings, blast resistant structures, or precast piles which must be hammered into the ground.

3. Components in which fibers are added to control cracking induced by humidity or temperature variations, as in slabs and pavements. In these applications, fibers are referred to as secondary reinforcement.

In general, fiber reinforcement is not a substitute for conventional reinforcement. Fibers and steel bars have different roles to play and there are many applications in which both fibers and continuous reinforcing bars should be used together. In applications 2 and 3, the fibers are not used to improve the strength of concrete but they are used to improve the ductility of the material or its energy absorption capacity.

Although the controlling factor in the use of FRC is its material properties, the cost is also important because the fibers are considerably expensive. Even though the use of FRC is still in its infancy, it will be much more widely used in the future if the economics of the material becomes more favorable.

2.2 Background on Design and Analysis of Experiments

Analysis of variance (ANOVA), general regression and response surface models are the analysis techniques used in this study with the full factorial and Taguchi statistical experimental designs.

The use of orthogonal arrays can be traced back to Euler's Greco-Latin Squares. Sir Ronald Fisher, who introduced ANOVA, was the primary promoter of the use of statistically designed experiments between the First and Second World Wars, 1918-1939. Since that time statistically designed experiments have played an increasingly important role in medical and R&D activities and have been a primary source in the use of statistics in industry [18].

A balanced matrix experiment consists of a set of experimental conditions where the settings of multiple product or process parameters are changed. The objective of these experiments is to be capable of studying the effect that these changes to settings have on the system under study. After conducting the matrix experiment, the data collected from these experiments can then be analyzed to separate and quantify the size and direction of the effects that each product or process parameter had on the system.

The objectives of the analysis of experiments may include [19]:

1. Determining which variables are most influential on the response y, which are compressive strength, flexural strength and impact resistance of steel fiber reinforced high strength concrete in this study.
2. Determining where to set the influential x's so that y is almost near the desired nominal value. The x's are the controllable factors, namely age

of testing, binder type, binder amount, curing type and steel fiber volume fraction in this study.

3. Determining where to set the influential x's so that the variability in y is small.
4. Determining where to set the influential x's so that the effects of the uncontrollable variables z_1, z_2,….., z_q are minimized. There are several uncontrollable variables in this study such as environmental conditions, human factors, steel fiber settlement and etc. However, these can not be introduced in the design.

One strategy of experimentation that is extensively used in concrete testing is the one factor at a time approach. This method consists of selecting a starting point or baseline set of levels for each factor, then successively varying each factor over its range with the other factors held constant at the baseline level [19]. After all tests are performed, a series of graphs are usually constructed showing how the response variable is affected by varying each factor with all other factors held constant. The major disadvantage of this strategy is that it fails to consider any possible interaction between the factors.

The correct approach to dealing with several factors is to conduct a factorial experiment. A factorial design is more efficient than one factor at a time experiments. A factorial design is necessary when interactions are present to avoid misleading conclusions. Also factorial designs allow the effects of a factor to be estimated at several levels of the other factors, yielding conclusions that are valid over a range of experimental conditions. By a full factorial design, in each complete trial or replication of the experiment all possible combinations of the levels of the factors are investigated. Consideration of all main factor and factor interaction effects generally produces good results. However, number of required experiments increases rapidly with an increase in number of analyzed parameters making usage of the full factorial designs infeasible.

If it is reasonably assumed that certain high order interactions are negligible, then information on the main effects and low order interactions may be obtained by running only a fraction of the complete factorial experiment. This approach is known as fractional factorial design. It saves considerable time and money but requires rigorous mathematical treatment, both in the design of the experiment and in the analysis of the results. Each experimenter may design a different set of fractional factorial experiments [20].

Taguchi simplified and standardized the fractional factorial designs in such a manner that two engineers conducting tests thousands of miles apart will always use similar designs and tend to obtain similar results [20]. Taguchi constructed a special set of orthogonal arrays (OAs) to lay out experiments. All common full factorial and fractional factorial plans of experiments are orthogonal arrays. But not all orthogonal arrays are common fractional factorial plans. According to Taguchi to design an experiment is to select the most suitable orthogonal array, assign the factors to the appropriate columns, and finally, describe the combinations of the individual experiments called the trial conditions [20]. The Taguchi approach of laying out the experimental conditions significantly reduces the number of tests and the overall testing time. The Taguchi method of analysis of results arrives at the best parameters for the optimum design configuration with the least number of analytical investigations.

The change in the quality characteristics of a product under investigation, in response to a factor introduced in the Taguchi experimental design is the signal of the desired effect. However, when an experiment is conducted, there are numerous external factors not designed into the experiment which influence the outcome. These external factors are called the noise factors and their effect on the outcome of the quality characteristic under test is termed the noise. The signal to ratio (S/N) measures the sensitivity of the quality characteristic being investigated to those external influencing factors not under control. The aim of any experiment is always to determine the highest possible S/N ratio for the result. A high value of S/N implies that the signal is much higher than the

random effects of the noise factors. Product design or process operation consistent with highest S/N always yields the optimum quality with minimum variance. There are three quality characteristics that the response measure will possess. These are the larger the better, the smaller the better and the nominal the best characteristics. The S/N ratio is computed from the Mean Squared Deviation (MSD). The MSD is a statistical quantity that reflects the deviation from the target value. The expressions for the MSD are different for different quality characteristics. For S/N to be large, the MSD must have a value that is small.

$$S/N = -10 \, Log_{10} (MSD) \tag{2.1}$$

For larger the better:

$$MSD = \frac{1}{n}\sum_{i=1}^{n}\frac{1}{y_i^2} \tag{2.2}$$

For smaller the better:

$$MSD = \frac{1}{n}\sum_{i=1}^{n} y_i^2 \tag{2.3}$$

For nominal is the best:

$$MSD = \frac{1}{n}\sum_{i=1}^{n}\left(y_i - m\right)^2 \tag{2.4}$$

where:

y_i = results of experiments, observations or quality characteristics

m = target value of results

n = number of repetitions

The analysis of variance (ANOVA) is the statistical treatment most commonly applied to the results of the experiment to determine the percent contribution of each factor and factor interactions. Study of the ANOVA table for a given analysis helps to determine which of the factors need control and which do not [20]. ANOVA employs sums of squares which are mathematical abstracts that are used to separate the overall variance in the response into variances due to the processing parameters and measurement errors. The correction factor for mean (CF), total, main effects, the interaction and error sum of squares are calculated as in the following equations:

$$CF = \frac{\left(\sum_{i=1}^{n} y_i\right)^2}{n} \tag{2.5}$$

$$SS_T = \sum_{i=1}^{n} y_i^2 - CF \tag{2.6}$$

$$SS_A = \frac{\sum_{i=1}^{a} A_i^2}{br} - CF \tag{2.7}$$

$$SS_B = \frac{\sum_{j=1}^{b} B_j^2}{ar} - CF \tag{2.8}$$

$$SS_{AB} = \frac{\sum_{j=1}^{b}\sum_{i=1}^{a} AB_{ij}^2}{r} - SS_A - SS_B - CF \tag{2.9}$$

$$SS_e = SS_T - SS_A - SS_B - SS_{AB} \tag{2.10}$$

where:

y_i = individual observations

a = number of levels of parameter A

b = number of levels of parameter B

r = number of measurements for each pair of levels of parameters A and B

n = total number of measurements = abr

A_i = total of all measurements of parameter A at level i ($i = 1, 2, \ldots, a$)

B_j = total of all measurements of parameter B at level j ($j = 1, 2, \ldots, b$)

AB_{ij} = total of all measurements at the i^{th} level of parameter A and at the j^{th} level of parameter B ($i = 1, 2, \ldots, a$; $j = 1, 2, \ldots, b$)

Mean squares (MS) for each factor is obtained by dividing the sum of squares by their respective degrees of freedom (df).

$$MS_A = \frac{SS_A}{df_A} \tag{2.11}$$

F ratios are calculated by dividing the mean squares by the mean square of error.

$$F_A = \frac{MS_A}{MS_e} \tag{2.12}$$

The relationship between the response variable and the factors is characterized by a mathematical model called a regression model. It provides a technique for building a statistical predictor of a response and places a bound on the error of prediction [21]. By employing least squares method it tries to find the levels of the design variables that result in the best values of the response.

Response surface methodology is a collection of mathematical and statistical techniques that are useful for the modeling and analysis of problems in which a response of interest is influenced by several variables and the objective is to optimize the response [19]. If the general regression model is:

$$y = f(x_1, x_2) + \epsilon$$

where ϵ represents the noise or error observed in the response y. If the expected response is denoted by $E(y) = f(x_1, x_2) = \eta$, then the surface represented by

$$\eta = f(x_1, x_2)$$

is called a response surface [19].

2.3 Literature Review

In the study of Tanigawa and Hatanaka, in early 1980s, [22] stress-strain curves of steel fiber reinforced concrete (SFRC) and mortar (SFRM) under uniaxial monotonic and repeated compressive loadings were examined in terms of the volume fraction and the aspect ratio of steel fiber. The fiber volume fractions for mortar were 0%, 1% and 2%; and for concrete 0%, 0.5%, 1% and 2%. Two types of straight steel fibers were used with the aspect ratios of 60 and 90. The experiments are conducted as full factorial design but there are no statistical models analyzing the experimental data. In this experiment the flexural strength and the tensile splitting strength were also measured. The addition of steel fibers was found to increase the fatigue resistance and the lower aspect ratio resulted in higher strains but lower fatigue resistance.

Hashemi, Cohen and Ertürk [23] showed the effects of prior cycling on the static tensile, microstructural and ultrasonic properties of fiber reinforced Portland cement pastes. Type III Portland cement samples reinforced with 0.01 volume fraction of chopped steel fibers were subjected to cyclic loading in tension. The fibers were 0.33x0.63 mm in rectangular cross section and 25 mm in length. It was concluded that steel fiber reinforced cement exhibited good fatigue resistance at stress amplitudes up to 38% above the first crack strength and penetrating 80% of the range between the first crack and the ultimate composite strengths. On the other hand, a rapid decay in the elastic modulus and a

substantial increase in ultrasonic attenuation, both indicative of prior fatigue damage, have been observed. Yet, the composite strength and post-cracking fiber pull-out behavior are not affected by pre-cycling.

In the mid 1990s, Issa, Shafiq and Hammad [24] investigated the effects of the reinforcement size, reinforcement spacing and specimen size on the fracture parameters of notched mortar specimens reinforced with long aligned steel fibers. 3 fibers with 2.0 mm diameter spaced at 37.5 mm, 6 fibers with 1.5mm diameter spaced at 15mm and 14 fibers with 1.0 mm diameter spaced at 5.7 mm were used in the 600x125x25 specimens. 9 fibers with 2.0 mm diameter spaced at 37.5 mm, 18 fibers with 1.5 mm diameter spaced at 15mm and 42 fibers with 1.0 mm diameter spaced at 5.7 mm were used in the 600x125x75 mm specimens. It was concluded that increasing the fiber size or the corresponding spacing between the fibers decreases the fracture energy. But the fracture energy and the energy release rate were independent of the specimen size.

Toutanji and Bayasi [25] investigated the effects of curing environments on the mechanical properties of steel-fiber reinforced concrete. Specimens were cured in three different environmental conditions: steam (80^{o}C and lasted 4 days), moisture and air. Results showed that steam curing, as compared to moisture curing, does not enhance the flexural strength of steel fiber reinforced concrete but does reduce flexural toughness. As expected, air curing showed detrimental effects on all aspects of the test results, as compared to steam and moisture curing.

Yan, Sun and Chen [26] studied the impact and fatigue performance of high-strength concrete (HSC), silica fume high-strength concrete (SIFUHSC), steel fiber high-strength concrete (SFRHSC), and steel fiber silica fume high-strength concrete (SSFHSC) under the action of repeated dynamic loading. Crushed granite was used as coarse aggregate. The impact performance was measured by the freely falling ball method. The weight and height of the falling ball were 4.5 kg and 457 mm, respectively. The flexural fatigue test results, involving 500

specimens, were analyzed by the linear regression analysis. It was found that the fatigue capacity is enhanced with the incorporation of silica fume, steel fibers or both. The effect of incorporating steel fibers alone was greater than that of incorporating silica fume alone. The composite effects of silica fume and steel fiber were greater than the sum of individual effects of silica fume or steel fibers.

In the work of Nataraja, Dhang and Gupta [1] the variation in impact resistance of steel fiber-reinforced concrete and plain concrete as determined from a drop weight test was reported. Granite was used as coarse aggregate. The goodness-of-fit (chi-square test) indicated poor fitness of the impact resistance test results produced in this study to normal distribution at 95% level of confidence for both fiber-reinforced and plain concrete. However, the postcrack resistance test results for both fiber-reinforced concrete as well as plain concrete fit to normal distribution as indicated by the goodness-of-fit test.

Yang, Zhang, Huang and He [27] studied the effects of 0% to 40% ground quartz sand (GQS) replacement of cement, SiO_2 content, and specific area of GQS on the compressive strength of concrete in the steam curing and autoclaved curing. Four types of natural quartz sand are used for producing GQS with varying specific area and having various SiO_2 content. Part of the specimens was stored 28 days in water (ordinary curing), and others were stored for 9 hours in steam-curing with a constant maximum temperature of 85^{o}C, and after 9 hours for 8 hours in autoclaved-curing with 1.0 MPa vapor pressure at 182^{o}C. It was found that the strength of concrete in steam curing and in ordinary curing for 28 days was reduced with the increase in the amount of GQS replacement of cement. The strength of concrete with GQS, cured in the steam-curing stage or in the autoclaved-curing stage, was enhanced with the increase in the SiO_2 content of GQS. The strength of concrete after autoclaving was enhanced when the specific area of GQS increases, but it had little influence on the strength of concrete cured in the steam-curing stage. These results are obtained with one factor at a time experimentation and with graphical analysis of the data.

In the study of Shannag [4], various combinations of a local natural pozzolan and silica fume were used to produce workable high to very high strength mortars and concretes. The mixtures were tested for workability, density, compressive strength, splitting tensile strength, and modulus of elasticity. Two high strength mortar mixes were optimized and used in this study. One mix contained 15% silica fume and different proportions of natural pozzolan (0%, 5%, 10%, 15%, 20%, and 25%) by weight of cement. The other mix contained 15% natural pozzolan and different proportions of silica fume (0%, 5%, 10%, 15%, 20%, and 25%) by weight of cement. The results of this study suggested that certain natural pozzolan-silica fume combinations can improve the compressive and splitting tensile strengths, workability, and elastic modulus of concretes, more than natural pozzolan and silica fume alone. Furthermore, the use of silica fume at 15% of the weight of cement was able to produce relatively the highest strength increase in the presence of about 15% pozzolan than without pozzolan. In this study all the combinations were tested and the results were analyzed graphically.

Luo, Sun and Chan [28] investigated the mechanical properties of steel fiber reinforced high performance concrete (SFRHPC) with different types of steel fibers and with varying fiber volume fractions. Also their resistance against impact testing was compared with reinforced high strength concrete (RHSC) with steel bars and without fiber reinforcement. 16% fly ash is used in the concrete mix. Five different types of steel fibers were used with different geometry. Two of them were straight fibers with aspect ratios of 60 and 40, one was hooked with an aspect ratio of 60, one was indented having an aspect ratio of 60 and the last one was steel-ingot-milled fiber with an aspect ratio of 35. Four different fiber volume fractions were adopted 4%, 6%, 8% and 10%. The projectiles used in the impact test were armor penetration projectiles with diameter of 37 mm and weight about 0.9 kg. In the impact tests, all the targets with their four side faces fixed in a rigid shelf were located to ensure that the projectiles hit the front faces vertically. With the increase in steel fiber volume fraction various mechanical properties of SFRHPC were considerably improved.

Impact test observations showed that SFRHPC exhibited different behavior from RHSC. RHSC targets were smashed up while SFRHPC targets kept intact with some radial cracks in the front faces and some minor cracks in the side faces. The projectiles were either embedded or rebounded for SFRHPC.

Wu, Chen, Yao and Zhang [14] tested the effect of the coarse aggregate type on the compressive strength, splitting tensile strength, fracture energy, characteristic length, and elastic modulus of concrete produced at different strength levels. Concretes considered were produced using crushed quartzite, crushed granite, limestone and marble coarse aggregate. The results showed that the strength, stiffness, and fracture energy of concrete for a given w/c ratio depend on the type of aggregate, especially for high-strength concrete. It was suggested that high-strength concrete with lower brittleness can be made by selecting high-strength aggregate with low brittleness.

In the study of Memon, Radin, Zain and Trottier [29], the effects of mineral and chemical admixtures namely fly ash, ground granulated blast furnace slag, silica fume and superplasticizers on the porosity, pore size distribution and compressive strength development of high-strength concrete in seawater curing condition exposed to tidal zone were investigated. Three levels of cement replacement (0%, 30%, 70%) were used. The objective was to identify the composition of cement matrix that would produce not only high strength but also durable concrete. Results of this study indicated that both 30% and 70% concrete mixes exhibited better performance than the normal Portland cement concrete in seawater exposed to tidal zone.

In the work of Srinivasan, Narasimhan and Ilango [30], an attempt has been made to make cost effective rapid-set high strength cement. The experiments were designed using orthogonal array technique in L9 array with three factors, namely ordinary Portland cement (OPC)/high-alumina cement (HAC)/anhydrous calcium sulphate, fineness of the cement, and type of additives, at three levels each. The responses studied were initial setting time,

final setting time, and compressive strength. The response data were analyzed using analysis of variance (ANOVA) technique with a software package, ANOVA by Taguchi Method. In the case of setting time, fineness of the cement and OPC/HAC/anhydrous calcium sulphate ratio plays a significant role. Additive type and the OPC/HAC/anhydrous calcium sulphate are significant factors affecting the compressive strength at different ages. The confirmatory trial results clearly indicate that the setting time and compressive strength at different ages targeted were achieved using design of experiments.

Li and Zhao [31] presented a laboratory study on the influence of combination of fly ash (FA) and ground granulated blast-furnace slag (GGBS) on the properties of high-strength concrete. A contrast study was carried out for the concrete (ground granulated blast-furnace slag fly ash concrete (GGFAC)) incorporating FA and GGBS, control Portland cement concrete and high-volume FA high-strength concrete (HFAC). The results showed that the combination of FA and GGBS can improve both short-and long-term properties of concrete, while HFAC requires a relatively longer time to get its beneficial effect.

In the investigation of Marzouk and Langdon [32], they used a potentially highly reactive aggregate and a potentially moderately reactive aggregate in the preparation of normal and high strength concretes. 13.5% of silica fume is used in the mix design of high-strength concrete with a constant w/c ratio of 0.34. After the initial 28 day curing period, the specimens were equally divided, and then submerged in a holding tank containing either a solution of a sodium hydroxide or de-ionized water at 80^{o}C for a period of 12 weeks. Normal strength concrete specimens containing the potentially highly reactive aggregate and exposed to the sodium hydroxide solution experienced more losses in mechanical properties than the concrete specimens prepared with potentially moderately reactive aggregates. However, in high strength concrete specimens exposed to the sodium hydroxide solution, there was a minimal loss in mechanical properties for both the specimens containing the highly reactive or moderately reactive aggregates.

Padmarajaiah and Ramaswamy [33] presented results from an experimental program for eight fully prestressed beams and seven partially prestressed beams made with high strength fiber-reinforced concrete. These studies mainly attempted to determine the influence of trough shaped steel fibers in altering the flexural strength, ductility and energy absorption capacity of the beams. The magnitude of the prestress, volume fraction of the fibers ranging from 0% to 1.5% as addition to conventional reinforcing steel bars and the location of fibers were the variables in the test program. It was seen that the ultimate flexural load increased as the fiber content increased. The inclusion of fibers in the fully prestressed beams resulted in higher ultimate strengths as compared to the corresponding partially prestressed beams. The placement of fibers over a partial depth in the tensile side of the prestressed flexural structural members provided equivalent flexural capacity as in a beam having the same amount of fiber over the full cross section.

The application of experimental design and analysis techniques to civil engineering is very rare. Some examples concerning civil engineering applications of experimental design and analysis can be found in the book of Montgomery D.C.'s Design and Analysis of Experiments [19]. Besides the study of Srinivasan, Narasimhan and Ilango [30] explained above, two other studies are found in the literature applying the experimental design and analysis methods. However, these two researches are not related with steel fiber reinforced high strength concretes. But, since they are civil engineering applications they are going to be included in the literature review.

In the study of Pan, Chang and Chou [34], solidification of low level radioactive (LLW) resin was optimized by using Taguchi analytical methodology. The ingredients in LLW mortar which caused the solidification of cement were evaluated through consecutive measurements of the effects of various concentrations of ingredients. Four ingredients, fly ash, furnace slag, cement and resin were mixed altogether with three different concentrations of each. Two different amounts of water were added to each combination. The samples

were organized into 18 groups according to Taguchi and still yield results with the same confidence as if they were to be considered separately. Results indicated that both furnace slag and fly ash were the dominant material resulting from the solidification of LLW mortar.

In the work Sonebi [35], statistical models are developed using a factorial design which was carried out to model the influence of key parameters on properties affecting the performance of underwater grout. A 2^3 statistical experimental design was used to evaluate the influence of water-to-cementitious materials ratio, the amount of anti-washout admixture by mass of binder and the amount of superplasticizer by mass of cementitious materials on the grout responses of mini-slump, flow time, washout resistance, unit weight and compressive strength. A central composite plan was selected where the responses could be modeled in a quadratic manner. The derived models enable the identification of primary factors and their interactions that influence the modeled responses of underwater cement grout. Also this study demonstrated the usefulness of the models to improve understanding of trade-offs between parameters.

CHAPTER 3

LABORATORY STUDIES

3.1. Process Parameter Selection

As noted by ACI committee 544, steel fiber reinforced concrete has potential for many applications, specially, in the area of structural elements [36]. Most research is now on the possibility of using the composite for structural applications. Because under seismic condition the structure may be subjected to large deformations, strength and ductility are among the important factors to be considered in the design of seismic resistant reinforced concrete structures. Therefore it is important to evaluate the compressive strength, flexural strength and impact resistance of steel fiber reinforced concrete. Since the aim is to obtain a high strength concrete, the process parameters of the steel fiber reinforced high strength concrete (SFRHSC) are optimized for increasing the compressive strength, flexural strength and impact resistance.

Most studies in literature are now on the effect of fine and coarse aggregate types (basalt, quartz, dolomite, granite, etc.) [3, 14, 15], fiber types (steel, polypropylene, carbon, bamboo, etc.) [37, 38, 39], fiber geometry (hooked, straight, anchored, etc.) [40, 41], fiber size (fiber aspect ratio) [42, 43], curing type (steam, water or air curing) [44], curing temperature [44, 45], curing time [44, 45], mineral and chemical admixtures namely fly ash, ground granulated blast furnace slag, silica fume and superplasticizers [4, 26, 29, 46] and water cement ratio (w/c) on the properties of fiber reinforced high strength concrete.

Apart from these, the mixing time of concrete in the mixer, the rodding time when fresh concrete is placed in the molds and the loading rate of the machines are other factors that affect the properties of the FRHSC.

However, only five processing parameters are analyzed in this study to reduce the required experiments to manageable numbers and also to reduce the enormous material costs. The analyzed processing parameters are the binder type, binder amount, curing type, testing age and steel fiber volume fraction. The remaining factors are kept constant.

High strength is made possible by reducing porosity, inhomogeneity and microcracks in concrete [4]. This can be achieved by using superplasticizers and supplementary cementing materials such as silica fume, fly ash, ground granulated blast furnace slag and natural pozzolan. Fortunately, most of these materials are industrial by-products and help in reducing the amount of cement required to make concrete less costly, more environmental friendly, and less energy intensive [4]. When they are used in the concrete mix, these by-products are called binders. Hence the effect of different types of binders and their amount on high strength steel fiber reinforced concrete should be considered.

The addition of steel fibers significantly improves many of the engineering properties of mortar and concrete, mainly impact strength and toughness. Flexural strength, fatigue strength, tensile strength and the ability to resist cracking and spalling are also enhanced [36, 42]. The main concern with high strength concrete is the increasing brittleness with increasing strength. Therefore, it becomes a more acute problem to improve the ductility of high strength concrete [2]. Most accumulated experience in normal strength fiber reinforced concrete may well be applicable to high strength concrete but the effectiveness of fiber reinforcement in high strength concrete may be different and thus needs to be investigated.

Loss of water from fresh and young concrete caused by inadequate curing can result in detrimental effects on the properties of concrete in the short and long run. These undesirable effects include appearance of plastic shrinkage cracks, reduction in strength, increase in permeability, and increase in porosity resulting in a shorter service life of the structure [45]. By hot water curing or steam curing, a 95% hydration rate can be achieved in a few hours [44]. However, this concrete easily cracks due to the temperature difference between the inside and the outside. In this study this problem is achieved by leaving the specimens in the steaming bath for half a day and gradually decreasing the temperature until it reaches to the outside temperature. Thus type of curing is an important factor affecting the mechanical properties of SFRHSC and different types should be analyzed.

Most of the previous research defines the workable ranges of the analyzed process parameters. Three types of binder are used in the mix design of the steel fiber reinforced concrete with different percentages. First mix contains only silica fume with 10%, 15% and 20% cement replacement levels. The second mix contains 10%, 20%, 30% of fly ash and a constant 15% of silica fume as cement replacement, and in the third mix 20%, 40%, 60% of ground granulated blast furnace slag is used with 15% of silica fume as cement replacements. Past research suggests using a certain amount of silica fume, mostly 10-15%, with fly ash and ground granulated blast furnace slag since they do not help to achieve very high strengths by themselves [29, 31, 39, 46].

The steel fibers are Dramix Bekaert 01 6/0.16 HC circular straight fibers with 6 mm in length and 0.16 mm in diameter. The fiber aspect ratio (l_f/l_d) is 37.5. The three different fiber volume fractions used in the study are 0%, 0.5% and 1% by volume. 0% is chosen as the minimum level in order to compare plain high strength concrete with steel fiber high strength concrete. 1% is chosen as the maximum level for economic reasons. The medium level is set as the average of maximum and minimum levels that is 0.5%. These values are also in accordance with the previous researches [33, 42, 43].

The effect of steam curing at 55^{o}C with a duration of five hours and the effect of normal water curing in an atmosphere of 90% humidity and 23^{o}C until the day of testing is analyzed in the study. The compressive strength, flexural strength and impact tests are performed at the age of 7, 28 and 90 days.

There are uncontrollable factors that can affect the whole process and cause unexpected variations in the response variables. The humidity and the temperature of the environment can cause rapid hydration of the fresh concrete and as a result, since it takes about one hour to pour the fresh concrete to the molds, the flow of the concrete can be different at the beginning and at the end of molding process. This unwanted hydration can also cause rodding problems as the concrete starts to set as time passes resulting in nonuniform rodding. As a result, concrete had not been placed in the molds properly causing excessive voids that decrease its strength. There is also human factor that can result in nonuniform rodding which is discussed above. Human factor also cause loading problems when the operator could not set the loading rate to the desired value as the machines operate manually not electronically. One of the uncontrollable factors is the fiber settlement. The micro steel fibers should be distributed in the concrete evenly during the mixing process. But, since the fresh concrete waits during the molding stage the fibers may settle to the bottom of the concrete, although this can happen rarely. During the molding and the curing stages undesired little voids and little fractures may occur. Another unwanted situation is the nonuniform distribution of load to all fibers in the specimen during the testing stage.

3.2 Concrete Mixtures

Twenty seven different concrete mixes having different amounts of reinforcements and mineral admixtures were produced to be used in the tests for the purpose of evaluating the performance characteristics which are compressive strength, flexural strength and impact resistance.

In order to produce a high strength concrete, a total mixture of aggregates were prepared consisting of 12.5% fine aggregate and 87.5% coarse aggregate. Both fine and coarse aggregates used in the study are natural basalt obtained from Tekirdağ region. The coarse aggregate is crushed basalt with a 4mm maximum particle size which is in coincidence with the literature for high strength concretes [47] and the fine aggregate is grounded basalt. The total cementitious material including the mineral admixtures (silica fume, fly ash, ground granulated blast furnace slag) was 690 kg/m^3. Portland cement is obtained from Bolu Cement Factory which has 42.5 MPa strength at the end of 28 days. Silica fume is obtained from industry, fly ash is from Seyit Ömer region and the ground granulated blast furnace slag was brought from İskenderun. Graded standard sand, which is natural river sand, is used in the mix since it acts as a good filler material. The Rilem Cembureau standard sand is obtained from Set Cement Industry. The concrete mix proportion used in the study is given in Table 3.1.

Table 3.1 Concrete mix proportions

Material Type	**Amount**
Total Binder (kg/m^3)	690,00
Graded Standard Sand (kg/m^3)	412,00
Fine Aggregate (kg/m^3)	2060,00
Coarse Aggregate (kg/m^3)	1442,00
Water (kg/m^3)	1860,00
w/c	0,27
Superplasticizer (kg/m^3)	17,25

When, for example, 15% silica fume and 20% fly ash is used as additional binders to portland cement, the concrete mix becomes as in Table 3.2 total binders amount adding up to 690 kg/m^3. The concrete mixes for all of the combinations of the factors are given in Appendix A.1.

Table 3.2 Concrete mix when 15% silica fume and 20% fly ash is used as additional binders to portland cement

Material Type	**Amount**
Silica Fume (kg/m^3)	103,50
Fly Ash (kg/m^3)	138,00
Portland Cement (kg/m^3)	448,50
Graded Standard Sand (kg/m^3)	412,00
Fine Aggregate (kg/m^3)	206,00
Coarse Aggregate (kg/m^3)	1442,00
Water (kg/m^3)	186,00
w/c	0,27
Superplasticizer (kg/m^3)	17,25

3.3 Making the Concrete in the Laboratory

The preparation of the concrete specimens in the laboratory is made in accordance with the ASTM C 192-90a. After the required amounts of all the materials are weighed properly, the next step is the mixing of concrete. The aim of the mixing is that all the aggregate particles should be surrounded by the cement paste and all the materials should be distributed homogeneously in the concrete mass. A power-driven tilting revolving drum mixer is used in the mixing process (Figure 3.1). It has an arrangement of interior fixed blades to ensure end-to-end exchange of material during mixing. Tilting drums have the advantage of a quick and clean discharge.

Figure 3.1 The power-driven tilting revolving drum mixer

The interior surfaces of the mixer should be clean before use. Prior to starting rotation of the mixer, the coarse aggregate, some of the mixing water and the superplasticizer, which is added to the mixer in solution in the mixing water, are poured into the mixer. Normal, drinkable tap water that was assumed to be free of oil, organic matter and alkalis, is used as mixing water. Then, the mixer is started and the fine aggregate, all the cementitious material and water is added with the mixer running. The powdered admixtures (in this study all the admixtures were powdered) such as silica fume, fly ash and GGBFS, are mixed with a portion of cement before introduction into the mixer so as to ensure thorough distribution throughout the concrete. The concrete is mixed after all ingredients are in the mixer for 3 minutes followed by 3 minutes rest, followed by 2 minutes final mixing. During the rest period the open end of the mixer is covered in order to prevent the evaporation. Before the final mixing, the steel fibers are added directly to the mixer once the other ingredients have been uniformly mixed. The mixer is rotating at full speed as the fibers are being added. After the final mixing the mixer is stopped and it is tilted so that the

open end turns up right down and the fresh homogeneous concrete is poured into a clean metal pan. To eliminate segregation, which is the separation of the components of fresh concrete, generally the coarse aggregate settles to the bottom of the fresh concrete, resulting in a nonuniform mix, the fresh concrete is remixed by shovel or trowel in the pan until it appears to be uniform. When the concrete is not being remixed or sampled it is covered to prevent evaporation.

3.4 Placing the Concrete

The reusable molds used in this study are made of steel which is nonreactive with concrete containing portland or other hydraulic cements. They are watertight and sufficiently stiff so that they do not deform excessively on use under severe conditions like steam curing. The molds are lightly coated with mineral oil before use in order to provide easy removal from the moulds.

50x50x50 mm cube molds for compressive strength and 25x25x300 mm prismatic molds for both flexural strength and impact resistance specimens are used in this study. The small size of the molds used for testing of steel fiber reinforced high strength concrete are in accordance with the literature [2, 3, 47, 48, 49]. The compressive strength molds have three cube compartments and they are separable into two parts. All the molds are placed on a firm, level surface that is free from vibration (Figure 3.2).

The concrete is placed in the molds using a blunted trowel. The fresh concrete is remixed in the pan with the trowel at random periods to prevent segregation during the molding process. The concrete is placed in the molds in two layers of approximately equal volume. The trowel is moved around the top edge of the mold as the concrete is discharged in order to ensure a symmetrical distribution of the concrete and to minimize segregation of coarse aggregate within the mold. Further the concrete is distributed by use of a 16 mm diameter tamping rod, which is a round, straight steel rod with the tamping end rounded to a hemispherical tip of the same diameter as the rod, prior to the step of

consolidation. The rodding type of consolidation is applied in this study since, the molds were too small for vibration type of consolidation.

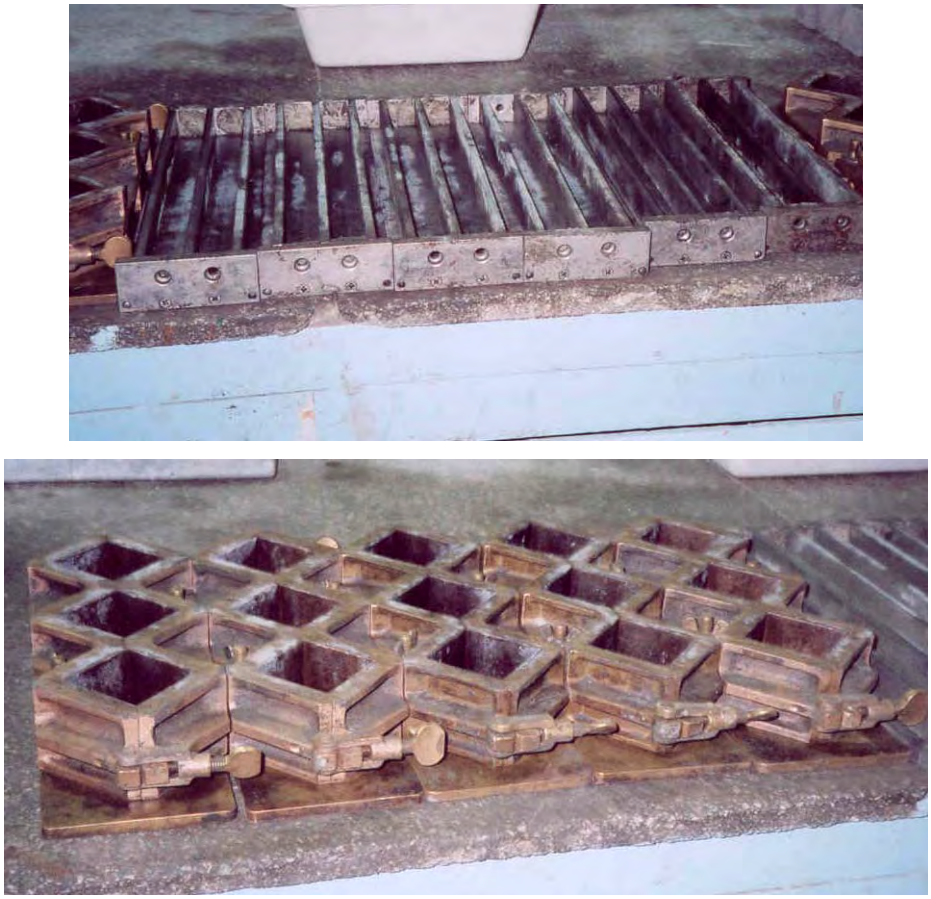

Figure 3.2 The 50x50x50 mm and 25x25x300 mm steel molds

Each layer is rodded with the rounded end of the rod 25 times. The bottom layer is rodded throughout its depth. The strokes are distributed uniformly over the cross section of the molds and for the upper layer the rod is allowed to penetrate about 12 mm into the underlying layer [50]. The reason for this rodding step is that a poorly compacted specimen has a lower strength than a properly compacted one. After each layer is rodded, the outsides of the molds are tapped

lightly 10 to 15 times with the mallet in order to close any holes left by rodding or to release any large air bubbles that may have been trapped. After consolidation, the top surface is finished by striking off with the trowel. All finishing is performed with the minimum manipulation necessary to produce a flat even surface that is level with the edge of the molds.

3.5 Curing the Concrete

To prevent evaporation of water from the unhardened concrete, the specimens are covered immediately after finishing, by a wet cotton cloth until the specimens are removed from the molds.

Figure 3.3 The specimens that are immersed in saturated lime water in the curing room

All the molds that are going to be moist cured are moved to the curing room after finishing, which is at 23 ± 1.7°C and having a relative humidity of 90% or above. Moist curing means that the test specimens must have free water maintained on the entire surface area at all times [50]. The specimens are demolded 24 h after casting, immersed in saturated lime water and stored in that position in the curing room until the time of testing (Figure 3.3). During curing, the desirable conditions are a suitable temperature as this governs the rate at which the chemical actions involving setting and hardening take place, the provision of ample moisture or the prevention of loss of moisture, and the avoidance of premature stressing or disturbance [51].

Figure 3.4 The specimens that are placed in the steam chamber after the initial setting

Figure 3.5 Intermittent low pressure steam curing machine at 55^{o}C

The molds which are going to be steam cured are placed into the steam chamber after the initial setting of concrete takes place (Figure 3.4). Until the time of initial setting the finished molds are covered with wet cotton clothes. Intermittent low pressure type of steam curing is employed in this study. The maturity of concrete is governed by the product of temperature and time and low pressure steam curing is effective in speeding up the gain of maturity but the temperature should not be raised too rapidly. The specimens are exposed to five hours 55^{o}C steam curing and left in the steam chamber until demolding which is again 24 h after casting (Figure 3.5). After the removal of the specimens from

the molds, they are placed in saturated lime water and stored in the curing room until the day of testing as done in moist curing.

3.6 Compressive Strength Measurement

A power operated hydraulic screw type RIEHLE Model RD-5B testing machine having a capacity of 200 t, with sufficient opening between the upper and lower bearing surface of the machine is used in compressive strength testing of the 50x50x50 cube specimens. The testing machine is equipped with two steel bearing blocks with hardened faces, one of which is a spherically seated block firmly attached at the center of the upper head of the machine that will bear on the upper surface of the specimen, and the other a solid block on which the specimen shall rest (Figure 3.6). The upper block is closely held in its spherical seat, but it is free of tilt in any direction. The upper platen of the machine can be raised or lowered, to suit the size of the test specimen, by means of very heavy screwed bolts. The two bearing surfaces of the machine shall not depart from plane surfaces by more than 0.013 mm [52]. The load applied to the concrete specimen under test is measured by the oil pressure in the hydraulic plunger as determined by a gauge.

The compressive strength test is made in accordance with the ASTM C39. Cubes stored in water are tested immediately they are removed from the water. Each specimen is wiped to a surface-dry condition and any loose sand grains or incrustations from the faces that will be in contact with the bearing blocks of the testing machine are removed. The cubes are placed in the testing machine so that the load is applied to opposite sides as cast and not to the top and bottom as cast. Therefore, the bearing faces of the specimen are sufficiently plane as to require no capping. If there is appreciable curvature, the face is grinded to plane surface using only a moderate pressure because, much lower results than the true strength are obtained by loading faces of the cube specimens that are not truly plane surfaces. Three cube specimens are tested for each different concrete mix. The cubes are accurately placed within the locating marks on the bottom platen

so that they are truly concentric with the spherical seat of the upper platen. As the spherically seated block is brought to bear on the specimen, its movable portion is rotated gently by hand so that uniform seating is obtained. The load is applied continuously and without shock with a rate of 0.25 MPa/s until the failure of the specimen [53]. The maximum load carried by the specimen is then recorded.

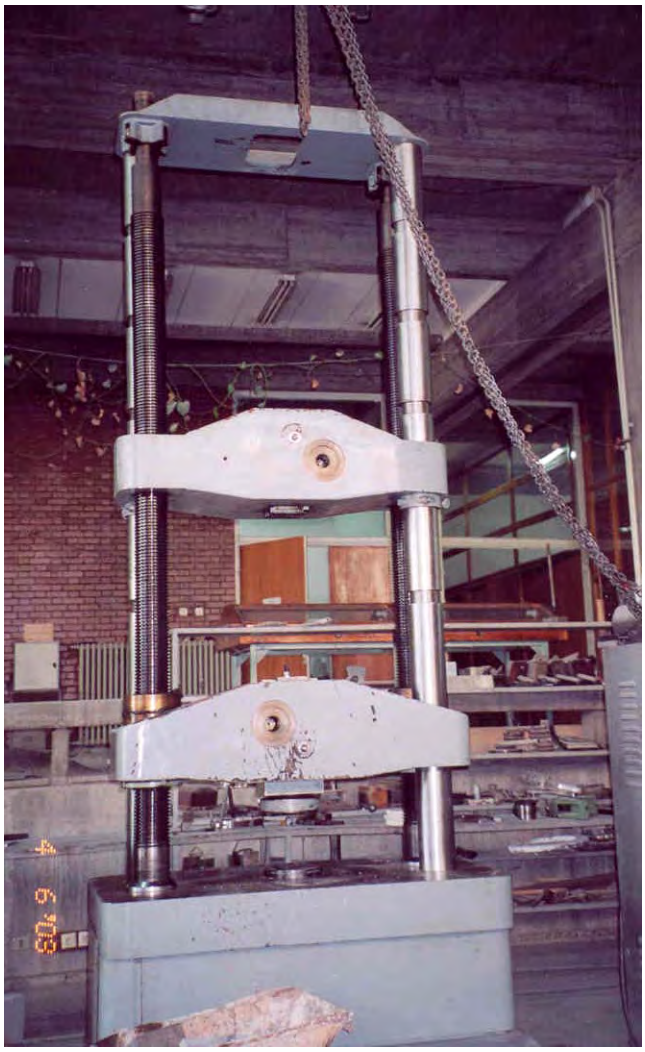

Figure 3.6 The hydraulic screw type compressive strength testing machine

The compressive strength of the specimen, σ_{comp} (in MPa), is calculated by dividing the maximum load carried by the cube specimen during the test by the cross sectional area of the specimen which is 25 cm^2.

$$\sigma_{comp} = \frac{P_{max}}{A} \tag{3.1}$$

3.7 Flexural Strength Measurement

The molds for the 25x25x300 mm prism specimens are double-gang molds and they are so designed that the specimens are molded with their longitudinal axes in a horizontal position. The flexural strengths of concrete specimens are determined by the use of simple beam with center point loading in accordance with ASTM C293. A hydraulic Losenhausen model testing machine is used for this purpose (Figure 3.7). The mechanism by which the forces are applied to the specimen employs a load applying block and two specimen support blocks (Figure 3.8). The machine is capable of applying all forces perpendicular to the face of the specimen without eccentricity. The load applying and support blocks extend across the full width of the specimen. They are maintained in a vertical position and in contact with the rod by means of spring loaded screws which hold them in contact with the pivot rod. Each hardened bearing surface in contact with the specimen shall not depart from a plane by more than 51 μm [54].

Three specimens are tested for each different concrete mix. Each beam is wiped to a surface dry condition, and any loose sand grains or incrustations are removed from the faces that will be in contact with the bearing surfaces of the points of support and the load application. Because the flexural strengths of the prisms are quickly affected by drying which produces skin tension, they are tested immediately after they are removed from the curing room.

Figure 3.7 The hydraulic Losenhausen model testing machine used in the flexural strength measurement of 25x25x300 mm concrete specimens

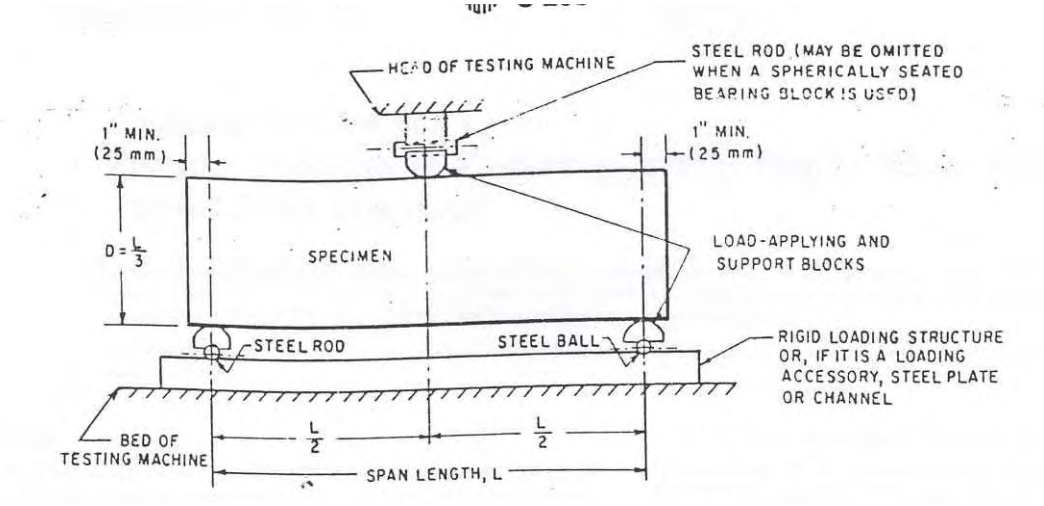

Figure 3.8 Diagrammatic view of the apparatus for flexure test of concrete by center-point loading method

The pedestal on the base plate of the machine is centered directly below the center of the upper spherical head, and the bearing plate and support edge assembly are placed on the pedestal. The center loading device is attaché to the spherical head. The test specimen is turned on its side with respect to its position as molded and it is placed on the supports of the testing device. This provides smooth, plane, and parallel faces for loading. The longitudinal center line of the specimen is set directly above the midpoint of both supports. The center point loading device is adjusted so that its bearing edge is at exactly right angles to the length of the beam and parallel to its top face as placed, with the center of the bearing edge directly above the center line of the beam and at the center of the span length. The load applying block is brought in contact with the surface of the specimen at the center. If full contact is not obtained between the specimen and the load applying or the support blocks so that there is a gap, the contact surfaces of the specimen are ground. Grinding of lateral surfaces is minimized as much as it was possible since grinding may change the physical characteristics of the specimens. The specimen is loaded continuously and without shock at a rate of 0.86 to 1.21 MPa/min until rupture occurs. Finally, the maximum load indicated by the testing machine is recorded.

The flexural strength of the beam, σ_{flex} (in MPa), is calculated as follows:

$$\sigma_{flex} = \frac{3\,P\,l}{2\,b\,d^2} \tag{3.2}$$

where:

P = maximum applied load indicated by the testing machine

l = span length (240 mm in this case)

b = average width of specimen, at the point of fracture (25 mm in this case)

d = average depth of specimen, at the point of fracture (25 mm in this case)

3.8 Impact Resistance Measurement

Civil engineering structures are often required to resist impact (dynamic) loads. Buildings in earthquake regions and bridges are common examples. Structural design for impact loads involves a careful consideration of material properties such as toughness. The toughness of a material is defined as the amount of energy that is absorbed until fracture.

There are several experimental methods for measuring the impact resistance of materials. One common method is the use of charpy impact machine together with notched specimens. This charpy V-notch impact test has been used extensively in mechanical testing of metals and mostly steel products by metallurgical engineers [55]. A similar study concerning the charpy impact test for concrete specimens, could not be found in literature. Mostly, drop weight test is employed for concrete specimens which are either large beams or plates. Since the specimens used in this study are small in size, charpy impact testing is employed to observe the impact resistance of the unnotched 25x25x150 mm beams and to identify whether this test procedure gives reasonable results. In order to illustrate the performance of the charpy impact testing, Losenhausen Model PSW 30 Pendulum Impact Tester (Figure 3.9) is used and testing is done in accordance with ASTM E23 “Methods for Notched Bar Impact Testing of

Metallic Material" since there is no other standard related to charpy impact testing of concrete specimens.

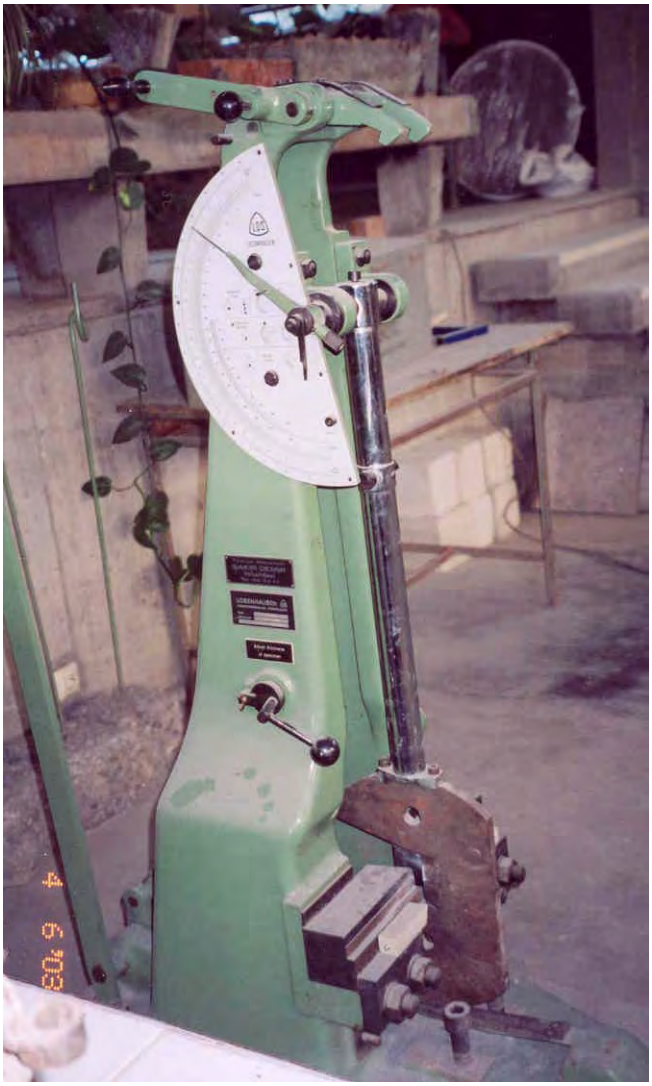

Figure 3.9 Brook's Model IT 3U Pendulum Impact Tester

The machine consists of a freely swinging pendulum which is released from a fixed height corresponding to a known energy at striking to the specimen (Figure 3.10). The specimen is supported at the ends and struck in the middle.

The height to which the pendulum rises in its swing after breaking the specimen is measured and indicated on a scale as the residual energy of the pendulum or as the energy absorbed by the specimen. There is not any drawback in using unnotched specimens, since this machine is equipped with adaptors that determine the energy required to fracture them.

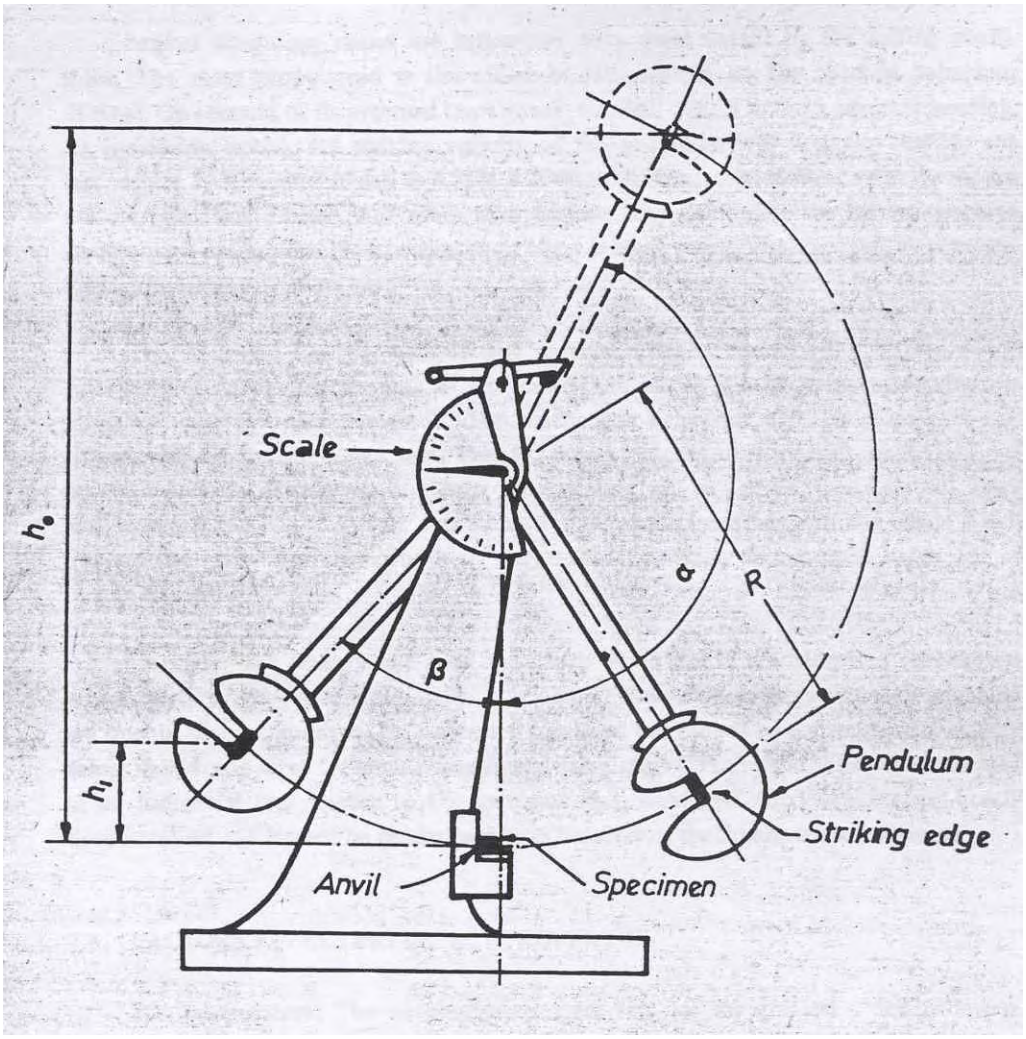

Figure 3.10 General view of pendulum type charpy impact testing machine

Each beam that is going to be tested is wiped to a surface dry condition, and any loose sand grains or incrustations are removed from the faces that will be in

contact with the pendulum surface and supports. The beams that are cast in 25x25x300 mm molds are cut into two pieces resulting two 25x25x150 mm beams since 300 mm is too long for this test and there were no available molds in the size of 25x25x150 mm or smaller. Then, the specimen is attached to the bottom of the machine on the supporting plates. The energy indicator scale is set to the maximum scale reading and the pendulum is released without vibration. Finally, the amount of energy required to fracture the specimen is read from the machine scale in kgf.m.

CHAPTER 4

EXPERIMENTAL DESIGN AND ANALYSIS WHEN THE RESPONSE IS COMPRESSIVE STRENGTH

4.1 Taguchi Experimental Design

For all of the responses (compressive strength, flexural strength and impact resistance), the same orthogonal array is used in order to have a consistent experimental design through the responses. To decide which orthogonal array will be used, the first step is the determination of the degrees of freedom needed to estimate all of the main effects and the important interaction effects. There are five main factors, four of them with three levels and one of them with two levels and two two-way interaction factors that are going to be included in the design. However, the levels of factor C (the binder amount) are not identical for different levels of factor B (binder type). Therefore this is a two-stage nested design with the levels of factor C nested under the levels of factor B. The main factors and their levels are given below:

Parameter A: Testing age (days)

Levels: -1: 7 days 0: 28 days 1: 90 days

Parameter B: Binder type used in the concrete mix

Levels: -1: Silica fume (SF) 0: Fly ash (FA)

1: Ground granulated blast furnace slag (GGBFS)

Parameter C: Binder amount used in the concrete mix (%)

Levels:	-1: 20%	0: 15%	1: 10%(for silica fume)
	-1: 10%	0: 20%	1: 30%(for fly ash)
	-1: 20%	0: 40%	1: 60%(for GGBFS)

Parameter D: Specimen curing type

Levels: -1: ordinary water curing 0: steam curing

1 = -1: ordinary water curing (dummy)

Parameter E: Steel fiber volume fraction (% by vol.)

Levels: -1: 0.0% 0: 0.5% 1: 1.0%

The levels of the silica fume binder amount are in descending order since it is known from the past researches that as the amount of silica fume decreases the strength of the concrete decreases also. Whereas, as the amounts of both fly ash and GGBFS increase, the strength of the concrete decreases. Therefore the level assignment is done according to the decreasing strength of concrete.

As a result the required degrees of freedom are:

Factors	dof
A	2
B	2
C within B	6
D	1
E	2
A*B	4
B*E	4
Overall Mean	1
TOTAL	22

It is obvious that an orthogonal array with 3 levels, 11 columns (4 for the main primary factors A, B, D, E, 3 for the nested factor C and 4 for the two interaction effects) and 18 rows (runs) is needed. So L_{27} (3^{13}) is found as the most suitable orthogonal array for this study. When this array is used two columns are left empty for the error estimation. Since all the factors have three levels except the Curing Type (D) factor, it must be dummy treated. So the ordinary water curing factor level is the repeated level for the dummy treatment. This level is chosen for as dummy because steam curing more expensive and a more time consuming process than the ordinary water curing. Therefore the 3rd level in the 10th column of L_{27} (3^{13}) array is replaced with its 1st level for the dummy treatment of the curing type factor.

The interaction between the binder type and steel fiber volume fraction is necessary. The behavior of SFRHSC changes as the binder type changes and steel fibers are very important especially when the responses are flexural strength and impact resistance since they prevent the smashing of concrete. As a result binder type and steel fiber volume fraction may interact and this interaction should be included in the design. Also the interaction between age and binder type should be considered because the binder types act differently with age and their amounts can affect this behavior. Figure 4.1 shows the linear graph used for the factor assignments. The L_{27} (3^{13}) orthogonal array and its interaction table is given in Appendix B.1 and B.2 respectively.

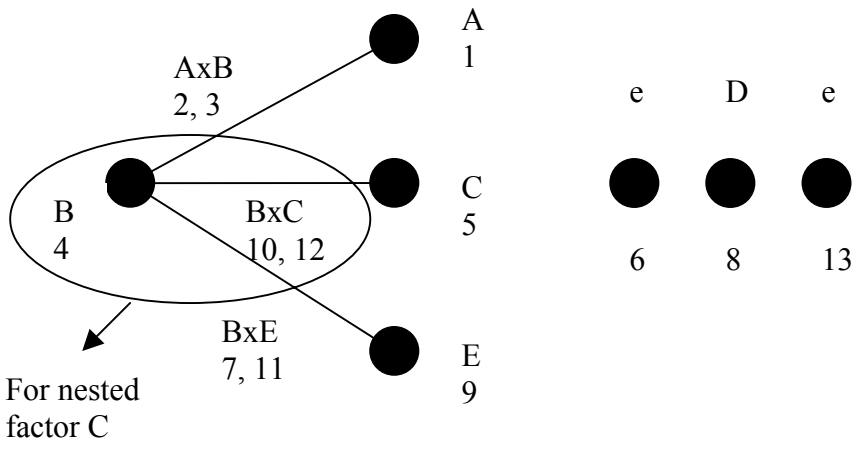

Figure 4.1 Linear graph used for assigning the main factor and two-way factor interaction effects to the orthogonal array L_{27} (3^{13})

Since three repetitions are made from each run signal to noise ratios (S/N) can effectively be calculated in order to minimize the variation in the response variables.

For all of the responses Taguchi analysis, general regression analysis and response surface analysis are performed.

4.1.1 Taguchi Analysis of the Mean Compressive Strength Based on the L_{27} (3^{13}) Design

Taguchi analysis investigates the importance of the process parameters by minimizing the variation of the response and optimizing the response separately by employing signal to noise data transformation, analysis of variance and F-test procedure. Also it employs a confirmation test to check the optimality of the offered best parameter levels.

The signal to noise ratio is calculated by using the larger-the-better criteria since our aim is to maximize the compressive strength. The S/N ratio is computed from the Mean Squared Deviation (MSD) by the equation:

$$S/N = -10 \log_{10} (MSD) \qquad MSD = \frac{1}{n}\sum_{i=1}^{n}\frac{1}{y_i^2} \qquad (4.1)$$

For S/N to be large, the MSD must have a value that is small. For larger-the-better characteristic, the inverse of each large value becomes a small value and the target is zero [20].

The results of the compressive strength experiments are shown in Table 4.1.

Table 4.1 The compressive strength experiment results developed by L_{27} (3^{13}) design

	Column numbers and factors					RESULTS				
	1	4	5	8	9					
Exp. Run	A	B	C	D	E	Run #1	Run#2	Run#3	μ (Mpa)	S/N ratio
1	-1	-1	-1	-1	-1	61,2	62,8	62,4	62,13	35,86
2	-1	-1	0	0	0	49,2	50,8	54,8	51,60	34,23
3	-1	-1	1	-1	1	67,2	69,6	70,8	69,20	36,80
4	-1	0	-1	0	1	57,2	53,2	56,8	55,73	34,91
5	-1	0	0	-1	-1	26,4	32,0	33,6	30,67	29,59
6	-1	0	1	-1	0	32,4	34,4	29,2	32,00	30,04
7	-1	1	-1	-1	0	67,6	61,2	64,8	64,53	36,17
8	-1	1	0	-1	1	54,0	53,6	51,2	52,93	34,47
9	-1	1	1	0	-1	41,6	40,0	50,0	43,87	32,72
10	0	1	-1	-1	-1	76,8	77,6	68,0	74,13	37,35
11	0	1	0	-1	0	61,2	60,0	66,0	62,40	35,88
12	0	1	1	0	1	57,6	56,8	55,2	56,53	35,04
13	0	-1	-1	-1	1	96,0	102,0	99,6	99,20	39,92
14	0	-1	0	0	-1	84,0	99,6	101,6	95,07	39,46
15	0	-1	1	-1	0	84,8	90,0	86,4	87,07	38,79
16	0	0	-1	0	0	88,0	92,0	86,0	88,67	38,95
17	0	0	0	-1	1	62,0	66,0	66,4	64,80	36,22
18	0	0	1	-1	-1	31,6	30,0	24,8	28,80	29,04
19	1	0	-1	0	-1	97,6	98,0	118,0	104,53	40,29
20	1	0	0	-1	0	82,0	74,4	74,8	77,07	37,71
21	1	0	1	-1	1	58,4	59,2	54,8	57,47	35,17
22	1	1	-1	-1	1	51,2	54,8	57,2	54,40	34,68
23	1	1	0	-1	-1	114,4	113,6	106,0	111,33	40,92
24	1	1	1	0	0	86,0	84,8	89,2	86,67	38,75
25	1	-1	-1	-1	0	118,8	112,0	122,4	117,73	41,40
26	1	-1	0	0	1	110,0	113,2	104,0	109,07	40,74
27	1	-1	1	-1	-1	76,4	90,0	82,0	82,80	38,30

If the results of the first experiment are used as an example for the computation then the S/N ratio becomes:

Results are: 61.20, 62.80, 62.40

$$MSD = \frac{1}{3}\left(\frac{1}{61.20^2}+\frac{1}{62.80^2}+\frac{1}{62.40^2}\right) \quad \Rightarrow \quad MSD = 0.000259$$

$$S/N = -10\ Log_{10}\ (0.000259) \quad \Rightarrow \quad S/N = 35.86$$

ANOVA for both of the mean compressive strength and the S/N ratio values are done by using the statistical software MINITAB. The ANOVA table for the mean compressive strength can be seen in Table 4.2. It indicates that only Age (A), Binder Type (B), Binder Amount (C(B)) and Curing Type (D) main factors significantly affect the compressive strength of the fiber reinforced high strength concrete since their F-ratio are greater than the tabulated F-ratio values of 95% confidence level. Also the Binder Type*Steel Fiber Volume Fraction (BE) interaction term can be accepted as significant with a 87% confidence. The insignificance of AB interaction can also be seen from the two-way interaction plot given in Figure 4.2. x-axis of each column and y-axis of each row represents the levels of the related factor. Each different line corresponds to the different levels of the second parameter. As it can be seen from the AB interaction plot, there is no interaction between A and B since the three lines are almost parallel. However, the BE plot indicates a strong interaction between 0.0 and 0.5% of steel fiber volume fraction and binder type because of the nonparallelizm of the lines and a very slight interaction for steel fiber volume fractions higher than 0.5%.

Table 4.2 ANOVA table for the mean compressive strength based on L_{27} (3^{13}) design

Source	df	Sum of Squares	Mean Square	F	P
A	2	6407,48	3203,74	40,22	0,001
B	2	3230,65	1615,33	20,28	0,004
C (B)	6	3445,66	574,28	7,21	0,023
D	1	1183,48	1183,48	14,86	0,012
E	2	251,64	125,82	1,58	0,294
AB	4	393,88	98,47	1,24	0,402
BE	4	953,54	238,39	2,99	0,130
Error	5	398,31	79,66		
TOTAL	26	16264,65			

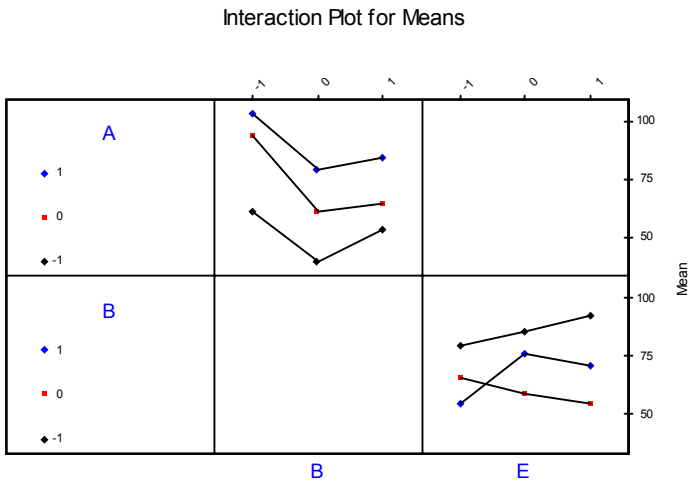

Figure 4.2 Two-way interaction plots for the mean compressive strength

The residual plots of the model for the mean compressive strength are given in Figures 4.3 and 4.4.

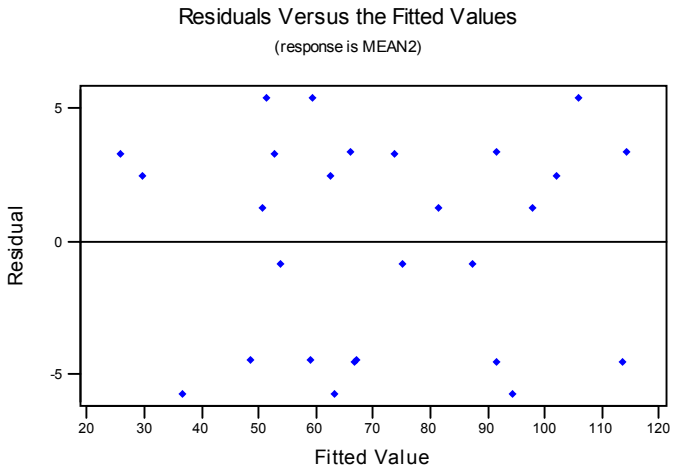

Figure 4.3 The residuals versus fitted values of the L_{27} (3^{13}) model found by ANOVA for the mean compressive strength

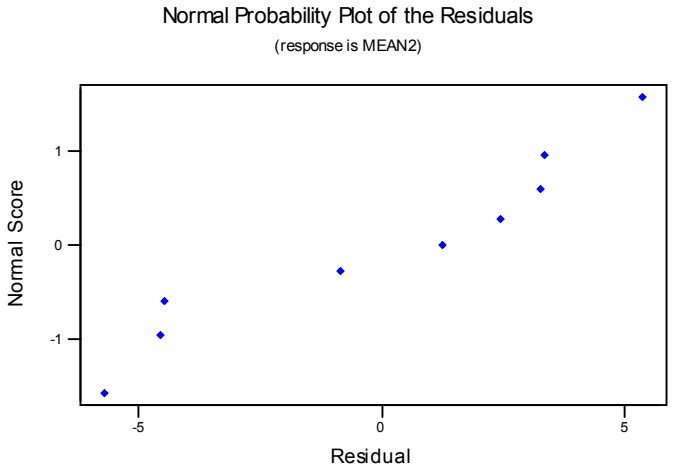

Figure 4.4 The residual normal probability plot for the L_{27} (3^{13}) model found by ANOVA for the mean compressive strength

It can be concluded from Figure 4.3 that the assumption of having a constant variance of the error term for all levels of the independent process parameters is not violated since there is no significant pattern. Also it can be seen from Figure

4.4 that there is a linear trend on the normal probability plot indicating that the assumption of the error term having a normal probability distribution is satisfied.

As ANOVA shows that the main factor E with AB interaction term are not significant within the experimental region, a new ANOVA is performed by pooling these terms to the error which is given in Table 4.3. Although the main factor E is insignificant, it can not be pooled because of the significance of the BE interaction term.

Table 4.3 Pooled ANOVA of the mean compressive strength based on $L_{27}(3^{13})$ design

Source	df	Sum of Squares	Mean Square	F	P
A	2	6407,48	3203,74	36,40	0,000
B	2	3230,65	1615,33	18,35	0,001
C (B)	6	3445,66	574,28	6,52	0,007
D	1	1183,48	1183,48	13,45	0,005
E	2	251,64	125,82	1,43	0,289
BE	4	953,54	238,39	2,71	0,099
Error	9	792,19	88,02		
TOTAL	26	16264,65			

The results show that with $\alpha = 0.05$ significance, all the main terms except steel fiber volume fraction, are significant and with $\alpha = 0.10$ significance the interaction term BE is significant on the compressive strength.

The residual plots of this new model for the mean compressive strength are given in Figures 4.5 and 4.6.

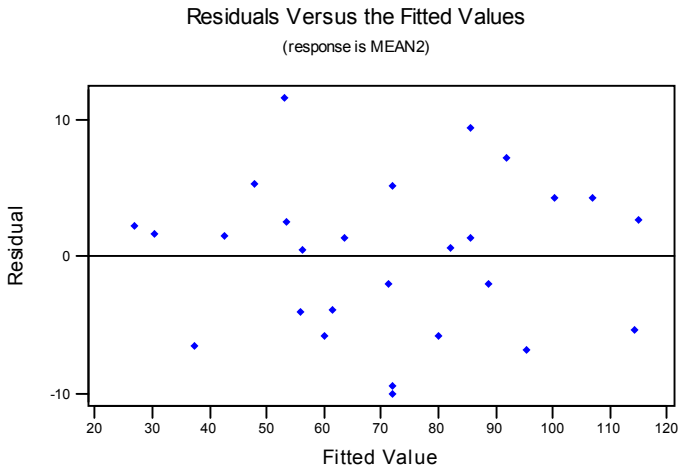

Figure 4.5 The residuals versus fitted values of the $L_{27}(3^{13})$ model found by the pooled ANOVA for the mean compressive strength

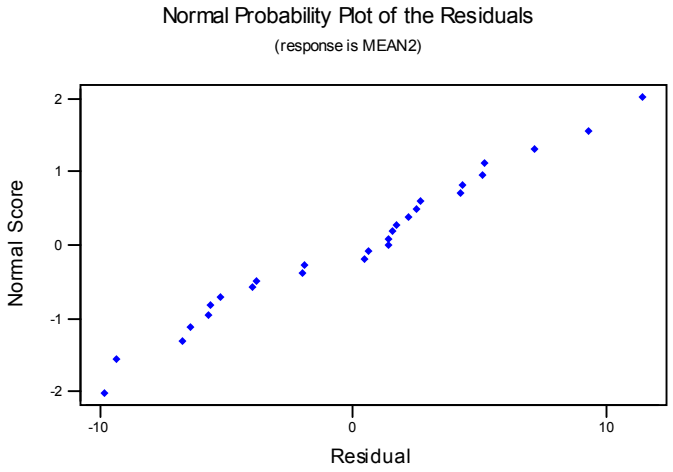

Figure 4.6 The residual normal probability plot for the $L_{27}(3^{13})$ model found by the pooled ANOVA for the mean compressive strength

When the insignificant terms are pooled in the error, the residual normal probability plot became better than the residual normal probability plot of the

unpooled model. Therefore this pooled model is kept as the best model. Therefore the prediction equation will be calculated only for the pooled model.

Figure 4.7 shows the main effects plot which is used for finding the optimum levels of the process parameters that increase the mean compressive strength.

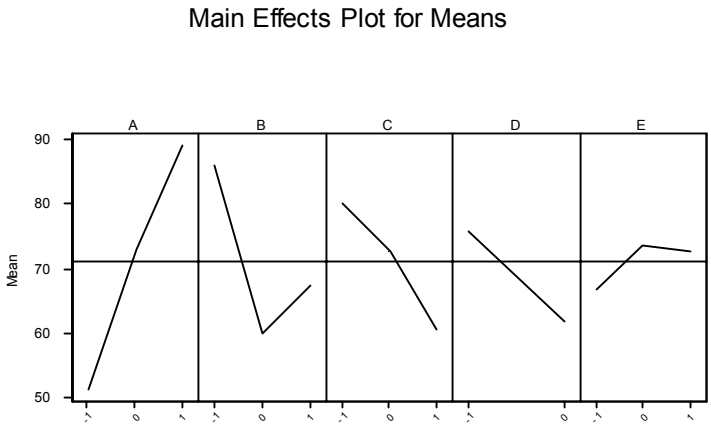

Figure 4.7 Main effects plot based on the L_{27} (3^{13}) design for the mean compressive strength

As it can be seen from Figure 4.7, the optimum points for the significant main factors are 3rd level for Age (90 days), 1st level for the Binder Type (Silica Fume), 1st level for the Binder Amount (20% as silica fume is selected for the binder type) and 1st level for Curing Type (water curing). Also it is needed to consider the significant two-way factor interactions when determining the optimum condition. From the interaction plot it can be seen that the optimum level for the interaction term are $B_{-1}xE_1$ which coincides with the optimum level of the main effect B. Although the main factor E is insignificant, it would be better to include it in the prediction equation because it should be used in the experiments. Therefore from the main effects plot (Figure 4.7) the level of

factor E that yields the highest compressive strength is the 2nd level for the Steel Fiber Volume Fraction (0.5%). But from the interaction plot it was decided that the 3rd level of factor E yields the highest compressive strength for the interaction term BE. So, the two optimum points should be calculated. The notations for optimum points are $A_1B_{-1}C_{-1}D_{-1}E_1$ for combination 1 and $A_1B_{-1}C_{-1}D_{-1}E_0$ for combination 2. The optimum performance is calculated by using the following expressions:

Combination 1: $A_1B_{-1}C_{-1}D_{-1}E_1$

$$\hat{\mu}_{A_1B_{-1}C_{-1}D_{-1}E_1} = \overline{T} + (\overline{A}_1 - \overline{T}) + (\overline{B}_{-1} - \overline{T}) + (\overline{C}_{-1} - \overline{T}) + (\overline{D}_{-1} - \overline{T}) + (\overline{E}_1 - \overline{T}) + (\overline{B_{-1} \times E_1} - \overline{T}) \quad (4.2)$$

Since $$\overline{B_{-1} \times E_1} = \left(\overline{B_{-1}E_1} - \overline{T}\right) - (\overline{B}_{-1} - \overline{T}) - (\overline{E}_1 - \overline{T}) \quad (4.3)$$

where:

$\overline{T}$ = overall average

$\overline{A}_1$ = average of the third level of process parameter A, age

$\overline{B}_{-1}$ = average of the first level of process parameter B, binder type

$\overline{C}_{-1}$ = average of the first level of process parameter C, binder amount

$\overline{D}_{-1}$ = average of the first level of process parameter D, curing type

$\overline{E}_1$ = average of the third level of process parameter E, steel fiber vol.

$\overline{B_{-1} \times E_1}$ = average of the 1st level and 3rd level interaction effect BxE

$\overline{B_{-1}E_1}$ = average of the 3rd and 1st level combinations of interaction effect BxE

When the interaction term is computed as stated in Equation 4.3 [18], the process estimate equation becomes:

$$\hat{\mu}_{A_1B_{-1}C_{-1}D_{-1}E_1} = \overline{T} + (\overline{A}_1 - \overline{T}) + (\overline{C}_{-1} - \overline{T}) + (\overline{D}_{-1} - \overline{T}) + (\overline{B_{-1}E_1} - \overline{T})$$

$$\hat{\mu}_{A_1B_{-1}C_{-1}D_{-1}E_1} = 71.13 + (89.01 - 71.13) + (80.12 - 71.13) + (75.81 - 71.13) + (92.49 - 71.13)$$

$$= 124.04 \text{ MPa}$$

The confidence interval is calculated from:

$$C.I. = \pm\sqrt{\frac{F_{\alpha,1,df_e} \times V_e}{n_e}} \qquad (4.4)$$

where:

$F_{\alpha,1,df_e}$ = tabulated F-value for 1-α (α = 0.95) confidence level with 1 and df_e degrees of freedom of error

V_e = variance of the error term

n_e = effective number of replications

$$= \frac{\text{total number of data}}{\text{df of all factors used in the estimate} + 1 \text{ df for mean}}$$

$$n_e = \frac{27}{16.5 + 1} = 1.54$$

$V_e = 88.02$

$F_{0.05,1,9} = 5.12$

$$C.I. = \sqrt{\frac{5.12 \times 88.02}{1.54}} = 17.11$$

When a dummy treated level is selected as the optimum level (water curing in this case), the effective degrees of freedom of the factor are used to determine n_e. The effective degrees of freedom of a factor whose dummy treated level is selected as the optimum, such as D_{-1} would be [18]:

$$\text{Effective degrees of freedom} = \frac{(\text{No. of levels before dummy treatment})}{(\text{No. of replications in dummy treated level})} - 1 \tag{4.5}$$

$$= \frac{3}{2} - 1 = 0.5$$

So the degrees of freedom used in the calculation of n_e become 16.5 + 1.

Therefore, the value of the mean compressive strength is expected in between;

$\hat{\mu}_{A_1B_{-1}C_{-1}D_{-1}E_1}$ = {106.93, 141.15} with 95% confidence interval.

Combination 2: $A_1B_{-1}C_{-1}D_{-1}E_0$

$$\hat{\mu}_{A_1B_{-1}C_{-1}D_{-1}E_0} = \overline{T} + (\overline{A}_1 - \overline{T}) + (\overline{B}_{-1} - \overline{T}) + (\overline{C}_{-1} - \overline{T}) + (\overline{D}_{-1} - \overline{T}) + (\overline{E}_0 - \overline{T}) + (\overline{B_{-1} \times E_0} - \overline{T}) \tag{4.6}$$

$$\hat{\mu}_{A_1B_{-1}C_{-1}D_{-1}E_0} = \overline{T} + (\overline{A}_1 - \overline{T}) + (\overline{C}_{-1} - \overline{T}) + (\overline{D}_{-1} - \overline{T}) + (\overline{B_{-1}E_0} - \overline{T})$$

$\hat{\mu}_{A_1B_{-1}C_{-1}D_{-1}E_0}$ = 71.13 + (89.09 – 71.13) + (80.12 – 71.13) + (75.81 – 71.13) + (85.47 – 71.13)

= 117.10 MPa

The confidence interval is the same as above which is 17.11. Therefore, the value of the mean compressive strength is expected in between;

$\hat{\mu}_{A_1B_{-1}C_{-1}D_{-1}E_0}$ = {99.99, 134.21} with 95% confidence interval.

Since the result of combination 1 gives higher compressive strength than combination 2, $A_1B_{-1}C_{-1}D_{-1}E_1$ is selected as the optimum setting for which the

confirmation experiment's results are expected to be between {106.93, 141.15} with 95% confidence.

In order to minimize the variation in the compressive strength, ANOVA for the S/N ratio values are performed (Table 4.4). The results of the ANOVA show that from the main factors A, B, C(B) and D and from the interaction factors only BE are significant on the S/N ratio of the compressive strength with 95% confidence. Figure 4.8 shows all the two-way factor interaction plots. As it can be seen from the figure that the three lines of AB seems almost parallel and does not contribute to the response. Whereas the contribution of BE is larger since the lines in the corresponding plots are intersecting each other. Also in the ANOVA table, the relatively small p-values of BE interaction support this.

Table 4.4 ANOVA of S/N ratio values of the compressive strength based on L_{27} (3^{13}) design

Source	df	Sum of Squares	Mean Square	F	P
A	2	104,901	52,450	48,74	0,001
B	2	63,203	31,602	29,37	0,002
C (B)	6	71,911	11,985	11,14	0,009
D	1	18,030	18,030	16,76	0,009
E	2	2,932	1,466	1,36	0,337
AB	4	8,307	2,077	1,93	0,244
BE	4	22,583	5,646	5,25	0,049
Error	5	5,381	1,076		
TOTAL	26	297,248			

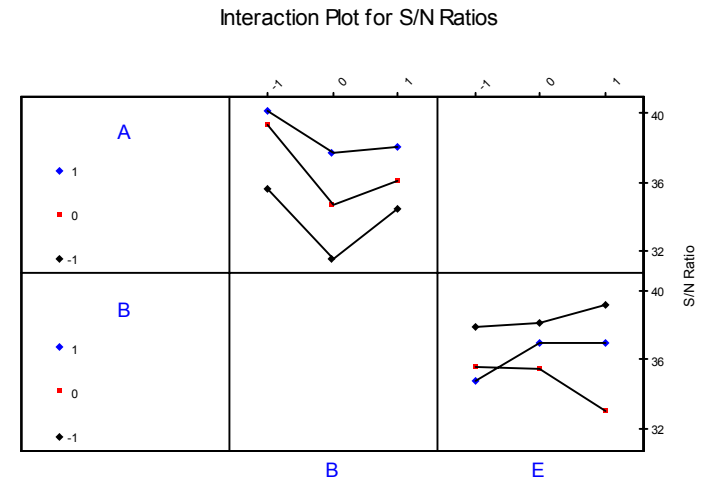

Figure 4.8 Two-way interaction plots for the S/N values of compressive strength

The residual plots for S/N ratio can be seen in Figures 4.9 and 4.10.

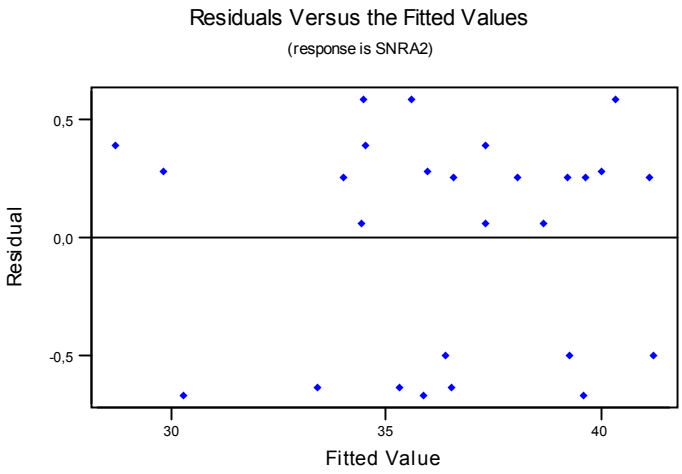

Figure 4.9 The residuals versus fitted values of the L_{27} (3^{13}) model found by ANOVA for S/N ratio for compressive strength

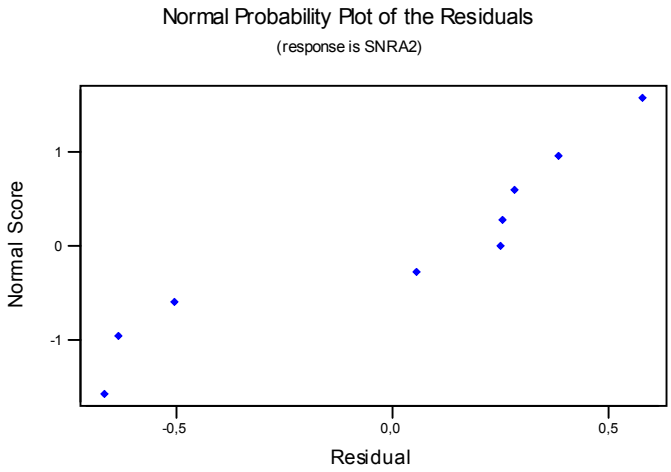

Figure 4.10 The residual normal probability plot for the L_{27} (3^{13}) model found by ANOVA for S/N ratio for compressive strength

In both figures it can be seen that the residual assumptions are violated. Figure 4.10 is not linear showing that the assumption of the normal distribution of the error terms is not satisfied and since the middle part of Figure 4.9 is empty, it can be said that the constant variance assumption of the errors is violated.

As ANOVA shows that the main factor E with AB interaction term does not significantly contribute to the response. However, factor E can not be pooled because of the significance of the BE interaction term. Therefore a new ANOVA is performed by pooling only AB to the error which is given in Table 4.5.

Table 4.5 Pooled ANOVA of the S/N values for the compressive strength based on L_{27} (3^{13}) design

Source	df	Sum of Squares	Mean Square	F	P
A	2	104,901	52,450	34,49	0,000
B	2	63,203	31,602	20,78	0,000
C (B)	6	71,911	11,985	7,88	0,004
D	1	18,030	18,030	11,86	0,007
E	2	2,932	1,466	0,96	0,418
BE	4	22,583	5,646	3,71	0,047
Error	9	13,688	1,521		
TOTAL	26	297,248			

In this model again all the terms except the main factor E are significant with 95% confidence on the response. The residual plots can be seen in Figures 4.11 and 4.12. By this model both residual plots are improved. As a result it can be concluded that the error term of the pooled model is distributed normally with a constant variance. The pooled model seems more adequate than the unpooled model. So the prediction equation for S/N values will be calculated only for the pooled model.

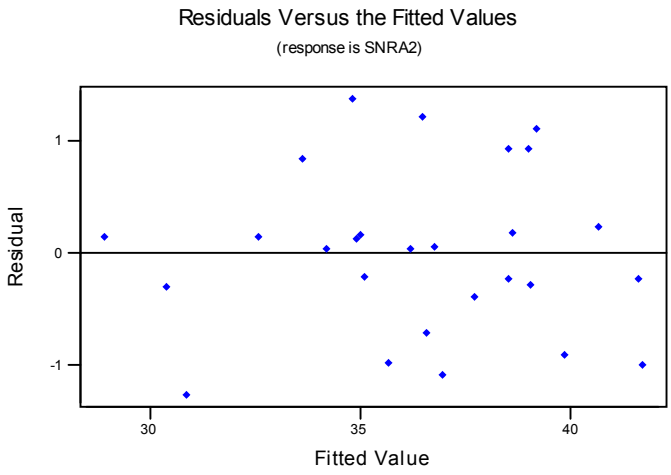

Figure 4.11 The residuals versus fitted values of the L_{27} (3^{13}) model found by the pooled ANOVA for the S/N ratio of compressive strength

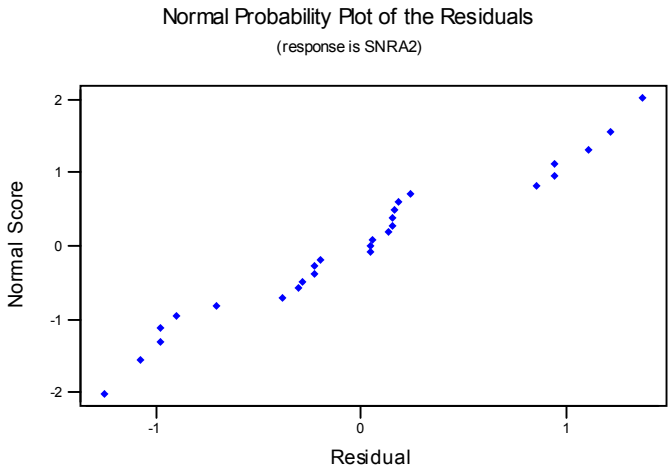

Figure 4.12 The residual normal probability plot for the L_{27} (3^{13}) model found by the pooled ANOVA for the S/N ratio of compressive strength

From the main effects plot (Figure 4.13), the optimum points are 3rd level for Age (90 days), 1st level for Binder Type (silica fume), 1st level for Binder Amount (20%), 1st level for Curing Type (water curing) and 2nd level for Steel Fiber Volume Fraction (0.5% vol.). Although factor E is insignificant, it should be included in the prediction equation because without it the experiments can not be conducted. From the interaction plot it is concluded that the best levels for BE interaction are 1st level for binder type and 3rd level for steel fiber volume fraction. However from the main plot the 2nd level of steel fiber volume fraction was found to be the best level maximizing the S/N ratio. As a result, the two different combinations should be computed for determining the optimum point.

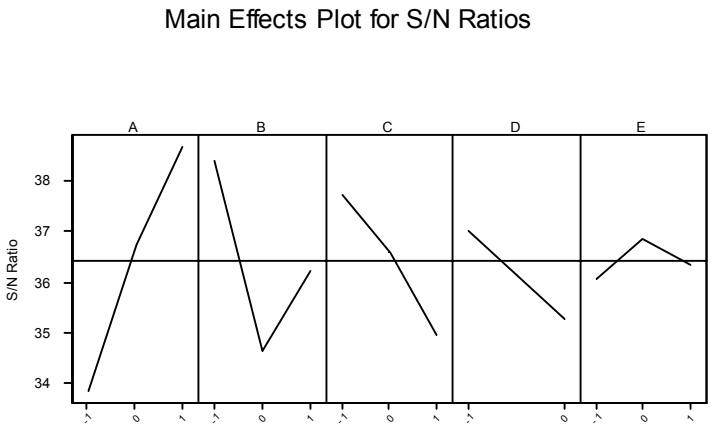

Figure 4.13 Main effects plot based on the L_{27} (3^{13}) design for S/N ratio for compressive strength

Combination 1: $A_1B_{-1}C_{-1}D_{-1}E_1$

$$\eta = \overline{T} + (\overline{A}_1 - \overline{T}) + (\overline{B}_{-1} - \overline{T}) + (\overline{C}_{-1} - \overline{T}) + (\overline{D}_{-1} - \overline{T}) + (\overline{E}_1 - \overline{T}) + (\overline{B_{-1} \times E_1} - \overline{T}) \quad (4.7)$$

$$\eta = \overline{T} + (\overline{A}_1 - \overline{T}) + (\overline{C}_{-1} - \overline{T}) - (\overline{D}_{-1} - \overline{T}) + (\overline{B_{-1}E_1} - \overline{T})$$

η = 36.42 + (38.66 – 36.42) + (37.73 – 36.42) – (37.00 – 36.42) + (39.15 - 36.42)

= 43.28

$$n_e = \frac{27}{16.5+1} = 1.54$$

$V_e = 1.521$

$F_{0.05,1,9} = 5.12$

$$C.I. = \sqrt{\frac{5.12 \times 1.521}{1.54}} = 2.25$$

As a result the value for the S/N ratio should fall in between:

η = {41.03, 45.53} with 95% confidence.

Combination 2: $A_1B_{-1}C_{-1}D_{-1}E_0$

$$\eta = \overline{T} + (\overline{A}_1 - \overline{T}) + (\overline{B}_{-1} - \overline{T}) + (\overline{C}_{-1} - \overline{T}) + (\overline{D}_{-1} - \overline{T}) + (\overline{E}_0 - \overline{T}) + (\overline{B_{-1} \times E_0} - \overline{T}) \quad (4.8)$$

$$\eta = \overline{T} + (\overline{A}_1 - \overline{T}) + (\overline{C}_{-1} - \overline{T}) - (\overline{D}_{-1} - \overline{T}) + (\overline{B_{-1}E_0} - \overline{T})$$

η = 36.42 + (38.66 – 36.42) + (37.73 – 36.42) – (37.00 – 36.42) + (38.14 – 36.42)

= 42.27

The value of the confidence interval is the same for all combinations which is calculated above as 2.25. As a result, the value for the S/N ratio should fall in between:

η = {40.02, 44.52} with 95% confidence.

From the two combinations the first one is chosen as the optimal level since its S/N ratio is larger than the others. It is less sensitive to the uncontrollable noise factors. Therefore, the best point selected is $A_1B_{-1}C_{-1}D_{-1}E_1$ combination resulting in the highest mean compressive strength (124.04 MPa) and the highest S/N value (43.28).

The confirmation experiment is performed for $A_1B_{-1}C_{-1}D_{-1}E_1$ combination three times. The results of the confirmation experiment yield the values of 136.00 MPa, 128.00 MPa and 121.60 MPa with an S/N ratio of 42.15, which are in the

prediction intervals. These results lead to the confirmation of the optimum setting $A_1B_{-1}C_{-1}D_{-1}E_1$ found by using the Taguchi method.

4.1.2 Regression Analysis of the Mean Compressive Strength Based on the L_{27} (3^{13}) Design

In order to model the mean compressive strength with general linear regression MINITAB software is used. The general regression equation used in this study is:

$$y = \beta_0 + \sum_{j=1}^{k} \beta_j x_j + \sum_{j=1}^{k} \sum_{i=1}^{k} \beta_{ji} x_j x_i + \sum_{j=1}^{k} \beta_{jj} x_j^2 + \varepsilon \qquad (4.9)$$

where:

y = the response

x = regressor variables (parameters)

β = regression coefficients determined by the least squares method

ε = normally distributed error term with a mean of 0 and constant variance of σ^2

Besides the main factor terms, these equations involve both interaction and square terms.

The binder type (B) and curing type (D) main factors are qualitative independent variables, so, a quantitative meaning to their given levels can not be attached. All that can be done is to describe them. As a result dummy (indicator) variables should be defined for these two main factors. Since factor B has three levels, it can only be described by two dummy variables, namely B_1 and B_2, and since factor D has two levels, it can be described by a single dummy variable D_1.

$$B_1 = \begin{cases} 1 \; if \; Fly \; Ash \; is \; used \\ 0 \; if \; not \end{cases} \qquad B_2 = \begin{cases} 1 \; if \; GGBFS \; is \; used \\ 0 \; if \; not \end{cases}$$

$$D_1 = \begin{Bmatrix} 1\, if\ steam\ curing\ is\ used \\ 0\, if\ not \end{Bmatrix}$$

The first employed regression analysis to model the mean compressive strength contains only the main factors. That is:

$$y = 90{,}4 + 18{,}6*A - 25{,}7*B_1 - 18{,}2*B_2 - 9{,}98*C - 14{,}4*D_1 + 3{,}03*E \qquad (4.10)$$

Table 4.6 shows the ANOVA for the significance of the above regression model. The hypothesis of having all β terms equal to zero is tested and refused with a confidence level of (1 – p)*100%, which is 99.9% for this model.

Table 4.6 ANOVA for the significance of the regression model developed for the mean compressive strength based on $L_{27}(3^{13})$ design

Source	df	Sum of Squares	Mean Squares	F	P
Regression	6	12663,6	2110,6	11,72	0,000
Residual Error	20	3601,0	180,1		
Total	26	16264,7			

$R^2 = 77.9\%$ $R^2_{(adj)} = 71.2\%$ $S = 13.42$

Durbin-Watson statistic = 2.07

The adjusted multiple coefficient of determination, $R^2_{(adj)}$, shows that 71.2% of the sample variation in the mean compressive strength can be explained by this model. The Durbin-Watson statistic states that there is not any indication of the presence of residual correlation because, the Durbin-Watson statistic is above the tabulated upper bound (d_U), which is 1.86 with 5 independent variables and 27 observations with 95% confidence.

The residual plots of this model are given in Figures 4.14 and 4.15. Although it is concluded from the residual plots that there is not any indication of violation of the assumptions of the error, a more adequate regression model will be searched to describe the mean compressive strength. The significance of β terms of the model is shown in Table 4.7. This table indicates that except the Curing Type, Steel Fiber Volume Fraction and B_2 dummy variable for Binder Type main effects, all the main factors are significant at the p(0.05) level of significance.

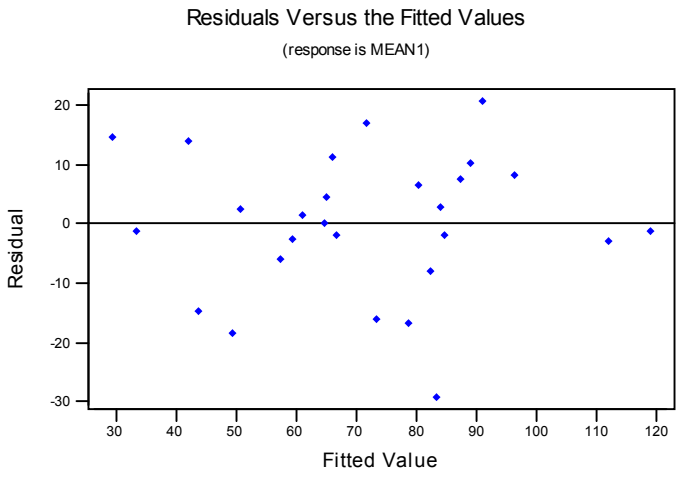

Figure 4.14 Residuals versus fitted values plot of the regression model based on L_{27} (3^{13}) design and developed for the mean compressive strength with only main factors

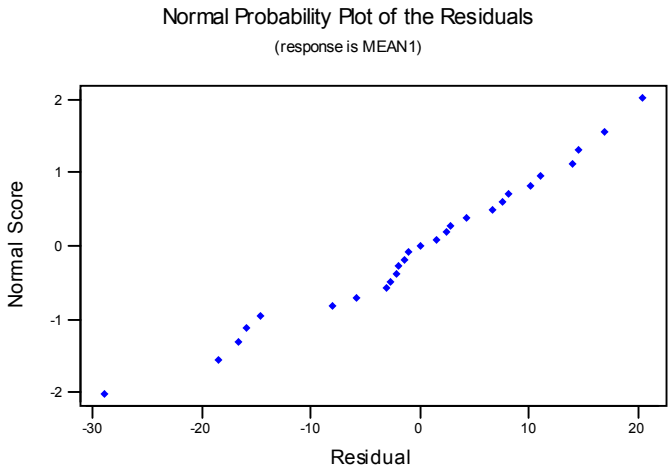

Figure 4.15 Residual normal probability plot of the regression model based on L_{27} (3^{13}) design and developed for the mean compressive strength with only main factors

Table 4.7 Significance of β terms of the regression model based on L_{27} (3^{13}) design and developed for the mean compressive strength with only main factors

Predictor	β Estimate	Standard Error	T	P
Constant	90,442	4,837	18,70	0,000
A	18,632	3,168	5,88	0,000
B_1	-25,678	6,336	-4,05	0,001
B_2	-18,226	6,336	-2,88	0,009
C	-9,983	3,168	-3,15	0,005
D_1	-14,381	5,490	-2,62	0,016
E	3,033	3,283	0,92	0,367

The MINITAB output with the sequential sum of squares of the regression model can be seen in Appendix B.3.

The second regression model is decided to include all the two-way interaction terms. There are three stages in writing the prediction equation that contains all

the two-way interaction and squared terms when there are both quantitative and qualitative variables in the model. These are [21]:

Stage 1. Write the second order model corresponding to the three quantitative independent variables.

$$y = \beta_0 + \beta_1 A + \beta_2 C + \beta_3 E + \beta_4 A^2 + \beta_5 C^2 + \beta_6 E^2 + \beta_7 AC + \beta_8 AE + \beta_9 CE$$

Stage 2. Add the main effect and interaction terms for the qualitative independent variables.

$$+ \beta_{10} B_1 + \beta_{11} B_2 + \beta_{12} D_1 + \beta_{13} B_1D_1 + \beta_{14} B_2D_1$$

Stage 3. Add terms that allow for interaction between the quantitative and qualitative independent variables.

$$+ \beta_{15} AB_1 + \beta_{16} CB_1 + \beta_{17} EB_1 + \beta_{18} A^2B_1 + \beta_{19} C^2B_1 + \beta_{20} E^2B_1 + \beta_{21} ACB_1 + \beta_{22} AEB_1 + \beta_{23} CEB_1 + \ldots\ldots + \beta_{51} AB_2D_1 + \beta_{52} CB_2D_1 + \beta_{53} EB_2D_1 + \beta_{54} A^2B_2D_1 + \beta_{55} C^2B_2D_1 + \beta_{56} C^2B_2D_1 + \beta_{57} ACB_2D_1 + \beta_{58} AEB_2D_1 + \beta_{59} CEB_2D_1$$

Because the experimental design has only 26 degrees of freedom, all of the above variables can not be included in the model since they exceed the 26 degrees of freedom. The squared terms are not included in the design. Therefore a pre-analysis is performed and it is seen that all the interactions with D_1 variable are insignificant. As a result they are omitted form the model. The equation and the ANOVA table for the regression model can be seen in Eqn. 4.11 and Table 4.8 respectively. By this model with 97.4% confidence the hypothesis that all β terms are equal to zero is rejected.

$$y = 98,5 + 17,2*A - 36,6*B_1 - 17,6*B_2 - 9,33*C - 29,7*D_1 + 5,47*E + 6,2*AC - 13,1*AE - 15,6*CE + 23,9*B_1D_1 - 10,6*B_2D_1 + 2,94*AB_1 - 12,4*CB_1 - 11,1*EB_1 - 8,2*ACB_1 + 17,8*AEB_1 + 15,7*CEB_1 + 1,94*AB_2 + 4,7*CB_2 + 16,4*EB_2 - 33,3*ACB_2 + 20,4*AEB_2 + 7,8*CEB_2 \quad (4.11)$$

Table 4.8 ANOVA for the significance of the regression model developed for the mean compressive strength based on L_{27} (3^{13}) design including main and interaction factors

Source	df	Sum of Squares	Mean Squares	F	P
Regression	23	15903,30	691,40	5,74	0,087
Residual Error	3	361,30	120,40		
Total	26	16264,70			

$R^2 = 97.8\%$ $R^2_{(adj)} = 80.7\%$ $S = 10.97$

Durbin-Watson statistic = 2.11

By this model a considerable improvement is achieved when compared with the previous one. The standard deviation of the error (S) is decreased from 16.75 to 10.97, the $R^2_{(adj)}$ value is raised from 77.9% to 80.7% explaining the 81% of the sample variation in the mean compressive strength. However the Durbin-Watson statistic is increased to 2.11 but still it shows that the residuals are uncorrelated. But the slight difference between R^2 and $R^2_{(adj)}$ value means that there are some unnecessary terms in the model.

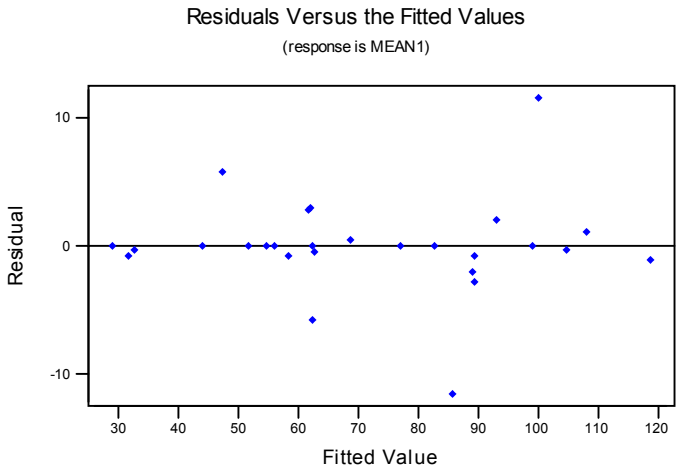

Figure 4.16 Residuals versus fitted values plot of the regression model in Eqn.4.11 developed for the mean compressive strength

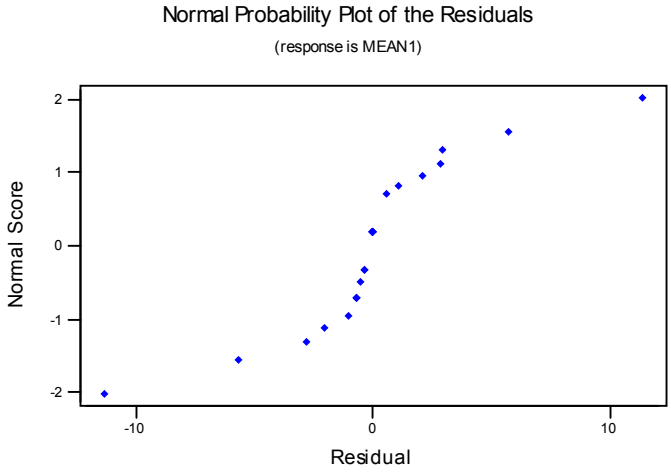

Figure 4.17 Residual normal probability plot of the regression model in Eqn.4.11 developed for the mean compressive strength

Although the residuals versus fitted values and the normal probability plot are not very good, it can be said that the error term has normal distribution with constant variance. The mid portion of Figure 4.17 can be accepted as linear.

However a better model explaining the mean response can be searched. Table 4.9 shows the significance of the β terms.

Table 4.9 Significance of β terms of the regression model in Eqn.4.11 developed for the mean compressive strength

Predictor	β Estimate	Standard Error	T	P
Constant	98,467	7,760	12,69	0,001
A	017,167	6,053	2,84	0,066
B_1	-36,566	9,046	-4,04	0,027
B_2	-17,620	10,970	-1,61	0,207
C	-9,330	7,381	-1,26	0,296
D_1	-29,700	16,040	-1,85	0,161
E	5,470	7,381	0,74	0,512
AC	6,200	14,040	0,44	0,689
AE	-13,070	15,220	-0,86	0,454
CE	-15,630	10,810	-1,45	0,244
B_1D_1	23,910	18,210	1,31	0,281
B_2D_1	-10,570	26,060	-0,41	0,712
AB_1	2,944	7,531	0,39	0,722
CB_1	-12,448	8,635	-1,44	0,245
EB_1	-11,092	8,635	-1,28	0,289
ACB_1	-8,240	15,610	-0,53	0,634
AEB_1	17,850	16,670	1,07	0,363
CEB_1	15,720	12,780	1,23	0,306
AB_2	1,944	9,546	0,20	0,852
CB_2	4,660	10,440	0,45	0,685
EB_2	16,350	11,610	1,41	0,254
ACB_2	-33,260	20,930	-1,59	0,210
AEB_2	20,410	19,220	1,06	0,366
CEB_2	7,770	15,960	0,49	0,660

The MINITAB output with the sequential sequential sum of squares of the regression model can be seen in Appendix B.4.

It can be seen from the small p-values that, only the factors A, B_1 and D_1 are significant on the mean compressive strength. The model can be improved by discarding the insignificant terms from the model one by one starting from the term having the largest p-value. After eliminating a factor, all the normality, constant variance and error correlation assumptions are checked and the best model is chosen.

The best model is achieved by pooling AB_2, AB_1, CEB_2, ACB_1 and CB_2 terms in the model to the error term. This model is much more adequate for explaining the mean compressive strength of SFRHSC whose regression equation, ANOVA table, residual plots and β significance test are given in Eqn.4.12, Table 4.10, Figures 4.18 and 4.19, and Table 4.11 respectively.

$$y = 94,5 + 19,6*A - 32,6*B_1 - 14,6*B_2 - 6,99*C - 20,8*D_1 + 2,87*E - 1,01*AC - 7,08*AE - 10,4*CE + 14,8*B_1D_1 - 16,7*B_2D_1 - 14,8*CB_1 - 8,49*EB_1 + 12,2*AEB_1 + 10,2*CEB_1 + 19,0*EB_2 - 26,1*ACB_2 + 17,5*AEB_2 \quad (4.12)$$

Table 4.10 ANOVA for the significance of the best regression model developed for the mean compressive strength based on the $L_{27}(3^{13})$ design

Source	df	Sum of Squares	Mean Squares	F	P
Regression	18	15819,75	878,88	15,80	0,000
Residual Error	8	444,90	55,61		
Total	26	16264,65			

$R^2 = 97.3\%$ $R^2_{(adj)} = 91.1\%$ $S = 7.457$

Durbin-Watson statistic = 1.84

Although R^2 is decreased from 97.8% to 97.3%, $R^2_{(adj)}$ is raised from 80.7% to 91.1% which is enough to explain the response. Also, R^2 and adjusted R^2 gets closer to each other meaning that there is not any indication of unnecessary

terms in the model. The Durbin-Watson statistic decreased to 1.84 stating that there is not enough information to reach any conclusion about the presence of residual correlation. Because, the Durbin-Watson statistic is in between the tabulated lower bound (d_L), which is 1.01 and upper bound (d_U), which is 1.86 with 5 independent variables and 27 observations with 95% confidence. Also Table 4.10 shows that this model has almost 100% confidence of refusing the hypothesis of having all β terms equal to zero.

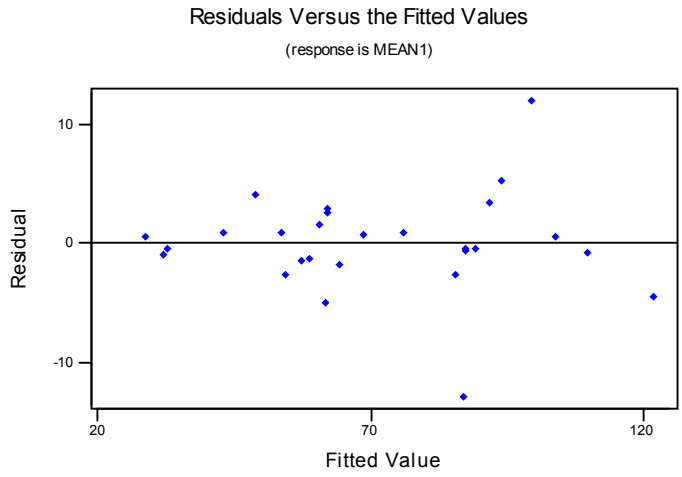

Figure 4.18 Residuals versus fitted values plot of the best regression model in Eqn.4.12 developed for the mean compressive strength

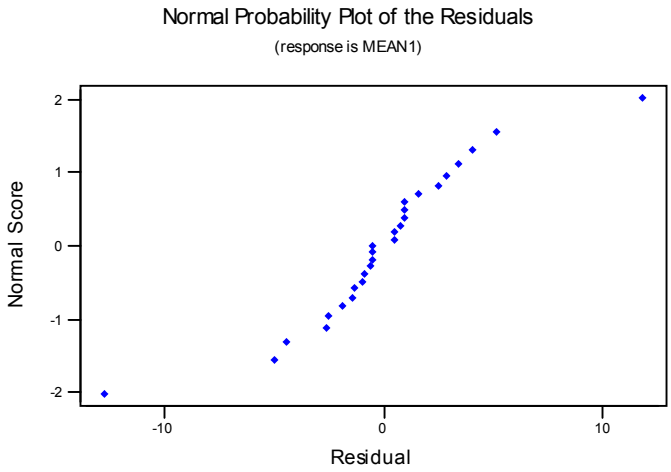

Figure 4.19 Residual normal probability plot of the best regression model in Eqn.4.12 developed for the mean compressive strength

The residuals normal probability and the residuals versus the fitted values plots are improved by this model showing no deviation from the assumptions of the error. From Figure 4.19 it can be concluded that the plot is linear and Figure 4.18 is paternless. When the β significance test is examined, the interaction factors AC, AE and CE still have slightly large p-value. But these interaction factors can not be pooled into the error term because in this new model the interaction terms containing these factors such as ACB_2 and AEB_2 became significant on the response.

Table 4.11 Significance of β terms of the best regression model in Eqn.4.12 developed for the mean compressive strength

Predictor	β Estimate	Standard Error	T	P
Constant	94,529	3,723	25,39	0,000
A	19,613	1,828	10,73	0,000
B_1	-32,559	4,799	-6,78	0,000
B_2	-14,624	6,345	-2,30	0,050
C	-6,988	2,792	-2,50	0,037
D_1	-20,756	6,835	-3,04	0,016
E	2,871	3,948	0,73	0,488
AC	-1,009	4,044	-0,25	0,809
AE	-7,076	6,125	-1,16	0,281
CE	-10,420	3,568	-2,92	0,019
B_1D_1	14,758	8,665	1,70	0,127
B_2D_1	-16,690	14,730	-1,13	0,290
CB_1	-14,790	4,131	-3,58	0,007
EB_1	-8,493	4,986	-1,70	0,127
AEB_1	12,162	8,162	1,49	0,175
CEB_1	10,201	5,680	1,80	0,109
EB_2	18,951	7,257	2,61	0,031
ACB_2	-26,060	11,300	-2,31	0,050
AEB_2	17,493	9,001	1,94	0,088

As a result this model is decided to be kept as the most adequate model explaining the mean compressive strength of the SFRHSC. The MINITAB output with the sequential sum of squares of the best regression model can be seen in Appendix B.5.

4.1.3 Response Surface Optimization of Mean Compressive Strength Based on the L_{27} (3^{13}) Design

The response optimization of the best regression model found in Eqn.4.12 in the previous section for the mean compressive strength is done by using the MINITAB Response Optimizer. Since the aim of this study is to maximize all

the responses, it is needed to define a target value and a lower bound for MINITAB to calculate the optimum solution. For high strength concrete the usual compressive strengths that can be reached are in between 50 and 100 Mpa. Therefore the lower bound is set to 50 Mpa. The maximum compressive strength achieved in literature is 128 Mpa. Therefore the target value is set to 130 Mpa.

MINITAB accomplishes the optimization by obtaining an individual desirability for each response and combining the individual desirabilities to obtain the composite desirability according to the specified target value and the lower bound. The measure of composite desirability is the weighted geometric mean of the individual desirabilities for the responses. The individual desirabilities are weighted according to the importance that is assigned by the user. But in this study the response optimization of each response is done separately, because they will have different models that best explains each one of them. Therefore we have only one response in each of the optimization process, so, the overall composite desirability is equal to the individual desirability. As a result there is no need to assign an importance for the responses. Finally, MINITAB employs a reduced gradient algorithm with multiple starting points that maximizes the composite desirability, which equals to the individual desirability in our situation, to determine the numerical optimal solution.

Thirteen different starting points are used in the response optimization process of the mean compressive strength based on the L_{27} (3^{13}) design. The results of the optimizer can be seen in Table 4.12. The starting points and the optimum points found by MINITAB response optimizer is shown in Table 4.13.

Table 4.12 The optimum response, its desirability, the confidence and prediction intervals computed by MINITAB Response Optimizer for the mean compressive strength based on the L_{27} (3^{13}) design

Optimum Points	Mean Comp.	Desirability	95% Conf. Int.	95% Pred. Int.
1	129,338	0,99172	(109,26; 147,45)	(102,66; 154,05)
2	119,140	0,80118	(94,82; 143,45)	(89,36; 148,91)
3	109,220	0,73447	(87,33; 131,11)	(81,38; 137,05)
4	133,572	1,00000	(99,61; 167,53)	(95,50; 171,64)
5	109,940	0,73931	(94,19; 125,68)	(86,62; 133,25)
6	138,780	1,00000	(103,35; 174,22)	(99,40; 178,17)
7	74,340	0,32330	(62,26; 86,42)	(53,32; 95,36)
8	131,760	1,00000	(106,92; 156,60)	(101,55; 161,97)
9	128,350	0,94900	(109,26; 147,45)	(102,66; 154,05)
10	138,780	1,00000	(103,35; 174,22)	(99,40; 178,17)
11	129,338	0,99172	(109,26; 147,45)	(102,66; 154,05)
12	138,780	1,00000	(103,35; 174,22)	(99,40; 178,17)
13	116,060	0,83556	(93,88; 138,25)	(87,99; 144,14)

Table 4.13 The starting and optimum points for MINITAB response optimizer developed for the mean compressive strength based on the L_{27} (3^{13}) design

	Starting Points					Optimum Points				
Points	**Age (days)**	**B. Type**	**B. Amount (%)**	**Cure**	**Steel (% vol.)**	**Age (days)**	**B. Type**	**B. Amount (%)**	**Cure**	**Steel (% vol.)**
1	90	SF	20	water	1,0	90	SF	20	water	1,0
2	No starting point					28	GGBFS	20	water	1,0
3	90	SF	20	steam	0,5	90	SF	20	steam	1,0
4	90	GGBFS	20	water	0,5	90	GGBFS	20	water	0,5
5	90	SF	10	water	1,0	90	SF	15	water	1,0
6	28	FA	40	steam	0,5	90	GGBFS	20	steam	1,0
7	7	SF	20	water	0,0	16,6	SF	20	water	0,03
8	90	GGBFS	60	water	1,0	90	GGBFS	40	water	1,0
9	90	FA	10	water	1,0	90	SF	20	water	1,0
10	28	GGBFS	20	steam	1,0	90	GGBFS	20	steam	1,0
11	90	SF	15	water	1,0	90	SF	20	water	1,0
12	90	GGBFS	20	steam	1,0	90	GGBFS	20	steam	1,0
13	90	SF	20	water	0,0	90	SF	20	water	0,01

The starting points 6, 10 and 12 gave the same result which is the best one found by the Response Optimizer as 138.780 MPa compressive strength. Also the starting points 1, 9 and 11 led to the same optimum point which is the second best point. But this second best point has narrower confidence and prediction intervals than the optimum. The results of the optimum points 4 and 8 are very close to the best points' results and point 8's intervals are better, so it is worth to do a confirmation run for them. Also points 2, 3, 5 and 13 will be tried because their confidence and prediction intervals are narrower than the others. The remaining points resulted in very low compressive strength values and therefore they are not taken into consideration for the confirmation experiments. Each experiment is repeated three times for convenience.

Optimum points 6, 10 and 12:

For this point the 3rd level for Age (90 days), 3rd level for Binder Amount (Ground Granulated Blast Furnace Slag), 1st level for Binder Amount (20% for GGBFS), 2nd level for Curing Type (steam curing) and the 3rd level for Steel Fiber Volume Fraction (1.0%) are assigned to the associated main factors. The results of the experiments are 81.20 MPa, 82.80 MPa and 80.80 MPa. These results are below the lower limits of both intervals. So it can be said that this point is a little overestimated by the chosen regression model.

Optimum points 1, 9 and 11:

For this point the 3rd level for Age (90 days), 1st level for Binder Amount (Silica Fume), 1st level for Binder Amount (20% for silica fume), 1st level for Curing Type (ordinary water curing) and the 3rd level for Steel Fiber Volume Fraction (1.0%) are assigned to the associated main factors. The results of the experiments are 136.0 MPa, 128.0 MPa and 121.60 MPa and all are in both the confidence and prediction intervals with 95%. They are also very close to the predicted optimum value of 129.338 MPa. As a result we can conclude that this point is well modeled by the chosen regression model.

Optimum point 4:

For this point the 3rd level for Age (90 days), 3rd level for Binder Amount (GGBFS), 1st level for Binder Amount (20% for GGBFS), 1st level for Curing Type (ordinary water curing) and the 2nd level for Steel Fiber Volume Fraction (0.5%) are assigned to the associated main factors. The results of the experiments are 88.00 MPa, 88.00 MPa and 116.60 MPa. Only the third result falls in the confidence and prediction intervals. The others are below the lower limits of both intervals. It is concluded that this point is overestimated by the chosen regression model and therefore is not very well modeled.

Optimum point 8:

For this point the 3rd level for Age (90 days), 3rd level for Binder Amount (GGBFS), 2nd level for Binder Amount (40% for GGBFS), 1st level for Curing Type (ordinary water curing) and the 3rd level for Steel Fiber Volume Fraction (1.0%) are assigned to the associated main factors. The results of the confirmation experiments are 98.00 MPa, 96.00 MPa and 96.00 MPa. None of the results fall in the confidence and prediction intervals. They are well below the lower limits of both intervals. It is concluded that this point is overestimated by the chosen regression model and therefore is not very well modeled.

Optimum point 2:

For this point the 2nd level for Age (28 days), 3rd level for Binder Amount (GGBFS), 1st level for Binder Amount (20% for GGBFS), 1st level for Curing Type (ordinary water curing) and the 3rd level for Steel Fiber Volume Fraction (1.0%) are assigned to the associated main factors. The results of the confirmation experiments are 67.60 MPa, 61.20 MPa and 64.80 MPa. None of the results fall in the confidence and prediction intervals. They are well below the lower limits of both intervals. It is concluded that this point is overestimated by the chosen regression model and therefore is not very well modeled.

Optimum point 13:

For this point the 3rd level for Age (90 days), 1st level for Binder Amount (SF), 1st level for Binder Amount (20% for SF), 1st level for Curing Type (ordinary water curing) and the 1st level for Steel Fiber Volume Fraction (0.0%) are assigned to the associated main factors. The results of the confirmation experiments are 88.00 MPa, 94.00 MPa and 90.40 MPa. Only the second result falls in the confidence interval and the others are below the lower limit. However all of them are in the prediction interval but closer to the lower side. So it can be said that this point is not very well modeled by the chosen regression model.

Optimum point 3:

For this point the 3rd level for Age (90 days), 1st level for Binder Amount (Silica Fume), 1st level for Binder Amount (20% for SF), 2nd level for Curing Type (steam curing) and the 3rd level for Steel Fiber Volume Fraction (1.0%) are assigned to the associated main factors. The results of the experiments are 110.00 MPa, 108.40 MPa and 104.40 MPa. These results are in the limits of both intervals and they are very close to the predicted value of 109.22 MPa. This point is well modeled by the chosen regression model but the predicted optimum value for this point is lower than the demanded value of 130.00 MPa.

Optimum point 5:

For this point the 3rd level for Age (90 days), 1st level for Binder Amount (SF), 2nd level for Binder Amount (15% for SF), 1st level for Curing Type (ordinary water curing) and the 3rd level for Steel Fiber Volume Fraction (1.0%) are assigned to the associated main factors. The results of the experiments are 110.00 MPa, 113.20 MPa and 104.00 MPa. These results are well fit to the results of the Response Optimizer. They are very close to the predicted optimum value of 109.94 MPa. It is concluded that this point is very well

modeled by the chosen regression model but again the predicted value is lower than the desired 130.00 MPa compressive strength.

The best point is chosen for the result of the regression analysis of the mean compressive strength is the optimum found by points 1, 9 and 11. Although points 5's intervals are narrower, there is almost 20 MPa gap in between the compressive strengths which is a considerable amount. Also the narrowness of the intervals is very close. As a result the best parameter level combination that maximizes the compressive strength of SFRHSC is found as $A_1B_{-1}C_{-1}D_{-1}E_1$.

4.2 Full Factorial Experimental Design

In order to analyze the effects of all three-way, four-way and five-way interaction effects on all of the responses it is decided to conduct all the experiments needed for full factorial design and analysis.

Since all possible combinations of the levels of the factors are experimented, there is enough data to select a $3^4 2^1$ full factorial design and analysis for the three responses that are compressive strength, flexural strength and impact resistance. The $3^4 2^1$ full factorial design requires all possible combinations of the maximum and minimum levels of the analyzed five process parameters. It lets the analysis of all two-way, three-way, four-way and five-way factor interaction effects in addition to the main factor effects. Therefore, it needs 162 different parameter level combinations and three replicates of each experiment condition are performed in order to take the noise factors into consideration. As a result 486 experiments are conducted for each of the response variables. The average and signal to noise ratio of the results are computed. The $3^4 2^1$ full factorial design and its results can be seen in Appendix B.6, B.7 and B.8 for all the response variables. Part of the design and its results is repeated in Table 4.14 in order to explain the factors and their levels. The same levels for all factors and the same notations in the Taguchi Design are used in the Full Factorial Design. They are repeated here for convenience.

Table 4.14 Part of the $3^4 2^1$ full factorial design and its results when the response variable is the compressive strength

$3^4 2^1$ Full Factorial Design for Compressive Strength										
Exp. Run No	Processing Parameters					Results				
	A	B	C	D	E	Run #1	Run #2	Run #3	μ (Mpa)	S/N ratio
1	-1	-1	-1	-1	-1	61,2	62,8	62,4	62,13	35,86
2	-1	-1	-1	-1	0	70,4	64,0	71,6	68,67	36,70
3	-1	-1	-1	-1	1	71,2	73,2	70,0	71,47	37,08
4	-1	-1	-1	1	-1	48,4	50,0	48,0	48,80	33,76
5	-1	-1	-1	1	0	56,0	60,6	59,6	58,73	35,36
6	-1	-1	-1	1	1	72,4	72,0	68,0	70,80	36,99
7	-1	-1	0	-1	-1	48,4	50,8	58,8	52,67	34,34
8	-1	-1	0	-1	0	66,8	75,2	61,2	67,73	36,52
9	-1	-1	0	-1	1	74,0	72,4	71,6	72,67	37,22
10	-1	-1	0	1	-1	45,6	46,8	49,2	47,20	33,47
11	-1	-1	0	1	0	49,2	50,8	54,8	51,60	34,23
12	-1	-1	0	1	1	59,6	59,6	68,0	62,40	35,85
13	-1	-1	1	-1	-1	54,0	58,4	56,8	56,40	35,01
14	-1	-1	1	-1	0	57,6	67,2	60,4	61,73	35,76
15	-1	-1	1	-1	1	67,2	69,6	70,8	69,20	36,80
16	-1	-1	1	1	-1	60,0	61,0	60,8	60,60	35,65
17	-1	-1	1	1	0	62,4	59,2	60,4	60,67	35,65
18	-1	-1	1	1	1	60,0	60,0	61,6	60,53	35,64
19	-1	0	-1	-1	-1	68,8	74,0	70,0	70,93	37,00
20	-1	0	-1	-1	0	56,0	54,4	55,2	55,20	34,84
21	-1	0	-1	-1	1	66,0	68,8	64,8	66,53	36,45
22	-1	0	-1	1	-1	52,0	48,0	48,8	49,60	33,89
23	-1	0	-1	1	0	57,2	53,2	56,8	55,73	34,91
24	-1	0	-1	1	1	59,6	64,8	58,4	60,93	35,67
25	-1	0	0	-1	-1	52,0	50,8	44,4	49,07	33,75
26	-1	0	0	-1	0	40,4	38,0	39,2	39,20	31,86
27	-1	0	0	-1	1	26,4	32,0	33,6	30,67	29,59

where:

μ: average of the three replicates

Parameter A: Testing age (days)

Levels: -1: 7 days 0: 28 days 1: 90 days

Parameter B: Binder type used in the concrete mix

Levels: -1: Silica fume (SF) 0: Fly ash (FA)

1: Ground granulated blast furnace slag (GGBFS)

Parameter C: Binder amount used in the concrete mix (%)

Levels: -1: 20% 0: 15% 1: 10%(for silica fume)

-1: 10% 0: 20% 1: 30%(for fly ash)

-1: 20% 0: 40% 1: 60%(for GGBFS)

Parameter D: Specimen curing type

Levels: -1: ordinary water curing 1: steam curing

Parameter E: Steel fiber volume fraction (% by vol.)

Levels: -1: 0.0% 0: 0.5% 1: 1.0%

The levels of the silica fume binder amount are in descending order since it is known from the past researches that as the amount of silica fume decreases the strength of the concrete decreases also. Whereas as the amounts of both fly ash and GGBFS increase the strength of the concrete decreases. Therefore the level assignment is done according to the decreasing strength of concrete.

For all of the responses Taguchi analysis, general linear regression analysis and response surface analysis are performed.

4.2.1 Taguchi Analysis of the Mean Compressive Strength Based on the Full Factorial Design

The ANOVA table for the mean compressive strength can be seen in Table 4.15. Since the factor interactions between the nested factor and its primary factor are insignificant in nested designs, they are omitted from the model. It indicates that except from the two-way interaction that is Cure*Steel (DE) and a three-way interaction that is Age*Cure*Steel (ADE), all the remaining sources significantly affect the compressive strength of the fiber reinforced high strength

concrete since their F-ratio are greater than the tabulated F-ratio values of 95% confidence level. The insignificance of DE interaction can also be seen from the two-way interaction plot given in Figure 4.20. x-axis of each column and y-axis of each row represents the levels of the related factor. Each different line corresponds to the different levels of the second parameter. Since the three lines in the Age*Cure (AD), Age*Steel (AE) and Cure*Binder Amount (DC(B)) interaction plots are almost parallel, their effect on the compressive strength can be accepted as insignificant. The relatively low F-ratios of AD, AE and DC(B) support this insignificance. The other plots indicate a strong interaction between all the remaining parameters because of the nonparallelizm of the lines in the interaction plot proving the results obtained from ANOVA.

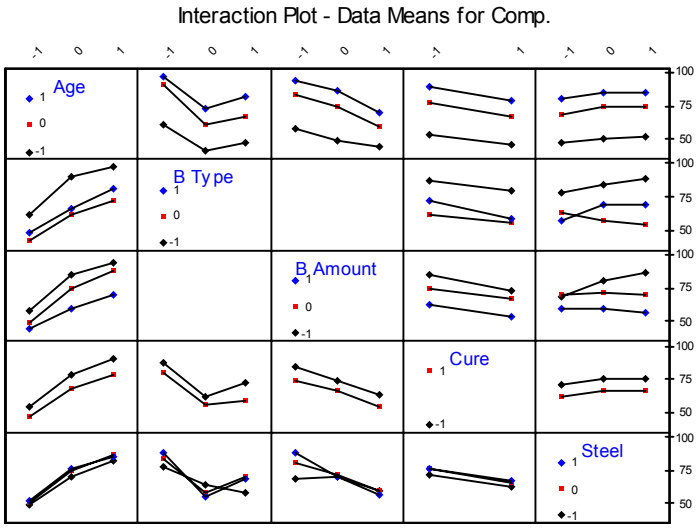

Figure 4.20 Two-way interaction plots for the mean compressive strength

Table 4.15 ANOVA table for the mean compressive strength based on the full factorial design

Source	Df	Sum of Squares	Mean Square	F	P
A	2	96911,4	48455,7	2017,02	0,000
B	2	52504,5	26252,3	1092,78	0,000
C (B)	6	49008,1	8168,0	340,00	0,000
D	1	10483,4	10483,4	436,38	0,000
E	2	2066,3	1033,1	43,01	0,000
AB	4	2245,5	561,4	23,37	0,000
AC(B)	12	4788,7	399,1	16,61	0,000
AD	2	322,1	161,0	6,70	0,001
AE	4	166,1	41,5	1,73	0,143
BD	2	1290,9	645,4	26,87	0,000
BE	4	8247,1	2061,8	85,82	0,000
DC(B)	6	656,8	109,5	4,56	0,000
EC(B)	12	9295,3	774,6	32,24	0,000
DE	2	19,8	9,9	0,41	0,663
ABD	4	249,3	62,3	2,59	0,036
ABE	8	1341,5	167,7	6,98	0,000
ADC(B)	12	797,6	66,5	2,77	0,001
AEC(B)	24	1709,1	71,2	2,96	0,000
ADE	4	107,2	26,8	1,12	0,349
BDE	4	1852,1	463,0	19,27	0,000
DEC(B)	12	1549,7	129,1	5,38	0,000
ABDE	8	772,3	96,5	4,02	0,000
ADEC(B)	24	1487,4	62,0	2,58	0,000
Error	324	7783,6	24,0		
TOTAL	485	255655,7			

The residual plots of the model for the mean compressive strength are given in Figures 4.21 and 4.22.

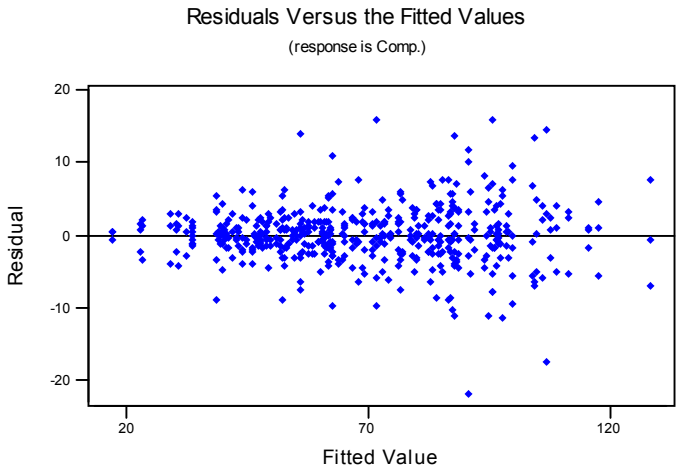

Figure 4.21 The residuals versus fitted values of the full factorial model found by ANOVA for the means for compressive strength

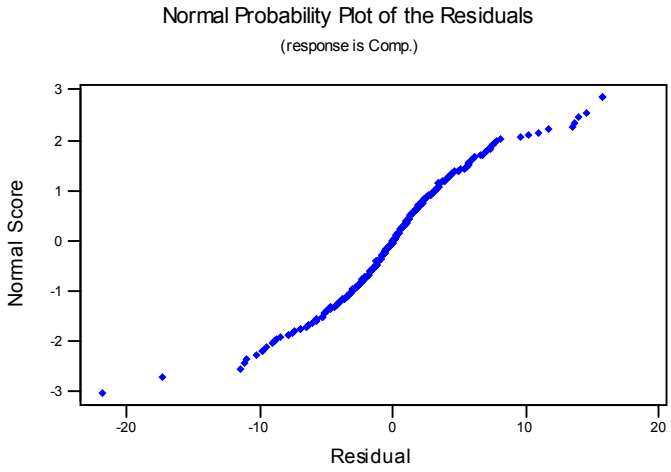

Figure 4.22 The residual normal probability plot for the full factorial model found by ANOVA for the means for compressive strength

It can be concluded from Figure 4.21 that the assumption of having a constant variance of the error term for all levels of the independent process parameters is not violated since there is no significant pattern. Also it can be seen from Figure

4.22 that there is a linear trend on the normal probability plot indicating that the assumption of the error term having a normal probability distribution is satisfied.

Figure 4.23 shows the main effects plot which is used for finding the optimum levels of the process parameters that increases the mean compressive strength.

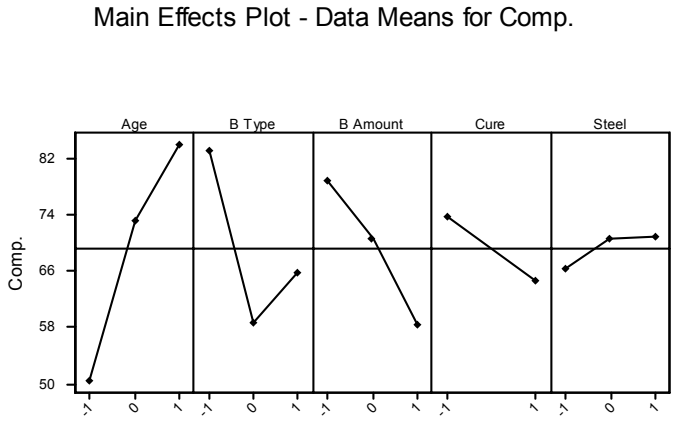

Figure 4.23 Main effects plot based on the full factorial design for the mean compressive strength

As it can be seen from Figure 4.23, the optimum points are 3rd level for Age (90 days), 1st level for the Binder Type (Silica Fume), 1st level for the Binder Amount (20% as silica fume is selected for the binder type), 1st level for Curing Type (water curing) and the 3rd level for the Steel Fiber Volume Fraction (1.0%). Since there is a slight difference between the 2nd level and the 3rd level of steel fiber volume fraction, the 2nd level can also be chosen for economic considerations. Also it is needed to consider the significant two-way factor interactions when determining the optimum condition. From the interaction plot it can be seen that the optimum levels for the interaction terms are A_1xB_{-1},

A_1xC_{-1}, $B_{-1}xD_{-1}$, $B_{-1}xE_1$, $E_1xC(B)_{-1}$ which coincide with the optimum levels of the main effects. The notation for optimum points is $A_1B_{-1}C_{-1}D_{-1}E_1$. This corresponds to the 111th trial run in the full factorial experiment. The optimum performance is calculated by using the following expression:

$A_1B_{-1}C_{-1}D_{-1}E_1$:

$$\hat{\mu}_{A_1B_{-1}C_{-1}D_{-1}E_1} = \overline{T} + (\overline{A}_1 - \overline{T}) + (\overline{B}_{-1} - \overline{T}) + (\overline{C}_{-1} - \overline{T}) + (\overline{D}_{-1} - \overline{T}) + (\overline{E}_1 - \overline{T}) + (\overline{A_1 \times B_{-1}} - \overline{T}) + (\overline{A_1 \times C_{-1}} - \overline{T}) + (\overline{B_{-1} \times D_{-1}} - \overline{T}) + (\overline{B_{-1} \times E_1} - \overline{T}) + (\overline{C_{-1} \times E_1} - \overline{T}) \quad (4.13)$$

Since $\overline{A_1 \times B_{-1}} = \overline{A_1 B_{-1}} - (\overline{A}_1 - \overline{T}) - (\overline{B}_{-1} - \overline{T})$ (4.14)

When the other interaction terms are computed as stated in Equation 4.14, the process estimate equation becomes:

$$\hat{\mu}_{A_1B_{-1}C_{-1}D_{-1}E_1} = \overline{T} - (\overline{A}_1 - \overline{T}) - 2(\overline{B}_{-1} - \overline{T}) - (\overline{C}_{-1} - \overline{T}) - (\overline{E}_1 - \overline{T}) + (\overline{A_1 B_{-1}} - \overline{T}) + (\overline{A_1 C_{-1}} - \overline{T}) + (\overline{B_{-1} D_{-1}} - \overline{T}) + (\overline{B_{-1} E_1} - \overline{T}) + (\overline{C_{-1} E_1} - \overline{T})$$

$$\hat{\mu}_{A_1B_{-1}C_{-1}D_{-1}E_1} = 69.30 - (84.25 - 69.30) - 2\,(83.45 - 69.30) - (79.02 - 69.30) - (66.40 - 69.30) + (97.8 - 69.30) + (94.85 - 69.30) + (87.06 - 69.30) + (88.59 - 69.30) + (87.21 - 69.30)$$

$$= 128.24 \text{ MPa}$$

The confidence interval is calculated by:

$$n_e = \frac{486}{47+1} = 10.13$$

$V_e = 24.0$

$F_{0.05,1,324} = 3.84$

$$C.I. = \sqrt{\frac{3.84 \times 24.0}{10.13}} = 3.02$$

Therefore, the value of the mean compressive strength is expected in between; $\hat{\mu}_{A_1B_{-1}C_{-1}D_{-1}E_1}$ = {125.22, 131.26} with 95% confidence interval.

The result of the 111th experiment, 128.53 MPa (the mean value), falls in the 95% confidence interval limits.

In order to minimize the variation in the compressive strength ANOVA for the S/N ratio values are performed (Table 4.16). The four-way interaction term (ADEC(B)) is omitted in order to leave 16 degrees of freedom to the error term. The results of the ANOVA show that all the main factors, six two-way interactions that are Age*Binder Type (AB), Age*Binder Amount (AC(B)), Binder Type*Cure (BD), Binder Type*Steel (BE), Cure*Binder Amount (DC(B)) and Steel*Binder Amount (EC(B)), and one three-way interaction which is Binder Type*Cure*Steel (BDE) are the significant factors with a 95% confidence interval. None of the four-way interaction factors is significant since all their p-values are bigger than 0.050. Figure 4.24 shows all the two-way factor interaction plots. As it can be seen from the figure that BE and EC(B) interactions significantly contribute to the compressive strength, whereas the contributions of AB and AC(B) are lesser since the lines in the corresponding plots are more or less parallel. Although the lines are parallel in the BD interaction plot, since its F-value is relatively higher it is accepted as significant on the response. Also in the ANOVA table, the relatively small F-values of AB and AC interactions support this. It is clear from the interaction plot that AD, AE, and DE have no significant effect on the compressive strength since the lines are parallel.

Table 4.16 ANOVA of S/N ratio values for the compressive strength based on the full factorial design

Source	Df	Sum of Squares	Mean Square	F	P
A	2	606,60	303,30	720,80	0,000
B	2	339,43	169,72	403,34	0,000
C(B)	6	371,75	61,96	147,24	0,000
D	1	60,23	60,23	143,14	0,000
E	2	5,63	2,82	6,69	0,005
AB	4	10,44	2,61	6,20	0,001
AC(B)	12	27,34	2,28	5,41	0,000
AD	2	0,55	0,27	0,65	0,532
AE	4	0,74	0,18	0,44	0,781
BD	2	9,38	4,69	11,14	0,000
BE	4	64,10	16,03	38,08	0,000
DC(B)	6	6,46	1,08	2,56	0,046
EC(B)	12	70,27	5,86	13,92	0,000
DE	2	0,00	0,00	0,00	1,000
ABD	4	1,74	0,44	1,04	0,409
ABE	8	6,02	0,75	1,79	0,129
ADC(B)	12	6,66	0,56	1,32	0,271
AEC(B)	24	11,75	0,49	1,16	0,357
ADE	4	0,89	0,22	0,53	0,715
BDE	4	8,52	2,13	5,06	0,004
DEC(B)	12	14,43	1,20	2,86	0,014
ABDE	8	2,68	0,34	0,80	0,611
Error	24	10,10	0,42		
TOTAL	161	1635,71			

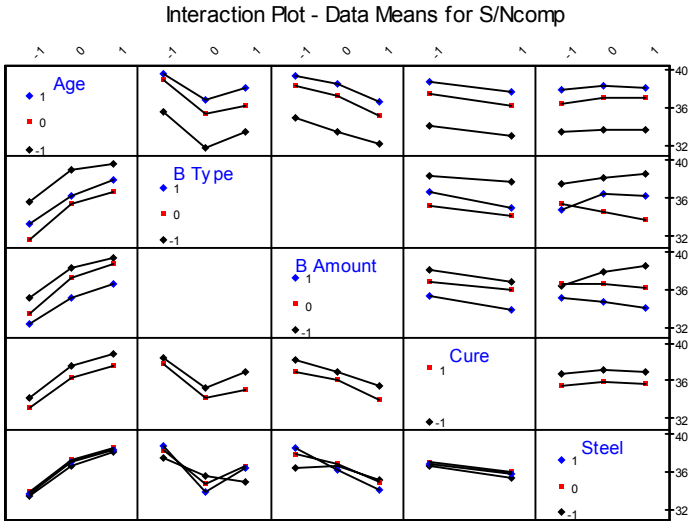

Figure 4.24 Two-way interaction plots for the S/N values of compressive strength

The residual plots for S/N ratio can be seen in Figures 4.25 and 4.26.

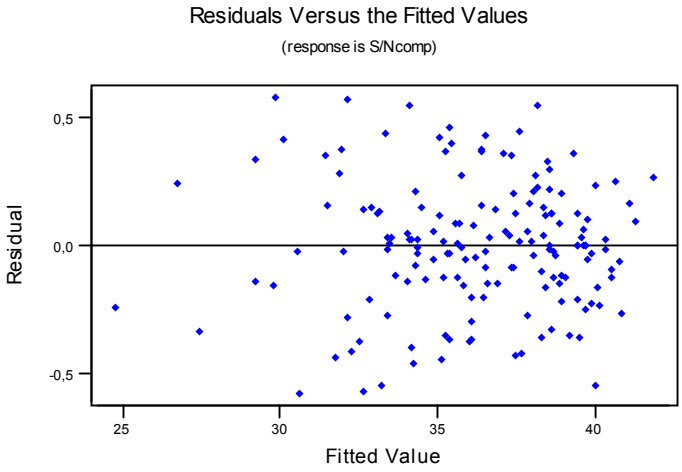

Figure 4.25 The residuals versus fitted values of the full factorial model found by ANOVA for S/N ratio for compressive strength

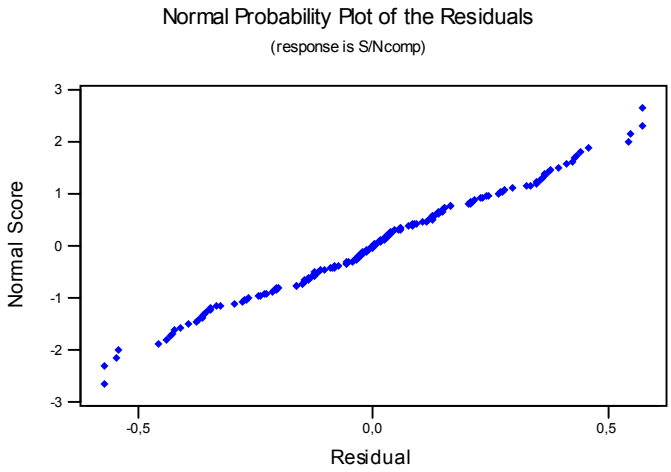

Figure 4.26 The residual normal probability plot for the full factorial model found by ANOVA for S/N ratio for compressive strength

Both figures show no abnormality for validation of the assumptions of the errors. It has constant variance and it is distributed normally.

From the main effects plot (Figure 4.27), the optimum points are 3rd level for Age (90 days), 1st level for Binder Type (silica fume), 1st level for Binder Amount (20%), 1st level for Curing Type (water curing) and 2nd level for Steel Fiber Volume Fraction (0.5% vol.). But from the interaction plot it is concluded that all the optimal levels of the factors are in coincidence with the determined values above except from the level of Steel Fiber Volume Fraction. The best points for both of the BE and EC(B) interactions correspond to the 3rd level of steel fiber volume fraction. So the two different combinations should be computed for determining the optimum point.

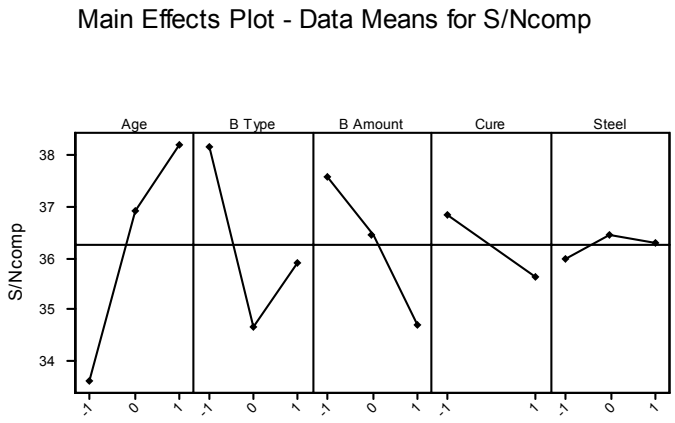

Figure 4.27 Main effects plot based on the full factorial design for S/N ratio for compressive strength

Combination 1: $A_1B_{-1}C_{-1}D_{-1}E_0$ (experiment no. 110)

$$\eta = \overline{T} + (\overline{A}_1 - \overline{T}) + (\overline{B}_{-1} - \overline{T}) + (\overline{C}_{-1} - \overline{T}) + (\overline{D}_{-1} - \overline{T}) + (\overline{E}_0 - \overline{T}) + (\overline{A_1 \times B_{-1}} - \overline{T}) + (\overline{A_1 \times C_{-1}} - \overline{T}) + (\overline{B_{-1} \times D_{-1}} - \overline{T}) + (\overline{B_{-1} \times E_0} - \overline{T}) + (\overline{C_{-1} \times E_0} - \overline{T}) \quad (4.15)$$

$$\eta = \overline{T} - (\overline{A}_1 - \overline{T}) - 2(\overline{B}_{-1} - \overline{T}) - (\overline{C}_{-1} - \overline{T}) - (\overline{E}_0 - \overline{T}) + (\overline{A_1 B_{-1}} - \overline{T}) + (\overline{A_1 C_{-1}} - \overline{T}) + (\overline{B_{-1} D_{-1}} - \overline{T}) + (\overline{B_{-1} E_0} - \overline{T}) + (\overline{C_{-1} E_0} - \overline{T})$$

$$\eta = 36.25 - (38.21 - 36.25) - 2\,(38.16 - 36.25) - (37.57 - 36.25) - (36.46 - 36.25) + (39.70 - 36.25) + (39.35 - 36.25) + (38.53 - 36.25) + (38.22 - 36.25) + (37.85 - 36.25)$$

$$= 41.24$$

$$n_e = \frac{162}{47+1} = 3.38$$

$$V_e = 0.42$$

$F_{0.05,1,24} = 4.26$

$$C.I. = \sqrt{\frac{4.26 \times 0.42}{3.38}} = 0.73$$

As a result the value for the S/N ratio should fall in between:

η = {40.51, 41.97} with 95% confidence.

Combination 2: $A_1B_{-1}C_{-1}D_{-1}E_1$ (experiment no. 111)

$$\eta = \overline{T} + (\overline{A}_1 - \overline{T}) + (\overline{B}_{-1} - \overline{T}) + (\overline{C}_{-1} - \overline{T}) + (\overline{D}_{-1} - \overline{T}) + (\overline{E}_1 - \overline{T}) + (\overline{A_1 \times B_{-1}} - \overline{T}) + (\overline{A_1 \times C_{-1}} - \overline{T}) + (\overline{B_{-1} \times D_{-1}} - \overline{T}) + (\overline{B_{-1} \times E_1} - \overline{T}) + (\overline{C_{-1} \times E_1} - \overline{T}) \quad (4.16)$$

$$\eta = \overline{T} - (\overline{A}_1 - \overline{T}) - 2(\overline{B}_{-1} - \overline{T}) - (\overline{C}_{-1} - \overline{T}) - (\overline{E}_1 - \overline{T}) + (\overline{A_1B_{-1}} - \overline{T}) + (\overline{A_1C_{-1}} - \overline{T}) + (\overline{B_{-1}D_{-1}} - \overline{T}) + (\overline{B_{-1}E_1} - \overline{T}) + (\overline{C_{-1}E_1} - \overline{T})$$

η = 36.25 – (38.21 – 36.25) – 2 (38.16 – 36.25) – (37.57 – 36.25) – (36.28 – 36.25) + (39.70 – 36.25) + (39.35 – 36.25) + (38.53 – 36.25) + (38.74 – 36.25) + (38.54 – 36.25)

= 42.74

$$n_e = \frac{162}{47+1} = 3.38$$

$V_e = 0.42$

$F_{0.05,1,16} = 4.26$

$$C.I. = \sqrt{\frac{4.26 \times 0.42}{3.38}} = 0.73$$

As a result the value for the S/N ratio should fall in between:

η = {42.01, 43.47} with 95% confidence.

From the two combinations the second one is chosen as the optimal level since it S/N ratio is larger than the first one. It is less sensitive to the uncontrollable noise factors. It can be seen from the result of experiment 111 that the S/N ratio is 42.15 and it falls within the determined values of the S/N ratio with 95% confidence.

As a result, Taguchi analysis has found $A_1B_{-1}C_{-1}D_{-1}E_1$ as the best levels considering both the mean and S/N ratio values of compressive strength with the predicted values of 128.24 MPa for mean compressive strength, 42.74 for S/N ratio. This corresponds to trial number 111 with mean compressive strength 128.53 MPa, S/N ratio 42.15 falling in the determined limits with 95% confidence. As a result trial number 111 confirms the results of the analysis. In the following sections regression and response surface methodologies are going to be compared with Taguchi analysis.

4.2.2 Regression Analysis of the Mean Compressive Strength Based on the Full Factorial Design

Again as in the Taguchi Design, the binder type (B) and curing type (D) main factors are qualitative independent variables, so, a quantitative meaning to their given levels can not be attached. All that can be done is to describe them. As a result dummy (indicator) variables should be defined for these two main factors. Since factor B has three levels, it can only be described by two dummy variables, namely B_1 and B_2, and since factor D has two levels, it can be described by a single dummy variable D_1.

$$B_1 = \begin{cases} 1 \, if \; Fly \; Ash \, is \, used \\ 0 \, if \; not \end{cases} \qquad B_2 = \begin{cases} 1 \, if \; GGBFS \, is \, used \\ 0 \, if \; not \end{cases}$$

$$D_1 = \begin{Bmatrix} 1\, if\ steam\ curing\ is\ used \\ 0\, if\ not \end{Bmatrix}$$

The first employed regression analysis to model the mean compressive strength contains only the main factors. That is:

$$y = 88{,}1 + 16{,}9*A - 24{,}7*B_1 - 17{,}8*B_2 - 10{,}4*C - 9{,}29*D_1 + 2{,}27*E \qquad (4.17)$$

Table 4.17 shows the ANOVA for the significance of the above regression model. ANOVA is performed on the individual results rather than the average of the three replicates. The hypothesis of having all β terms equal to zero is tested and refused with almost 100% confidence by this model since the p-value of the regression is 0.000 as shown in Table 4.17.

Table 4.17 ANOVA for the significance of the regression model developed for the mean compressive strength based on the full factorial design including only the main factors

Source	df	Sum of Squares	Mean Squares	F	P
Regression	6	192433	32072	242,99	0,000
Residual Error	479	63223	132		
Total	485	255656			

$R^2 = 75.3\%$ $R^2_{(adj)} = 75.0\%$ $S = 11.49$

Durbin-Watson statistic = 1.43

The adjusted multiple coefficient of determination, $R^2_{(adj)}$, shows that 75% of the sample variation in the mean compressive strength can be explained by this model. The Durbin-Watson statistic states that there is a strong evidence of positive residual correlation with 95% confidence since it is less than the tabulated lower bound (d_L), which is 1.57 with 5 independent variables and 486 observations. The residual plots of this model are given in Figures 4.28 and

4.29. Although it is concluded from the residual plots that there is not any indication of violation of the assumptions of the error, a more adequate regression model will be searched to describe the mean compressive strength. The significance of β terms of the model is shown in Table 4.18. This table indicates that all the main factors are significant at the p(0.05) level of significance.

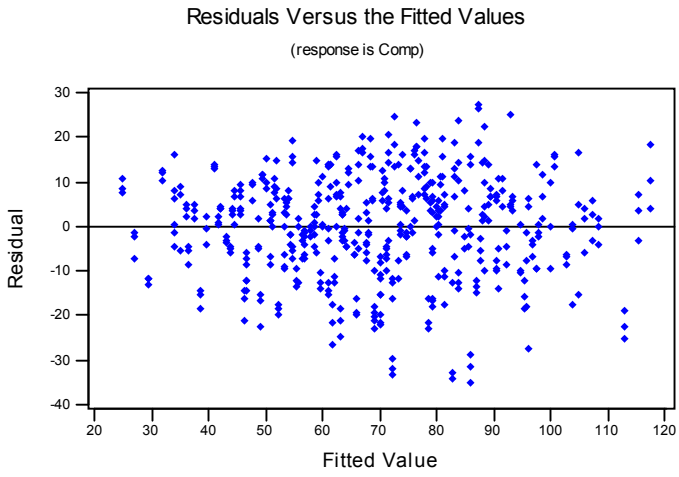

Figure 4.28 Residuals versus fitted values plot of the regression model developed for the mean compressive strength with only main factors

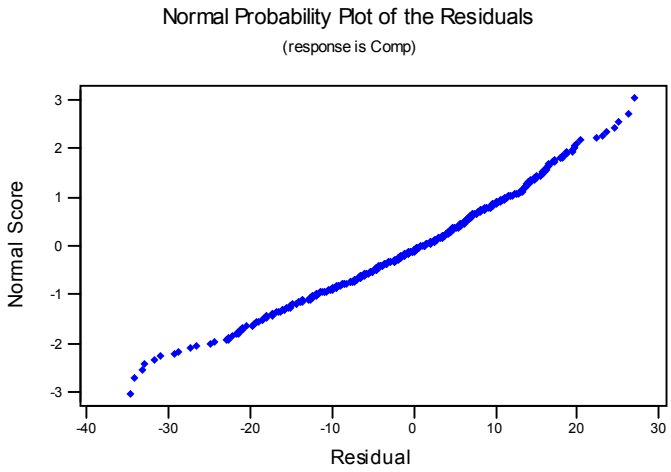

Figure 4.29 Residual normal probability plot of the regression model developed for the mean compressive strength with only main factors

Table 4.18 Significance of β terms of the regression model developed for the mean compressive strength with only main factors

Predictor	β Estimate	Standard Error	T	P
Constant	88,096	1,0420	84,52	0,000
A	16,9444	0,6383	26,55	0,000
B_1	-24,677	1,2770	-19,33	0,000
B_2	-17,765	1,2770	-13,92	0,000
C	-10,3556	0,6383	-16,22	0,000
D	-9,289	1,0420	-8,91	0,000
E	2,2735	0,6383	3,56	0,000

The MINITAB output with the sequential sum of squares of the regression model can be seen in Appendix B.9.

The second regression model is decided to include all the two-way interaction terms and the square of the main factors. The equation and the ANOVA table for the regression equation can be seen in Eqn. 4.18 and Table 4.19 respectively.

Again the hypothesis of having all β terms equal to zero is refused with 100% confidence by this model.

$$y = 97,0 + 18,6*A - 35,3*B_1 - 14,6*B_2 - 7,89*C - 9,32*D_1 + 6,83*E - 11,3*A^2 - 1,24*C^2 - 2,33*E^2 - 4,51*AC + 1,13*AE - 4,73*CE + 2,85*B_1D_1 - 1,70*B_2D_1 - 2,53*AB_1 - 11,2*CB_1 - 14,0*EB_1 + 4,87*A^2B_1 + 7,01*C^2B_1 + 3,79*E^2B_1 + 2,77*ACB_1 - 3,42*AEB_1 + 1,18*CEB_1 + 0,39*AB_2 + 2,06*CB_2 + 0,99*EB_2 + 8,72*A^2B_2 - 5,39*C^2B_2 - 3,13*E^2B_2 + 3,81*ACB_2 + 0,77*AEB_2 - 0,42*CEB_2 - 0,64*AD_1 + 3,36*CD_1 - 2,88*ED_1 - 0,75*A^2D_1 + 0,81*C^2D_1 + 3,11*E^2D_1 - 0,90*ACD_1 - 3,63*AED_1 - 0,08*CED_1 - 0,44*AB_1D_1 - 2,78*CB_1D_1 + 8,84*EB_1D_1 + 4,82*A^2B_1D_1 - 6,27*C^2B_1D_1 - 2,17*E^2B_1D_1 + 0,91*ACB_1D_1 + 6,19*AEB_1D_1 - 4,11*CEB_1D_1 - 3,01*AB_2D_1 - 3,77*CB_2D_1 - 1,51*EB_2D_1 + 1,93*A^2B^2D_1 - 3,47*C^2B_2D_1 - 5,94*E^2B_2D_1 - 1,34*ACB_2D_1 + 4,23*AEB_2D_1 - 1,37*CEB_2D_1 \quad (4.18)$$

Table 4.19 ANOVA for the significance of the regression model developed for the mean compressive strength based on the full factorial design including main, interaction and squared factors

Source	df	Sum of Squares	Mean Squares	F	P
Regression	59	235794,3	3996,5	85,72	0,000
Residual Error	426	19861,4	46,6		
Total	485	255655,7			

$R^2 = 92.2\%$ $R^2_{(adj)} = 91.2\%$ $S = 6.828$

Durbin-Watson statistic = 2.17

This model seems more adequate than the previous one, the standard deviation of the error (S) decreased considerably and the $R^2_{(adj)}$ value is improved explaining the 91% of the sample variation in the mean compressive strength by this model. Also the Durbin-Watson statistic is increased by this model. (4 – Durbin-Watson statistic), 1.83 is above the tabulated upper bound value for 5 independent variables and 486 observations which is 1.78. Therefore it is concluded that the residuals are independent.

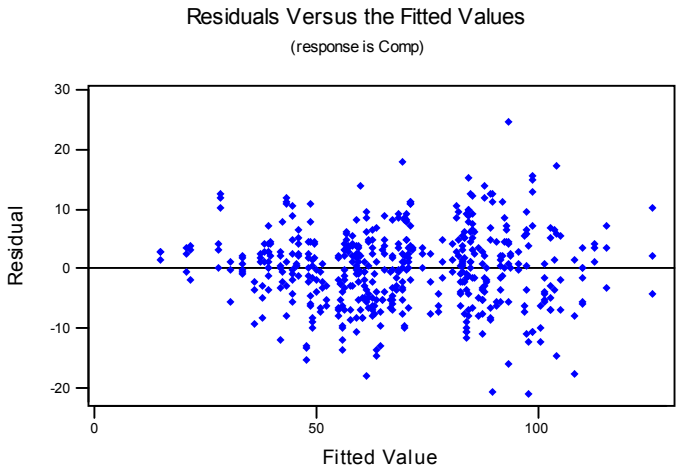

Figure 4.30 Residuals versus fitted values plot of the regression model in Eqn.4.18 developed for the mean compressive strength

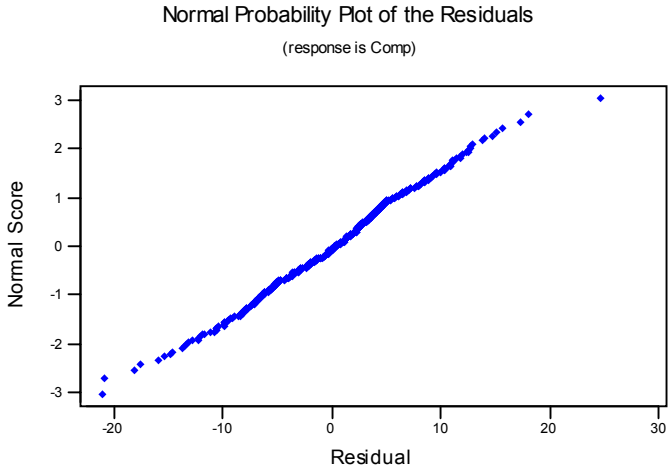

Figure 4.31 Residual normal probability plot of the regression model in Eqn.4.18 developed for the mean compressive strength

Residuals versus fitted values and the normal probability plot indicate that the error term has normal distribution with constant variance. As a result an adequate model explaining the mean response is achieved. Table 4.20 shows the significance of the β terms.

It can be seen from the large p-values that, there are several insignificant factors in the model. The model can be improved by discarding the insignificant terms from the model one by one starting from the term having the largest p-value. After eliminating a factor, all the normality, constant variance and error correlation assumptions are checked and the best model is chosen.

Table 4.20 Significance of β terms of the regression model in Eqn.4.18 developed for the mean compressive strength

Predictor	β Estimate	Standard Error	T	P
Constant	96,9530	2,0070	48,30	0,000
A	18,5556	0,9292	19,97	0,000
B_1	-35,3430	2,8390	-12,45	0,000
B_2	-14,5580	2,8390	-5,13	0,000
C	-7,8889	0,9292	-8,49	0,000
D_1	-9,3210	2,8390	-3,28	0,001
E	6,8296	0,9292	7,35	0,000
A^2	-11,2810	1,6090	-7,01	0,000
C^2	-1,2370	1,6090	-0,77	0,443
E^2	-2,3260	1,6090	-1,45	0,149
AC	-4,5510	1,1380	-3,96	0,000
AE	1,1330	1,1380	1,00	0,320
CE	-4,7330	1,1380	-4,16	0,000
B_1D_1	2,8520	4,0150	0,71	0,478
B_2D_1	-1,6960	4,0150	-0,42	0,673
AB_1	-2,5330	1,3140	-1,93	0,055
CB_1	-11,2300	1,3140	-8,55	0,000
EB_1	-14,0070	1,3140	-10,66	0,000
A^2B_1	4,8740	2,2760	2,14	0,033
C^2B_1	7,0070	2,2760	3,08	0,002
E^2B_1	3,7850	2,2760	1,66	0,097
ACB_1	2,7670	1,6090	1,72	0,086
AEB_1	-3,4220	1,6090	-2,13	0,034
CEB_1	1,1780	1,6090	0,73	0,465
AB_2	0,3930	1,3140	0,30	0,765
CB_2	2,0590	1,3140	1,57	0,118
EB_2	0,9930	1,3140	0,76	0,450
A^2B_2	8,7190	2,2760	3,83	0,000
C^2B_2	-5,3930	2,2760	-2,37	0,018
E^2B_2	-3,1260	2,2760	-1,37	0,170
ACB_2	3,8110	1,6090	2,37	0,018
AEB_2	0,7670	1,6090	0,48	0,634
CEB_2	-0,4220	1,6090	-0,26	0,793
AD_1	-0,6440	1,3140	-0,49	0,624
CD_1	3,3630	1,3140	2,56	0,011
ED_1	-2,8780	1,3140	-2,19	0,029
A^2D_1	-0,7480	2,2760	-0,33	0,743
C^2D_1	0,8070	2,2760	0,35	0,723
E^2D_1	3,1070	2,2760	1,37	0,173
ACD_1	-0,9000	1,6090	-0,56	0,576

Table 4.20 Continued

Predictor	β Estimate	Standard Error	T	P
AED_1	-3,6280	1,6090	-2,25	0,025
CED_1	-0,0830	1,6090	-0,05	0,959
AB_1D_1	-0,4370	1,8580	-0,24	0,814
CB_1D_1	-2,7780	1,8580	-1,49	0,136
EB_1D_1	8,8410	1,8580	4,76	0,000
$A^2B_1D_1$	4,8220	3,2190	1,50	0,135
$C^2B_1D_1$	-6,2670	3,2190	-1,95	0,052
$E^2B_1D_1$	-2,1670	3,2190	-0,67	0,501
ACB_1D_1	0,9110	2,2760	0,40	0,689
AEB_1D_1	6,1940	2,2760	2,72	0,007
CEB_1D_1	-4,1060	2,2760	-1,80	0,072
AB_2D_1	-3,0150	1,8580	-1,62	0,105
CB_2D_1	-3,7700	1,8580	-2,03	0,043
EB_2D_1	-1,5150	1,8580	-0,82	0,415
$A^2B_2D_1$	1,9330	3,2190	0,60	0,548
$C^2B_2D_1$	-3,4670	3,2190	-1,08	0,282
$E^2B_2D_1$	-5,9440	3,2190	-1,85	0,065
ACB_2D_1	-1,3440	2,2760	-0,59	0,555
AEB_2D_1	4,2280	2,2760	1,86	0,064
CEB_2D_1	-1,3720	2,2760	-0,60	0,547

The MINITAB output with the sequential sum of squares of the regression model can be seen in Appendix B.10.

There is only a slight improvement in the best model whose regression equation, ANOVA table, residual plots and β significance test are given in Eqn.4.19, Table 4.21, Figures 4.32 and 4.33, and Table 4.22 respectively. This was obvious from the previous model because, the R^2 value and $R^2_{(adj)}$ value are very close to each other. This new model is achieved by pooling the ACB_1D_1, AB_1D_1, ACB_2D_1, $A^2B_2D_1$, CEB_2D_1, ACD_1, CEB_2, $E^2B_1D_1$ and $C^2B_2D_1$ interaction terms. The hypothesis of having all β terms equal to zero is tested and refused with almost 100% confidence by this model since the p-value of the regression is 0.000 as shown in Table 4.20. No change in both R^2 and adjusted

R^2 values can be obtained by this new model. However, the Durbin-Watson statistic is decreased to 2.14 showing that the residuals are uncorrelated.

$$y = 96,3 + 18,7*A - 34,4*B_1 - 13,7*B_2 - 7,89*C - 8,09*D_1 + 6,83*E - 11,8*A^2 - 0,37*C^2 - 1,78*E^2 - 4,96*AC + 1,13*AE - 4,94*CE + 0,90*B_1D_1 - 3,44*B_2D_1 - 2,75*AB_1 - 11,2*CB_1 - 14,0*EB_1 + 5,36*A^2B_1 + 6,14*C^2B_1 + 2,70*E^2B_1 + 3,22*ACB_1 - 3,42*AEB_1 + 1,39*CEB_1 + 0,28*AB_2 + 2,06*CB_2 + 0,99*EB_2 + 9,69*A^2B_2 - 7,13*C^2B_2 - 3,67*E^2B_2 + 3,14*ACB_2 + 0,77*AEB_2 - 0,86*AD_1 + 3,36*CD_1 - 2,88*ED_1 + 0,22*A^2D_1 - 0,93*C^2D_1 + 2,02*E^2D_1 - 3,63*AED_1 - 0,77*CED_1 - 2,78*CB_1D_1 + 8,84*EB_1D_1 + 3,86*A^2B_1D_1 - 4,53*C^2B_1D_1 + 6,19*AEB_1D_1 - 3,42*CEB_1D_1 - 2,80*AB_2D_1 - 3,77*CB_2D_1 - 1,51*EB_2D_1 - 4,86*E^2B_2D_1 + 4,23*AEB_2D_1 \quad (4.19)$$

Table 4.21 ANOVA for the significance of the best regression model developed for the mean compressive strength based on the full factorial design

Source	df	Sum of Squares	Mean Squares	F	P
Regression	50	235533,3	4710,7	101,83	0,000
Residual Error	435	20122,4	46,3		
Total	485	255655,7			

$R^2 = 92.1\%$ $R^2_{(adj)} = 91.2\%$ $S = 6.801$

Durbin-Watson statistic = 2.14

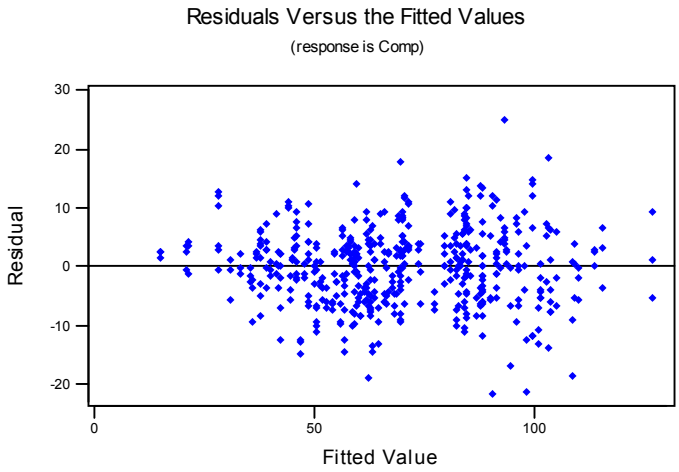

Figure 4.32 Residuals versus fitted values plot of the best regression model in Eqn.4.19 developed for the mean compressive strength

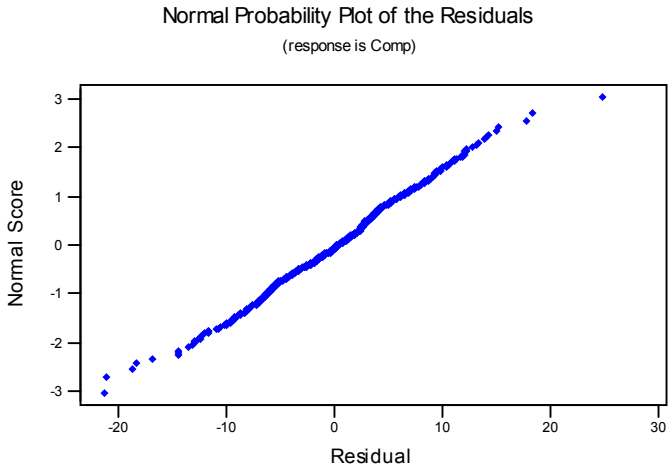

Figure 4.33 Residual normal probability plot of the best regression model in Eqn.4.19 developed for the mean compressive strength

Table 4.22 Significance of β terms of the best regression model in Eqn.4.19 developed for the mean compressive strength

Predictor	β Estimate	Standard Error	T	P
Constant	96,3360	1,7720	54,36	0,000
A	18,6648	0,8015	23,29	0,000
B_1	-34,3650	2,5060	-13,71	0,000
B_2	-13,6860	2,3290	-5,88	0,000
C	-7,8889	0,9255	-8,52	0,000
D_1	-8,0880	2,1370	-3,78	0,000
E	6,8296	0,9255	7,38	0,000
A^2	-11,7650	1,3880	-8,47	0,000
C^2	-0,3700	1,3880	-0,27	0,790
E^2	-1,7840	1,3880	-1,29	0,199
AC	-4,9611	0,8015	-6,19	0,000
AE	1,1330	1,1340	1,00	0,318
CE	-4,9444	0,8015	-6,17	0,000
B_1D_1	0,8960	3,0230	0,30	0,767
B_2D_1	-3,4410	2,3900	-1,44	0,151
AB_1	-2,7519	0,9255	-2,97	0,003
CB_1	-11,2300	1,3090	-8,58	0,000
EB_1	-14,0070	1,3090	-10,70	0,000
A^2B_1	5,3570	2,1210	2,53	0,012
C^2B_1	6,1410	2,1210	2,90	0,004
E^2B_1	2,7020	1,6030	1,69	0,093
ACB_1	3,2220	1,1340	2,84	0,005
AEB_1	-3,4220	1,6030	-2,13	0,033
CEB_1	1,3890	1,3880	1,00	0,318
AB_2	0,2830	1,2240	0,23	0,817
CB_2	2,0590	1,3090	1,57	0,116
EB_2	0,9930	1,3090	0,76	0,449
A^2B_2	9,6850	1,6030	6,04	0,000
C^2B_2	-7,1260	1,6030	-4,45	0,000
E^2B_2	-3,6680	2,1210	-1,73	0,084
ACB_2	3,1390	1,1340	2,77	0,006
AEB_2	0,7670	1,6030	0,48	0,633
AD_1	-0,8630	0,9255	-0,93	0,352
CD_1	3,3630	1,3090	2,57	0,011
ED_1	-2,8780	1,3090	-2,20	0,028
A^2D_1	-0,2190	1,6030	0,14	0,892
C^2D_1	-0,9260	1,6030	-0,58	0,564
E^2D_1	2,0240	1,6030	1,26	0,207
AED_1	-3,6280	1,6030	-2,26	0,024
CED_1	-0,7690	1,1340	-0,68	0,498

Table 4.22 Continued

Predictor	β Estimate	Standard Error	T	P
CB_1D_1	-2,7780	1,8510	-1,50	0,134
EB_1D_1	8,8410	1,8510	4,78	0,000
$A^2B_1D_1$	3,8560	2,7770	1,39	0,166
$C^2B_1D_1$	-4,5330	2,7770	-1,63	0,103
AEB_1D_1	6,1940	2,2670	2,73	0,007
CEB_1D_1	-3,4190	1,9630	-1,74	0,082
AB_2D_1	-2,7960	1,6030	-1,74	0,082
CB_2D_1	-3,7700	1,8510	-2,04	0,042
EB_2D_1	-1,5150	1,8510	-0,82	0,414
$E^2B_2D_1$	-4,8610	2,7770	-1,75	0,081
AEB_2D_1	4,2280	2,2670	1,86	0,063

As a result this model is decided to be kept as the most adequate model explaining the compressive strength of the SFRHSC. The MINITAB output with the sequential sum of squares of the regression model can be seen in Appendix B.11.

4.2.3 Response Surface Optimization of Compressive Strength Based on the Full Factorial Design

The response optimization of the best regression model found in Eqn.4.19 in the previous section for the mean compressive strength is done by using the MINITAB Response Optimizer. Again as in the Taguchi design, the lower bound is set to 50 Mpa and the target value is set to 130 Mpa.

The same thirteen starting points are used in the response optimization process of the mean compressive strength based on the full factorial design. The results of the optimizer can be seen in Table 4.23. The starting points and the optimum points found by MINITAB response optimizer is shown in Table 4.24.

Table 4.23 The optimum response, its desirability, the confidence and prediction intervals computed by MINITAB Response Optimizer for the mean compressive strength based on the full factorial design

Optimum Points	Mean Comp.	Desirability	95% Conf. Int.	95% Pred. Int.
1	126,839	0,9231	(121,969; 131,709)	(112,612; 141,066)
2	78,410	0,4206	(74,342; 82,478)	(64,437; 92,383)
3	110,106	0,8013	(105,236; 114,976)	(95,879; 124,333)
4	108,890	0,6925	(103,908; 113,871)	(94,624; 123,155)
5	109,415	0,7404	(105,181; 113,649)	(95,393; 123,437)
6	87,542	0,4831	(82,560; 92,523)	(73,276; 101,807)
7	74,711	0,3994	(70,597; 78,824)	(60,725; 88,697)
8	109,967	0,7432	(101,102; 118,832)	(93,927; 126,007)
9	126,839	0,9231	(121,969; 131,709)	(112,612; 141,066)
10	108,890	0,6925	(103,908; 113,871)	(94,624; 123,155)
11	126,839	0,9231	(121,969; 131,709)	(112,612; 141,066)
12	108,890	0,6925	(103,908; 113,871)	(94,624; 123,155)
13	102,169	0,6474	(97,508; 106,830)	(88,012; 116,326)

Table 4.24 The starting and optimum points for MINITAB response optimizer developed for the mean compressive strength based on the full factorial design

	Starting Points					Optimum Points				
Points	**Age (days)**	**B. Type**	**B. Amount (%)**	**Cure**	**Steel (% vol.)**	**Age (days)**	**B. Type**	**B. Amount (%)**	**Cure**	**Steel (% vol.)**
1	90	SF	20	water	1,0	90	SF	20	water	1,0
2	No starting point					28	GGBFS	20	water	1,0
3	90	SF	20	steam	0,5	90	SF	20	steam	1,0
4	90	GGBFS	20	water	0,5	90	GGBFS	20	water	1,0
5	90	SF	10	water	1,0	90	SF	15	water	1,0
6	28	FA	40	steam	0,5	90	GGBFS	20	steam	1,0
7	7	SF	20	water	0,0	13,4	SF	20	water	0,0
8	90	GGBFS	60	water	1,0	90	GGBFS	40	water	1,0
9	90	FA	10	water	1,0	90	SF	20	water	1,0
10	28	GGBFS	20	steam	1,0	90	GGBFS	20	water	1,0
11	90	SF	15	water	1,0	90	SF	20	water	1,0
12	90	GGBFS	20	steam	1,0	90	GGBFS	20	water	1,0
13	90	SF	20	water	0.0	90	SF	20	water	0,04

The starting points 1, 9 and 11 gave the same result which is the best one found by the Response Optimizer as 126.84 MPa compressive strength. Point 3 gave 110.11 MPa, which is the second best point but this is far from the target value of 130.0 MPa. Also the starting points 4, 10 and 12 led to the same optimum point which is 108.89 MPa. Points 5 and 8 are close to the second best and therefore they are worth to try. The remaining points resulted in very low compressive strength values and therefore they are not going to be interpreted.

Optimum points 1, 9 and 11:

For this point the 3rd level for Age (90 days), 1st level for Binder Amount (Silica Fume), 1st level for Binder Amount (20% for silica fume), 1st level for Curing Type (ordinary water curing) and the 3rd level for Steel Fiber Volume Fraction (1.0%) are assigned to the associated main factors. The optimum combination of the factor levels for these points corresponds to experiment 111. The results of it are 136.0 MPa, 128.0 MPa and 121.60 MPa and all are in the prediction interval with 95%. But 136.0 MPa is outside the upper limit of the confidence interval. They are also very close to the predicted optimum value of 126.89 MPa. As a result we can conclude that these points are well modeled by the chosen regression model.

Optimum point 3:

For this experiment age, binder type, binder amount, curing type and steel fiber volume fraction are set to 90 days, Silica Fume, 20% for SF, steam curing and 1.0% vol. respectively. The results of the experiments are 110.0 MPa, 108.4 MPa and 104.4 MPa. Only the third one is below the lower limit of the confidence interval and all three are in the prediction interval. Also they are close to the fitted value of 110.11 MPa. So it can be said that this point is well modeled by the chosen regression model.

Optimum point 8:

For this experiment age, binder type, binder amount, curing type and steel fiber volume fraction are set to 90 days, GGBFS, 40% for GGBFS, ordinary water curing and 1.0% vol. respectively. The results of the experiments are 98.0 MPa, 96.0 MPa and 96.0 MPa. None of the results are in the confidence interval. However all are in the prediction interval but close to the lower side. Also there is around 15 MPa gap between the results of the confirmation tests and the predicted compressive strength which is 109.97 MPa. As a result it can be concluded that this point is a little overestimated by the chosen regression model.

Optimum point 5:

For this experiment age, binder type, binder amount, curing type and steel fiber volume fraction are set to 90 days, SF, 15% for SF, ordinary water curing and 1.0% vol. respectively. The results of the experiments are 110.0 MPa, 113.2 MPa and 104.0 MPa. All of the results are in both the confidence and prediction intervals and they are very close to the predicted compressive strength of 109.42 MPa by the model. Therefore it can be said that this point is well modeled by the chosen regression model.

Optimum points 4, 10 and 12:

For these points the 3rd level for Age (90 days), 3rd level for Binder Amount (GGBFS), 1st level for Binder Amount (20% for GGBFS), 1st level for Curing Type (ordinary water curing) and the 3rd level for Steel Fiber Volume Fraction (1.0%) are assigned to the associated main factors. The optimum combination of the factor levels for these points corresponds to experiment 147. The results of the experiments are 109.60 MPa, 100.00 MPa and 90.40 MPa. Only 90.4 MPa is outside the lower boundary of the confidence and prediction intervals. This point is somewhat modeled by the chosen regression model but we should

have obtain larger compressive strengths because the predicted optimum value for this point is 107.51 MPa and our confirmation experiments resulted in lower values.

The best optimum combination of the parameter levels chosen for the regression analysis of the mean compressive strength is the results obtained by points 1, 9 and 11. Although point 3's intervals are narrower, there is almost 15 MPa gap in between the compressive strengths which is a considerable amount. Also the narrowness of the intervals is very close.

CHAPTER 5

EXPERIMENTAL DESIGN AND ANALYSIS WHEN THE RESPONSE IS FLEXURAL STRENGTH

5.1 Taguchi Experimental Design

The same methodology discussed in Chapter 4 when the response variable was compressive strength is applied for the flexural strength response variable. The same L_{27} (3^{13}) orthogonal array is employed with the same main factors and interaction terms.

5.1.1 Taguchi Analysis of the Mean Flexural Strength Based on the L_{27} (3^{13}) Design

The results of the flexural strength experiments are shown in Table 5.1.

The ANOVA table for the mean flexural strength can be seen in Table 5.2. It indicates that only Age (A) and Binder Type (B) main factors significantly affect the flexural strength of the fiber reinforced high strength concrete since their F-ratio are greater than the tabulated F-ratio values of 95% confidence level. Also the Curing Type (D) main factor can be accepted as significant with 89.5% confidence. The insignificance of AB interaction can also be seen from the two-way interaction plot given in Figure 5.1. As it can be seen from the Age*Binder Type (AB) interaction plot, all the lines are almost parallel supporting the large p-value of the interaction term in the ANOVA table. When Binder Type*Steel (BE) interaction plot is examined it is seen that the three

lines are not parallel and an interaction may exist in between them when the insignificant factors are pooled into the error term in ANOVA. Also the BE interaction term has relatively small p-value when compared with the p-value of the other interaction term AB.

Table 5.1 The flexural strength experiment results developed by L_{27} (3^{13}) design

	Column numbers and factors					**RESULTS**				
	1	**4**	**5**	**8**	**9**					
Exp. Run	**A**	**B**	**C**	**D**	**E**	**Run #1**	**Run#2**	**Run#3**	**μ (Mpa)**	**S/N ratio**
1	-1	-1	-1	-1	-1	10,14	9,91	9,22	9,76	19,76
2	-1	-1	0	0	0	8,06	8,52	7,49	8,02	18,05
3	-1	-1	1	-1	1	8,29	10,25	9,33	9,29	19,26
4	-1	0	-1	0	1	6,45	5,99	5,99	6,14	15,75
5	-1	0	0	-1	-1	4,61	4,15	4,72	4,49	13,01
6	-1	0	1	-1	0	4,72	5,41	4,84	4,99	13,92
7	-1	1	-1	-1	0	8,41	9,79	10,02	9,41	19,39
8	-1	1	0	-1	1	4,61	6,91	3,68	5,07	13,25
9	-1	1	1	0	-1	6,45	5,99	6,45	6,30	15,97
10	0	1	-1	-1	-1	7,03	7,37	8,06	7,49	17,44
11	0	1	0	-1	0	9,10	9,68	8,18	8,99	19,01
12	0	1	1	0	1	9,68	10,02	10,60	10,10	20,07
13	0	-1	-1	-1	1	10,25	10,14	10,71	10,37	20,31
14	0	-1	0	0	-1	11,98	12,44	12,10	12,17	21,70
15	0	-1	1	-1	0	13,48	13,71	13,25	13,48	22,59
16	0	0	-1	0	0	11,52	11,52	11,75	11,60	21,29
17	0	0	0	-1	1	8,29	7,60	8,06	7,98	18,03
18	0	0	1	-1	-1	5,07	5,18	5,76	5,34	14,51
19	1	0	-1	0	-1	10,83	10,14	8,87	9,95	19,86
20	1	0	0	-1	0	9,91	10,83	10,48	10,41	20,33
21	1	0	1	-1	1	6,45	5,76	9,10	7,10	16,56
22	1	1	-1	-1	1	8,52	8,41	7,72	8,22	18,27
23	1	1	0	-1	-1	15,21	14,28	13,82	14,44	23,17
24	1	1	1	0	0	11,98	13,48	12,44	12,63	22,00
25	1	-1	-1	-1	0	14,28	13,48	13,36	13,71	22,73
26	1	-1	0	0	1	14,63	12,79	13,59	13,67	22,68
27	1	-1	1	-1	-1	11,40	11,75	11,52	11,56	21,25

Table 5.2 ANOVA table for the mean flexural strength based on $L_{27}(3^{13})$ design

Source	df	Sum of Squares	Mean Square	F	P
A	2	82,918	41,459	12,29	0,012
B	2	64,731	32,365	9,60	0,019
C (B)	6	20,617	3,436	1,02	0,502
D	1	13,156	13,156	3,90	0,105
E	2	0,037	0,018	0,01	0,995
AB	4	4,012	1,003	0,30	0,868
BE	4	20,368	5,092	1,51	0,327
Error	5	16,864	3,373		
TOTAL	26	222,702			

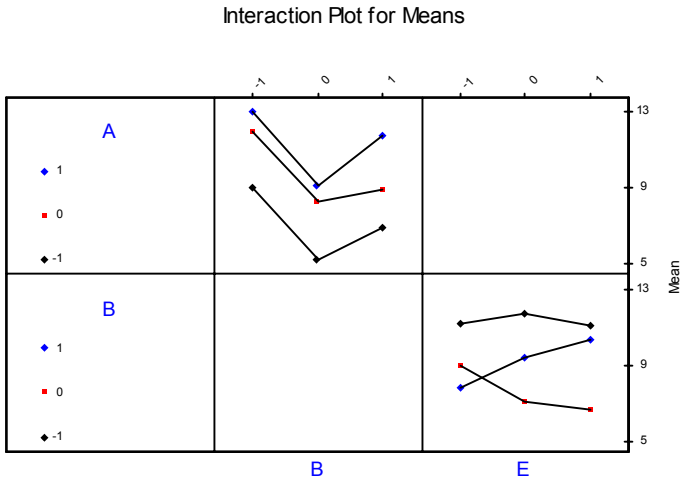

Figure 5.1 Two-way interaction plots for the mean flexural strength

The residual plots of the model for the mean flexural strength are given in Figures 5.2 and 5.3.

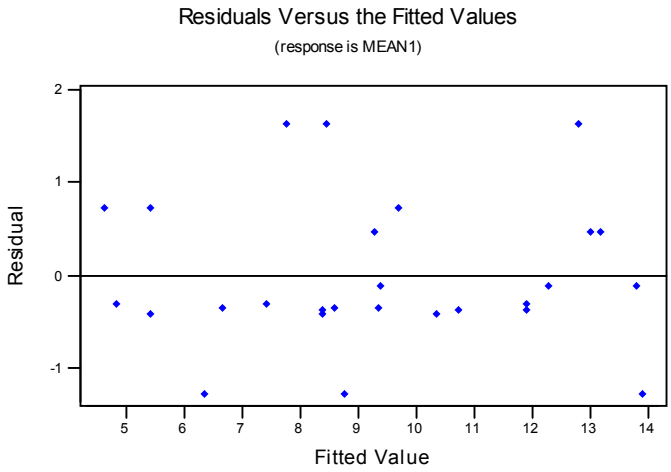

Figure 5.2 The residuals versus fitted values of the L_{27} (3^{13}) model found by ANOVA for the mean flexural strength

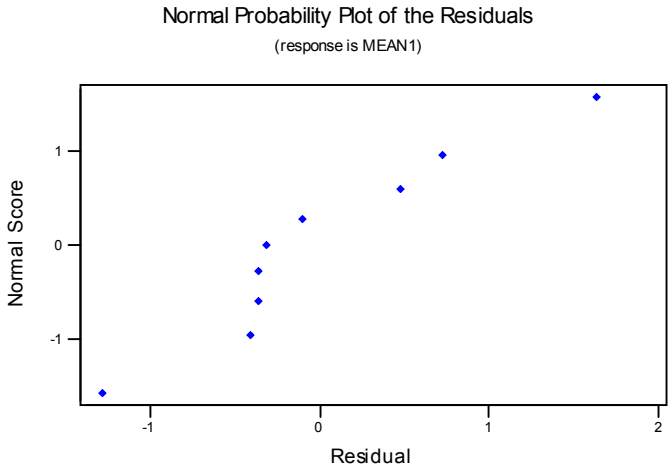

Figure 5.3 The residual normal probability plot for the L_{27} (3^{13}) model found by ANOVA for the mean flexural strength

Although most of the residuals are collected at the lower part of the residuals versus the fitted values plot in Figure 5.2, it can be concluded that the assumption of having a constant variance of the error term for all levels of the

independent process parameters is not violated because it can be assumed as patternless. However, there is not a linear trend in Figure 5.3 indicating the violation of the normal distribution of the error terms assumption.

As ANOVA shows that the main factor C(B) with AB interaction term are not significant within the experimental region. Therefore, a new ANOVA is performed by pooling only the interaction term to the error which is given in Table 5.3. When C(B) term is pooled, the model became worse. Although the main factor E is insignificant, it can not be pooled because of the slight significance of the BE interaction term.

Table 5.3 Pooled ANOVA of the mean flexural strength based on L_{27} (3^{13}) design

Source	df	Sum of Squares	Mean Square	F	P
A	2	82,918	41,459	17,87	0,001
B	2	64,731	32,365	13,95	0,002
C (B)	6	20,617	3,436	1,48	0,286
D	1	13,156	13,156	5,67	0,041
E	2	0,037	0,018	0,01	0,992
BE	4	20,368	5,092	2,20	0,150
Error	4	20,368	2,320		
TOTAL	26	222,702			

The results show that with $\alpha = 0.05$ significance, all the terms except the main factors binder amount and steel fiber volume fraction, are significant. However the binder amount term can be accepted as significant on the response with 71.4% confidence.

The residual plots of this new model for the mean flexural strength are given in Figures 5.4 and 5.5.

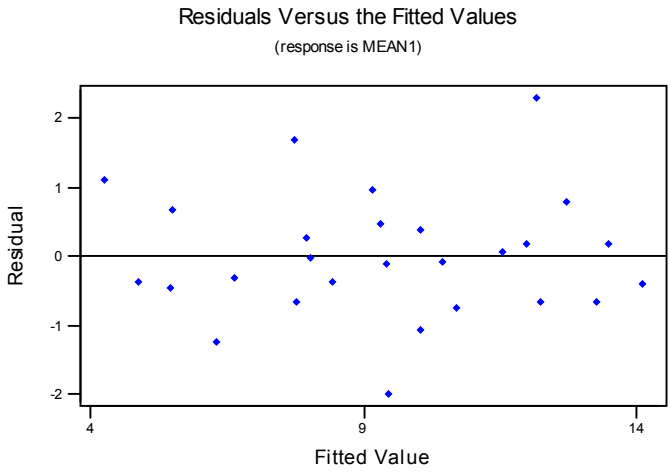

Figure 5.4 The residuals versus fitted values of the $L_{27}(3^{13})$ model found by the pooled ANOVA for the mean flexural strength

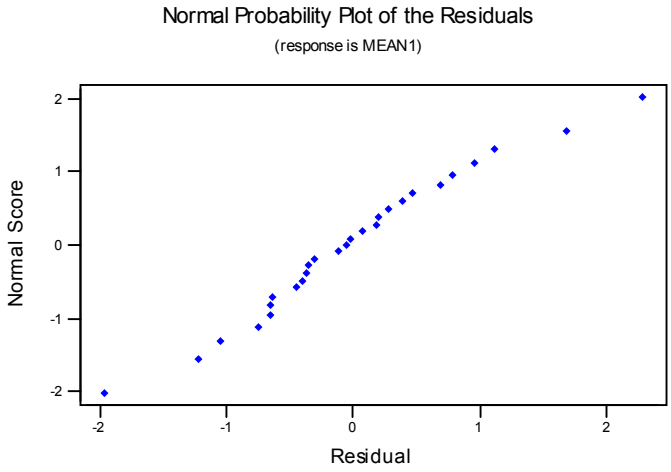

Figure 5.5 The residual normal probability plot for the $L_{27}(3^{13})$ model found by the pooled ANOVA for the mean flexural strength

When the insignificant term AB is pooled in the error, the constant variance and the normality assumptions of the error term are satisfied because Figure 5.4 is

patternless and Figure 5.5 is linear. Therefore the pooled model is decided to be kept and the prediction equation will be calculated for the pooled one.

Figure 5.6 shows the main effects plot which is used for finding the optimum levels of the process parameters that increase the mean flexural strength.

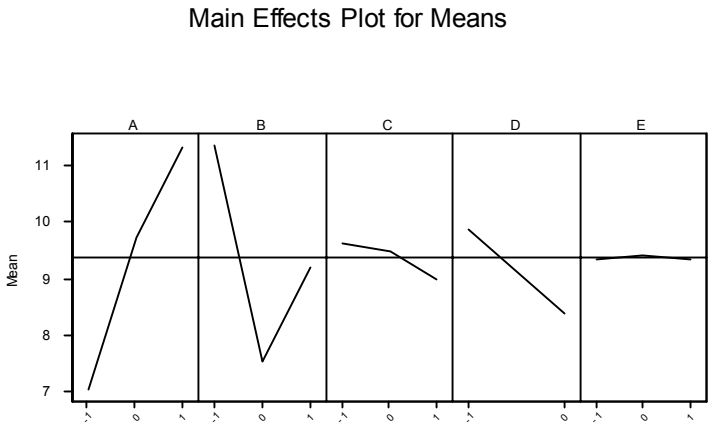

Figure 5.6 Main effects plot based on the $L_{27}(3^{13})$ design for the mean flexural strength

As it can be seen from Figure 5.6, the optimum points for the significant main factors are 3rd level for Age (90 days), 1st level for the Binder Type (Silica Fume), 1st level for the Binder Amount (20% as silica fume is selected for the binder type) and 1st level for Curing Type (ordinary water curing). Also it is needed to consider the significant two-way factor interactions when determining the optimum condition. From the interaction plot it can be seen that the optimum level for the interaction term is $B_{-1}xE_0$ which coincides with the optimum level of the main effect B. Although the main factor E is insignificant, it would be better to include it in the prediction equation because it should be used in the experiments. Therefore from the main effects plot (Figure 5.6), the

level that yield the highest flexural strength is the 2nd level for the Steel Fiber Volume Fraction (0.5%) which is in coincidence with the findings of the interaction table. However the 3rd level of steel fiber volume fraction (1.0%) can be used in the design since the line in the main effects plot is almost parallel for factor E. So, both combinations $A_1B_{-1}C_{-1}D_{-1}E_0$ and $A_1B_{-1}C_{-1}D_{-1}E_1$ will be calculated in the prediction equation below. The optimum performance is calculated by using the following expressions:

Combination 1: $A_1B_{-1}C_{-1}D_{-1}E_1$

$$\hat{\mu}_{A_1B_{-1}C_{-1}D_{-1}E_1} = \overline{T} + (\overline{A}_1 - \overline{T}) + (\overline{B}_{-1} - \overline{T}) + (\overline{C}_{-1} - \overline{T}) + (\overline{D}_{-1} - \overline{T}) + (\overline{E}_1 - \overline{T}) + (\overline{B_{-1} \times E_1} - \overline{T}) \quad (5.1)$$

$$\hat{\mu}_{A_1B_{-1}C_{-1}D_{-1}E_1} = \overline{T} + (\overline{A}_1 - \overline{T}) + (\overline{C}_{-1} - \overline{T}) + (\overline{D}_{-1} - \overline{T}) + (\overline{B_{-1}E_1} - \overline{T})$$

$$\hat{\mu}_{A_1B_{-1}C_{-1}D_{-1}E_1} = 9.36 + (11.30 - 9.36) + (9.63 - 9.36) + (9.85 - 9.36) + (11.11 - 9.36)$$

$$= 13.81 \text{ MPa}$$

$$n_e = \frac{27}{16.5+1} = 1.64$$

$$V_e = 2.32$$

$$F_{0.05,1,9} = 5.12$$

$$C.I. = \sqrt{\frac{5.12 \times 2.32}{1.64}} = 2.69$$

As a result the mean flexural strength should fall in between:

$\hat{\mu}_{A_1B_{-1}C_{-1}D_{-1}E_1}$ = {11.12, 16.50} with 95% confidence.

Combination 2: $A_1B_{-1}C_{-1}D_{-1}E_0$

$$\hat{\mu}_{A_1B_{-1}C_{-1}D_{-1}E_0} = \overline{T} + (\overline{A}_1 - \overline{T}) + (\overline{B}_{-1} - \overline{T}) + (\overline{C}_{-1} - \overline{T}) + (\overline{D}_{-1} - \overline{T}) + (\overline{E}_0 - \overline{T}) + (\overline{B_{-1} \times E_0} - \overline{T}) \quad (5.2)$$

$$\hat{\mu}_{A_1B_{-1}C_{-1}D_{-1}E_0} = \overline{T} + (\overline{A}_1 - \overline{T}) + (\overline{C}_{-1} - \overline{T}) + (\overline{D}_{-1} - \overline{T}) + (\overline{B_{-1}E_0} - \overline{T})$$

$$\hat{\mu}_{A_1B_{-1}C_{-1}D_{-1}E_0} = 9.36 + (11.30 - 9.36) + (9.63 - 9.36) + (9.85 - 9.36) + (11.74 - 9.36)$$
$$= 14.44 \text{ MPa}$$

The value of the confidence interval is the same for all combinations which is calculated above as 2.69. As a result, the value for the mean flexural strength should fall in between:

$\hat{\mu}_{A_1B_{-1}C_{-1}D_{-1}E_0}$ = {11.75, 17.13} with 95% confidence.

Since the result of combination 2 gives higher flexural strength than combination 1, $A_1B_{-1}C_{-1}D_{-1}E_0$ is selected as the optimum setting for which the confirmation experiment's results are expected to be between {11.75, 17.13} with 95% confidence.

The ANOVA results of the S/N ratio values can be seen in Table 5.4. The results of the ANOVA show that from the main factors, only A and B are significant on the S/N ratio of the flexural strength with 95% confidence. Also factor D and the interaction term BE are accepted as significant with 77.4% and 69.6% confidences respectively. Figure 5.7 shows all the two-way factor interaction plots. As it can be seen from the figure that the three lines of AB seems almost parallel and does not contribute to the response. Whereas the contribution of BE is larger since the lines in the corresponding plot are

intersecting each other. Also in the ANOVA table, the relatively small p-value of BE interaction supports this.

Table 5.4 ANOVA of S/N ratio values of the flexural strength based on L_{27} (3^{13}) design

Source	df	Sum of Squares	Mean Square	F	P
A	2	86,249	43,125	11,30	0,014
B	2	68,771	34,386	9,01	0,022
C (B)	6	25,515	4,253	1,11	0,462
D	1	7,280	7,280	1,91	0,226
E	2	0,011	0,005	0,00	0,999
AB	4	4,153	1,038	0,27	0,884
BE	4	24,558	6,139	1,61	0,304
Error	5	19,080	3,816		
TOTAL	26	235,617			

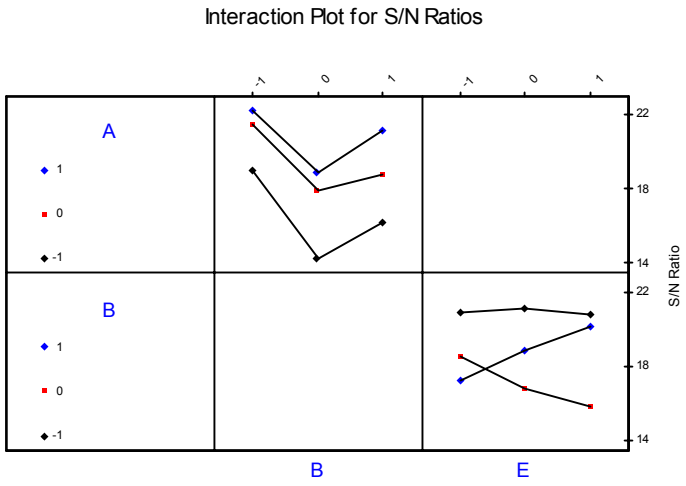

Figure 5.7 Two-way interaction plots for the S/N values of flexural strength

The residual plots for S/N ratio can be seen in Figures 5.8 and 5.9.

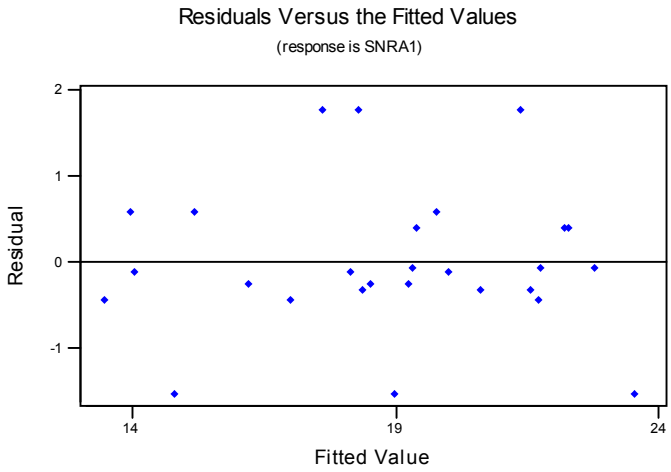

Figure 5.8 The residuals versus fitted values of the L_{27} (3^{13}) model found by ANOVA for S/N ratio for flexural strength

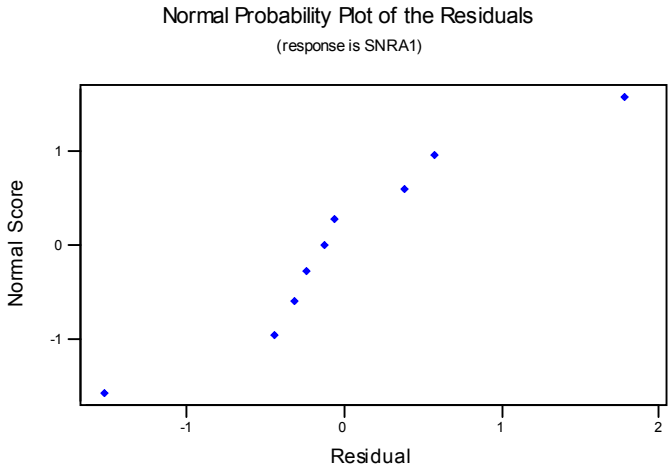

Figure 5.9 The residual normal probability plot for the L_{27} (3^{13}) model found by ANOVA for S/N ratio for flexural strength

Figure 5.8 seems patternless and Figure 5.9 is close to linear. Therefore, the error terms have constant variance and distributed normally.

As ANOVA shows that the main factor C(B) with interaction BE are not significantly contributing to the response. Therefore a new ANOVA is performed by pooling these terms to the error which is given in Table 5.5. However, factor C(B) is not pooled because the model becomes worse. Although the main factor E is insignificant, it can not be pooled because of the significance of the AE interaction term.

Table 5.5 Pooled ANOVA of the S/N values for the flexural strength based on $L_{27}(3^{13})$ design

Source	df	Sum of Squares	Mean Square	F	P
A	2	86,249	43,125	16,71	0,001
B	2	68,771	34,386	13,32	0,002
C (B)	6	25,515	4,253	1,65	0,240
D	1	7,280	7,280	2,82	0,127
E	2	0,011	0,005	0,00	0,998
BE	4	24,558	6,139	2,38	0,129
Error	9	23,232	2,581		
TOTAL	26	235,617			

This model caused the C(B) and D main terms and BE interaction term to be significant with 76%, 87.3% and 87.1% confidence respectively. The residual plots can be seen in Figures 5.10 and 5.11. When the residual plots are examined it can easily be seen that the normal plot is linear and the normality assumption holds. No obvious pattern is observed in the residuals versus the fitted values graph of the pooled model. Therefore the constant variance assumption of the error is satisfied. The pooled model seems more adequate than the unpooled model. So the prediction equation for S/N values will be calculated for the pooled model.

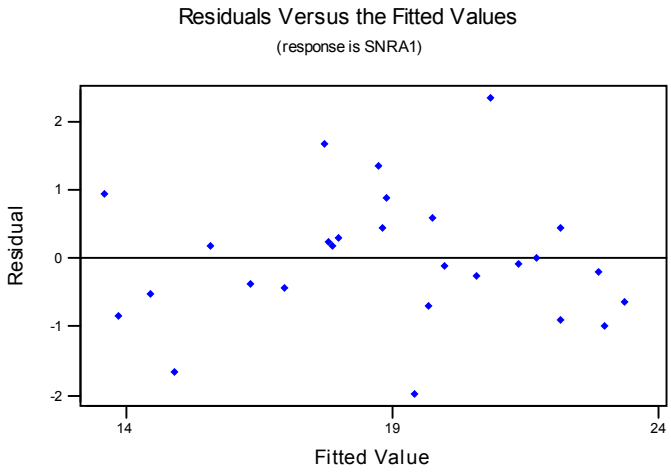

Figure 5.10 The residuals versus fitted values of the L_{27} (3^{13}) model found by the pooled ANOVA for the S/N ratio of flexural strength

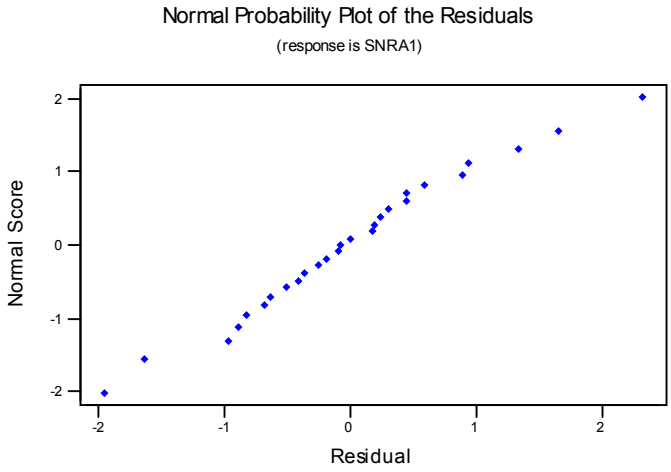

Figure 5.11 The residual normal probability plot for the L_{27} (3^{13}) model found by the pooled ANOVA for the S/N ratio of flexural strength

From the main effects plot in Figure 5.12, the optimum points are 3rd level for Age (90 days), 1st level for Binder Type (silica fume), 1st level for Binder Amount (20%), 1st level for Curing Type (water curing) and 2nd level for Steel

Fiber Volume Fraction (0.5% vol.). Although factors D and E are insignificant, they should be included in the prediction equation because without these main factors the experiments can not be conducted. From the interaction plot it is concluded that all the optimal levels of the factors are in coincidence with the determined values above. The best points for the BE interaction corresponds to the 2nd level of steel fiber volume fraction and the 1st level of binder type. However there is no significant difference between all the levels of factor E, in other words they contribute to the flexural strength nearly the same amount. Therefore anyone of the three levels can be selected in the calculation of the prediction equation. For convenience, the prediction equation will be computed for $A_1B_{-1}C_{-1}D_{-1}E_0$ and $A_1B_{-1}C_{-1}D_{-1}E_1$.

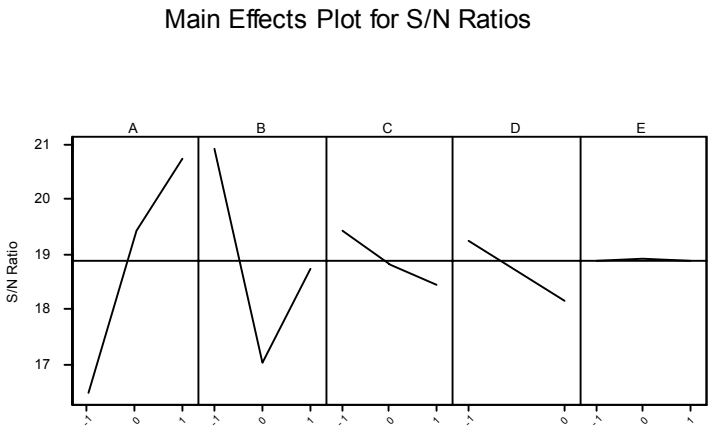

Figure 5.12 Main effects plot based on the L_{27} (3^{13}) design for S/N ratio for flexural strength

Combination 1: $A_1B_{-1}C_{-1}D_{-1}E_1$

$$\eta = \overline{T} + (\overline{A}_1 - \overline{T}) + (\overline{B}_{-1} - \overline{T}) + (\overline{C}_{-1} - \overline{T}) + (\overline{D}_{-1} - \overline{T}) + (\overline{E}_1 - \overline{T}) + (\overline{B_{-1} \times E_1} - \overline{T}) \quad (5.3)$$

$$\eta = \overline{T} + (\overline{A}_1 - \overline{T}) + (\overline{C}_{-1} - \overline{T}) + (\overline{D}_{-1} - \overline{T}) + (\overline{B_{-1}E_1} - \overline{T})$$

η = 18.89 + (20.76 – 18.89) + (19.42 – 18.89) + (19.26 – 18.89) + (20.75 – 18.89)

= 23.52 MPa

$$n_e = \frac{27}{16.5+1} = 1.64$$

$V_e = 2.58$

$F_{0.05,1,9} = 5.12$

$$C.I. = \sqrt{\frac{5.12 \times 2.58}{1.64}} = 2.84$$

As a result the mean flexural strength should fall in between:

η = {20.68, 26.36} with 95% confidence.

Combination 2: $A_1B_{-1}C_{-1}D_{-1}E_0$

$$\eta = \overline{T} + (\overline{A}_1 - \overline{T}) + (\overline{B}_{-1} - \overline{T}) + (\overline{C}_{-1} - \overline{T}) + (\overline{D}_{-1} - \overline{T}) + (\overline{E}_0 - \overline{T}) + (\overline{B_{-1} \times E_0} - \overline{T}) \quad (5.4)$$

$$\eta = \overline{T} + (\overline{A}_1 - \overline{T}) + (\overline{C}_{-1} - \overline{T}) + (\overline{D}_{-1} - \overline{T}) + (\overline{B_{-1}E_0} - \overline{T})$$

η = 18.89 + (20.76 – 18.89) + (19.42 – 18.89) + (19.26 – 18.89) + (21.12 – 18.89)

= 23.89 MPa

The value of the confidence interval is the same for all combinations which is calculated above as 2.84. As a result, the value for the mean flexural strength should fall in between:

η = {21.05, 26.73} with 95% confidence.

The confirmation experiment is performed for $A_1B_{-1}C_{-1}D_{-1}E_0$ combination three times. The results of the confirmation experiment yield the values of 14.28 MPa, 13.48 MPa and 13.36 MPa with an S/N ratio of 22.73. All of the results are in the confidence interval and 14.28 MPa is very close to the predicted optimum value found by Taguchi analysis which is 14.44 MPa. Also the S/N value calculated from the results of the confirmation experiments falls in the confidence interval of S/N ratio obtained by Taguchi analysis. As a result, it can be concluded that these results lead to the confirmation of the optimum setting $A_1B_{-1}C_{-1}D_{-1}E_0$ found by using the Taguchi method.

The confirmation trials are performed for $A_1B_{-1}C_{-1}D_{-1}E_1$ combination also in order to show that this combination can be also be selected due to the results of compressive strength and therefore to show that there is not so much difference in between the two. The results of the confirmation experiment yield the values of 14.05 MPa, 15.09 MPa and 13.71 MPa with an S/N ratio of 23.08 which are greater than the selected optimum combination above. All of the results are in the confidence interval and they are above the predicted optimum value found by Taguchi analysis which is 13.81 MPa. Also the S/N value calculated from the results of the confirmation experiments falls in the confidence interval of S/N ratio obtained by Taguchi analysis. As a result, it can be concluded that the confirmation runs for this combination gave better results and this combination can also be selected as optimum.

5.1.2 Regression Analysis of the Mean Flexural Strength Based on the L_{27} (3^{13}) Design

The first employed regression analysis to model the mean flexural strength contains only the main factors. That is:

$$y = 11,8 + 2,12*A - 3,78*B_1 - 2,16*B_2 - 0,323*C - 1,48*D_1 - 0,019*E \quad (5.5)$$

Table 5.6 shows the ANOVA for the significance of the above regression model. The hypothesis of having all β terms equal to zero is tested and refused with a confidence level of (1 – p)*100%, which is almost 100% for this model.

Table 5.6 ANOVA for the significance of the regression model developed for the mean flexural strength based on L_{27} (3^{13}) design

Source	df	Sum of Squares	Mean Squares	F	P
Regression	6	160,899	26,816	8,68	0,000
Residual Error	20	61,803	3,090		
Total	26	222,702			

$R^2 = 72.2\%$ $R^2_{(adj)} = 63.9\%$ $S = 1.758$

Durbin-Watson statistic = 2.18

The adjusted multiple coefficient of determination, $R^2_{(adj)}$, shows that only 64% of the sample variation in the mean flexural strength can be explained by this model. The Durbin-Watson statistic states that there is not enough information to reach any conclusion about the presence of residual correlation. Because, (4 - Durbin-Watson statistic), which is 1.82, is in between the tabulated lower bound (d_L), which is 1.01 and upper bound (d_U), which is 1.86 with 5 independent variables and 27 observations with 95% confidence. The residual plots of this model are given in Figures 5.13 and 5.14. Although it is concluded from the residual plots that there is not any indication of violation of the assumptions of the error, a more adequate regression model will be searched to describe the mean flexural strength. The significance of β terms of the model is shown in Table 5.7. This table indicates that Age, Binder Type and Curing Type are significant at the p(0.05) level of significance.

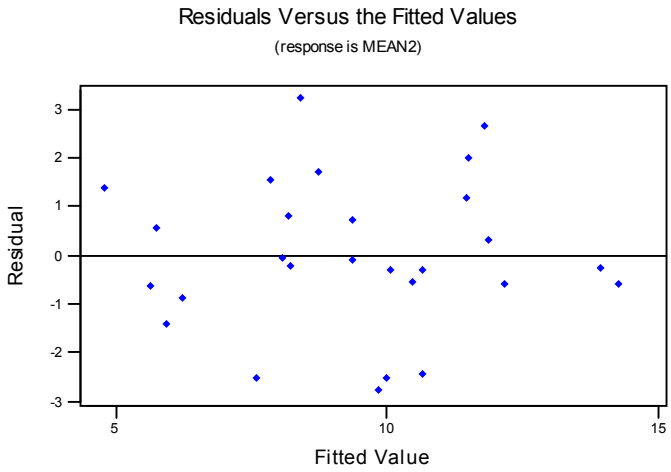

Figure 5.13 Residuals versus fitted values plot of the regression model based on L_{27} (3^{13}) design and developed for the mean flexural strength with only main factors

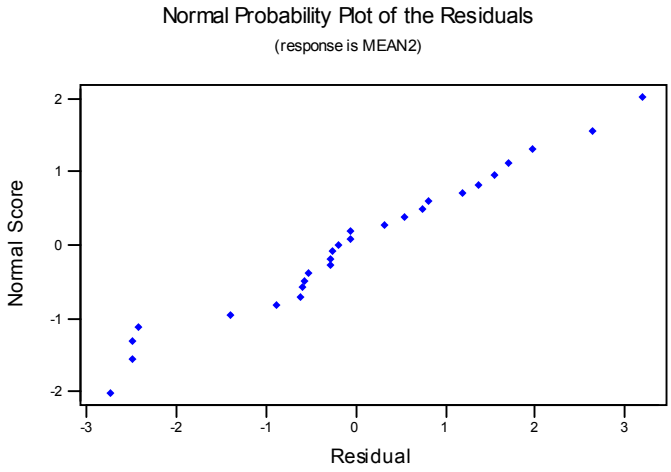

Figure 5.14 Residual normal probability plot of the regression model based on L_{27} (3^{13}) design and developed for the mean flexural strength with only main factors

Table 5.7 Significance of β terms of the regression model based on L_{27} (3^{13}) design and developed for the mean flexural strength with only main factors

Predictor	β Estimate	Standard Error	T	P
Constant	11,8309	0,6337	18,67	0,000
A	2,1239	0,4150	5,12	0,000
B_1	-3,7825	0,8301	-4,56	0,000
B_2	-2,1570	0,8301	-2,60	0,017
C	-0,3234	0,4150	-0,78	0,445
D_1	-1,4786	0,7192	-2,06	0,053
E	-0,0194	0,4301	-0,05	0,965

The MINITAB output with the sequential sum of squares of the regression model can be seen in Appendix C.1.

The second regression model is decided to include all the two-way interaction terms. Because the experimental design has only 26 degrees of freedom, all of the variables can not be included in the model since they exceed the 26 degrees of freedom. Therefore a pre-analysis is performed and it is seen that ACB_2, AEB_2, CEB_2 and except from AD_1 and CD_1, all the interactions with D_1 variable are insignificant. As a result they are omitted form the model. The equation and the ANOVA table for the regression model can be seen in Eqn. 5.6 and Table 5.8 respectively. By this model with 95.9% confidence the hypothesis that all β terms are equal to zero is rejected.

$$y = 12,8 + 1,97*A - 5,09*B_1 - 3,42*B_2 + 0,006*C - 3,74*D_1 + 0,175*E + 1,21*AC - 0,96*AE - 1,32*CE + 3,23*B_1D_1 + 3,10*B_2D_1 + 0,304*AB_1 - 1,66*CB_1 - 1,63*EB_1 - 2,38*ACB_1 + 0,40*AEB_1 + 2,15*CEB_1 + 1,61*AB_2 + 0,63*CB_2 + 0,24*EB_2 - 1,11*AD_1 + 0,40*CD_1 \quad (5.6)$$

Table 5.8 ANOVA for the significance of the regression model developed for the mean flexural strength based on L_{27} (3^{13}) design including main and interaction factors

Source	df	Sum of Squares	Mean Squares	F	P
Regression	22	216,584	9,845	6,44	0,041
Residual Error	4	6,117	1,529		
Total	26	222,702			

R^2 = 97.3% $R^2_{(adj)}$ = 82.1% S = 1.237

Durbin-Watson statistic = 2.22

By this model a considerable improvement is achieved when compared with the previous one. The $R^2_{(adj)}$ value is raised from 63.9% to 82.1% which explains the sample variation in the mean flexural strength adequately. But the Durbin-Watson statistic is deviated from 2 more than the previous model. Nevertheless it is still in between the tabulated lower and upper bounds meaning that there is not enough information to say that the residual are correlated. The difference between R^2 and $R^2_{(adj)}$ value is an evidence of the unnecessary terms in the model.

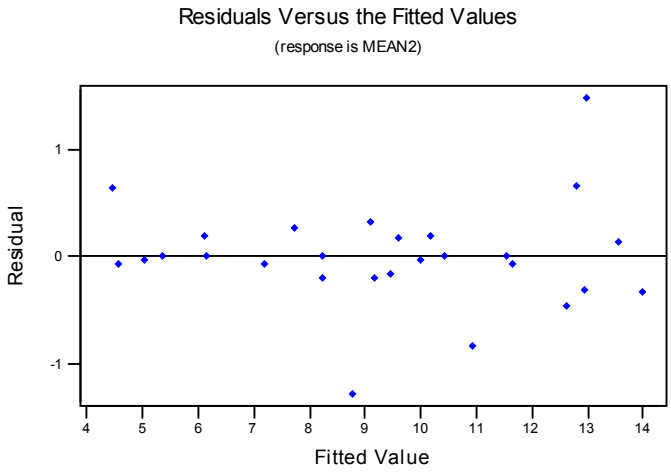

Figure 5.15 Residuals versus fitted values plot of the regression model in Eqn.5.6 developed for the mean flexural strength

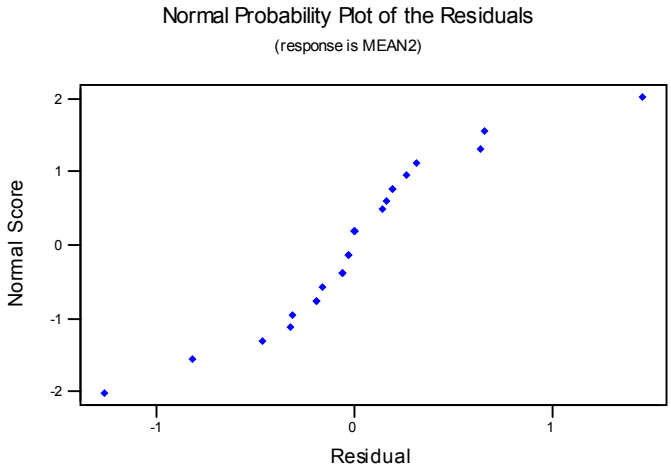

Figure 5.16 Residual normal probability plot of the regression model in Eqn.5.6 developed for the mean flexural strength

There is a significant pattern in the residuals versus fitted values plot, it resembles an arrow, indicating that the constant variance assumption may be violated. But the residual normal probability plot is linear and therefore the

normal distribution assumption of the error is satisfied. As a result a more adequate model explaining the mean response should be achieved by pooling the unnecessary terms. Table 5.9 shows the significance of the β terms.

Table 5.9 Significance of β terms of the regression model in Eqn.5.6 developed for the mean flexural strength

Predictor	β Estimate	Standard Error	T	P
Constant	12,8153	0,6130	20,91	0,000
A	1,9700	1,3400	1,47	0,215
B_1	-5,0929	0,8064	-6,32	0,003
B_2	-3,4240	0,9730	-3,52	0,024
C	0,0056	0,8045	0,01	0,995
D_1	-3,7360	1,3080	-2,86	0,046
E	0,1752	0,9115	0,19	0,857
AC	1,2100	1,5180	0,80	0,470
AE	-0,9610	1,2530	-0,77	0,486
CE	-1,3220	1,1960	-1,11	0,331
B_1D_1	3,2350	1,6280	1,99	0,118
B_2D_1	3,1050	2,318	1,34	0,251
AB_1	0,3042	0,9178	0,33	0,757
CB_1	-1,6630	0,9448	-1,76	0,153
EB_1	-1,6280	1,2120	-1,34	0,250
ACB_1	-2,3810	2,7460	-0,87	0,435
AEB_1	0,3980	1,1570	0,34	0,748
CEB_1	2,1510	1,2510	1,72	0,161
AB_2	1,6110	1,8480	0,87	0,432
CB_2	0,6270	1,0980	0,57	0,598
EB_2	0,2430	1,7260	0,14	0,895
AD_1	-1,1060	1,8390	-0,60	0,580
CD_1	0,3970	1,4640	0,27	0,800

The MINITAB output with the sequential sum of squares of the regression model can be seen in Appendix C.2.

It can be seen from the small p-values that, only the factors B_1, B_2, D_1, B_1D_1, CB_1, CEB_1, A, EB_1 and B_2D_1 are significant on the mean flexural strength. The model can be improved by discarding the insignificant terms from the model one by one starting from the term having the largest p-value. After eliminating a factor, all the normality, constant variance and error correlation assumptions are checked and the best model is chosen.

The best model is achieved by pooling EB_2, CD_1, AEB_1, CB_2 in the error term and by adding ACB_2 and ED_1 terms into the model. This model is much more adequate for explaining the mean flexural strength of SFRHSC whose regression equation, ANOVA table, residual plots and β significance test are given in Eqn.5.7, Table 5.10, Figures 5.17 and 5.18, and Table 5.11 respectively.

$$y = 12{,}8 + 2{,}58*A - 5{,}07*B_1 - 3{,}31*B_2 + 0{,}375*C - 3{,}90*D_1 + 0{,}048*E + 1{,}73*AC - 1{,}30*AE - 0{,}83*CE + 3{,}41*B_1D_1 + 2{,}98*B_2D_1 + 0{,}171*AB_1 - 1{,}86*CB_1 - 1{,}80*EB_1 - 3{,}53*ACB_1 + 1{,}54*CEB_1 + 1{,}03*AB_2 - 0{,}39*ACB_2 - 2{,}00*AD_1 + 0{,}65*ED_1 \quad (5.7)$$

Table 5.10 ANOVA for the significance of the best regression model developed for the mean flexural strength based on the $L_{27}(3^{13})$ design

Source	df	Sum of Squares	Mean Squares	F	P
Regression	20	216,116	10,806	9,84	0,005
Residual Error	6	6,586	1,098		
Total	26	222,702			

$R^2 = 97.0\%$ $R^2_{(adj)} = 87.2\%$ $S = 1.048$

Durbin-Watson statistic = 2.15

Although R^2 is decreased from 97.3% to 97.0%, $R^2_{(adj)}$ is raised from 82.1% to 87.2% which is enough to explain the response. Also, R^2 and adjusted R^2 gets closer to each other meaning that there is not any indication of unnecessary terms in the model. The Durbin-Watson statistic becomes 2.15 by this best model and this can be accepted as no indication of residual correlation since it is close to 2. Also Table 5.10 shows that this model has 95% confidence of refusing the hypothesis of having all β terms equal to zero.

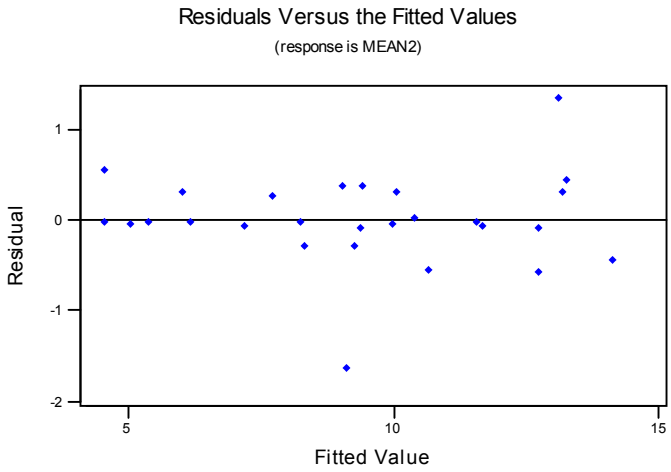

Figure 5.17 Residuals versus fitted values plot of the best regression model in Eqn.5.7 developed for the mean flexural strength

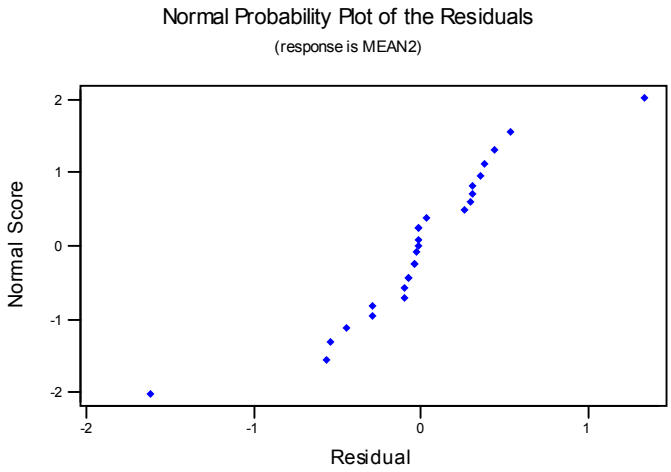

Figure 5.18 Residual normal probability plot of the best regression model in Eqn.5.7 developed for the mean flexural strength

The residuals normal probability and the residuals versus the fitted values plots do not indicate any deviation from the assumptions of the error although Figure 5.18 is a little wavy. When the β significance test is examined, factors E, AB_1, ACB_2 and ED_1 still have large p-values. But E and AB_1 can not be pooled into the error term because the interaction terms containing these main factors such as AE, CE, EB_1, ACB_1, etc. are significant on the response. When ACB_2 is pooled, the model becomes worse, so it is kept in the regression equation.

Table 5.11 Significance of β terms of the best regression model in Eqn.5.7 developed for the mean flexural strength

Predictor	β Estimate	Standard Error	T	P
Constant	12,7944	0,5026	25,46	0,000
A	2,5760	0,9152	2,81	0,031
B_1	-5,0743	0,6664	-7,61	0,000
B_2	-3,3080	0,8443	-3,92	0,008
C	0,3751	0,3160	1,19	0,280
D_1	-3,8992	0,9838	-3,96	0,007
E	0,0485	0,5957	0,08	0,938
AC	1,7290	0,8888	1,95	0,100
AE	-1,3020	0,9337	-1,39	0,213
CE	-0,8290	1,0160	-0,82	0,445
B_1D_1	3,4050	1,2740	2,67	0,037
B_2D_1	2,9830	1,7750	1,68	0,144
AB_1	0,1710	0,7135	0,24	0,819
CB_1	-1,8603	0,5831	-3,19	0,019
EB_1	-1,8024	0,6871	-2,62	0,039
ACB_1	-3,5340	1,4250	-2,48	0,048
CEB_1	1,5400	1,6290	0,95	0,381
AB_2	1,3040	1,0590	0,98	0,367
ACB_2	-0,3870	1,5660	-0,25	0,813
AD_1	-1,9990	1,0630	-1,88	0,109
ED_1	0,6540	1,2340	0,53	0,615

As a result this model is decided to be kept as the most adequate model explaining the mean flexural strength of the SFRHSC. The MINITAB output with the sequential sum of squares of the best regression model can be seen in Appendix C.3.

5.1.3 Response Surface Optimization of Mean Flexural Strength Based on the L_{27} (3^{13}) Design

For the MINITAB response optimization the best regression model found in Eqn.5.7 in the previous section for the mean flexural strength will be used. In literature the usual flexural strength obtained for SFRHSC is around 6.0 MPa and the maximum one reached is around 15 MPa. So, for flexural strength in MINITAB Response Optimizer, the lower bound is set to 6.0 MPa and the target value is set to 15 MPa.

The same thirteen starting points which were used in the response optimization process of the mean compressive strength are used in the maximization of the mean flexural strength also. The results of the optimizer can be seen in Table 5.12. The starting points and the optimum points found by MINITAB response optimizer is shown in Table 5.13.

Table 5.12 The optimum response, its desirability, the confidence and prediction intervals computed by MINITAB Response Optimizer for the mean flexural strength based on the L_{27} (3^{13}) design

Optimum Points	Mean Flex.	Desirability	95% Conf. Int.	95% Pred. Int.
1	12,907	0,77470	(8,019; 17,795)	(7,388; 18,427)
2	13,690	0,85652	(7,223; 20,158)	(6,733; 20,648)
3	12,907	0,77470	(8,019; 17,795)	(7,388; 18,427)
4	11,379	0,60774	(7,297; 15,461)	(6,558; 16,200)
5	15,391	1,00000	(11,569; 19,214)	(10,789; 19,995)
6	14,377	0,93127	(10,580; 18,175)	(9,795; 18,960)
7	9,976	0,30585	(7,889; 12,062)	(6,670; 13,282)
8	12,730	0,75867	(10,397; 15,063)	(9,263; 16,197)
9	12,907	0,77470	(8,019; 17,795)	(7,388; 18,427)
10	10,469	0,49499	(5,380; 15,557)	(4,771; 16,167)
11	14,117	0,90712	(11,781; 16,453)	(10,648; 17,586)
12	11,078	0,58671	(5,124; 17,033)	(4,595; 17,562)
13	13,699	0,85792	(7,408; 19,990)	(6,871; 20,482)

Table 5.13 The starting and optimum points for MINITAB response optimizer developed for the mean flexural strength based on the L_{27} (3^{13}) design

	Starting Points					Optimum Points				
Points	**Age (days)**	**B. Type**	**B. Amount (%)**	**Cure**	**Steel (% vol.)**	**Age (days)**	**B. Type**	**B. Amount (%)**	**Cure**	**Steel (% vol.)**
1	90	SF	20	water	1,0	90	SF	20	water	1,0
2	No starting point					90	SF	20	water	0,0
3	90	SF	20	steam	0,5	90	SF	20	water	1,0
4	90	GGBFS	20	water	0,5	90	GGBFS	20	water	0,5
5	90	SF	10	water	1,0	90	SF	10	water	1,0
6	28	FA	40	steam	0,5	90	FA	10	steam	0,0
7	7	SF	20	water	0,0	12,6	SF	20	water	0,0
8	90	GGBFS	60	water	1,0	90	GGBFS	60	water	1,0
9	90	FA	10	water	1,0	90	SF	20	water	1,0
10	28	GGBFS	20	steam	1,0	90	GGBFS	60	steam	1,0
11	90	SF	15	water	1,0	90	SF	15	water	1,0
12	90	GGBFS	20	steam	1,0	90	GGBFS	23	water	1,0
13	90	SF	20	water	0,0	90	SF	20	water	0,02

The starting point 5 gave the highest flexural strength which is 15.4 MPa and it is a little above the desired value of 15.0 MPa. Points 6 and 11 resulted in around 14.0 MPa flexural strength and their confidence and prediction intervals are narrower. Therefore confirmation runs will be performed for these two points also. The starting points 2 and 13 resulted in the third highest flexural strength, around 13.7 MPa, so they are worth to try. However the intervals of point 2 are too wide. The starting points 1, 3, 8 and 9 gave nearly the same result which is around 12.9 MPa. The confidence and prediction intervals of points 1, 3 and 9 are relatively wider but, point 8 has the narrowest intervals with point 11. The remaining points resulted in very low flexural strength values and therefore they are not taken into consideration for the confirmation experiments. Each experiment is repeated three times for convenience.

Optimum point 5:

For this experiment age, binder type, binder amount, curing type and steel fiber volume fraction are set to 90 days, Silica Fume, 10% for SF, ordinary water curing and 1.0% respectively. The results of the experiments are 14.40 MPa, 14.05 MPa and 13.59 MPa and all are in the confidence and prediction intervals with 95%. However all are below the predicted value of 15.4 MPa. It can be said that this point is well modeled by the chosen regression model but a little overestimated.

Optimum point 6:

For this experiment age, binder type, binder amount, curing type and steel fiber volume fraction are set to 90 days, Fly Ash, 10% for FA, steam curing and 0.0% respectively. The results of the experiments are 10.14 MPa, 9.68 MPa and 11.87 MPa. Only 11.87 falls into the confidence interval limits and 10.14 and 11.87 are in the prediction interval but they are closer to the lower limit. Also none of the results are near to the predicted optimum value of 14.4 MPa. So it can be said that this point is a little overestimated by the chosen regression

model. We could have an improvement by conducting the experiments of this point but this could not achieved.

Optimum point 11:

For this experiment age, binder type, binder amount, curing type and steel fiber volume fraction are set to 90 days, Silica Fume, 15% for SF, ordinary water curing and 1.0% respectively. The results of the experiments are 14.63 MPa, 12.79 MPa and 13.59 MPa. All the results are in the confidence and prediction intervals but their mean value, 13.67 MPa, is a little below the optimum predicted value found by the response optimizer which is 14.12 MPa. However the intervals of this point are one of the narrowest. Thus it can be said that this point is confirmed by the results of the experiments and well modeled.

Optimum points 2 and 13:

One confirmation experiment will be done for these two points since their optimum performance levels are very close. For these points the 3rd level for Age (90 days), 1st level for Binder Amount (Silica Fume), 1st level for Binder Amount (20% for silica fume), 1st level for Curing Type (ordinary water curing) and the 1st level for Steel Fiber Volume Fraction (0.0%) are assigned to the associated main factors. The results of the experiments are 14.63 MPa, 13.13 MPa and 12.33 MPa and all are in the confidence and prediction intervals of both points with 95%. However the intervals of both points are the widest ones. As a result, it can be said that these two points are well modeled by the chosen regression model because the results of the confirmation runs are around the optimum predicted values of 13.7 MPa.

Optimum points 1, 3 and 9:

One confirmation experiment will be done for these two points since they all resulted in the same optimum parameter level combination. For these points the

3rd level for Age (90 days), 1st level for Binder Amount (Silica Fume), 1st level for Binder Amount (20% for silica fume), 1st level for Curing Type (ordinary water curing) and the 3rd level for Steel Fiber Volume Fraction (1.0%) are assigned to the associated main factors. The results of the experiments are 14.05 MPa, 15.09 MPa and 13.71 MPa and all are in the confidence and prediction intervals of both points with 95%. However they are above the predicted value of 12.9 MPa which is found by the regression model. Thus, it can be concluded that these points are modeled but underestimated by the chosen regression model.

Optimum point 8:

For this experiment the 3rd level for Age (90 days), 3rd level for Binder Amount (GGBFS), 3rd level for Binder Amount (60% for SF), 1st level for Curing Type (ordinary water curing) and the 3rd level for Steel Fiber Volume Fraction (1.0%) are assigned to the associated main factors. The results of the experiments are 11.98 MPa, 13.48 MPa and 12.44 MPa. All the results are in the confidence and prediction intervals and their mean value, 12.44 MPa is very close to the optimum predicted value found by the response optimizer which is 12.73 MPa. Also this point has one of the narrowest confidence and prediction intervals. Therefore, it can be said that these results well confirm the findings of the regression analysis for point 8.

The best point is chosen for the result of the regression analysis of the mean flexural strength is the optimum 5, since its predicted value obtained by the Response Optimizer has reached to the desired value of 15.0 MPa. Also its intervals are relatively narrower when compared with the other points. However the confirmation runs could not reach to the predicted value obtained by the regression model. Therefore, the points 1, 3 and 9 can also be chosen because the results of the confirmation runs are very close to the results of point 5 even a little higher. So, the best modeled point that maximizes the flexural strength of

SFRHSC by the regression analysis has the combination of $A_1B_{-1}C_1D_{-1}E_1$, but $A_1B_{-1}C_{-1}D_{-1}E_1$ can also be chosen.

5.2 Full Factorial Experimental Design

As in Chapter 4, again in order to analyze the effects of all three-way, four-way and five-way interaction effects on all of the responses it is decided to conduct all the experiments for flexural strength needed for $3^4 2^1$ full factorial design and analysis.

5.2.1 Taguchi Analysis of the Mean Flexural Strength Based on the Full Factorial Design

The ANOVA table for the mean flexural strength can be seen in Table 5.14. Since the factor interactions between the nested factor and its primary factor are insignificant in nested designs, they are omitted from the model. It indicates that except from the three two-way interactions that are Age*Cure (AD), Age*Steel (AE) and Cure*Steel (DE), and one three-way interaction that is Age*Cure*Binder Amount (ADC(B)), all the remaining sources significantly affect the flexural strength of FRHSC since their F-ratio are greater than the tabulated F-ratio values of 95% confidence level. The insignificance of AD, AE, and DE interactions can also be seen from the two-way interaction plot given in Figure 5.19 since the three lines in the interaction plots are almost parallel.

Table 5.14 ANOVA table for the mean flexural strength based on the full factorial design

Source	df	Sum of Squares	Mean Square	F	P
A	2	1245,250	622,625	1052,88	0,000
B	2	1243,036	621,518	1051,01	0,000
C (B)	6	354,959	59,160	100,04	0,000
D	1	214,735	214,735	363,12	0,000
E	2	3,813	1,907	3,22	0,041
AB	4	43,491	10,873	18,39	0,000
AC(B)	12	48,541	4,045	6,84	0,000
AD	2	3,061	1,531	2,59	0,077
AE	4	2,710	0,677	1,15	0,335
BD	2	35,977	17,989	30,42	0,000
BE	4	176,609	44,152	74,66	0,000
DC(B)	6	22,825	3,804	6,43	0,000
EC(B)	12	138,741	11,562	19,55	0,000
DE	2	1,370	0,685	1,16	0,315
ABD	4	6,251	1,563	2,64	0,034
ABE	8	11,443	1,430	2,42	0,015
ADC(B)	12	11,372	0,948	1,60	0,089
AEC(B)	24	36,257	1,511	2,55	0,000
ADE	4	19,047	4,762	8,05	0,000
BDE	4	23,736	5,934	10,03	0,000
DEC(B)	12	45,859	3,822	6,46	0,000
ABDE	8	24,013	3,002	5,08	0,000
ADEC(B)	24	68,415	2,851	4,82	0,000
Error	324	191,599	0,591		
TOTAL	485	3973,111			

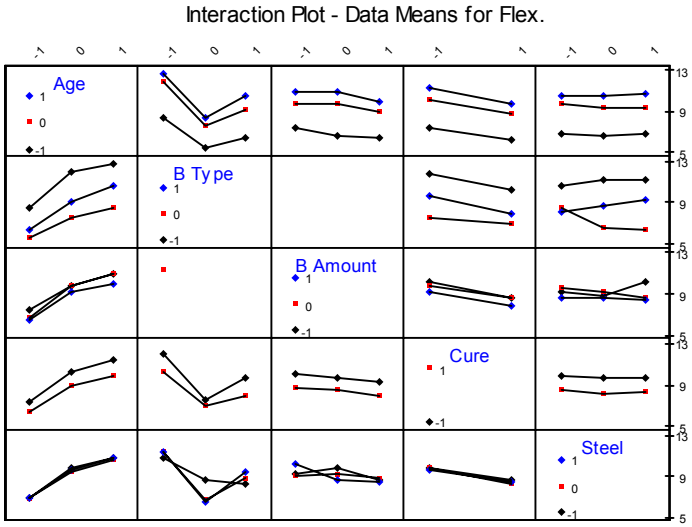

Figure 5.19 Two-way interaction plots for the mean flexural strength

The residual plots of the model for the mean flexural strength are given in Figures 5.20 and 5.21.

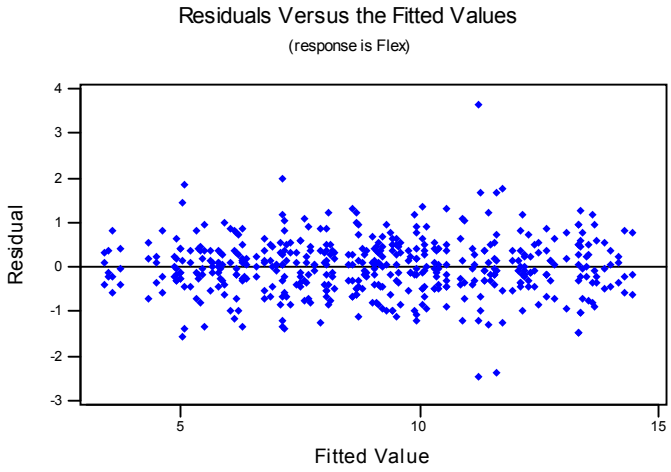

Figure 5.20 The residuals versus fitted values of the full factorial model found by ANOVA for the means for flexural strength

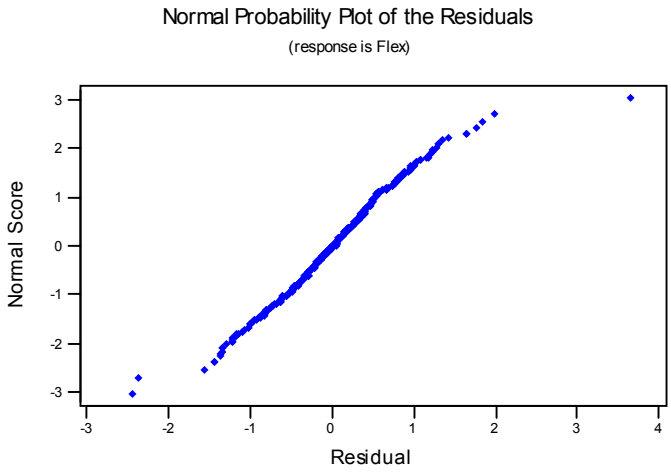

Figure 5.21 The residual normal probability plot for the full factorial model found by ANOVA for the means for flexural strength

It can be concluded from Figure 5.20 that the assumption of having a constant variance of the error term for all levels of the independent process parameters is not violated since there is no significant pattern. Also it can be seen from Figure 5.21 that there is a linear trend on the normal probability plot indicating that the assumption of the error term having a normal probability distribution is satisfied.

Figure 5.22 shows the main effects plot which is used for finding the optimum levels of the process parameters that increases the mean flexural strength.

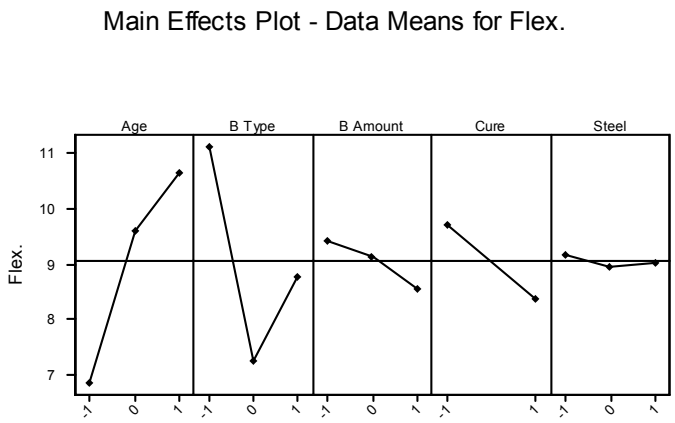

Figure 5.22 Main effects plot based on the full factorial design for the mean flexural strength

As it can be seen from Figure 5.22, the optimum points are 3rd level for Age (90 days), 1st level for the Binder Type (Silica Fume), 1st level for the Binder Amount (20% as silica fume is selected for the binder type), 1st level for Curing Type (water curing) and the 1st level for the Steel Fiber Volume Fraction (0.0%). From the interaction plot it can be seen that the optimum levels for the interaction terms are A_1xB_{-1}, $A_1xC(B)_{-1}$, $B_{-1}xD_{-1}$, $B_{-1}xE_1$, $D_{-1}xC(B)_{-1}$, $E_1xC(B)_{-1}$ which coincides with the optimum levels of the main effects except for factor E. Therefore the two combinations of the optimum levels should be calculated for both the 1st and 3rd level of factor E. The two combinations are $A_1B_{-1}C_{-1}D_{-1}E_{-1}$ and $A_1B_{-1}C_{-1}D_{-1}E_1$ respectively.

Combination 1: $A_1B_{-1}C_{-1}D_{-1}E_{-1}$ (experiment no. 109)

$$\begin{aligned}\hat{\mu}_{A_1B_{-1}C_{-1}D_{-1}E_{-1}} = {} & \overline{T} + (\overline{A}_1 - \overline{T}) + (\overline{B}_{-1} - \overline{T}) + (\overline{C}_{-1} - \overline{T}) + (\overline{D}_{-1} - \overline{T}) + (\overline{E}_{-1} - \overline{T}) + \\ & (\overline{A_1 \times B_{-1}} - \overline{T}) + (\overline{A_1 \times C_{-1}} - \overline{T}) + (\overline{B_{-1} \times D_{-1}} - \overline{T}) + (\overline{B_{-1} \times E_{-1}} - \overline{T}) \\ & + (\overline{C_{-1} \times D_{-1}} - \overline{T}) + (\overline{C_{-1} \times E_{-1}} - \overline{T})\end{aligned} \tag{5.8}$$

$$\hat{\mu}_{A_1B_{-1}C_{-1}D_{-1}E_{-1}} = \overline{T} - (\overline{A}_1 - \overline{T}) - 2(\overline{B}_{-1} - \overline{T}) - 2(\overline{C}_{-1} - \overline{T}) - (\overline{D}_{-1} - \overline{T}) - (\overline{E}_{-1} - \overline{T}) + (\overline{A_1B_{-1}} - \overline{T}) + (\overline{A_1C_{-1}} - \overline{T}) + (\overline{B_{-1}D_{-1}} - \overline{T}) + (\overline{B_{-1}E_{-1}} - \overline{T}) + (\overline{C_{-1}D_{-1}} - \overline{T}) + (\overline{C_{-1}E_{-1}} - \overline{T})$$

$$\hat{\mu}_{A_1B_{-1}C_{-1}D_{-1}E_{-1}} = 9.04 - (10.65 - 9.04) - 2\,(11.12 - 9.04) - 2\,(9.41 - 9.04) - (9.70 - 9.04) - (9.15 - 9.04) + (12.81 - 9.04) + (10.93 - 9.04) + (11.96 - 9.04) + (10.73 - 9.04) + (10.13 - 9.04) + (9.23 - 9.04)$$

$$= 13.31 \text{ MPa}$$

The confidence interval is:

$$n_e = \frac{486}{53+1} = 9.00$$

$V_e = 0.591$

$F_{0.05,1,324} = 3.84$

$$\text{C.I.} = \sqrt{\frac{3.84 \times 0.591}{9.00}} = 0.50$$

Therefore, the value of the mean flexural strength is expected in between;

$\hat{\mu}_{A_1B_{-1}C_{-1}D_{-1}E_{-1}}$ = {12.81, 13.81} with 95% confidence interval.

Combination 2: $A_1B_{-1}C_{-1}D_{-1}E_1$ (experiment no. 111)

$$\hat{\mu}_{A_1B_{-1}C_{-1}D_{-1}E_1} = \overline{T} + (\overline{A}_1 - \overline{T}) + (\overline{B}_{-1} - \overline{T}) + (\overline{C}_{-1} - \overline{T}) + (\overline{D}_{-1} - \overline{T}) + (\overline{E}_1 - \overline{T}) + (\overline{A_1 \times B_{-1}} - \overline{T}) + (\overline{A_1 \times C_{-1}} - \overline{T}) + (\overline{B_{-1} \times D_{-1}} - \overline{T}) + (\overline{B_{-1} \times E_1} - \overline{T}) + (\overline{C_{-1} \times D_{-1}} - \overline{T}) + (\overline{C_{-1} \times E_1} - \overline{T}) \quad (5.9)$$

$$\hat{\mu}_{A_1B_{-1}C_{-1}D_{-1}E_1} = \overline{T} - (\overline{A}_1 - \overline{T}) - 2(\overline{B}_{-1} - \overline{T}) - 2(\overline{C}_{-1} - \overline{T}) - (\overline{D}_{-1} - \overline{T}) - (\overline{E}_1 - \overline{T}) + (\overline{A_1B_{-1}} - \overline{T}) + (\overline{A_1C_{-1}} - \overline{T}) + (\overline{B_{-1}D_{-1}} - \overline{T}) + (\overline{B_{-1}E_1} - \overline{T}) + (\overline{C_{-1}D_{-1}} - \overline{T}) + (\overline{C_{-1}E_1} - \overline{T})$$

$$\hat{\mu}_{A_1B_{-1}C_{-1}D_{-1}E_1} = 9.04 - (10.65 - 9.04) - 2\,(11.12 - 9.04) - 2\,(9.41 - 9.04) - (9.70 - 9.04) - (9.03 - 9.04) + (12.81 - 9.04) + (10.93 - 9.04) + (11.96 - 9.04) + (11.32 - 9.04) + (10.13 - 9.04) + (10.12 - 9.04)$$

$$= 14.91 \text{ MPa}$$

The confidence interval is the same as the one calculated above, 0.50. Therefore, the value of the mean flexural strength is expected in between;

$\hat{\mu}_{A_1B_{-1}C_{-1}D_{-1}E_1}$ = {14.41, 15.41} with 95% confidence interval.

Since the maximum flexural strength is obtained by combination 2, the optimum levels are accepted as $A_1B_{-1}C_{-1}D_{-1}E_1$. This point corresponds to experiment 111 with a mean flexural strength of 14.28 MPa, which is an acceptable result according to Taguchi analysis.

In order to determine the most robust set of operating condition from variations within the results of flexural strength, ANOVA for the S/N ratio values are performed (Table 5.15). Again the four-way interaction term (ADEC(B)) is omitted in order to leave 24 degrees of freedom to the error term. The results of the ANOVA show that all the main factors, four two-way interactions that are Age*Binder Amount (AC(B)), Binder Type*Cure (BD), Binder Type*Steel (BE), Steel*Binder Amount (EC(B)), two three-way interactions which are Age*Cure*Steel (ADE) and Binder Type*Cure*Steel (BDE) and one four-way interaction that is Age*Binder Type*Cure*Steel (ABDE) are the significant factors with a 90% confidence interval. Figure 5.23 shows all the two-way factor interaction plots. As it can be seen from the figure that BE and EC(B) interactions significantly contribute to the flexural strength, whereas the

contributions of AC(B) and BD are lesser since the lines in the corresponding plots are more or less parallel. Also in the ANOVA table, the relatively small F-values of AC(B) and BD interactions support this. It is clear from the interaction plot that AB, AD, AE, DC(B) and DE have no significant effect on the flexural strength since the lines are parallel.

Table 5.15 ANOVA of S/N ratio values for the flexural strength based on the full factorial design

Source	df	Sum of Squares	Mean Square	F	P
A	2	461,606	230,803	273,46	0,000
B	2	449,238	224,619	266,13	0,000
C (B)	6	179,581	29,930	35,46	0,000
D	1	60,742	60,742	71,97	0,000
E	2	4,136	2,068	2,45	0,108
AB	4	5,008	1,252	1,48	0,238
AC(B)	12	21,024	1,752	2,08	0,062
AD	2	0,746	0,373	0,44	0,648
AE	4	0,589	0,147	0,17	0,949
BD	2	7,864	3,932	4,66	0,020
BE	4	78,644	19,661	23,29	0,000
DC(B)	6	7,973	1,329	1,57	0,198
EC(B)	12	58,174	4,848	5,74	0,000
DE	2	1,078	0,539	0,64	0,537
ABD	4	0,713	0,178	0,21	0,930
ABE	8	5,991	0,749	0,89	0,542
ADC(B)	12	6,252	0,521	0,62	0,807
AEC(B)	24	11,301	0,471	0,56	0,920
ADE	4	8,453	2,113	2,50	0,069
BDE	4	8,071	2,018	2,39	0,079
DEC(B)	12	13,686	1,140	1,35	0,255
ABDE	8	12,952	1,619	1,92	0,104
Error	24	20,256	0,844		
TOTAL	161	1424,081			

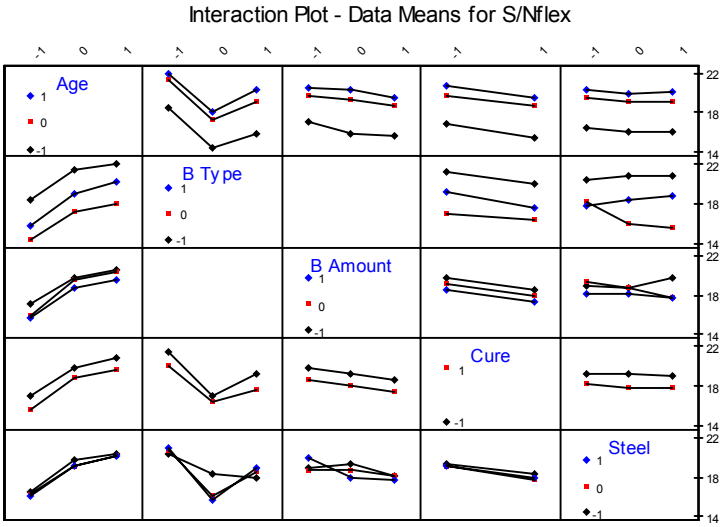

Figure 5.23 Two-way interaction plots for the S/N values of flexural strength

The residual plots for S/N ratio can be seen in Figures 5.24 and 5.25.

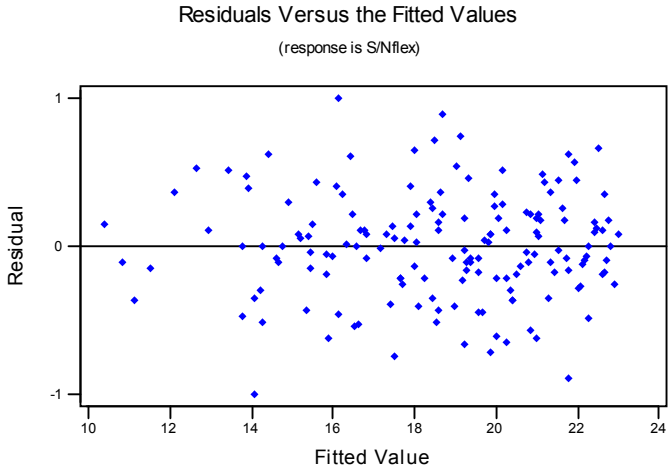

Figure 5.24 The residuals versus fitted values of the full factorial model found by ANOVA for S/N ratio for flexural strength

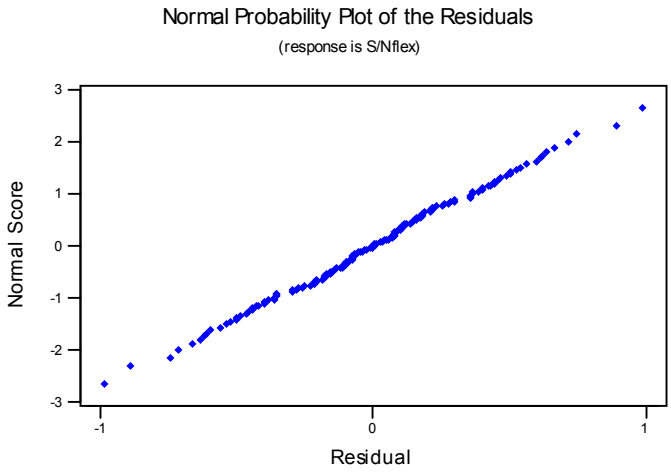

Figure 5.25 The residual normal probability plot for the full factorial model found by ANOVA for S/N ratio for flexural strength

Both figures show no abnormality for validation of the assumptions of the errors. It has constant variance and it is distributed normally.

From the main effects plot (Figure 5.26), the optimum points are 3rd level for Age (90 days), 1st level for Binder Type (silica fume), 1st level for Binder Amount (20%), 1st level for Curing Type (water curing) and 1st level for Steel Fiber Volume Fraction (0.0% vol.). But from the interaction plot it is concluded that all the optimal levels of the factors are in coincidence with the determined values above except from the level of Steel Fiber Volume Fraction. The best points for both of the BE and EC(B) interactions correspond to the 3rd level of steel fiber volume fraction. So the two different combinations should be computed for determining the optimum point which are $A_1B_{-1}C_{-1}D_{-1}E_{-1}$ and $A_1B_{-1}C_{-1}D_{-1}E_1$.

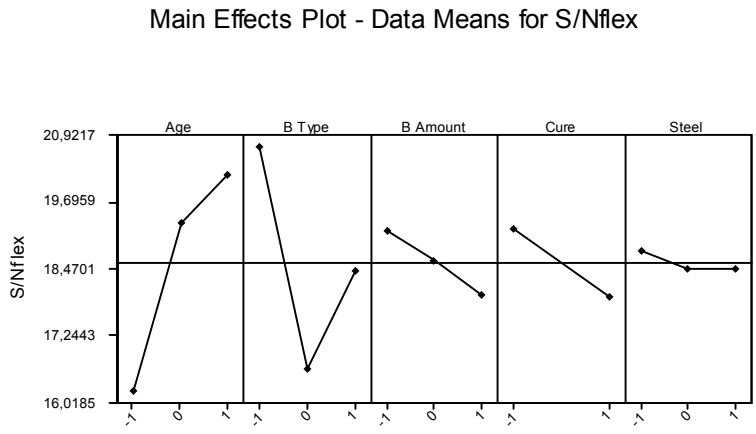

Figure 5.26 Main effects plot based on the full factorial design for S/N ratio for flexural strength

Combination 1: $A_1B_{-1}C_{-1}D_{-1}E_{-1}$ (experiment no. 109)

$$\eta = \overline{T} + (\overline{A}_1 - \overline{T}) + (\overline{B}_{-1} - \overline{T}) + (\overline{C}_{-1} - \overline{T}) + (\overline{D}_{-1} - \overline{T}) + (\overline{E}_{-1} - \overline{T}) + (\overline{A_1 \times C_{-1}} - \overline{T}) + (\overline{B_{-1} \times D_{-1}} - \overline{T}) + (\overline{B_{-1} \times E_{-1}} - \overline{T}) + (\overline{C_{-1} \times E_{-1}} - \overline{T}) \quad (5.10)$$

$$\eta = \overline{T} - (\overline{B}_{-1} - \overline{T}) - (\overline{C}_{-1} - \overline{T}) - (\overline{E}_{-1} - \overline{T}) + (\overline{A_1 C_{-1}} - \overline{T}) + (\overline{B_{-1} D_{-1}} - \overline{T}) + (\overline{B_{-1} E_{-1}} - \overline{T}) + (\overline{C_{-1} E_{-1}} - \overline{T})$$

$$\eta = 18.58 - (20.70 - 18.58) - (19.19 - 18.58) - (18.81 - 18.58) + (20.59 - 18.58) + (21.40 - 18.58) + (20.40 - 18.58) + (18.98 - 18.58)$$
$$= 22.67$$

$$n_e = \frac{162}{43+1} = 3.68$$

$V_e = 0.844$

$F_{0.05,1,24} = 4.26$

$$C.I. = \sqrt{\frac{4.26 \times 0.844}{3.68}} = 0.99$$

As a result the value for the S/N ratio should fall in between:

η = {21.68, 23.66} with 95% confidence.

Combination 2: $A_1B_{-1}C_{-1}D_{-1}E_1$ (experiment no. 111)

$$\eta = \overline{T} + (\overline{A}_1 - \overline{T}) + (\overline{B}_{-1} - \overline{T}) + (\overline{C}_{-1} - \overline{T}) + (\overline{D}_{-1} - \overline{T}) + (\overline{E}_1 - \overline{T}) + (\overline{A_1 \times C_{-1}} - \overline{T}) + (\overline{B_{-1} \times D_{-1}} - \overline{T}) + (\overline{B_{-1} \times E_1} - \overline{T}) + (\overline{C_{-1} \times E_1} - \overline{T}) \quad (5.11)$$

$$\eta = \overline{T} - (\overline{B}_{-1} - \overline{T}) - (\overline{C}_{-1} - \overline{T}) - (\overline{E}_1 - \overline{T}) + (\overline{A_1 C_{-1}} - \overline{T}) + (\overline{B_{-1} D_{-1}} - \overline{T}) + (\overline{B_{-1} E_1} - \overline{T}) + (\overline{C_{-1} E_1} - \overline{T})$$

$$\eta = 18.58 - (20.70 - 18.58) - (19.16 - 18.58) - (18.46 - 18.58) + (20.59 - 18.58) + (21.40 - 18.58) + (20.87 - 18.58) + (19.84 - 18.58)$$
$$= 24.38$$

The confidence interval is the same as the one calculated above, 0.99. Therefore, the value of the S/N ratio for the flexural strength is expected in between;

η = {23.39, 25.37} with 95% confidence.

From the two combinations the second one is chosen as the optimal level since it S/N ratio is the largest one. As a result it is the least sensitive one to the uncontrollable noise factors. It can be seen from the result of experiment 111 that the S/N ratio is 23.08 but it falls a little below the confidence interval.

5.2.2 Regression Analysis of the Mean Flexural Strength Based on the Full Factorial Design

The first employed regression analysis to model the mean flexural strength contains only the main factors. That is:

$$y= 11,8 + 1,90*A - 3,89*B_1 - 2,36*B_2 - 0,427*C - 1,33*D_1 - 0,0586*E \quad (5.12)$$

Table 5.16 shows the ANOVA for the significance of the above regression model. ANOVA is performed on the individual results rather than the average of the three replicates. The hypothesis of having all β terms equal to zero is tested and refused with a confidence level of (1-p)*100, almost 100%.

Table 5.16 ANOVA for the significance of the regression model developed for the mean flexural strength based on the full factorial design including only the main factors

Source	df	Sum of Squares	Mean Squares	F	P
Regression	6	2685,44	447,57	166,49	0,000
Residual Error	479	1287,67	2,69		
Total	485	3973,11			

$R^2 = 67.6\%$ $R^2_{(adj)} = 67.2\%$ $S = 1.640$

Durbin-Watson statistic = 1.45

The adjusted multiple coefficient of determination, $R^2_{(adj)}$, shows that only 67.2% of the sample variation in the mean flexural strength can be explained by this model. The Durbin-Watson statistic states that there is a strong evidence of positive residual correlation with 95% confidence since it is less than the tabulated lower bound (d_L), which is 1.57 with 5 independent variables and 486

observations. The residual plots of this model are given in Figures 5.27 and 5.28. Although it is concluded from the residual plots that there is not any indication of violation of the assumptions of the error, a more adequate regression model will be searched to describe the mean flexural strength. The significance of β terms of the model is shown in Table 5.17. This table indicates that all the main factors are significant except the steel fiber volume fraction at the p(0.05) level of significance.

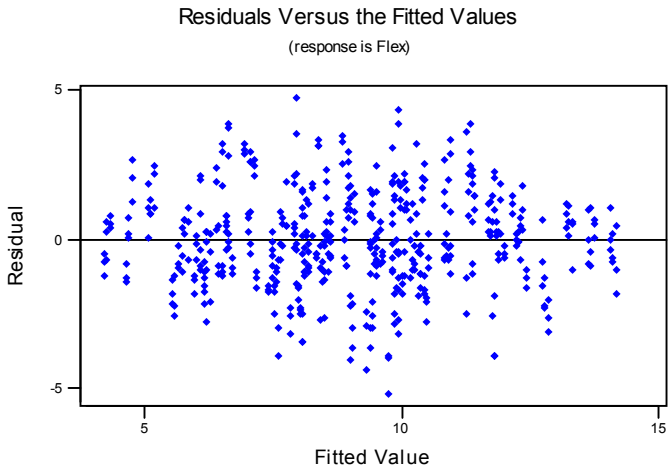

Figure 5.27 Residuals versus fitted values plot of the regression model developed for the mean flexural strength with only main factors

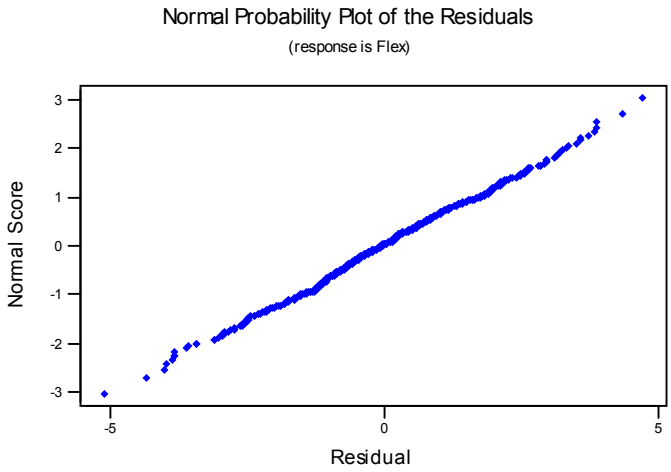

Figure 5.28 Residual normal probability plot of the regression model developed for the mean flexural strength with only main factors

Table 5.17 Significance of β terms of the regression model developed for the mean flexural strength with only main factors

Predictor	β Estimate	Standard Error	T	P
Constant	11,7848	0,1487	79,23	0,000
A	1,8982	0,0911	20,84	0,000
B_1	-3,8885	0,1822	-21,34	0,000
B_2	-2,3556	0,1822	-12,93	0,000
C	-0,4270	0,0911	-4,69	0,000
D_1	-1,3294	0,1487	-8,94	0,000
E	-0,0586	0,0911	-0,64	0,520

The MINITAB output with the sequential sum of squares of the regression model can be seen in Appendix C.4.

The second regression model is decided to include all the two-way interaction terms and the square of the main factors. The equation and the ANOVA table for the regression equation can be seen in Eqn. 5.13 and Table 5.18 respectively. Table 5.18 shows that the model has almost 100% confidence level for refusing the hypothesis stating that all β terms equal to zero.

$$y = 12,8 + 2,23*A - 5,13*B_1 - 2,54*B_2 - 0,041*C - 0,895*D_1 + 0,201*E - 1,22*A^2 - 0,015*C^2 - 0,073*E^2 + 0,141*AC - 0,022*AE - 0,025*CE - 0,184*B_1D_1 - 1,14*B_2D_1 - 0,855*AB_1 - 1,80*CB_1 - 1,45*EB_1 + 0,545*A^2B_1 - 0,166*C^2B_1 + 0,647*E^2B_1 - 0,219*ACB_1 - 0,221*AEB_1 + 0,288*CEB_1 + 0,154*AB_2 + 0,553*CB_2 + 0,652*EB_2 + 0,619*A^2B_2 - 0,002*C^2B_2 - 0,289*E^2B_2 + 0,229*ACB_2 - 0,297*AEB_2 - 0,848*CEB_2 - 0,217*AD_1 + 0,609*CD_1 + 0,192*ED_1 - 0,158*A^2D_1 - 0,575*C^2D_1 - 0,439*E^2D_1 - 0,221*ACD_1 + 0,148*AED_1 - 0,246*CED_1 + 0,370*AB_1D_1 - 0,474*CB_1D_1 + 0,287*EB_1D_1 + 0,211*A^2B_1D_1 + 0,757*C^2B_1D_1 + 0,980*E^2B_1D_1 - 0,239*ACB_1D_1 + 0,360*AEB_1D_1 - 0,327*CEB_1D_1 - 0,298*AB_2D_1 - 1,18*CB_2D_1 - 0,819*EB_2D_1 + 0,154*A^2B_2D_1 + 0,437*C^2B_2D_1 + 1,01*E^2B_2D_1 + 0,108*ACB_2D_1 + 0,604*AEB_2D_1 + 0,768*CEB_2D_1 \quad (5.13)$$

Table 5.18 ANOVA for the significance of the regression model developed for the mean flexural strength based on the full factorial design including main, interaction and squared factors

Source	df	Sum of Squares	Mean Squares	F	P
Regression	59	3450,165	58,477	47,64	0,000
Residual Error	426	522,946	1,228		
Total	485	3973,11			

$R^2 = 86.8\%$ $R^2_{(adj)} = 85.0\%$ S = 1.108

Durbin-Watson statistic = 2.18

This model seems more adequate than the previous one. The standard deviation of the error (S) is decreased from 1.640 to 1.108. Besides, the $R^2_{(adj)}$ value is improved considerably explaining 85% of the sample variation in the mean flexural strength by this model. Also the Durbin-Watson statistic is increased by this model through the uncorrelated region showing that the residuals are independent.

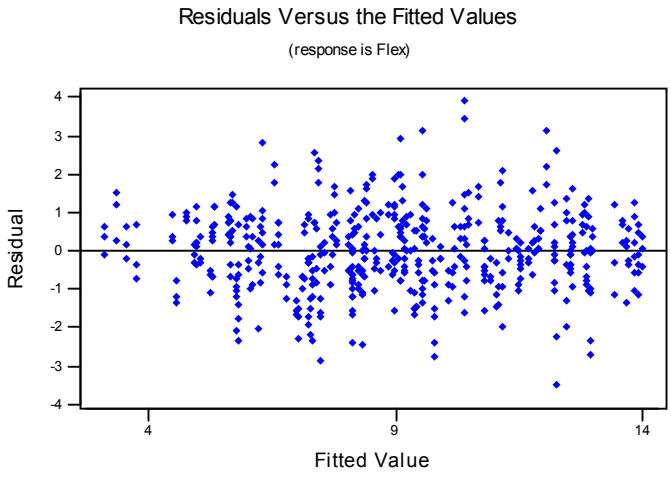

Figure 5.29 Residuals versus fitted values plot of the regression model in Eqn.5.13 developed for the mean flexural strength

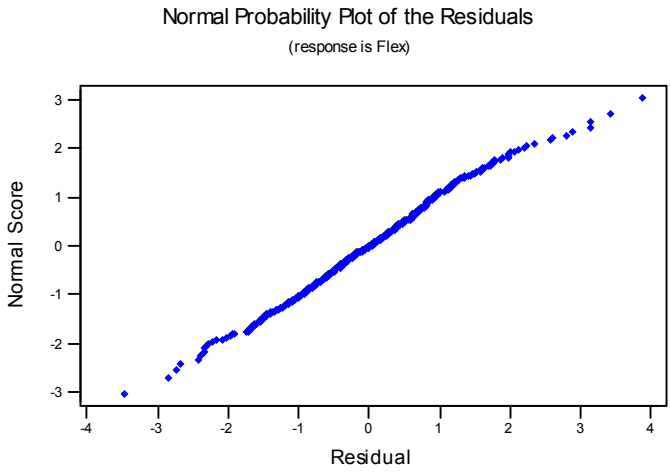

Figure 5.30 Residual normal probability plot of the regression model in Eqn.5.13 developed for the mean flexural strength

Residuals versus fitted values and the normal probability plot indicate that the error term has normal distribution with constant variance. As a result an adequate model explaining the mean response is achieved. Table 5.19 shows the significance of the β terms.

The MINITAB output with the sequential sum of squares of the regression model can be seen in Appendix C.5.

Table 5.19 Significance of β terms of the regression model in Eqn.5.13 developed for the mean flexural strength

Predictor	β Estimate	Standard Error	T	P
Constant	12,8290	0,3257	39,39	0,000
A	2,2285	0,1508	14,78	0,000
B_1	-5,1291	0,4606	-11,14	0,000
B_2	-2,5362	0,4606	-5,51	0,000
C	-0,0409	0,1508	-0,27	0,786
D_1	-0,8946	0,4606	-1,94	0,053
E	0,2006	0,1508	1,33	0,184
A^2	-1,2181	0,2611	-4,66	0,000
C^2	-0,0154	0,2611	-0,06	0,953
E^2	-0,0731	0,2611	-0,28	0,780
AC	0,1414	0,1847	0,77	0,444
AE	-0,0225	0,1847	-0,12	0,903
CE	-0,0253	0,1847	-0,14	0,891
B_1D_1	-0,1836	0,6514	-0,28	0,778
B_2D_1	-1,1428	0,6514	-1,75	0,080
AB_1	-0,8550	0,2132	-4,01	0,000
CB_1	-1,7957	0,2132	-8,42	0,000
EB_1	-1,4520	0,2132	-6,81	0,000
A^2B_1	0,5446	0,3693	1,47	0,141
C^2B_1	-0,1665	0,3693	-0,45	0,652
E^2B_1	0,6469	0,3693	1,75	0,081
ACB_1	-0,2186	0,2611	-0,84	0,403
AEB_1	-0,2206	0,2611	-0,84	0,399
CEB_1	0,2881	0,2611	1,10	0,271
AB_2	0,1541	0,2132	0,72	0,470
CB_2	0,5528	0,2132	2,59	0,010
EB_2	0,6524	0,2132	3,06	0,002
A^2B_2	0,6185	0,3693	1,67	0,095
C^2B_2	-0,0020	0,3693	-0,01	0,996
E^2B_2	-0,2887	0,3693	-0,78	0,435
ACB_2	0,2286	0,2611	0,88	0,382
AEB_2	-0,2969	0,2611	-1,14	0,256
CEB_2	-0,8481	0,2611	-3,25	0,001
AD_1	-0,2172	0,2132	-1,02	0,309
CD_1	0,6087	0,2132	2,85	0,005
ED_1	0,1920	0,2132	0,90	0,368

Table 5.19 Continued

Predictor	β Estimate	Standard Error	T	P
A^2D_1	-0,1580	0,3693	-0,43	0,669
C^2D_1	-0,5746	0,3693	-1,56	0,120
E^2D_1	-0,4391	0,3693	-1,19	0,235
ACD_1	-0,2214	0,2611	-0,85	0,397
AED_1	0,1481	0,2611	0,57	0,571
CED_1	-0,2464	0,2611	-0,94	0,346
AB_1D_1	0,3696	0,3015	1,23	0,221
CB_1D_1	-0,4743	0,3015	-1,57	0,117
EB_1D_1	0,2874	0,3015	0,95	0,341
$A^2B_1D_1$	0,2107	0,5223	0,40	0,687
$C^2B_1D_1$	0,7569	0,5223	1,45	0,148
$E^2B_1D_1$	0,9796	0,5223	1,88	0,061
ACB_1D_1	-0,2394	0,3693	-0,65	0,517
AEB_1D_1	0,3597	0,3693	0,97	0,331
CEB_1D_1	-0,3267	0,3693	-0,88	0,377
AB_2D_1	-0,2978	0,3015	-0,99	0,324
CB_2D_1	-1,1826	0,3015	-3,92	0,000
EB_2D_1	-0,8191	0,3015	-2,72	0,007
$A^2B_2D_1$	0,1541	0,5223	0,29	0,768
$C^2B_2D_1$	0,4374	0,5223	0,84	0,403
$E^2B_2D_1$	1,0091	0,5223	1,93	0,054
ACB_2D_1	0,1078	0,3693	0,29	0,771
AEB_2D_1	0,6036	0,3693	1,63	0,103
CEB_2D_1	0,7683	0,3693	2,08	0,038

It can be seen from the large p-values that several factors are insignificant with 95% confidence. The model can be improved by discarding the insignificant terms from the model one by one starting from the term having the largest p-value. After eliminating a factor, all the normality, constant variance and error correlation assumptions are checked and the best model is chosen. The main factors are left in the model without considering their p-value.

There is only a slight improvement in the best model whose regression equation, ANOVA table, residual plots and β significance test are given in Eqn.5.14, Table 5.20, Figures 5.31 and 5.32, and Table 5.21 respectively. It is achieved by pooling the ACB_2D_1, $A^2B_2D_1$, $A^2B_1D_1$, $C^2B_2D_1$, CEB_1D_1, ACB_1D_1, A^2D_1, C^2B_2, AEB_1D_1 and AEB_1 interaction terms. R^2 and adjusted R^2 gets a little closer to each other meaning that there is not any indication of unnecessary terms in the model. Also, the Durbin-Watson statistic became closer to 2 by this new model showing that the residuals are independent.

$$y = 12{,}9 + 2{,}23*A - 5{,}20*B_1 - 2{,}59*B_2 - 0{,}041*C - 1{,}15*D_1 + 0{,}201*E - 1{,}30*A^2 - 0{,}016*C^2 - 0{,}073*E^2 + 0{,}163*AC - 0{,}133*AE + 0{,}056*CE + 0{,}103*B_1D_1 - 0{,}749*B_2D_1 - 0{,}855*AB_1 - 1{,}80*CB_1 - 1{,}45*EB_1 + 0{,}650*A^2B_1 - 0{,}165*C^2B_1 + 0{,}647*E^2B_1 - 0{,}338*ACB_1 + 0{,}125*CEB_1 + 0{,}154*AB_2 + 0{,}553*CB_2 + 0{,}652*EB_2 + 0{,}696*A^2B_2 - 0{,}289*E^2B_2 + 0{,}282*ACB_2 - 0{,}187*AEB_2 - 0{,}930*CEB_2 - 0{,}217*AD_1 + 0{,}609*CD_1 + 0{,}192*ED_1 - 0{,}356*C^2D_1 - 0{,}439*E^2D_1 - 0{,}265*ACD_1 + 0{,}328*AED_1 - 0{,}410*CED_1 + 0{,}370*AB_1D_1 - 0{,}474*CB_1D_1 + 0{,}287*EB_1D_1 + 0{,}538*C^2B_1D_1 + 0{,}980*E^2B_1D_1 - 0{,}298*AB_2D_1 - 1{,}18*CB_2D_1 - 0{,}819*EB_2D_1 + 1{,}01*E^2B_2D_1 + 0{,}424*AEB_2D_1 + 0{,}932*CEB_2D_1 \quad (5.14)$$

Table 5.20 ANOVA for the significance of the best regression model developed for the mean flexural strength based on the full factorial design

Source	df	Sum of Squares	Mean Squares	F	P
Regression	49	3444,888	70,304	58,03	0,000
Residual Error	436	528,223	1,212		
Total	485	3973,110			

$R^2 = 86.7\%$ $R^2_{(adj)} = 85.2\%$ S = 1.101

Durbin-Watson statistic = 2.15

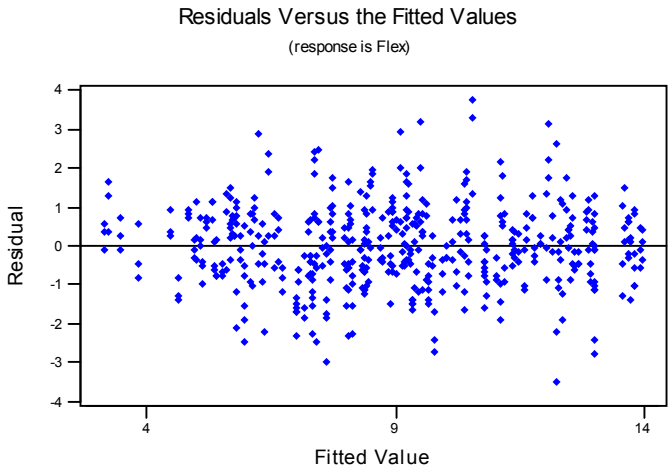

Figure 5.31 Residuals versus fitted values plot of the best regression model in Eqn.5.14 developed for the mean flexural strength

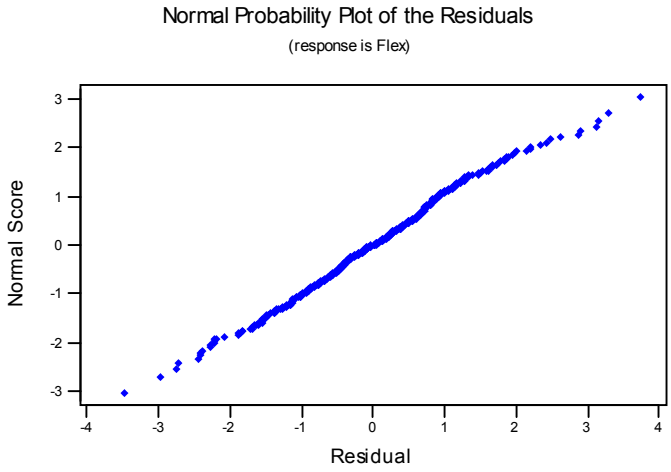

Figure 5.32 Residual normal probability plot of the best regression model in Eqn.5.14 developed for the mean flexural strength

Table 5.21 Significance of β terms of the best regression model in Eqn.5.14 developed for the mean flexural strength

Predictor	β Estimate	Standard Error	T	P
Constant	12,8823	0,2735	47,11	0,000
A	2,2285	0,1498	14,88	0,000
B_1	-5,2001	0,4056	-12,82	0,000
B_2	-2,5889	0,3459	-7,48	0,000
C	-0,0409	0,1498	-0,27	0,785
D_1	-1,1457	0,3459	-3,31	0,001
E	0,2006	0,1498	1,34	0,181
A^2	-1,2971	0,1834	-7,07	0,000
C^2	-0,0164	0,1834	-0,09	0,929
E^2	-0,0731	0,2594	-0,28	0,778
AC	0,1633	0,1498	1,09	0,276
AE	-0,1328	0,1297	-1,02	0,307
CE	0,0564	0,1589	0,35	0,723
B_1D_1	0,1027	0,5189	0,20	0,843
B_2D_1	-0,7485	0,4237	-1,77	0,078
AB_1	-0,8550	0,2118	-4,04	0,000
CB_1	-1,7957	0,2118	-8,48	0,000
EB_1	-1,4520	0,2118	-6,85	0,000
A^2B_1	0,6500	0,2594	2,51	0,013
C^2B_1	-0,1665	0,3177	-0,52	0,603
E^2B_1	0,6469	0,3669	1,76	0,079
ACB_1	-0,3383	0,1834	-1,84	0,066
CEB_1	0,1247	0,1834	0,68	0,497
AB_2	0,1541	0,2118	0,73	0,467
CB_2	0,5528	0,2118	2,61	0,009
EB_2	0,6524	0,2118	3,08	0,002
A^2B_2	0,6956	0,2594	2,68	0,008
E^2B_2	-0,2887	0,3669	-0,79	0,432
ACB_2	0,2825	0,1834	1,54	0,124
AEB_2	-0,1867	0,2247	-0,83	0,407
CEB_2	-0,9297	0,2427	-3,83	0,000
AD_1	-0,2172	0,2118	-1,03	0,306
CD_1	0,6087	0,2118	2,87	0,004
ED_1	0,1920	0,2118	0,91	0,365
C^2D_1	-0,3559	0,2594	-1,37	0,171
E^2D_1	-0,4391	0,3669	-1,20	0,232

Table 5.21 Continued

Predictor	β Estimate	Standard Error	T	P
ACD_1	-0,2653	0,1498	-1,77	0,077
AED_1	0,3279	0,1834	1,79	0,075
CED_1	-0,4097	0,1834	-2,23	0,026
AB_1D_1	0,3696	0,2996	1,23	0,218
CB_1D_1	-0,4743	0,2996	-1,58	0,114
EB_1D_1	0,2874	0,2996	0,96	0,338
$C^2B_1D_1$	0,5381	0,4494	1,20	0,232
$E^2B_1D_1$	0,9796	0,5189	1,89	0,060
AB_2D_1	-0,2978	0,2996	-0,99	0,321
CB_2D_1	-1,1826	0,2996	-3,95	0,000
EB_2D_1	-0,8191	0,2996	-2,73	0,007
$E^2B_2D_1$	1,0091	0,5189	1,94	0,052
AEB_2D_1	0,4237	0,3177	1,33	0,183
CEB_2D_1	0,9317	0,3177	2,93	0,004

As a result this model is decided to be kept as the most adequate model explaining the flexural strength of the SFRHSC. The MINITAB output with the sequential sum of squares of the regression model can be seen in Appendix C.6.

5.2.3 Response Surface Optimization of Mean Flexural Strength Based on the Full Factorial Design

For the MINITAB response optimization the best regression model found in Eqn.5.14 in the previous section for the mean flexural strength will be used. Again as in Taguchi design, in MINITAB Response Optimizer, the lower bound is set to 6.0 MPa and the target value is set to 15 MPa.

The same thirteen starting points are used in the maximization of the mean flexural strength also. The results of the optimizer can be seen in Table 5.22. The starting points and the optimum points found by MINITAB response optimizer is shown in Table 5.23.

Table 5.22 The optimum response, its desirability, the confidence and prediction intervals computed by MINITAB Response Optimizer for the mean flexural strength based on the full factorial design

Optimum Points	Mean Flex.	Desirability	95% Conf. Int.	95% Pred. Int.
1	13,6132	0,85137	(12,8228; 14,4036)	(11,3100; 15,9164)
2	13,5940	0,84942	(12,8000; 14,3808)	(11,2872; 15,8936)
3	13,6132	0,85137	(12,8228; 14,4036)	(11,3100; 15,9164)
4	12,1454	0,69468	(11,2956; 12,9952)	(9,8211; 14,4697)
5	13,9708	0,88257	(13,1804; 14,7612)	(11,6676; 16,2740)
6	13,5940	0,84942	(12,8000; 14,3808)	(11,2872; 15,8936)
7	10,2294	0,48022	(9,5236; 10,9351)	(7,9538; 12,5049)
8	12,3141	0,71523	(11,4643; 13,1639)	(9,9888; 14,6384)
9	13,6132	0,85137	(12,8228; 14,4036)	(11,3100; 15,9164)
10	12,1454	0,69468	(11,2956; 12,9952)	(9,8211; 14,4697)
11	13,8084	0,86942	(13,1781; 14,4386)	(11,5551; 16,0616)
12	12,1454	0,69468	(11,2956; 12,9952)	(9,8211; 14,4697)
13	13,5940	0,84942	(12,8000; 14,3808)	(11,2872; 15,8936)

Table 5.23 The starting and optimum points for MINITAB response optimizer developed for the mean flexural strength based on the full factorial design

	Starting Points					Optimum Points				
Points	**Age (days)**	**B. Type**	**B. Amount (%)**	**Cure**	**Steel (% vol.)**	**Age (days)**	**B. Type**	**B. Amount (%)**	**Cure**	**Steel (% vol.)**
1	90	SF	20	water	1,0	90	SF	20	water	1,0
2	No starting point					90	SF	20	water	0,0
3	90	SF	20	steam	0,5	90	SF	20	water	1,0
4	90	GGBFS	20	water	0,5	90	GGBFS	20	water	1,0
5	90	SF	10	water	1,0	90	SF	10	water	1,0
6	28	FA	40	steam	0,5	90	SF	20	water	0,0
7	7	SF	20	water	0,0	11,8	SF	20	water	0,0
8	90	GGBFS	60	water	1,0	90	GGBFS	60	water	1,0
9	90	FA	10	water	1,0	90	SF	20	water	1,0
10	28	GGBFS	20	steam	1,0	90	GGBFS	20	water	1,0
11	90	SF	15	water	1,0	90	SF	15	water	1,0
12	90	GGBFS	20	steam	1,0	90	GGBFS	20	water	1,0
13	90	SF	20	water	0,0	90	SF	20	water	0,0

The starting point 5 resulted in the highest flexural strength of 13.97 MPa among the others. Following point 5, point 11 is the second best with 13.81 MPa flexural strength. The starting points 1, 3, and 9 gave exactly the same result which is 13.61 MPa which very close to the previous two points ant therefore confirmation runs will be performed for these points. Points 2, 6 and 13 resulted in 13.59 MPa flexural strength and they will be evaluated also. The confidence and prediction intervals of all the points are nearly the same except point 11 which has the narrowest intervals. The starting points 8, 4, 10 and 12 will also be evaluated because their desirabilities are around 70% and can be acceptable. The remaining point 7 resulted in very low flexural strength value with around 50% desirability and therefore it is not taken into consideration for confirmation.

Optimum point 5:

For these points the 3rd level for Age (90 days), 1st level for Binder Amount (Silica Fume), 3rd level for Binder Amount (10% for silica fume), 1st level for Curing Type (ordinary water curing) and the 3rd level for Steel Fiber Volume Fraction (1.0%) are assigned to the associated main factors. This combination corresponds to experiment number 123 which resulted in 14.40 MPa, 14.05 MPa and 13.59 MPa flexural strengths. All are in the prediction and confidence intervals. Therefore, it can be concluded that the results of the experiment are fitting to the findings of the optimizer. Also, the mean of the three flexural strengths, 14.01 MPa, is very close to the fitted value of 13.97 MPa. As a result, it can be said that this point is well modeled by the chosen regression model.

Optimum point 11:

For this experiment age, binder type, binder amount, curing type and steel fiber volume fraction are set to 90 days, Silica Fume, 15% for SF, ordinary water curing and 1.0% respectively. This combination corresponds to experiment

number 117 with 14.63 MPa, 12.79 MPa and 13.59 MPa flexural strengths. 12.79 MPa and 14.63 MPa are outside the limits of the confidence interval. But all the results fall in the prediction limits. Also, the mean of them, 13.67 MPa, confirms the optimum fitted value, which is 13.81 MPa, found by the Response Optimizer. So it can be said that this point is well modeled by the determined best regression model in the previous section.

Optimum points 1, 3 and 9:

For these points the 3rd level for Age (90 days), 1st level for Binder Amount (Silica Fume), 1st level for Binder Amount (20% for silica fume), 1st level for Curing Type (ordinary water curing) and the 3rd level for Steel Fiber Volume Fraction (1.0%) are assigned to the associated main factors. This combination corresponds to experiment number 111 which resulted in 14.05 MPa, 15.09 MPa and 13.71 MPa flexural strengths. All are in the prediction interval but 15.09 MPa is above the upper confidence limit. Also, the mean of the three flexural strengths, 14.28 MPa, is above the fitted value of 13.61 MPa. As a result, it can be said that these points are modeled by the chosen regression model but a little underestimated.

Optimum points 2, 6 and 13:

For this experiment age, binder type, binder amount, curing type and steel fiber volume fraction are set to 90 days, Silica Fume, 20% for SF, ordinary water curing and 0.0% respectively. This combination corresponds to experiment number 109 with 14.63 MPa, 13.13 MPa and 12.33 MPa flexural strengths. 12.33 MPa and 14.63 MPa are outside the limits of the confidence interval. But all the results fall in the prediction limits. Also, the mean of them, 13.36 MPa, confirms the optimum fitted value, which is 13.59 MPa, found by the Response Optimizer. So it can be said that these points are well modeled by the determined best regression model in the previous section.

Optimum point 8:

For this experiment age, binder type, binder amount, curing type and steel fiber volume fraction are set to 90 days, GGBFS, 60% for GGBFS, ordinary water curing and 1.0% respectively. This combination corresponds to experiment number 159 with 11.98 MPa, 13.48 MPa and 12.44 MPa flexural strengths. 13.48 MPa is outside the upper limit of the confidence interval. But all the results fall in the prediction limits. Also, the mean of them, 12.63 MPa, confirms the optimum fitted value, which is 12.31 MPa, found by the Response Optimizer. So it can be said that this point is well modeled by the determined best regression model in the previous section.

Optimum points 4, 10 and 12:

For these points the 3rd level for Age (90 days), 3rd level for Binder Amount (GGBFS), 1st level for Binder Amount (20% for silica fume), 1st level for Curing Type (ordinary water curing) and the 3rd level for Steel Fiber Volume Fraction (1.0%) are assigned to the associated main factors. This combination corresponds to experiment number 147 which resulted in 12.33 MPa, 11.98 MPa and 12.90 MPa flexural strengths. All are in the confidence and prediction intervals and it can be concluded that the results of the experiment are fitting to the findings of the optimizer. Also, the mean of the three flexural strengths, 12.40 MPa, is very close to the fitted value of 12.15 MPa. As a result, it can be said that these points are well modeled by the chosen regression model.

The best point chosen for the result of the regression analysis of the mean flexural strength is the optimum 5 since it is well modeled by the regression model and gives the maximum flexural strength among the other factor level combinations. Therefore, the best modeled point that maximizes the flexural strength of SFRHSC by the regression analysis has the combination of $A_1B_{-1}C_1D_{-1}E_1$. On the other hand, point 1 (also the points 3 and 9 because they

resulted in the same combination of the main factor levels) can be selected as the optimum parameter level combination also, because, the confirmation experiments for these points resulted in the highest mean flexural strength, even higher than the chosen point 5. However, these points are underestimated by the chosen regression model. Hence, the best point that maximizes the flexural strength of SFRHSC can have the combination of $A_1B_{-1}C_{-1}D_{-1}E_1$ which is point 1.

CHAPTER 6

EXPERIMENTAL DESIGN AND ANALYSIS WHEN THE RESPONSE IS IMPACT RESISTANCE

6.1 Taguchi Experimental Design

The same methodology discussed in Chapter 4 when the response variable was compressive strength is applied for the impact resistance response variable. The same L_{27} (3^{13}) orthogonal array is employed with the same main factors and interaction terms.

6.1.1 Taguchi Analysis of the Mean Impact Resistance Based on the L_{27} (3^{13}) Design

The results of the impact resistance experiments are shown in Table 6.1.

The ANOVA table for the mean impact resistance can be seen in Table 6.2. It indicates that only Steel Fiber Volume Fraction (E) main factor significantly affects the impact resistance of the fiber reinforced high strength concrete with 95% confidence level. Binder Type (B) and Curing Type (D) main factors affect the response with 88.6% and 86.1% confidences respectively. None of the remaining main factors and two-way interaction factors is significant on the response. The insignificance of the interactions can also be seen from the two-way interaction plot given in Figure 6.1. As it can be seen from the AB interaction plot, at level 1 and 3 of factor age there is no interaction between age and binder type but, level 2 of factor A interacts with factor B. In the interaction

plot of BE, at level 1 and 3 of factor binder type there is no interaction between binder type and steel fiber volume fraction but, level 2 of factor B interacts with factor E.

Table 6.1 The impact resistance experiment results developed by L_{27} (3^{13}) design

	Column numbers and factors					RESULTS				
	1	4	5	8	9					
Exp. Run	A	B	C	D	E	Run #1	Run#2	Run#3	μ (Mpa)	S/N ratio
1	-1	-1	-1	-1	-1	3,80	2,10	2,60	2,83	8,30
2	-1	-1	0	0	0	5,20	5,70	7,80	6,23	15,52
3	-1	-1	1	-1	1	4,60	3,60	6,20	4,80	13,00
4	-1	0	-1	0	0	4,80	5,00	3,60	4,47	12,71
5	-1	0	0	-1	1	4,40	2,40	7,60	4,80	10,92
6	-1	0	1	-1	-1	5,80	3,20	3,60	4,20	11,66
7	-1	1	-1	-1	1	15,60	11,80	3,20	10,20	14,40
8	-1	1	0	-1	-1	3,80	2,10	3,00	2,97	8,67
9	-1	1	1	0	0	6,90	5,20	10,00	7,37	16,45
10	0	1	-1	-1	0	7,60	6,10	9,90	7,87	17,42
11	0	1	0	0	1	3,40	5,40	5,40	4,73	12,87
12	0	1	1	-1	-1	5,00	8,90	3,60	5,83	13,64
13	0	-1	-1	0	1	3,60	3,60	3,20	3,47	10,76
14	0	-1	0	-1	-1	3,60	5,00	3,00	3,87	11,19
15	0	-1	1	-1	0	4,90	5,20	4,20	4,77	13,46
16	0	0	-1	-1	-1	4,70	4,20	6,10	5,00	13,67
17	0	0	0	-1	0	13,00	2,50	2,40	5,97	9,46
18	0	0	1	0	1	4,80	3,00	4,60	4,13	11,72
19	1	0	-1	-1	1	16,80	4,00	7,60	9,47	15,56
20	1	0	0	0	-1	3,60	5,90	5,40	4,97	13,30
21	1	0	1	-1	0	4,60	5,40	2,80	4,27	11,57
22	1	1	-1	0	-1	4,40	3,00	4,20	3,87	11,36
23	1	1	0	-1	0	9,90	4,40	6,70	7,00	15,52
24	1	1	1	-1	1	9,60	5,80	8,80	8,07	17,49
25	1	-1	-1	-1	0	6,60	6,80	5,50	6,30	15,87
26	1	-1	0	-1	1	5,50	5,70	7,70	6,30	15,70
27	1	-1	1	0	-1	2,30	4,00	5,20	3,83	10,17

Table 6.2 ANOVA table for the mean impact resistance based on L_{27} (3^{13}) design

Source	df	Sum of Squares	Mean Square	F	P
A	2	4,243	2,121	1,05	0,416
B	2	13,963	6,982	3,46	0,114
C (B)	6	20,015	3,336	1,65	0,299
D	1	6,247	6,247	3,10	0,139
E	2	23,461	11,731	5,82	0,050
AB	4	4,504	1,126	0,56	0,704
BE	4	9,907	2,477	1,23	0,405
Error	5	10,086	2,017		
TOTAL	26	92,426			

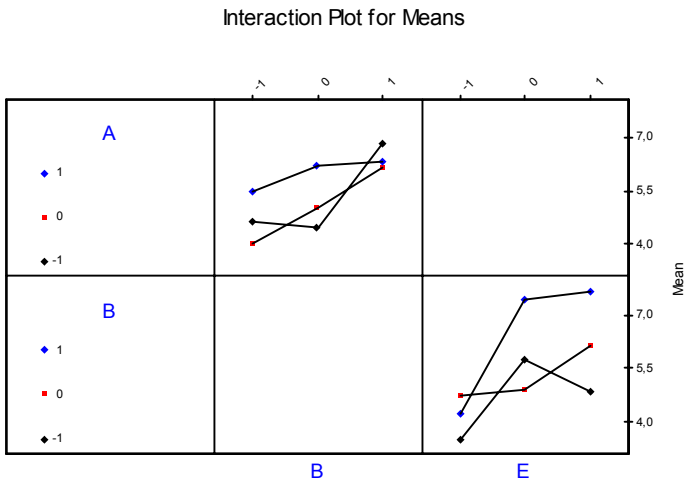

Figure 6.1 Two-way interaction plots for the mean impact resistance

The residual plots of the model for the mean impact resistance are given in Figures 6.2 and 6.3.

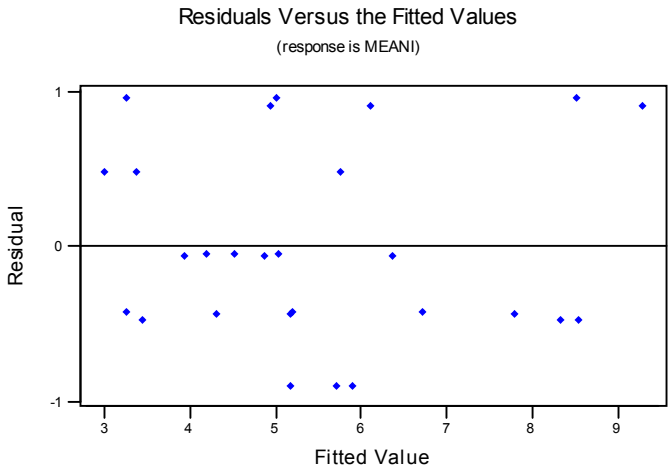

Figure 6.2 The residuals versus fitted values of the L_{27} (3^{13}) model found by ANOVA for the mean impact resistance

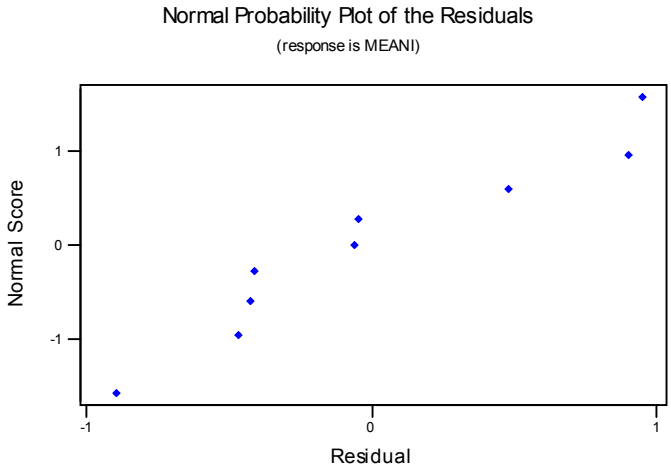

Figure 6.3 The residual normal probability plot for the L_{27} (3^{13}) model found by ANOVA for the mean impact resistance

In Figure 6.2, it can be seen that most of the residuals are in the lower side of the fitted values. This may violate the assumption of having a constant variance of the error term for all levels of the independent process parameters. But a linear

trend can be observed in Figure 6.3 indicating that the assumption of the error term having a normal probability distribution is satisfied.

As ANOVA shows that none of the terms except factor B, D and E are significant within the experimental region, a new ANOVA is performed by pooling A and AB terms to the error which is given in Table 6.3.

Table 6.3 Pooled ANOVA of the mean impact resistance based on L_{27} (3^{13}) design

Source	df	Sum of Squares	Mean Square	F	P
B	2	13,963	6,982	4,08	0,047
C (B)	6	20,015	3,336	1,95	0,160
D	1	6,247	6,247	3,65	0,083
E	2	23,461	11,731	6,85	0,012
BE	4	9,907	2,477	1,45	0,283
Error	11	18,833	1,712		
TOTAL	26	92,426			

The results show that with $\alpha = 0.05$ significance, only the main factors E and B are significant on the mean impact resistance of SFRHSC. But factors C(B), D and BE are accepted significant on the response with 84.0%, 91.7% and 71.7% confidences respectively.

The residual plots of this new model for the mean flexural strength are given in Figures 6.4 and 6.5.

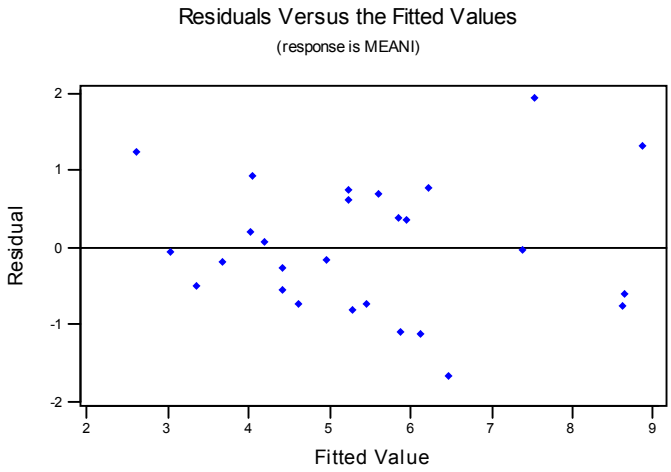

Figure 6.4 The residuals versus fitted values of the $L_{27}(3^{13})$ model found by the pooled ANOVA for the mean impact resistance

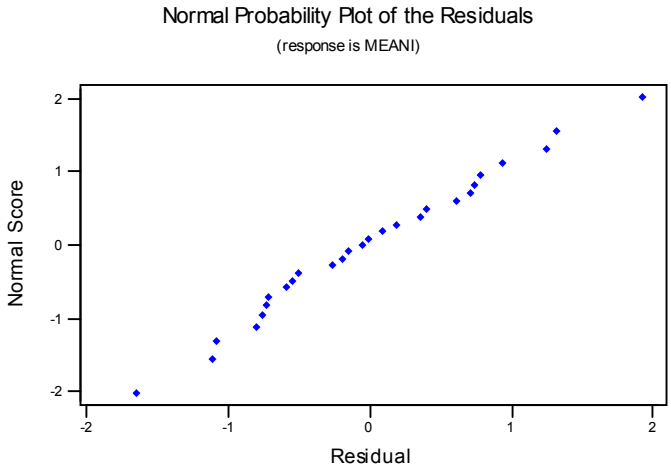

Figure 6.5 The residual normal probability plot for the $L_{27}(3^{13})$ model found by the pooled ANOVA for the mean impact resistance

When the insignificant terms are pooled in the error, the residuals versus the fitted values plot did not improve so much meaning that the constant variance assumption of the error still may be violated. The residual normal probability

plot seems better, the linear trend can be observed and the normality assumption is valid. Therefore the pooled model is decided to be kept and the prediction equation will be calculated for the pooled one.

Figure 6.6 shows the main effects plot which is used for finding the optimum levels of the process parameters that increase the mean impact resistance.

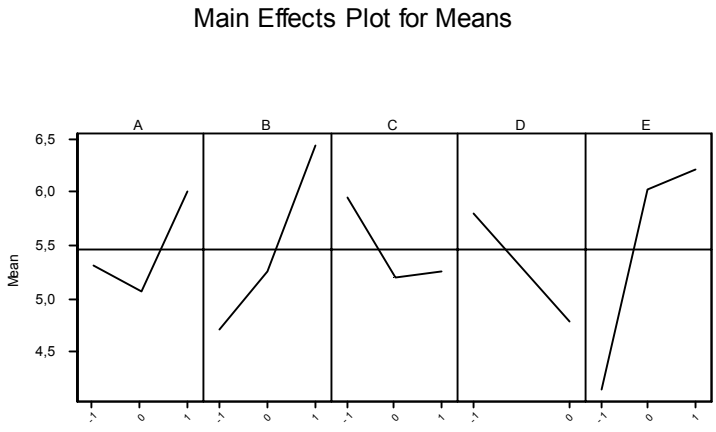

Figure 6.6 Main effects plot based on the $L_{27}(3^{13})$ design for the mean impact resistance

As it can be seen from Figure 6.6, the optimum points for the significant main factors are 3rd level for the Binder Type (Ground Granulated Blast Furnace Slag), 1st level for Binder Amount (20% for GGBFS) 1st level for Curing Type (ordinary water curing) and 3rd level for Steel Fiber Volume Fraction (1.0% vol.). Although the main factor A is insignificant, it would be better to include it in the prediction equation because it should be used in the experiments. Therefore form the main effects plot (Figure 6.6) the level that yield the highest flexural strength is the 3rd level for Age (90 days). Since the interaction term BE is significant on the response with only 70% confidence, it will not be included in the calculation of the prediction equation. The notation for the

optimum point is $A_1B_1C_{-1}D_{-1}E_1$. The optimum performance is calculated by using the following expressions:

$A_1B_1C_{-1}D_{-1}E_1$:

$$\hat{\mu}_{A_1B_1C_{-1}D_{-1}E_1} = \overline{T} + (\overline{A}_1 - \overline{T}) + (\overline{B}_1 - \overline{T}) + (\overline{C}_{-1} - \overline{T}) + (\overline{D}_{-1} - \overline{T}) + (\overline{E}_1 - \overline{T}) \qquad (6.1)$$

$$\hat{\mu}_{A_1B_1C_{-1}D_{-1}E_1} = 5.47 + (6.01 - 5.47) + (6.43 - 5.47) + (5.94 - 5.47) + (5.81 - 5.47) + (6.22 - 5.47)$$
$$= 8.53 \text{ kgf.m}$$

$$n_e = \frac{27}{12.5+1} = 2.00$$

$V_e = 1.712$

$F_{0.05,1,11} = 4.84$

$$C.I. = \sqrt{\frac{4.84 \times 1.712}{2.00}} = 2.04$$

The value of the mean impact resistance is expected in between;

$\hat{\mu}_{A_1B_1C_{-1}D_{-1}E_1}$ = {6.49, 10.57} with 95% confidence.

As a result, combination $A_1B_1C_{-1}D_{-1}E_1$ is selected as the optimum setting for which the confirmation experiment's results are expected to be between {6.49, 10.57} with 95% confidence.

The ANOVA results of the S/N ratio values can be seen in Table 6.4. The results of the ANOVA show that from the factors A, B, C(B), E and BE are significant on the S/N ratio of the impact resistance with 95% confidence. Figure 6.7 shows all the two-way factor interaction plots. As it can be seen from the figure that the three lines of AB seems almost parallel and does not

contribute to the response. The contribution of BE seems larger since the lines in the corresponding plots are intersecting each other at least for one level of the related interaction terms.

Table 6.4 ANOVA of S/N ratio values of the impact resistance based on $L_{27}(3^{13})$ design

Source	df	Sum of Squares	Mean Square	F	P
A	2	14,1352	7,0676	10,13	0,017
B	2	18,5041	9,2520	13,26	0,010
C (B)	6	42,0297	7,0050	10,04	0,011
D	1	1,1225	1,1225	1,61	0,260
E	2	41,6993	20,8497	29,89	0,002
AB	4	4,4425	1,1106	1,59	0,308
BE	4	46,2091	11,5523	16,56	0,004
Error	5	3,4876	0,6975		
TOTAL	26	171,6300			

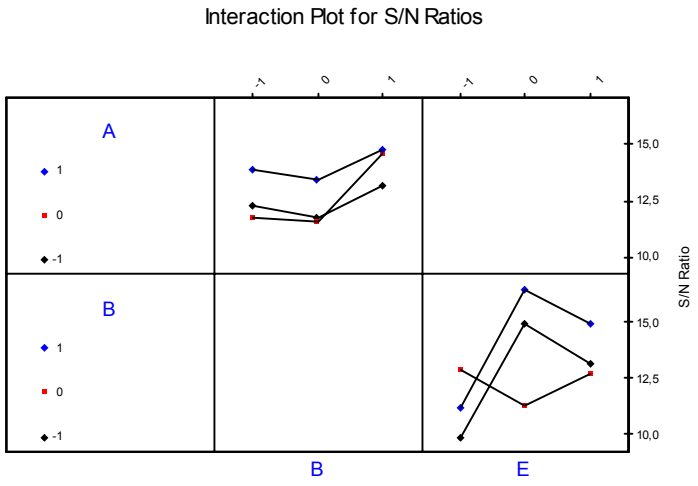

Figure 6.7 Two-way interaction plots for the S/N values of impact resistance

The residual plots for S/N ratio can be seen in Figures 6.8 and 6.9.

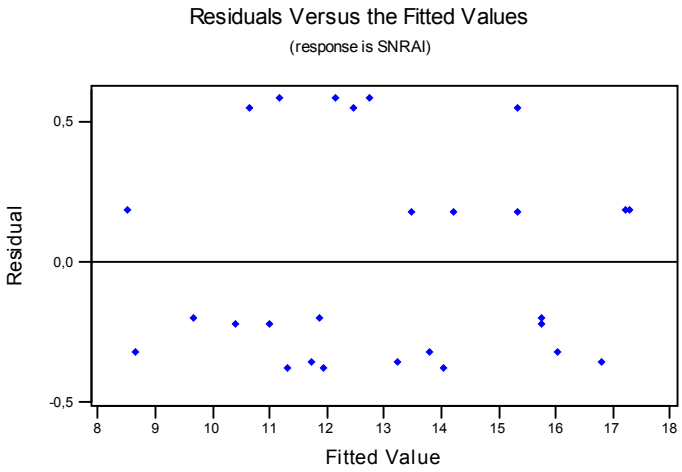

Figure 6.8 The residuals versus fitted values of the L_{27} (3^{13}) model found by ANOVA for S/N ratio for impact resistance

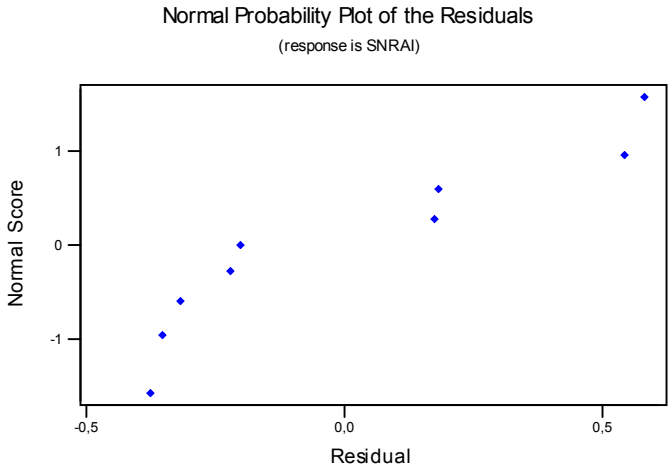

Figure 6.9 The residual normal probability plot for the L_{27} (3^{13}) model found by ANOVA for S/N ratio for impact resistance

Figure 6.8 shows no abnormality for validation of the constant variance assumption of the error. However Figure 6.9 is a little away from linearity but it can be said that the normal distribution assumption of the error still holds.

As ANOVA shows that factors D and AB are insignificant on the response within the experimental region and therefore, a new ANOVA is performed by pooling D and AB terms to the error which is given in Table 6.5.

Table 6.5 Pooled ANOVA of the S/N values for the impact resistance based on $L_{27}(3^{13})$ design

Source	df	Sum of Squares	Mean Square	F	P
A	2	14,1352	7,0676	7,81	0,009
B	2	18,5041	9,2520	10,22	0,004
C (B)	6	42,0297	7,0050	7,74	0,003
E	2	41,6993	20,8497	23,03	0,000
BE	4	46,2091	11,5523	12,76	0,001
Error	10	9,0530	0,9050		
TOTAL	26	171,6300			

The results show that with $\alpha = 0.05$ significance, all of the factors are significant on the mean impact resistance of SFRHSC.

The residual plots of this new model for the mean flexural strength are given in Figures 6.10 and 6.11. When the residual plots are examined it is seen that none of the assumption of the error term is violated. No obvious pattern is observed in the residuals versus the fitted values graph of the pooled model. Therefore the constant variance assumption of the error holds. The linearity of the residual normal plot shows that the errors are distributed normally. The pooled model seems more adequate than the unpooled model. So the prediction equation for S/N values will be calculated for the pooled model.

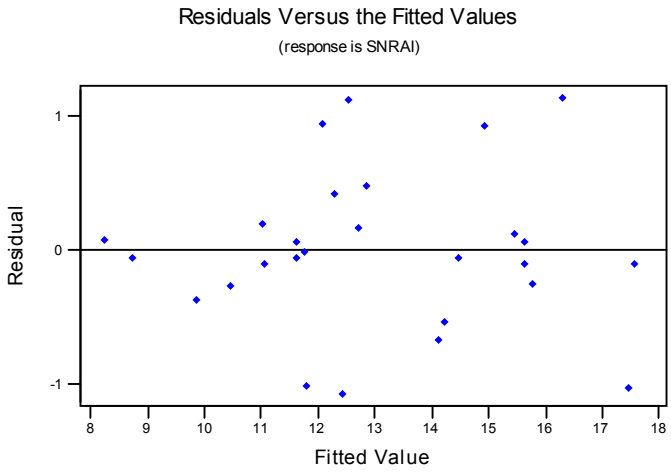

Figure 6.10 The residuals versus fitted values of the L_{27} (3^{13}) model found by the pooled ANOVA for the S/N ratio of impact resistance

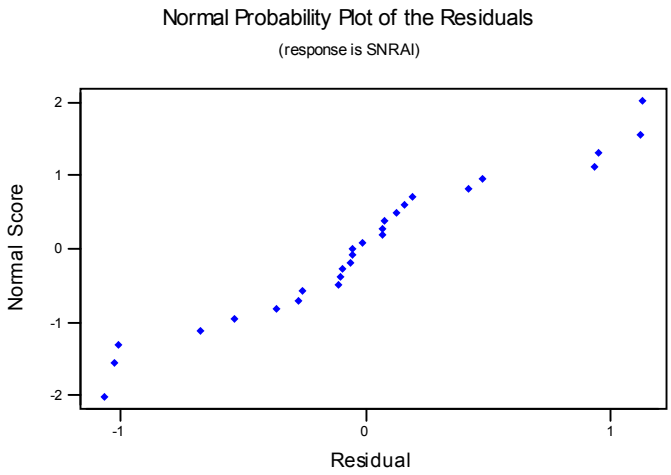

Figure 6.11 The residual normal probability plot for the L_{27} (3^{13}) model found by the pooled ANOVA for the S/N ratio of impact resistance

From the main effects plot in Figure 6.12, the optimum points are 3rd level for Age (90 days), 3rd level for Binder Type (GGBFS), 1st level for Binder Amount (20% for GGBFS) and 2nd level for Steel Fiber Volume Fraction (0.5% vol.). Factor C can also be set to its 3rd level (60% for GGBFS) , since their affects are

almost the same, as it can be seen from Figure 6.12. Although factor D is insignificant, it should be included in the prediction equation because without this main factor the experiments can not be conducted. Therefore, factor D is set to its 1st level (ordinary water curing). The levels of the significant interaction factor BE are determined from the interaction plot in Figure 6.7 as the 3rd level for Binder Type and 2nd level for steel fiber volume fraction which are in coincidence with the results that are obtained from the main effects plot. As a result, the prediction equation will be computed for both $A_1B_1C_{-1}D_{-1}E_0$ and $A_1B_1C_1D_{-1}E_0$. When both level averages of $C(B)_{-1}$ and $C(B)_1$ are calculated, it is seen that $C(B)_{-1}$ is a little larger. Thus, both combinations will give approximately the same result. Either the 1st level or the 3rd level of factor C(B) can be selected as the optimal level. If economy is important, 1st level should be selected. But here 1st level is selected for convenience.

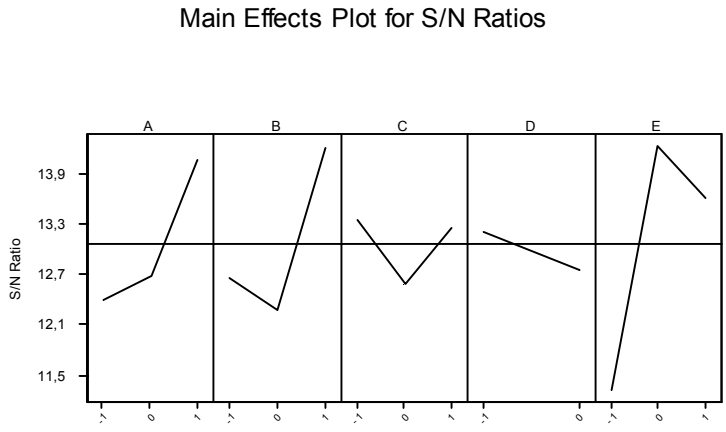

Figure 6.12 Main effects plot based on the L_{27} (3^{13}) design for S/N ratio for impact resistance

$A_1B_1C_{-1}D_{-1}E_0$:

$$\eta = \overline{T} + (\overline{A}_1 - \overline{T}) + (\overline{B}_1 - \overline{T}) + (\overline{C}_{-1} - \overline{T}) + (\overline{D}_{-1} - \overline{T}) + (\overline{E}_0 - \overline{T}) + (\overline{B_1 \times E_0} - \overline{T}) \quad (6.2)$$

$$\eta = \overline{T} + (\overline{A}_1 - \overline{T}) + (\overline{C}_{-1} - \overline{T}) + (\overline{D}_{-1} - \overline{T}) + (\overline{B_1 E_0} - \overline{T})$$

η = 13.05 + (14.06 – 13.05) + (13.34 – 13.05) + (13.19 – 13.05) + (16.46 – 13.05)

= 17.90

$$n_e = \frac{27}{16.5+1} = 1.54$$

$V_e = 0.905$

$F_{0.05,1,10} = 4.96$

$$C.I. = \sqrt{\frac{4.96 \times 0.905}{1.54}} = 1.71$$

As a result the value for the S/N ratio should fall in between:

η = {16.19, 19.61} with 95% confidence.

Since the obtained parameter level combinations are different for the mean impact resistance and S/N ratio, for $A_1B_1C_{-1}D_{-1}E_0$ combination the predicted mean impact resistance should be calculated.

$A_1B_1C_{-1}D_{-1}E_0$:

$$\hat{\mu}_{A_1B_1C_{-1}D_{-1}E_0} = \overline{T} + (\overline{A}_1 - \overline{T}) + (\overline{B}_1 - \overline{T}) + (\overline{C}_{-1} - \overline{T}) + (\overline{D}_{-1} - \overline{T}) + (\overline{E}_0 - \overline{T}) \quad (6.3)$$

$$\hat{\mu}_{A_1B_1C_{-1}D_{-1}E_0} = 5.47 + (6.01 - 5.47) + (6.43 - 5.47) + (5.94 - 5.47) + (5.81 - 5.47) + (6.03 - 5.47)$$
$$= 8.34 \text{ kgf.m}$$

$$n_e = \frac{27}{12.5+1} = 2.00$$

$V_e = 1.712$

$F_{0.05,1,11} = 4.84$

$$C.I. = \sqrt{\frac{4.84 \times 1.712}{2.00}} = 2.04$$

The value of the mean impact resistance is expected in between;

$\hat{\mu}_{A_1B_1C_{-1}D_{-1}E_0}$ = {6.30, 10.38} with 95% confidence

Also, predicted S/N ratio should be calculated for $A_1B_1C_{-1}D_{-1}E_1$ combination in order to see the difference between the two combinations.

$A_1B_1C_{-1}D_{-1}E_1$:

$$\eta = \overline{T} + (\overline{A}_1 - \overline{T}) + (\overline{B}_1 - \overline{T}) + (\overline{C}_{-1} - \overline{T}) + (\overline{D}_{-1} - \overline{T}) + (\overline{E}_1 - \overline{T}) + (\overline{B_1 \times E_1} - \overline{T}) \quad (6.4)$$

$$\eta = \overline{T} + (\overline{A}_1 - \overline{T}) + (\overline{C}_{-1} - \overline{T}) + (\overline{D}_{-1} - \overline{T}) + (\overline{B_1 E_1} - \overline{T})$$

$$\eta = 13.05 + (14.06 - 13.05) + (13.34 - 13.05) + (13.19 - 13.05) + (14.92 - 13.05)$$
$$= 16.36$$

$$n_e = \frac{27}{16.5+1} = 1.54$$

$V_e = 0.905$

$F_{0.05,1,10} = 4.96$

$$C.I. = \sqrt{\frac{4.96 \times 0.905}{1.54}} = 1.71$$

As a result the value for the S/N ratio should fall in between:

η = {14.65, 18.07} with 95% confidence.

Since the difference in between the two combinations for mean impact resistance is very low and the difference in S/N ratios are relatively higher, $A_1B_1C_{-1}D_{-1}E_0$ combination is selected as the optimum parameter level combination. The confirmation experiment is performed for $A_1B_1C_{-1}D_{-1}E_0$ combination three times. The results of the confirmation experiment yield the values of 3.50 kgf.m, 3.20 kgf.m and 3.80 kgf.m with an S/N ratio of 10.82. None of the results are in the confidence interval. The S/N value calculated from the results of the confirmation experiment is also below the lower limit of the confidence interval. All the results are very far from the calculated predicted values of 8.34 kgf.m mean impact resistance and 17.90 S/N ratio. Hence, it can be concluded that these results do not confirm the optimum setting $A_1B_1C_{-1}D_{-1}E_0$ found by using the Taguchi method. Confirmation experiment is performed for $A_1B_1C_{-1}D_{-1}E_1$ combination also and the results of the confirmation experiment yield the values of 4.20 kgf.m, 5.50 kgf.m and 10.10 kgf.m with an S/N ratio of 14.79. Only 10.10 is in the confidence interval and the other two are below the lower limit. However, the S/N value falls in the confidence interval. Also the variation between the three confirmation runs are too much. Nevertheless, this second combination better confirms the results of Taguchi analysis. Therefore, $A_1B_1C_{-1}D_{-1}E_1$ combination is selected as the optimum parameter level combination.

6.1.2 Regression Analysis of the Mean Impact Resistance Based on the L_{27} (3^{13}) Design

The first employed regression analysis to model the mean impact resistance again contains only the main factors. That is:

$$y = 4{,}97 + 0{,}283*A + 0{,}663*B_1 + 1{,}84*B_2 - 0{,}406*C - 1{,}14*D_1 + 1{,}10*E \quad (6.5)$$

Table 6.6 shows the ANOVA for the significance of the above regression model. The hypothesis of having all β terms equal to zero is tested and refused with a confidence level of (1 – p)*100%, which is 97.5% for this model.

Table 6.6 ANOVA for the significance of the regression model developed for the mean impact resistance based on the L_{27} (3^{13}) design including only the main factors

Source	df	Sum of Squares	Mean Squares	F	P
Regression	6	44,755	7,459	3,13	0,025
Residual Error	20	47,670	2,384		
Total	26	92,426			

$R^2 = 48.4\%$ $R^2_{(adj)} = 32.9\%$ $S = 1.544$

Durbin-Watson statistic = 2.67

The adjusted multiple coefficient of determination, $R^2_{(adj)}$, shows that only 32.9% of the sample variation in the mean impact resistance can be explained by this model which is not acceptable. The Durbin-Watson statistic states that there is insufficient evidence to conclude that the residuals are negatively correlated because (4 - Durbin-Watson statistic), which results in 1.33, falls in between the tabulated lower (1.01) and upper bounds (1.86) with 95% confidence with 5 independent variables and 27 observations. The residual plots of this model are

given in Figures 6.13 and 6.14. The residuals versus the fitted values plot seems patternless, showing that there is not an indication of violation of the constant variance assumption of the error. The normality assumption is somewhat satisfied because of the linearity of the residual normal plot in Figure 6.14. A more adequate regression model will be searched to describe the mean impact resistance. The significance of β terms of the model is shown in Table 6.7. This table indicates that only B_2, D_1 and E are significant on the mean impact resistance.

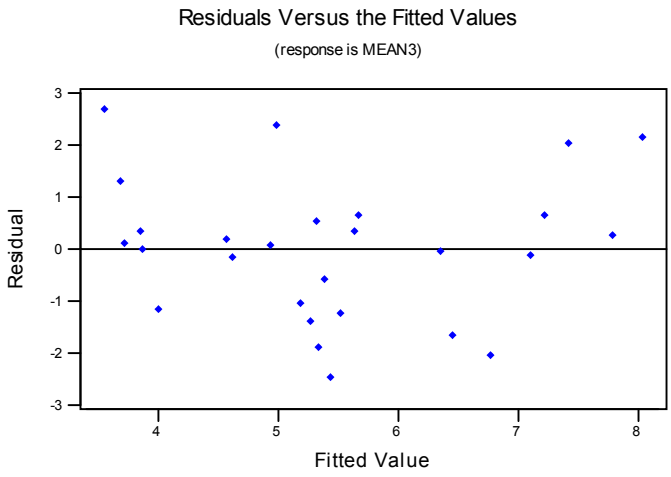

Figure 6.13 Residuals versus fitted values plot of the regression model developed for the mean impact resistance with only main factors based on the L_{27} (3^{13}) design

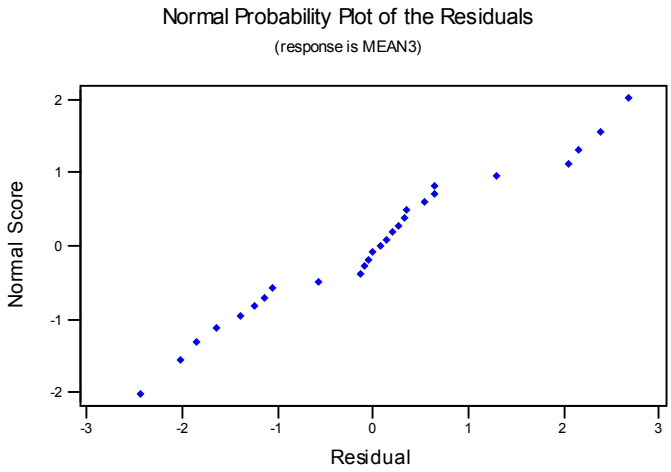

Figure 6.14 Residual normal probability plot of the regression model developed for the mean impact resistance with only main factors based on the L_{27} (3^{13}) design

Table 6.7 Significance of β terms of the regression model developed for the mean impact resistance with only main factors based on the L_{27} (3^{13}) design

Predictor	β Estimate	Standard Error	T	P
Constant	4,9696	0,5566	8,93	0,000
A	0,2832	0,3645	0,78	0,446
B_1	0,6632	0,7290	0,91	0,374
B_2	1,8446	0,7290	2,53	0,020
C	-0,4056	0,3645	-1,11	0,279
D_1	-1,1428	0,6317	-1,81	0,085
E	1,1017	0,3777	2,92	0,009

The MINITAB output with the sequential sum of squares of the regression model can be seen in Appendix D.1.

The second regression model is decided to include all the two-way interaction terms. Because the experimental design has only 26 degrees of freedom, all of the variables can not be included in the model since they exceed the 26 degrees

of freedom. Therefore a pre-analysis is performed and it is seen that all the interactions with D_1 variable are insignificant. As a result they are omitted form the model. The equation and the ANOVA table for the regression model can be seen in Eqn. 6.6 and Table 6.8 respectively. By this model with 93.2% confidence the hypothesis that all β terms are equal to zero is rejected.

$$y = 3{,}23 + 0{,}198*A + 2{,}13*B1 + 5{,}65*B_2 + 1{,}38*C + 3{,}20*D_1 - 0{,}794*E - 4{,}18*AC + 3{,}75*AE + 0{,}787*CE - 3{,}52*B_1D_1 - 10{,}5*B_2D_1 + 0{,}674*AB_1 - 2{,}44*CB_1 + 1{,}50*EB_1 + 3{,}42*ACB_1 - 3{,}51*AEB_1 - 1{,}34*CEB_1 - 1{,}40*AB_2 + 0{,}301*CB_2 + 3{,}98*EB_2 + 1{,}25*ACB_2 - 7{,}34*AEB_2 + 1{,}09*CEB_2 \quad (6.6)$$

Table 6.8 ANOVA for the significance of the regression model developed for the mean impact resistance based on the L_{27} (3^{13}) design including main and interaction factors

Source	df	Sum of Squares	Mean Squares	F	P
Regression	23	90,7217	3,9444	6,95	0,068
Residual Error	3	1,7039	0,5680		
Total	26	92,4255			

$R^2 = 98.2\%$ $R^2_{(adj)} = 84.0\%$ $S = 0.7536$

Durbin-Watson statistic = 2.19

This model is enough to explain the mean impact resistance of SFRHSC since $R^2_{(adj)}$ is 84.0%. The Durbin-Watson statistic is 2.19 showing that there is not enough information to decide on the independence of the errors, because, (4-Durbin-Watson statistic), 1.81, is below the upper boundary, 1.86. Also the R^2 value is improved by this model from 48.4% to 98.2% but the slight difference between R^2 and $R^2_{(adj)}$ means that there are unnecessary terms in the model.

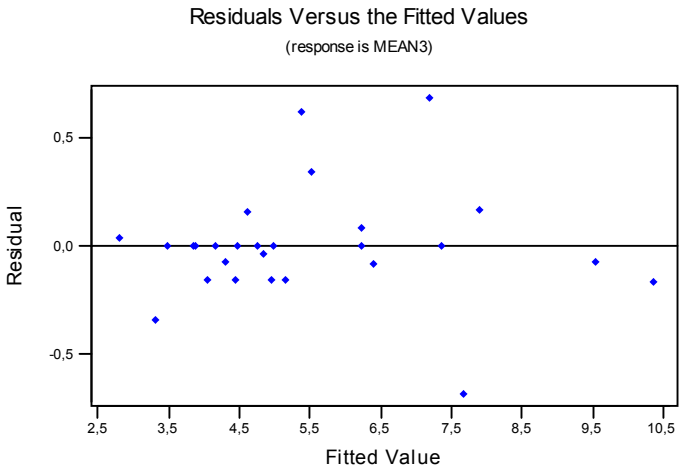

Figure 6.15 Residuals versus fitted values plot of the regression model in Eqn.6.6 developed for the mean impact resistance and based on the L_{27} (3^{13}) design

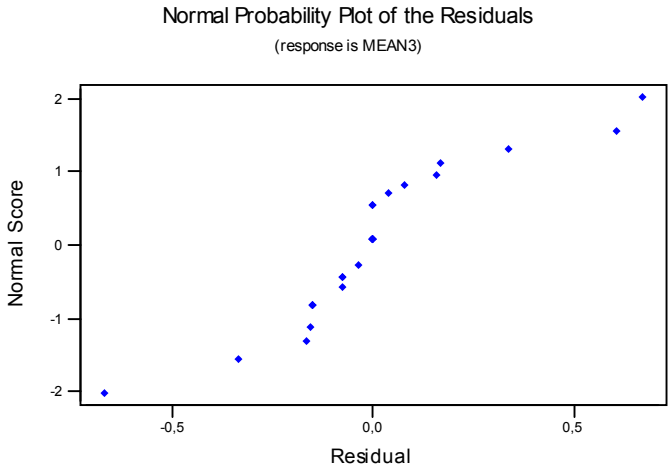

Figure 6.16 Residual normal probability plot of the regression model in Eqn.6.6 developed for the mean impact resistance and based on the L_{27} (3^{13}) design

Most of the residuals are collected at the lower side of the fitted values in the residuals versus the fitted values plot (Figure 6.15). The normal probability plot in Figure 6.16 indicates that the error term has a normal distribution since it is

almost linear, especially the mid portion. A more adequate model having better residual plots should be searched. Table 6.9 shows the level of significance of the β terms.

The MINITAB output with the sequential sum of squares of the regression model can be seen in Appendix D.2.

Table 6.9 Significance of β terms of the regression model in Eqn.6.6 developed for the mean impact resistance and based on the L_{27} (3^{13}) design

Predictor	β Estimate	Standard Error	T	P
Constant	3,2278	0,5329	6,06	0,009
A	0,1981	0,4157	0,48	0,666
B_1	2,1303	0,6212	3,43	0,042
B_2	5,6500	0,7536	7,50	0,005
C	1,3833	0,5069	2,73	0,072
D_1	3,2040	1,1020	2,91	0,062
E	-0,7944	0,5069	-1,57	0,215
AC	-4,1796	0,9644	-4,33	0,023
AE	3,7460	1,0450	3,58	0,037
CE	0,7870	0,7426	1,06	0,367
B_1D_1	-3,5230	1,2500	-2,82	0,067
B_2D_1	-10,5370	1,7890	-5,89	0,010
AB_1	0,6741	0,5172	1,30	0,283
CB_1	-2,4389	0,5929	-4,11	0,026
EB_1	1,5000	0,5929	2,53	0,085
ACB_1	3,4240	1,0720	3,19	0,050
AEB_1	-3,5070	1,1450	-3,06	0,055
CEB_1	-1,3430	0,8774	-1,53	0,223
AB_2	-1,4029	0,6555	-2,14	0,122
CB_2	0,3008	0,7168	0,42	0,703
EB_2	3,9833	0,7972	5,00	0,015
ACB_2	1,2460	1,4370	0,87	0,450
AEB_2	-7,3370	1,3200	-5,56	0,011
CEB_2	1,0890	1,0960	0,99	0,393

It can be seen from Table 6.9 except from factors A, E, CE, AB_1, CEB_1, CB_2, ACB_2 and CEB_2, all the other factors are significant on the mean impact resistance with p(0.10) confidence. The model will be tried to improve by discarding the insignificant terms from the model one by one starting from the term having the largest p-value. The new model is reached by pooling ACB_2, CEB_2, CB_2, AEB_1 and adding AD_1. In the previous model AEB_1 was significant but, after adding AD_1 term in the equation it becomes very insignificant and therefore it is discarded from the model. $R^2_{(adj)}$ term of the model seen in Eqn.6.7 became 91.4%. But the Durbin-Watson statistic increased a little bit by this model but still there is not enough evidence to say that whether the residuals are negatively correlated or not. The equation and ANOVA of the model can be seen in Eqn.6.7 and Table 6.10.

$$y = 4{,}93 + 2{,}95*A + 0{,}432*B_1 + 2{,}28*B_2 - 0{,}160*C - 0{,}757*D_1 + 0{,}857*E + 1{,}95*AC - 2{,}30*AE + 1{,}78*CE + 0{,}438*B_1D_1 - 1{,}56*B_2D_1 - 0{,}388*AB_1 - 0{,}052*CB_1 - 0{,}996*EB_1 - 5{,}24*ACB_1 - 2{,}33*CEB_1 - 2{,}42*AB_2 - 0{,}953*EB_2 - 1{,}12*AEB_2 - 5{,}07*AD_1 \quad (6.7)$$

Table 6.10 ANOVA for the significance of the regression model in Eqn.6.7 developed for the mean impact resistance based on the L_{27} (3^{13}) design

Source	df	Sum of Squares	Mean Squares	F	P
Regression	20	90,5852	4,5293	14,77	0,002
Residual Error	6	1,8404	0,3067		
Total	26	92,4255			

$R^2 = 98.0\%$ $R^2_{(adj)} = 91.4\%$ $S = 0.5538$

Durbin-Watson statistic = 2.26

The residual plots can be seen in Figures 6.17 and 6.18.

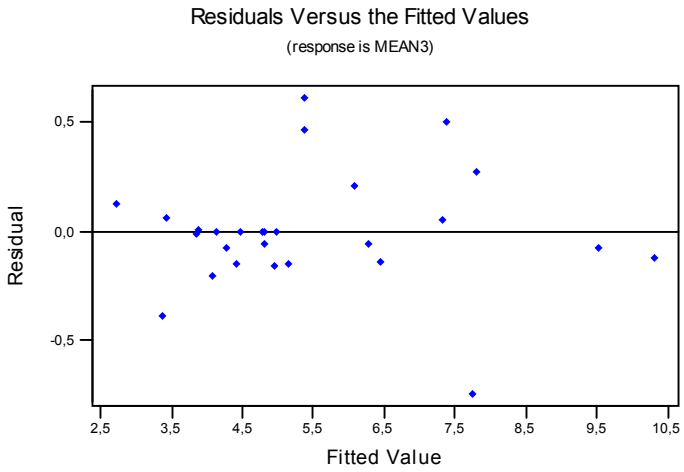

Figure 6.17 Residuals versus fitted values plot of the regression model in Eqn.6.7 developed for the mean impact resistance and based on the L_{27} (3^{13}) design

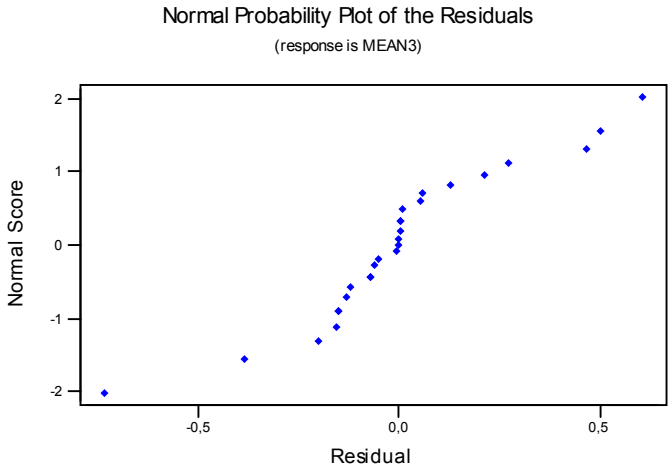

Figure 6.18 Residual normal probability plot of the regression model in Eqn.6.7 developed for the mean impact resistance and based on the L_{27} (3^{13}) design

Most of the residuals are collected at the lower side of the fitted values in the residuals versus the fitted values plot (Figure 6.17). The normal probability plot in Figure 6.18 seems linear indicating that the error term has a normal

distribution. As a result an adequate model explaining the mean response can not be achieved without any variance stabilizing data transformation. Table 6.11 shows the significance of the β terms. In this model A, B_2, D_1, E, AC, CE, EB_1, ACB_1, CEB_1, AB_2, AEB_2 and AD_1 are the significant terms on the mean impact resistance of SFRHSC.

The MINITAB output with the sequential sum of squares of the regression model can be seen in Appendix D.3.

Table 6.11 Significance of β terms of the regression model in Eqn.6.7 developed for the mean impact resistance and based on the L_{27} (3^{13}) design

Predictor	β Estimate	Standard Error	T	P
Constant	4,9261	0,3335	14,77	0,000
A	2,9491	0,5300	5,56	0,001
B_1	0,4323	0,3981	1,09	0,319
B_2	2,2791	0,6055	3,76	0,009
C	-0,1596	0,2610	-0,61	0,563
D_1	-0,7573	0,7305	-1,04	0,340
E	0,8569	0,3995	2,14	0,076
AC	1,9477	0,9110	2,14	0,076
AE	-2,2971	0,7165	-3,21	0,018
CE	1,7776	0,4039	4,40	0,005
B_1D_1	0,4378	0,8182	0,54	0,612
B_2D_1	-1,5580	1,5360	-1,01	0,350
AB_1	-0,3881	0,3717	-1,04	0,337
CB_1	-0,0515	0,4489	-0,11	0,912
EB_1	-0,9957	0,5610	-1,77	0,126
ACB_1	-5,2380	1,4670	-3,57	0,012
CEB_1	-2,3345	0,5408	-4,32	0,005
AB_2	-2,4158	0,4957	-4,87	0,003
EB_2	-0,9529	0,9587	-0,99	0,359
AEB_2	-1,1183	0,6828	-1,64	0,153
AD_1	-5,0663	0,9732	-5,21	0,002

A logarithmic transformation, y* = log y, is decided to be applied for the mean impact resistance. The log y values of the mean impact resistance of SFRHSC are given in Appendix D.4. The mean of the replicates is logarithmically transformed instead of the transformation of the individual results.

The best model achieved and the ANOVA table of the regression analysis of the transformed mean impact resistance values can be seen in Eqn.6.8 and Table 6.12.

$$\log \mu = 0{,}707 + 0{,}105*A + 0{,}0091*B_1 + 0{,}101*B_2 - 0{,}0288*C - 0{,}0802*D_1 + 0{,}0959*E + 0{,}0558*AC - 0{,}104*AE - 0{,}0381*CE + 0{,}0492*B_1D_1 - 0{,}0001*AB_1 - 0{,}0055*CB_1 - 0{,}0583*EB_1 - 0{,}197*ACB_1 + 0{,}0566*AEB_1 + 0{,}0398*CEB_1 - 0{,}259*AD_1 + 0{,}0831*CD_1 - 0{,}156*ED_1 \quad (6.8)$$

Table 6.12 ANOVA for the significance of the best regression model developed for the transformed mean impact resistance based on the L_{27} (3^{13}) design

Source	df	Sum of Squares	Mean Squares	F	P
Regression	19	0,517495	0,027237	11,08	0,002
Residual Error	7	0,017212	0,002459		
Total	26	0,534707			

$R^2 = 96.8\%$ $R^2_{(adj)} = 88.0\%$ $S = 0.04959$

Durbin-Watson statistic = 2.05

By this transformed quadratic model the Durbin-Watson statistic is improved showing that the residuals are uncorrelated but, $R^2_{(adj)}$ term degraded. However, this model seems enough to explain the impact resistance of SFRHSC. The residuals versus the fitted values and normal probability plots are given in Figures 6.19 and 6.20.

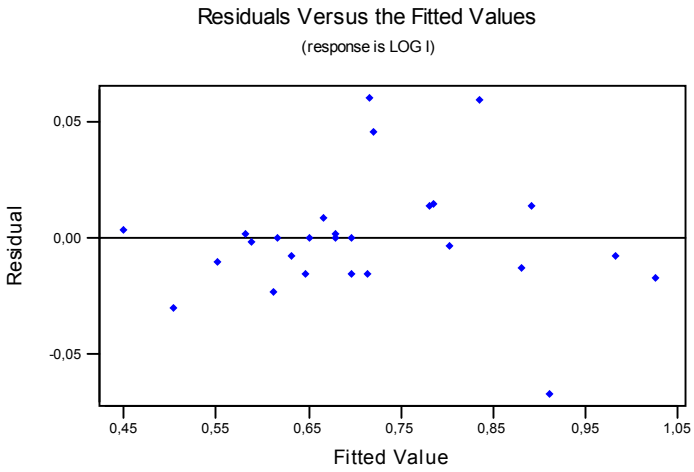

Figure 6.19 Residuals versus fitted values plot of the quadratic regression model in Eqn.6.8 developed for the log transformed mean impact resistance

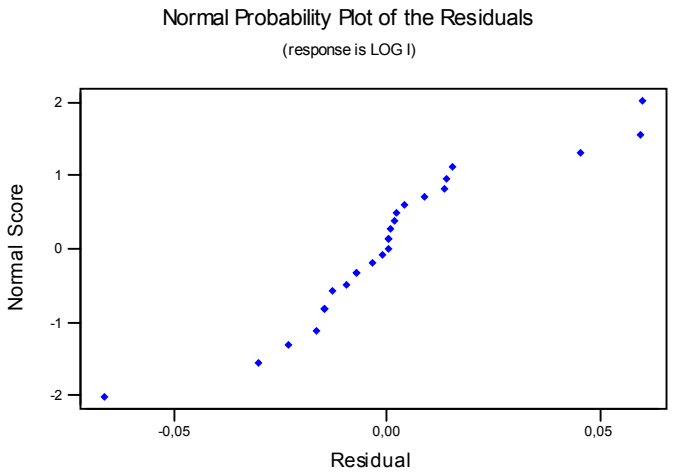

Figure 6.20 Residual normal probability plot of the quadratic regression model in Eqn.6.8 developed for the log transformed mean impact resistance

By the variance stabilizing data transformation the constant variance of the error assumption is validated since there is no obvious pattern in the residuals versus fitted values plot. Also the normal probability plot of the residuals is linear indicating that the error term has a normal distribution. Although this model has

lower $R^2_{(adj)}$, since all of the assumptions of the error terms are satisfied, this transformed model overcomes the nontransformed one and this model is decided to be kept as the best regression model. Table 6.13 shows the β significance of the factors. It is concluded that, except from the factors B_1, B_1D_1, AB_1, CB_1, AEB_1 and CEB_1, all the remaining factors are significant on the mean impact resistance with 90% confidence. The MINITAB output with the sequential sum of squares of the transformed model can be found in Appendix D.5.

Table 6.13 Significance of β terms of the quadratic regression model in Eqn.6.8 developed for the log transformed mean impact resistance

Predictor	β Estimate	Standard Error	T	P
Constant	0,70658	0,01931	36,60	0,000
A	0,10464	0,02232	4,69	0,002
B_1	0,00907	0,02853	0,32	0,760
B_2	0,10061	0,02404	4,19	0,004
C	-0,02882	0,01807	-1,59	0,155
D_1	-0,08019	0,02752	-2,91	0,023
E	0,09594	0,02231	4,30	0,004
AC	0,05585	0,02442	2,29	0,056
AE	-0,10411	0,03125	-3,33	0,013
CE	-0,03810	0,02547	-1,50	0,178
B_1D_1	0,04918	0,04765	1,03	0,336
AB_1	-0,00010	0,02627	-0,00	0,997
CB_1	-0,00549	0,02767	-0,20	0,848
EB_1	-0,05831	0,02675	-2,18	0,066
ACB_1	-0,19661	0,05588	-3,52	0,010
AEB_1	0,05658	0,04009	1,41	0,201
CEB_1	0,03975	0,05774	0,69	0,513
AD_1	-0,25942	0,04213	-6,16	0,000
CD_1	0,08309	0,03285	2,53	0,039
ED_1	-0,15640	0,04875	-3,21	0,015

6.1.3 Response Surface Optimization of Mean Impact Resistance Based on the L_{27} (3^{13}) Design

For the MINITAB response optimization the best regression model found in Eqn.6.8 in the previous section for the mean impact resistance will be used. Since a similar impact resistance test that is employed in this study can not be found in literature, the minimum and target values are determined according to the results of this study. The lower bound is set to 5.0 kgf.m because the average of all the readings is around 5.50 kgf.m and the target value is set to 10.0 kgf.m since the average of the maximum readings is around 10. The same thirteen starting points are tried again and additionally the optimum combination found in Taguchi analysis $A_1B_{-1}C_{-1}D_1E_1$ is tried. The results of the optimizer can be seen in Table 6.14. The starting points and the optimum points found by MINITAB response optimizer is shown in Table 6.15.

Table 6.14 The optimum response, its desirability, the confidence and prediction intervals computed by MINITAB Response Optimizer for the mean impact resistance based on the L_{27} (3^{13}) design

Optimum Points	log μ	Desirability	95% Conf. Int.	95% Pred. Int.	Mean Impact
1	0,8142	0,46292	(0,6401; 0,9881)	(0,6043; 1,0240)	6,5181
2	0,9512	0,83582	(0,7843; 1,1180)	(0,7472; 1,1551)	8,9363
3	0,7738	0,35225	(0,6907; 0,8569)	(0,6300; 0,9176)	5,9405
4	0,9147	0,71329	(0,7418; 1,0877)	(0,7057; 1,1237)	8,2173
5	0,8062	0,43746	(0,6967; 0,9157)	(0,6457; 0,9667)	6,4001
6	0,7897	0,38952	(0,5626; 1,0168)	(0,5341; 1,0453)	6,1617
7	0,6906	0,13313	(0,5052; 0,8761)	(0,4712; 0,9101)	4,9050
8	0,9037	0,67865	(0,8071; 1,0002)	(0,7517; 1,0556)	8,5030
9	0,9837	0,95329	(0,8671; 1,1003)	(0,8183; 1,1491)	9,6319
10	0,9147	0,71329	(0,7418; 1,0877)	(0,7057; 1,1237)	8,2173
11	0,8142	0,46292	(0,6401; 0,9881)	(0,6043; 1,0240)	6,5181
12	0,9188	0,72359	(0,7650; 1,0726)	(0,7253; 1,1123)	8,2945
13	0,8016	0,43999	(0,6831; 0,9200)	(0,6349; 0,9683)	6,3327
14	0,9147	0,71329	(0,7418; 1,0877)	(0,7057; 1,1237)	8,2173

Table 6.15 The starting and optimum points for MINITAB response optimizer developed for the mean impact resistance based on the L_{27} (3^{13}) design

	Starting Points					Optimum Points				
Points	**Age (days)**	**B. Type**	**B. Amount (%)**	**Cure**	**Steel (% vol.)**	**Age (days)**	**B. Type**	**B. Amount (%)**	**Cure**	**Steel (% vol.)**
1	90	SF	20	water	1,0	90	SF	20	water	1,0
2	No starting point					82	GGBFS	60	water	0,0
3	90	SF	20	steam	0,5	80	SF	20	water	0,5
4	90	GGBFS	20	water	0,5	90	GGBFS	20	water	1,0
5	90	SF	10	water	1,0	90	SF	16,5	water	1,0
6	28	FA	40	steam	0,5	90	FA	10	steam	0,0
7	7	SF	20	water	0,0	11	SF	19	steam	0,0
8	90	GGBFS	60	water	1,0	90	GGBFS	40	water	1,0
9	90	FA	10	water	1,0	90	FA	10	water	1,0
10	28	GGBFS	20	steam	1,0	90	GGBFS	20	water	1,0
11	90	SF	15	water	1,0	90	SF	20	water	1,0
12	90	GGBFS	20	steam	1,0	82	GGBFS	21	water	1,0
13	90	SF	20	water	0,0	90	SF	20	water	0,8
14	90	SF	20	steam	1,0	90	GGBFS	20	water	1,0

The starting point 9 resulted in the highest impact resistance, 9.63 kgf.m, which is very close to the desired impact resistance of 10.0 kgf.m and its confidence and prediction intervals are relatively narrower. Point 2 is the second best with 8.94 kgf.m impact resistance. Although its intervals are wider, it is worth to do a confirmation run for this point. Point 8 resulted in 8.5 kgf.m impact resistance and it has the narrowest confidence and prediction interval and therefore it is worth to try this point. Points 4, 10, 12, and 14 gave nearly the same result around 8.2 kgf.m. The confidence and prediction intervals of all points are relatively wider, but the confirmation runs will be performed for them. One of the combinations that resulted in relatively lower impact resistance will be tried also and points 1 and 11 are chosen for the confirmation trials since they are the highest among the remaining points and they gave exactly the same results. The remaining points resulted in relatively lower impact resistance values and therefore they are not taken into consideration for the confirmation experiments. Each experiment is repeated three times for convenience.

Optimum point 9:

For this point the 3rd level for Age (90 days), 2nd level for Binder Amount (Fly Ash), 1st level for Binder Amount (10% for fly ash), 1st level for Curing Type (ordinary water curing) and the 3rd level for Steel Fiber Volume Fraction (1.0%) are assigned to the associated main factors. The results of the experiments are 16.80 kgf.m, 4.0 kgf.m and 7.60 kgf.m and their logarithmic transformed values are 1.23, 0.60 and 0.88. Only 0.88 is in the confidence and prediction intervals' limits. 1.23 is above the upper boundary and 0.60 is below the lower boundary showing that there is a considerable amount of variation. Also, they are very far from the optimum fitted value of 9.63 kgf.m found by the Response Optimizer. As a result, it can be said that this point is not very well modeled by the regression model in Eqn.6.8.

Optimum point 2:

For this experiment age, binder type, binder amount, curing type and steel fiber volume fraction are set to 90 days, GGBFS, 60% for GGBFS, ordinary water curing and 0.0% respectively. The results of the experiments are 4.20 kgf.m, 3.20 kgf.m and 4.40 kgf.m with the transformed values of 0.62, 0.51 and 0.64. None of them falls in both intervals. Also none of the results are near to the predicted optimum value of 8.94 kgf.m. So it can be said that this point is overestimated by the chosen regression model.

Optimum point 8:

For this point the 3rd level for Age (90 days), 3rd level for Binder Amount (GGBFS), 2nd level for Binder Amount (40% for GGBFS), 1st level for Curing Type (ordinary water curing) and the 3rd level for Steel Fiber Volume Fraction (1.0%) are assigned to the associated main factors. The results of the experiments are 3.80 kgf.m, 6.20 kgf.m and 8.60 kgf.m with the transformed values of 0.58, 0.79 and 0.93. Only 0.93 is in the confidence interval and 0.79 and 0.93 are in the prediction interval. The remaining confirmation run results are below the lower limits of the intervals. Also the mean value of the experiments, which is 6.2 kgf.m, is very far from the fitted value found by the regression analysis, around 8.5 kgf.m. It can be concluded that the results of the confirmation experiments are very far from the findings of the regression analysis. Therefore these points could not be modeled very well. We could have an improvement by conducting the experiments of this point but this could not achieved.

Optimum points 4, 10, 12 and 11:

One confirmation experiment is done for these points since their optimum performance levels are very close. For these points the 3rd level for Age (90 days), 3rd level for Binder Amount (GGBFS), 1st level for Binder Amount (20%

for GGBFS), 1st level for Curing Type (ordinary water curing) and the 3rd level for Steel Fiber Volume Fraction (1.0%) are assigned to the associated main factors. The results of the experiments are 4.20 kgf.m, 5.50 kgf.m and 10.10 kgf.m with the transformed values of 0.62, 0.74 and 1.00. Only 1.00 is in the confidence interval and 0.74 and 1.00 are in the prediction interval for all the points. The remaining confirmation run results are below the lower limits of the intervals. Also the mean value of the experiments, which is 6.6 kgf.m, is very far from the fitted values of all points, around 8.2 kgf.m. It can be concluded that the results of the confirmation experiments are very far from the findings of the Response Optimizer. Therefore these points could not be modeled very well.

Optimum points 1 and 11:

For these points the 3rd level for Age (90 days), 1st level for Binder Amount (Silica Fume), 1st level for Binder Amount (20% for silica fume), 1st level for Curing Type (ordinary water curing) and the 3rd level for Steel Fiber Volume Fraction (1.0%) are assigned to the associated main factors. The results of the experiments are 9.20 kgf.m, 5.30 kgf.m and 5.50 kgf.m and their logarithmic transformed values are 0.96, 0.72 and 0.74. These transformed values are in both the confidence and prediction intervals and the two results, 5.30 kgf.m and 5.50 kgf.m, are not very far from the optimum fitted value of 6.5 kgf.m found by the regression model. As a result, it can be said that this point is well modeled by the regression model in Eqn.6.8.

The best point chosen for the result of the regression analysis of the mean impact resistance is the optimum 1. Although it did not give high values of impact resistance, it is well modeled by the regression model. Also among the three replicates of the confirmation run for this point, two of them are very consistent with each other. There are more variations in the results of the other confirmation runs. Therefore $A_1B_{-1}C_{-1}D_{-1}E_1$ combination can be selected as the

optimal levels for the mean impact resistance of SFRHSC. But none of the points can be well modeled by the chosen regression equation in Eqn.6.8.

6.2. Full Factorial Experimental Design

As in Chapter 4, again in order to analyze the effects of all three-way, four-way and five-way interaction effects on all of the responses it is decided to conduct all the experiments for impact resistance needed for $3^4 2^1$ full factorial design and analysis.

6.2.1 Taguchi Analysis of the Mean Impact Resistance Based on the Full Factorial Design

The ANOVA table for the impact resistance of SFRHSC can be seen in Table 6.16. It indicates that with 90% confidence interval, from the main factors Age, Binder Type, Curing Type and Steel significantly affect the impact resistance. From the two-way interactions, Age*Binder Type (AB), Age*Cure (AD), Age*Steel (AE), Binder Amount*Cure (DC(B)), Binder Amount*Steel (EC(B)), and from the three-way interactions only Age*Cure*Steel (ADE) are the significant factors on the impact resistance. The ABDE and ADEC(B) interactions can be accepted as significant on the mean impact resistance with 86.4% and 81.8% confidences respectively. From the two-way interaction plot in Figure 6.21, it seems that additional to the significant factors determined from the ANOVA table, AC and BE slightly affect the response variable because the three lines cross. They are not accepted as significant terms as their p-values are not small enough.

Table 6.16 ANOVA table for the mean impact resistance based on the full factorial design

Source	df	Sum of Squares	Mean Square	F	P
A	2	149,463	74,732	11,80	0,000
B	2	30,302	15,151	2,39	0,093
C (B)	6	45,992	7,665	1,21	0,300
D	1	28,456	28,456	4,49	0,035
E	2	600,814	300,407	47,45	0,000
AB	4	55,677	13,919	2,20	0,069
AC(B)	12	57,600	4,800	0,76	0,694
AD	2	47,274	23,637	3,73	0,025
AE	4	77,501	19,375	3,06	0,017
BD	2	0,758	0,379	0,06	0,942
BE	4	31,854	7,963	1,26	0,287
DC(B)	6	90,854	15,142	2,39	0,028
EC(B)	12	129,627	10,802	1,71	0,064
DE	2	14,514	7,257	1,15	0,319
ABD	4	8,021	2,005	0,32	0,867
ABE	8	46,568	5,821	0,92	0,500
ADC(B)	12	94,567	7,881	1,24	0,251
AEC(B)	24	114,328	4,764	0,75	0,795
ADE	4	67,396	16,849	2,66	0,033
BDE	4	14,626	3,657	0,58	0,679
DEC(B)	12	81,700	6,808	1,08	0,380
ABDE	8	79,06	9,883	1,56	0,136
ADEC(B)	24	192,750	8,031	1,27	0,182
Error	324	2051,407	6,332		
TOTAL	485	4111,108			

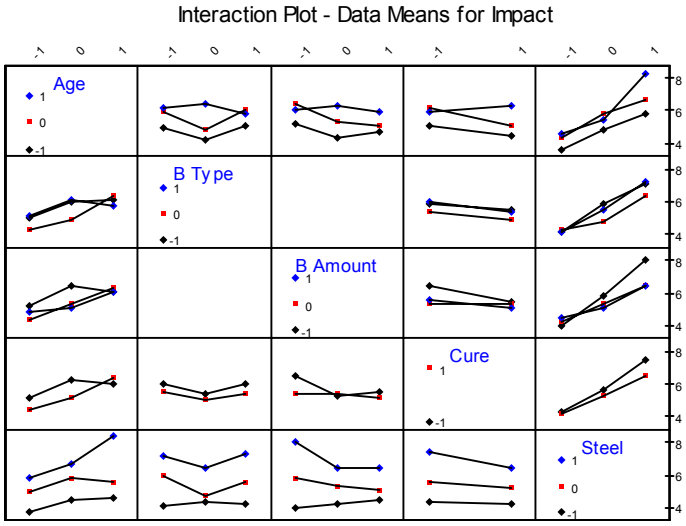

Figure 6.21 Two-way interaction plots for the mean impact resistance

The residual plots of the model for the mean impact resistance are given in Figures 6.22 and 6.23.

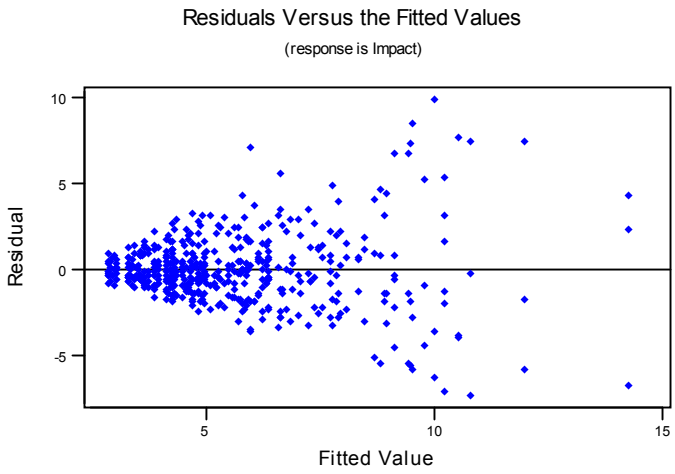

Figure 6.22 The residuals versus fitted values of the full factorial model found by ANOVA for the means for impact resistance

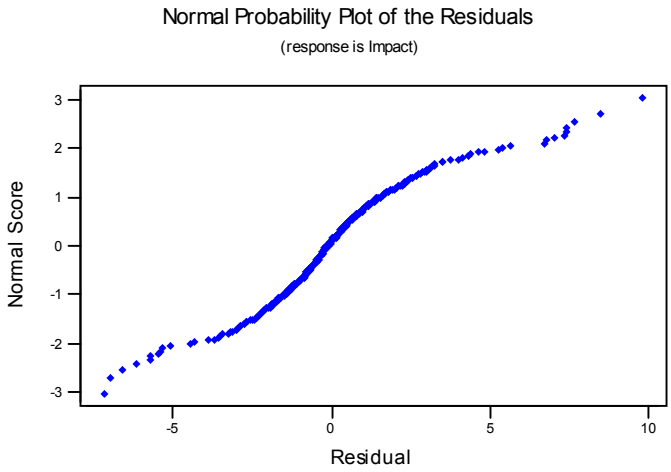

Figure 6.23 The residual normal probability plot for the full factorial model found by ANOVA for the means for impact resistance

It can be concluded from both figures that assumptions of having a constant variance and normal distribution of the error term are violated. There is an increasing trend of the residuals as the fitted values are increased and the residual normal probability plot is not linear. So a variance stabilizing data transformation is necessary.

Figure 6.24 shows the main effects plot which is used for finding the optimum levels of the process parameters that increases the mean impact resistance.

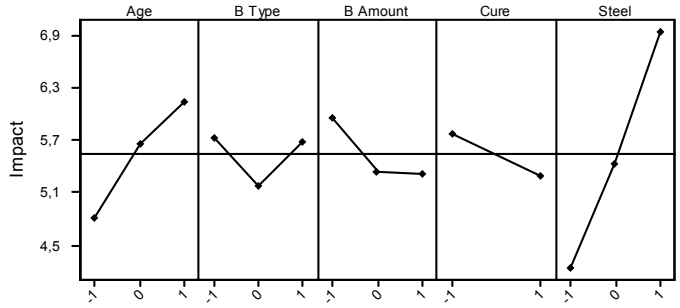

Figure 6.24 Main effects plot based on the full factorial design for the mean impact resistance

As it can be seen from Figure 6.24, the optimum points are 3rd level for Age (90 days), 1st level for the Binder Type (Silica Fume), 1st level for the Binder Amount (20% as silica fume is selected for the binder type), 1st level for Curing Type (water curing) and the 3rd level for the Steel Fiber Volume Fraction (1.0%). Also for the binder type GGBFS can be selected as the most resistance binder to impact with an amount of 20%. From the interaction plot it can be seen that the optimum levels for the 95% significant interaction terms are A_1xD_1, A_1xE_1, $C_{-1}xD_{-1}$ which coincides with the optimum levels of the main effects except for factor D. Therefore the two combinations of the optimum levels should be calculated for both the 1st and 3rd level of factor D. The two combinations are $A_1B_{-1}C_{-1}D_{-1}E_1$ and $A_1B_{-1}C_{-1}D_1E_1$ respectively.

Combination 1: $A_1B_{-1}C_{-1}D_{-1}E_1$ (experiment no. 111)

$$\hat{\mu}_{A_1B_{-1}C_{-1}D_{-1}E_1} = \overline{T} + (\overline{A}_1 - \overline{T}) + (\overline{B}_{-1} - \overline{T}) + (\overline{C}_{-1} - \overline{T}) + (\overline{D}_{-1} - \overline{T}) + (\overline{E}_1 - \overline{T}) + (\overline{A_1 \times D_{-1}} - \overline{T}) + (\overline{A_1 \times E_1} - \overline{T}) + (\overline{C_{-1} \times D_{-1}} - \overline{T}) \quad (6.9)$$

$$\hat{\mu}_{A_1B_{-1}C_{-1}D_{-1}E_1} = \overline{T} + (\overline{B}_{-1} - \overline{T}) - (\overline{A}_1 - \overline{T}) - (\overline{D}_{-1} - \overline{T}) + (\overline{A_1D_{-1}} - \overline{T}) + (\overline{A_1E_1} - \overline{T}) + (\overline{C_{-1}D_{-1}} - \overline{T})$$

$$\hat{\mu}_{A_1B_{-1}C_{-1}D_{-1}E_1} = 5.54 + (5.74 - 5.54) - (6.14 - 5.54) - (5.78 - 5.54) + (5.96 - 5.54) + (8.34 - 5.54) + (6.48 - 5.54)$$

$$= 9.06 \text{ kgf.m}$$

The confidence interval is:

$$n_e = \frac{486}{25+1} = 18.69$$

$V_e = 6.332$

$F_{0.05,1,324} = 3.84$

$$\text{C.I.} = \sqrt{\frac{3.84 \times 6.332}{18.69}} = 1.14$$

Therefore, the value of the mean impact resistance is expected in between;

$\hat{\mu}_{A_1B_{-1}C_{-1}D_{-1}E_1}$ = {7.92, 10.20} with 95% confidence interval.

Combination 2: $A_1B_{-1}C_{-1}D_1E_1$ (experiment no. 114)

$$\hat{\mu}_{A_1B_{-1}C_{-1}D_1E_1} = \overline{T} + (\overline{A}_1 - \overline{T}) + (\overline{B}_{-1} - \overline{T}) + (\overline{C}_{-1} - \overline{T}) + (\overline{D}_1 - \overline{T}) + (\overline{E}_1 - \overline{T}) + (\overline{A_1 \times D_1} - \overline{T}) + (\overline{A_1 \times E_1} - \overline{T}) + (\overline{C_{-1} \times D_1} - \overline{T}) \quad (6.10)$$

$$\hat{\mu}_{A_1B_{-1}C_{-1}D_1E_1} = \overline{T} + (\overline{B}_{-1} - \overline{T}) - (\overline{A}_1 - \overline{T}) - (\overline{D}_1 - \overline{T}) + (\overline{A_1D_1} - \overline{T}) + (\overline{A_1E_1} - \overline{T}) + (\overline{C_1D_1} - \overline{T})$$

$$\hat{\mu}_{A_1B_{-1}C_{-1}D_1E_1} = 5.54 + (5.74 - 5.54) - (6.14 - 5.54) - (5.29 - 5.54) + (6.33 - 5.54) + (8.34 - 5.54) + (5.33 - 5.54)$$

$$= 8.77 \text{ kgf.m}$$

The confidence interval is the same as the one calculated above, 1.14. Therefore, the value of the mean flexural strength is expected in between;

$\hat{\mu}_{A_1B_{-1}C_{-1}D_1E_1} = \{7.63, 9.91\}$ with 95% confidence interval.

Since the maximum impact resistance is obtained by combination 1, the optimum levels are accepted as $A_1B_{-1}C_{-1}D_{-1}E_1$.

In order to determine the most robust set of operating condition from variations within the results of impact resistance, ANOVA for the S/N ratio values are performed (Table 6.17). Again the four-way interaction term (ADEC(B)) is omitted in order to leave 24 degrees of freedom to the error term. The results of the ANOVA show that all the main factors except factor C(B) (Binder Amount) are significant on the impact resistance of SFRHSC. The two-way interaction factors AB and BE are also significant with 95% confidence. Additional to these two-way interaction factors, AE and DC(B) are accepted as significant with 82.8% and 86.6% confidence respectively. None of the three-way and four-way interaction factors are significant on the impact resistance. Figure 6.25 shows all the two-way factor interaction plots. As it can be seen from the figure that AB, AE, BE and DC(B) interactions significantly contribute to the impact resistance since, the lines in the corresponding plots are not parallel.

Table 6.17 ANOVA of S/N ratio values for the impact resistance based on the full factorial design

Source	df	Sum of Squares	Mean Square	F	P
A	2	96,661	48,330	11.91	0,000
B	2	47,29	23,645	5,83	0,009
C (B)	6	21,909	3,651	0,90	0,511
D	1	21,962	21,962	5,41	0,029
E	2	257,007	128,504	31,67	0,000
AB	4	44,067	11,017	2,72	0,054
AC(B)	12	52,946	4,412	1,09	0,412
AD	2	4,459	2,230	0,55	0,584
AE	4	28,406	7,102	1,75	0,172
BD	2	1,882	0,941	0,23	0,795
BE	4	53,452	13,363	3,29	0,028
DC(B)	6	44,780	7,463	1,84	0,134
EC(B)	12	65,627	5,469	1,35	0,257
DE	2	11,813	5,907	1,46	0,253
ABD	4	3,671	0,918	0,23	0,921
ABE	8	9,831	1,229	0,30	0,958
ADC(B)	12	50,171	4,181	1,03	0,454
AEC(B)	24	57,456	2,394	0,59	0,898
ADE	4	22,178	5,544	1,37	0,275
BDE	4	24,754	6,189	1,53	0,226
DEC(B)	12	46,473	3,873	0,95	0,514
ABDE	8	34,886	4,361	1,07	0,413
Error	24	97,367	4,057		
TOTAL	161	1099,050			

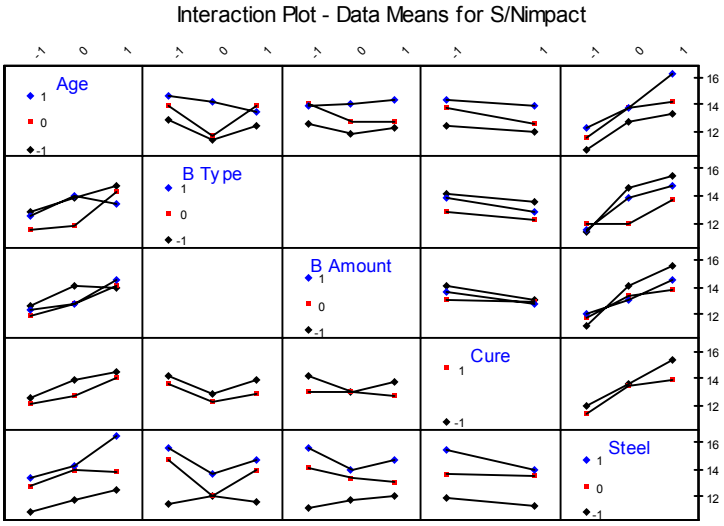

Figure 6.25 Two-way interaction plots for the S/N values of impact resistance

The residual plots for S/N ratio can be seen in Figures 6.26 and 6.27.

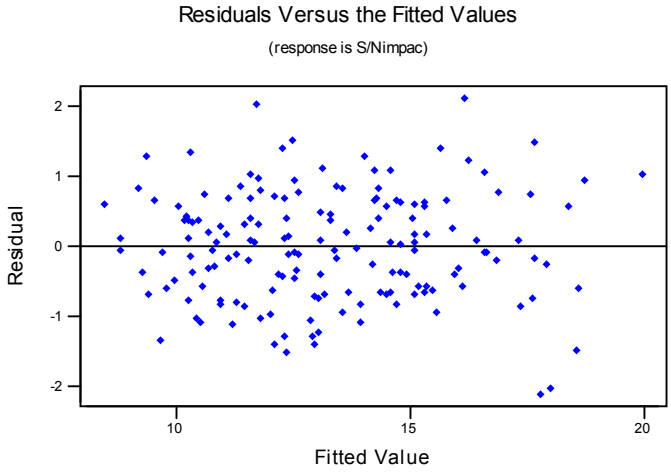

Figure 6.26 The residuals versus fitted values of the full factorial model found by ANOVA for S/N ratio for impact resistance

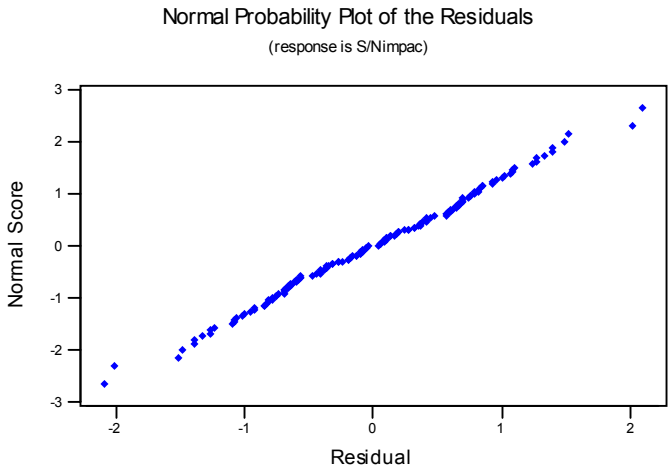

Figure 6.27 The residual normal probability plot for the full factorial model found by ANOVA for S/N ratio for impact resistance

Both figures show no abnormality for validation of the assumptions of the errors. It has constant variance and it is distributed normally.

From the main effects plot (Figure 6.28), the optimum points are 3rd level for Age (90 days), 1st level for Binder Type (silica fume), 1st level for Binder Amount (20%), 1st level for Curing Type (water curing) and 3rd level for Steel Fiber Volume Fraction (1.0% vol.). Also from the interaction plot it is concluded that all the optimal levels of the factors are in coincidence with the determined values above. So the optimum point for determining the predicted value of S/N ratio is $A_1B_{-1}C_{-1}D_{-1}E_1$ which corresponds to trial number 111. This optimum point conflicts with the one that is determined according to the results of the mean impact resistance, which is $A_1B_{-1}C_{-1}D_1E_1$. Therefore the two combinations should be calculated for the optimum performance of S/N ratio.

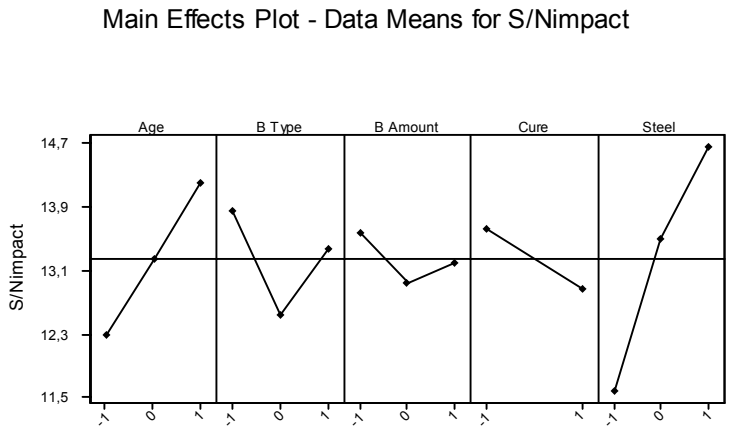

Figure 6.28 Main effects plot based on the full factorial design for S/N ratio for impact resistance

Combination 1: $A_1B_{-1}C_{-1}D_{-1}E_1$ (experiment no. 111)

$$\eta = \overline{T} + (\overline{A}_1 - \overline{T}) + (\overline{B}_{-1} - \overline{T}) + (\overline{C}_{-1} - \overline{T}) + (\overline{D}_{-1} - \overline{T}) + (\overline{E}_1 - \overline{T}) + (\overline{A_1 \times B_{-1}} - \overline{T}) + (\overline{A_1 \times E_1} - \overline{T}) + (\overline{B_{-1} \times E_1} - \overline{T}) + (\overline{C_{-1} \times D_{-1}} - \overline{T}) \quad (6.11)$$

$$\eta = \overline{T} - (\overline{A}_1 - \overline{T}) - (\overline{B}_{-1} - \overline{T}) - (\overline{E}_1 - \overline{T}) + (\overline{A_1 B_{-1}} - \overline{T}) + (\overline{A_1 E_1} - \overline{T}) + (\overline{B_{-1} E_1} - \overline{T}) + (\overline{C_{-1} D_{-1}} - \overline{T})$$

$$\eta = 13.25 - (14.19 - 13.25) - (13.85 - 13.25) - (14.65 - 13.25) + (14.74 - 13.25) + (16.38 - 13.25) + (15.55 - 13.25) + (14.16 - 13.25)$$
$$= 18.14$$

$$n_e = \frac{162}{31+1} = 5.06$$

$$V_e = 4.057$$

$$F_{0.05,1,24} = 4.26$$

$$C.I. = \sqrt{\frac{4.26 \times 4.057}{5.06}} = 1.85$$

As a result the value for the S/N ratio should fall in between:

η = {16.29, 19.99} with 95% confidence.

Combination 2: $A_1B_{-1}C_{-1}D_1E_1$ (experiment no. 114)

$$\eta = \overline{T} + (\overline{A}_1 - \overline{T}) + (\overline{B}_{-1} - \overline{T}) + (\overline{C}_{-1} - \overline{T}) + (\overline{D}_1 - \overline{T}) + (\overline{E}_1 - \overline{T}) + (\overline{A_1 \times B_{-1}} - \overline{T}) + (\overline{A_1 \times E_1} - \overline{T}) + (\overline{B_{-1} \times E_1} - \overline{T}) + (\overline{C_{-1} \times D_1} - \overline{T}) \quad (6.12)$$

$$\eta = \overline{T} - (\overline{A}_1 - \overline{T}) - (\overline{B}_{-1} - \overline{T}) - (\overline{E}_1 - \overline{T}) + (\overline{A_1B_{-1}} - \overline{T}) + (\overline{A_1E_1} - \overline{T}) + (\overline{B_{-1}E_1} - \overline{T}) + (\overline{C_1D_1} - \overline{T})$$

$$\eta = 13.25 - (14.19 - 13.25) - (13.85 - 13.25) - (14.65 - 13.25) + (14.74 - 13.25) + (16.38 - 13.25) + (15.55 - 13.25) + (13.00 - 13.25)$$
$$= 16.98$$

The confidence interval is the same as the one calculated above, 1.85. Therefore, the value of the mean flexural strength is expected in between;

η = {15.13, 18.83} with 95% confidence interval.

As stated before, the optimum point selected was $A_1B_{-1}C_{-1}D_{-1}E_1$ (experiment no. 111) from the results of mean impact resistance. The results of S/N also states that the optimum point should be $A_1B_{-1}C_{-1}D_{-1}E_1$ (experiment no. 111) in order to minimize the variation in the response with a predicted mean impact resistance of 9.06 kgf.m and 18.14 S/N ratio.

Experiment 111 resulted in 9.20 kgf.m, 5.30 kgf.m and 5.50 kgf.m impact resistances with 15.71 S/N ratio. However, the S/N ratio is 15.71 is below the lower limit of the determined values of the S/N ratio with 95% confidence. Also, the mean impact resistance of trial 111, 6.67 kgf.m, does not fall into the determined confidence interval limits. However, from the three replicates one of them is in between the limits, 9.20 kgf.m. When we look at the results of experiment number 114 which corresponds to the combination $A_1B_{-1}C_{-1}D_1E_1$, the S/N ratio is 18.26. It is in between the determined confidence limits and higher than the predicted value, 16.98, which confirms the findings of Taguchi analysis. The mean impact resistance values are 7.10 kgf.m, 8.90 kgf.m and 9.00 kgf.m that are closer to the predicted value of 8.77 kgf.m. Also, two of them lie in the confidence interval. Therefore the combination of $A_1B_{-1}C_{-1}D_1E_1$ is better represented by the Taguchi analysis and the optimum point selected is changed to $A_1B_{-1}C_{-1}D_1E_1$ combination.

6.2.2 Regression Analysis of the Mean Impact Resistance Based on the Full Factorial Design

The first employed regression analysis to model the mean impact resistance again contains only the main factors. That is:

$$y = 5{,}98 + 0{,}670*A - 0{,}552*B_1 - 0{,}048*B_2 - 0{,}312*C - 0{,}484*D_1 + 1{,}36*E \quad (6.13)$$

Table 6.18 shows the ANOVA for the significance of the above regression model. ANOVA is performed on the individual results rather than the average of the three replicates.

Table 6.18 ANOVA for the significance of the regression model developed for the mean impact resistance based on the full factorial design including only the main factors

Source	df	Sum of Squares	Mean Squares	F	P
Regression	6	833,52	138,92	20,30	0,000
Residual Error	479	3277,59	6,84		
Total	485	4111,11			

R^2 = 20,3% $R^2_{(adj)}$ = 19.3% S = 2.616

Durbin-Watson statistic = 1.94

The model has almost 100% confidence for refusing the hypothesis of β terms equal to zero. The adjusted multiple coefficient of determination, $R^2_{(adj)}$, shows that only 19.3% of the sample variation in the mean impact resistance can be explained by this model which is not acceptable. The Durbin-Watson statistic states that the residuals are uncorrelated with 95% confidence since it is larger than the tabulated upper bound (d_U), which is 1.78 with 5 independent variables and 486 observations. The residual plots of this model are given in Figures 6.29 and 6.30. It is concluded from the residuals versus the fitted values plot that there is an indication of violation of the constant variance assumption of the error, since the residuals are increasing with increasing fitted values. The normality assumption is somewhat satisfied because of the linearity of the residual normal plot in Figure 6.30, but it is skewed to the left. Therefore a variance stabilizing data transformation is needed for this model or a more adequate regression model will be searched to describe the mean impact resistance. The significance of β terms of the model is shown in Table 6.19. This table indicates that all the main factors are significant except B_2 at the p(0.05) level of significance.

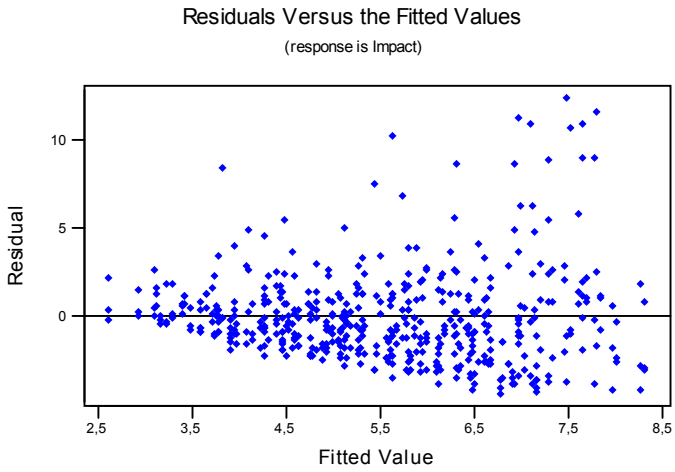

Figure 6.29 Residuals versus fitted values plot of the regression model developed for the mean impact resistance with only main factors

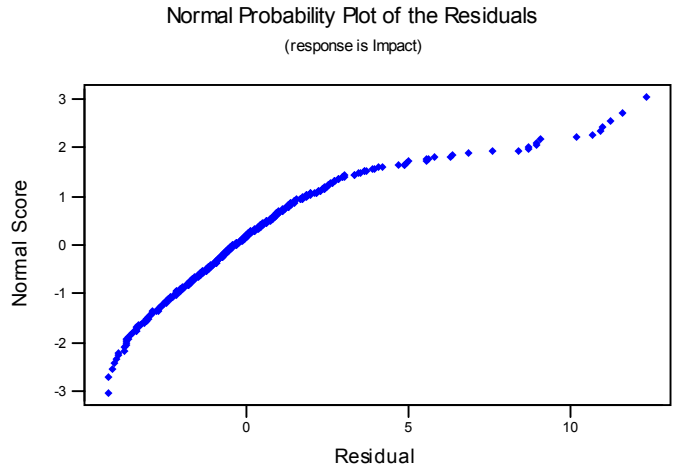

Figure 6.30 Residual normal probability plot of the regression model developed for the mean impact resistance with only main factors

Table 6.19 Significance of β terms of the regression model developed for the mean impact resistance with only main factors

Predictor	β Estimate	Standard Error	T	P
Constant	5,9784	0,2373	25,19	0,000
A	0,6701	0,1453	4,61	0,000
B_1	-0,5519	0,2906	-1,90	0,058
B_2	-0,0475	0,2906	-0,16	0,870
C	-0,3117	0,1453	-2,15	0,032
D_1	-0,4840	0,2373	-2,04	0,042
E	1,3583	0,1453	9,35	0,000

The MINITAB output with the sequential sum of squares of the regression model can be seen in Appendix D.6.

The second regression model is decided to include all the two-way interaction terms and the square of the main factors. While performing the regression analysis MINITAB has found that the Cure*Cure (D^2) squared term was essentially constant and it automatically removed it from the regression equation. The equation and the ANOVA table for the regression model can be seen in Eqn.6.14 and Table 6.20 respectively. The hypothesis of having all β terms equal to zero is tested and refused with an almost 100% of confidence.

$$y = 6,22 + 0,317*A - 1,90*B_1 - 0,07*B_2 - 0,913*C - 0,10*D_1 + 1,69*E - 1,10*A^2 + 1,05*C^2 - 0,365*E^2 + 0,667*AC + 0,117*AE - 1,11*CE - 0,40*B_1D_1 - 0,58*B_2D_1 + 0,593*AB_1 + 0,300*CB_1 - 0,674*EB_1 + 0,970*A^2B_1 - 0,119*C^2B_1 + 1,18*E^2B_1 - 0,575*ACB_1 + 0,394*AEB_1 + 0,525*CEB_1 - 0,346*AB_2 + 1,05*CB_2 + 0,307*EB_2 + 0,350*A^2B_2 - 0,844*C^2B_2 + 0,656*E^2B_2 - 0,333*ACB_2 - 0,858*AEB_2 + 0,606*CEB_2 + 0,554*AD_1 + 1,15*CD_1 - 0,391*ED_1 + 1,29*A^2D_1 - 1,86*C^2D_1 + 0,083*E^2D_1 - 0,808*ACD_1 + 0,478*AED_1 + 1,47*CED_1 - 0,217*AB_1D_1 - 0,698*CB_1D_1 + 0,470*EB_1D_1 - 0,07*A^2B_1D_1 + 1,08*C^2B_1D_1 - 0,44*E^2B_1D_1 + 1,11*ACB_1D_1 - 0,364*AEB_1D_1 - 1,34*CEB_1D_1 + 0,183*AB_2D_1 - 1,84*CB_2D_1 - 0,537*EB_2D_1 - 1,02*A^2B_2D_1 + 1,92*C^2B_2D_1 - 0,29*E^2B_2D_1 - 0,325*ACB_2D_1 + 1,61*AEB_2D_1 - 1,80*CEB_2D_1 \quad (6.14)$$

Table 6.20 ANOVA for the significance of the regression model developed for the mean impact resistance based on the full factorial design including main, interaction and squared factors

Source	df	Sum of Squares	Mean Squares	F	P
Regression	59	1393,028	23,611	3,70	0,000
Residual Error	426	2718,080	6,380		
Total	485	4111,108			

R^2 = 33.9.2% $R^2_{(adj)}$ = 24.7% S = 2.526

Durbin-Watson statistic = 2.08

This model again is not enough to explain the mean impact resistance of SFRHSC since $R^2_{(adj)}$ is 24.7% which is very low. The Durbin-Watson statistic is 2.08 showing that the independence assumption on the errors is not violated since it is very close to 2 which means the residuals are uncorrelated.

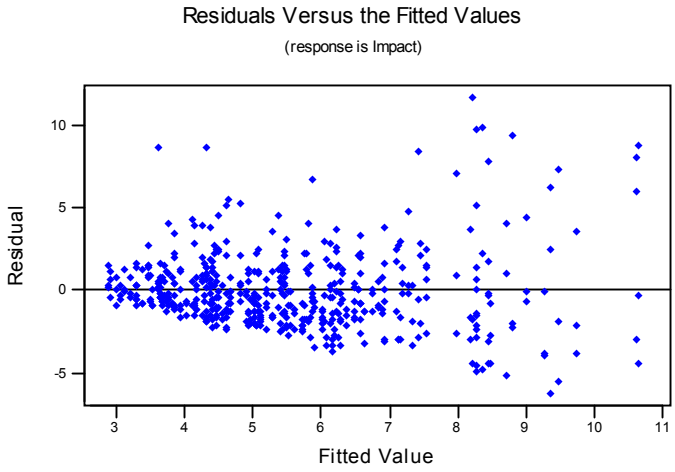

Figure 6.31 Residuals versus fitted values plot of the regression model in Eqn.6.14 developed for the mean impact resistance

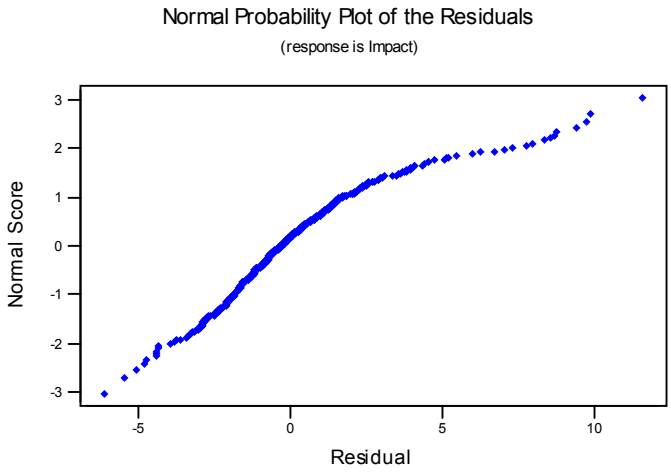

Figure 6.32 Residual normal probability plot of the regression model in Eqn.6.14 developed for the mean impact resistance

Residuals versus fitted values and the normal probability plot indicate that the error term has normal distribution skewed to the left but the constant variance assumption is violated. As a result an adequate model explaining the mean response can not be achieved. Certainly a variance stabilizing data transformation is necessary. Table 6.21 shows the significance of the β terms.

The MINITAB output with the sequential sum of squares of the regression model can be seen in Appendix D.7.

Table 6.21 Significance of β terms of the regression model in Eqn.6.14 developed for the mean impact resistance

Predictor	β Estimate	Standard Error	T	P
Constant	6,2235	0,7426	8,38	0,000
A	0,3167	0,3437	0,92	0,357
B_1	-1,8980	1,0500	-1,81	0,071
B_2	-0,0670	1,0500	-0,06	0,949
C	-0,9130	0,3437	-2,66	0,008
D_1	-0,0960	1,0500	-0,09	0,927
E	1,9870	0,3437	4,91	0,000
A^2	-1,0981	0,5954	-1,84	0,066
C^2	1,0463	0,5954	1,76	0,080
E^2	-0,3648	0,5954	-0,61	0,540
AC	0,6667	0,4210	1,58	0,114
AE	0,1167	0,4210	0,28	0,782
CE	-1,1083	0,4210	-2,63	0,009
B_1D_1	-0,3980	1,4850	-0,27	0,789
B_2D_1	-0,5800	1,4850	-0,39	0,696
AB_1	0,5926	0,4861	1,22	0,224
CB_1	0,3000	0,4861	0,62	0,537
EB_1	-0,6741	0,4861	-1,39	0,166
A^2B_1	0,9704	0,8420	1,15	0,250
C^2B_1	-0,1185	0,8420	-0,14	0,888
E^2B_1	1,1818	0,8420	1,40	0,161
ACB_1	-0,5750	0,5954	-0,97	0,335
AEB_1	0,3944	0,5954	0,66	0,508
CEB_1	0,5250	0,5954	0,88	0,378
AB_2	-0,3463	0,4861	-0,71	0,477
CB_2	1,0481	0,4861	2,16	0,032
EB_2	0,3074	0,4861	0,63	0,527
A^2B_2	0,3500	0,8420	0,42	0,678
C^2B_2	-0,8444	0,8420	-1,00	0,316
E^2B_2	0,6556	0,8420	0,78	0,437
ACB_2	-0,3333	0,5954	-0,56	0,576
AEB_2	-0,8583	0,5954	-1,44	0,150
CEB_2	0,6056	0,5654	1,02	0,310
AD_1	0,5537	0,4861	1,14	0,255
CD_1	1,1500	0,4861	2,37	0,018
ED_1	-0,3907	0,4861	-0,80	0,422

Table 6.21 Continued

Predictor	β Estimate	Standard Error	T	P
A^2D_1	1,2944	0,8420	1,54	0,125
C^2D_1	-1,8611	0,8420	-2,21	0,028
E^2D_1	0,0833	0,8420	0,10	0,921
ACD_1	-0,8083	0,5954	-1,36	0,175
AED_1	0,4778	0,5954	0,80	0,423
CED_1	1,4667	0,5954	2,46	0,014
AB_1D_1	-0,2167	0,6875	-0,32	0,753
CB_1D_1	-0,6981	0,6875	-1,02	0,310
EB_1D_1	0,4704	0,6875	0,68	0,494
$A^2B_1D_1$	-0,0690	1,1910	-0,06	0,954
$C^2B_1D_1$	1,0760	1,1910	0,90	0,367
$E^2B_1D_1$	-0,4410	1,1910	-0,37	0,711
ACB_1D_1	1,1111	0,8420	1,32	0,188
AEB_1D_1	-0,3639	0,8420	-0,43	0,666
CEB_1D_1	-1,3389	0,8420	-1,59	0,113
AB_2D_1	0,1833	0,685	0,27	0,790
CB_2D_1	-1,8407	0,6875	-2,68	0,008
EB_2D_1	-0,5370	0,6875	-0,78	0,435
$A^2B_2D_1$	-1,0200	1,1910	-0,86	0,392
$C^2B_2D_1$	1,9190	1,1910	1,61	0,108
$E^2B_2D_1$	-0,2930	1,1910	-0,25	0,806
ACB_2D_1	-0,3250	0,8420	-0,39	0,700
AEB_2D_1	1,6139	0,8420	1,92	0,056
CEB_2D_1	-1,7972	0,8420	-2,13	0,033

It can be seen from the large p-values that, several factors are insignificant on the response. The model can be improved by discarding the insignificant terms from the model one by one starting from the term having the largest p-value. But by doing this a slight improvement is reached since the R^2 term of the model seen in Eqn.6.14 is 33.9% and could not be improved without any data transformation. But for convenience, this improvement operation is done and the best model is tried to be achieved by pooling $A^2B_1D_1$, $E^2B_2D_1$, $E^2B_1D_1$, ACB_2D_1, AEB_1D_1, E^2D_1, AEB_1, $C^2B_1D_1$, C^2B_1, E^2B_2, $A^2B_2D_1$, A^2B_2 and ACB_2

terms. It has an $R^2_{(adj)}$ value of 26.1% with a 2.06 Durbin-Watson statistic. The model and its residual plots can be seen Appendix D.8 and D.9 respectively.

From the pattern of the residuals versus the fitted values (Figures 6.29 and 6.31), it is understood that the variance of mean impact resistance grows proportionally to the square of its mean [21]. Therefore a logarithmic transformation, y* = log y, is appropriate for the mean impact resistance. The log y values of the impact resistance of SFRHSC are given in Appendix D.10.

The model and the ANOVA table of the regression analysis of the transformed mean impact resistance values can be seen in Eqn.6.15 and Table 6.22.

$$\begin{aligned}\text{Log } \mu = {} & 0{,}760 + 0{,}0369*A - 0{,}197*B_1 + 0{,}0141*B_2 - 0{,}0406*C + 0{,}0072*D_1 + \\ & 0{,}116*E - 0{,}0576*A^2 + 0{,}0580*C^2 - 0{,}0448*E^2 + 0{,}0258*AC + \\ & 0{,}0033*AE - 0{,}0694*CE - 0{,}0005*B_1D_1 - 0{,}0647*B_2D_1 + 0{,}0322*AB_1 \\ & - 0{,}0011*CB_1 - 0{,}0641*EB_1 + 0{,}0778*A^2B_1 + 0{,}0233*C^2B_1 + \\ & 0{,}119*E^2B_1 - 0{,}0064*ACB_1 + 0{,}0178*AEB_1 + 0{,}0375*CEB_1 - \\ & 0{,}0239*AB_2 + 0{,}0661*CB_2 + 0{,}0231*EB_2 - 0{,}0006*A^2B_2 - \\ & 0{,}0539*C^2B_2 + 0{,}0306*E^2B_2 - 0{,}0056*ACB_2 - 0{,}0536*AEB_2 + \\ & 0{,}0394*CEB_2 + 0{,}0220*AD_1 + 0{,}0524*CD_1 - 0{,}0165*ED_1 + \\ & 0{,}0746*A^2D_1 - 0{,}113*C^2D_1 - 0{,}0120*E^2D_1 - 0{,}0319*ACD_1 + \\ & 0{,}0244*AED_1 + 0{,}102*CED_1 - 0{,}0007*AB_1D_1 - 0{,}0187*CB_1D_1 + \\ & 0{,}0407*EB_1D_1 - 0{,}0193*A^2B_1D_1 + 0{,}0569*C^2B_1D_1 - 0{,}0448*E^2B_1D_1 + \\ & 0{,}0606*ACB_1D_1 - 0{,}0200*AEB_1D_1 - 0{,}106*CEB_1D_1 + 0{,}0002*AB_2D_1 \\ & - 0{,}111*CB_2D_1 - 0{,}0617*EB_2D_1 - 0{,}0687*A^2B_2D_1 + 0{,}134*C^2B_2D_1 + \\ & 0{,}0002*E^2B_2D_1 - 0{,}0386*ACB_2D_1 + 0{,}111*AEB_2D_1 - 0{,}116*CEB_2D_1 \end{aligned} \quad (6.15)$$

Table 6.22 ANOVA for the significance of the regression model developed for the transformed mean impact resistance based on the full factorial design including main, interaction and squared factors

Source	df	Sum of Squares	Mean Squares	F	P
Regression	59	6,50728	0,11029	4,17	0,000
Residual Error	426	11,27645	0,02647		
Total	485	17,78372			

$R^2 = 36.6\%$ $R^2_{(adj)} = 27.8\%$ $S = 0.1627$

Durbin-Watson statistic = 2.06

This transformed quadratic model seems better than that of the non-transformed model, however, $R^2_{(adj)}$ value is still low. So this model is not enough to explain the impact resistance of SFRHSC. The Durbin-Watson statistic is close to 2, showing that there is no correlation between the residuals of quadratic regression model for the transformed mean impact resistance. The residuals versus the fitted values and normal probability plots are given in Figures 6.33 and 6.34.

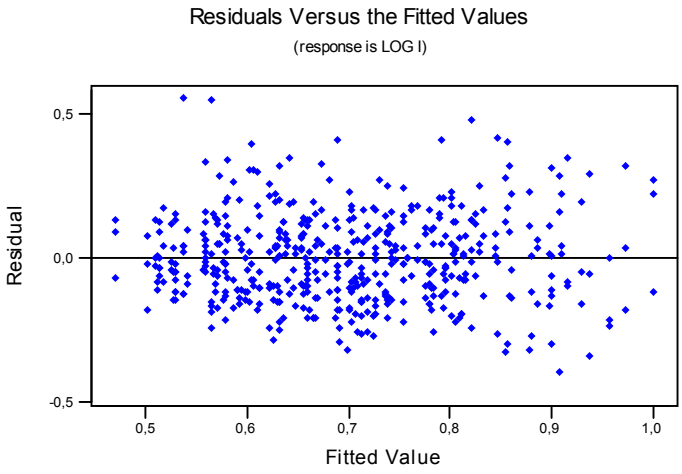

Figure 6.33 Residuals versus fitted values plot of the quadratic regression model in Eqn.6.15 developed for the log transformed mean impact resistance

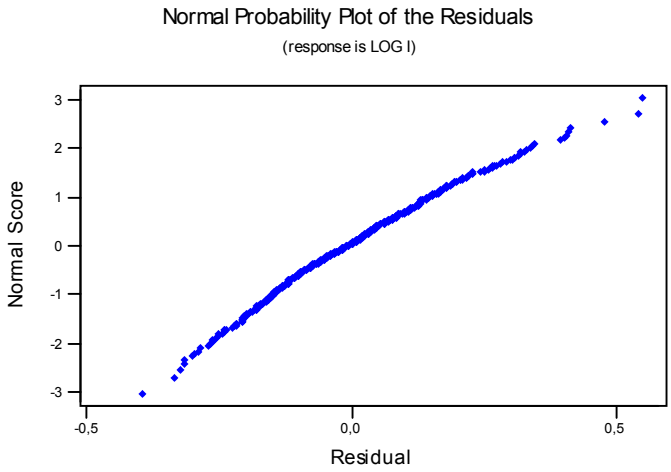

Figure 6.34 Residual normal probability plot of the quadratic regression model in Eqn.6.15 developed for the log transformed mean impact resistance

By the variance stabilizing data transformation the constant variance of the error assumption is validated since there is no obvious pattern in the residuals versus fitted values plot. Also the normal probability plot of the residuals is linear indicating that the error term has a normal distribution. But the β significance test of the parameters show that some improvements are needed to be made in order to obtain a more explanatory model. Table 6.23 shows the β significance of the factors and the MINITAB output with the sequential sum of squares can be found in Appendix D.11.

Table 6.23 Significance of β terms of the quadratic regression model in Eqn.6.15 developed for the log transformed mean impact resistance

Predictor	β Estimate	Standard Error	T	P
Constant	0,76160	0,04783	15,92	0,000
A	0,03685	0,02214	1,66	0,097
B_1	-0,19667	0,06764	-2,91	0,004
B_2	0,01407	0,06764	0,21	0,835
C	-0,04056	0,02214	-1,83	0,068
D_1	0,00716	0,06764	0,11	0,916
E	0,11630	0,02214	5,25	0,000
A^2	-0,05759	0,03835	-1,50	0,134
C^2	0,05796	0,03835	1,51	0,131
E^2	-0,04481	0,03835	-1,17	0,243
AC	0,02583	0,02712	0,95	0,341
AE	0,00333	0,02712	0,12	0,902
CE	-0,06944	0,02712	-2,56	0,011
B_1D_1	0,00049	0,09566	0,01	0,996
B_2D_1	-0,06469	0,09566	-0,68	0,499
AB_1	0,03222	0,03131	1,03	0,304
CB_1	-0,00111	0,03131	-0,04	0,972
EB_1	-0,06407	0,03131	-2,05	0,041
A^2B_1	0,07778	0,05423	1,43	0,152
C^2B_1	0,02333	0,05423	0,43	0,667
E^2B_1	0,11889	0,05423	2,19	0,029
ACB_1	-0,00639	0,03835	-0,17	0,868
AEB_1	0,01778	0,03835	0,46	0,643
CEB_1	0,03750	0,03835	0,98	0,329
AB_2	-0,02389	0,03131	-0,76	0,446
CB_2	0,06611	0,03131	2,11	0,035
EB_2	0,02315	0,03131	0,74	0,460
A^2B_2	-0,00056	0,05423	-0,01	0,992
C^2B_2	-0,05389	0,05423	-0,99	0,321
E^2B_2	0,03056	0,05423	0,56	0,573
ACB_2	-0,00556	0,03835	-0,14	0,885
AEB_2	-0,05361	0,03835	-1,40	0,163
CEB_2	0,03944	0,03835	1,03	0,301
AD_1	0,02204	0,03131	0,70	0,482
CD_1	0,05241	0,03131	1,67	0,095
ED_1	-0,01648	0,03131	-0,53	0,599

Table 6.23 Continued

Predictor	β Estimate	Standard Error	T	P
A^2D_1	0,07463	0,05423	1,38	0,170
C^2D_1	-0,11315	0,05423	-2,09	0,038
E^2D_1	-0,01204	0,05423	-0,22	0,824
ACD_1	-0,03194	0,03835	-0,83	0,405
AED_1	0,02444	0,03835	0,64	0,524
CED_1	0,10222	0,03835	2,67	0,008
AB_1D_1	-0,00074	0,04428	-0,02	0,987
CB_1D_1	-0,01870	0,04428	-0,42	0,673
EB_1D_1	0,04074	0,04428	0,92	0,358
$A^2B_1D_1$	-0,01926	0,07670	-0,25	0,802
$C^2B_1D_1$	0,05685	0,07670	0,74	0,459
$E^2B_1D_1$	-0,04481	0,07670	-0,58	0,559
ACB_1D_1	0,06056	0,05423	1,12	0,265
AEB_1D_1	-0,02000	0,05423	-0,37	0,712
CEB_1D_1	-0,10639	0,05423	-1,96	0,050
AB_2D_1	0,00019	0,04428	0,00	0,997
CB_2D_1	-0,11130	0,04428	-2,51	0,012
EB_2D_1	-0,06167	0,04428	-1,39	0,164
$A^2B_2D_1$	-0,06870	0,07670	-0,90	0,371
$C^2B_2D_1$	0,13352	0,07670	1,74	0,082
$E^2B_2D_1$	0,00019	0,07670	0,00	0,998
ACB_2D_1	-0,03861	0,05423	-0,71	0,477
AEB_2D_1	0,11083	0,05423	2,04	0,042
CEB_2D_1	-0,11556	0,05423	-2,13	0,034

It can be seen from the large p-values that some of the terms in the model are unnecessary. As a result, the model can be improved by discarding the insignificant terms from the model one by one starting from the term having the largest p-value. The main factors are left in the model without considering their p-value. After several trials, the best model having the largest $R^2_{(adj)}$ value is obtained by pooling $E^2B_2D_1$, $A^2B_1D_1$, AEB_1D_1, AEB_1, $E^2B_1D_1$, ACB_2D_1, $C^2B_1D_1$, CB_1D_1, E^2B_2, $A^2B_2D_1$, E^2D_1, A^2B_2 and ACB_2 terms as in Eqn.6.16. ANOVA of this model is given in Table 6.24.

$$\log \mu = 0{,}767 + 0{,}0369*A - 0{,}196*B_1 + 0{,}0246*B_2 - 0{,}0359*C - 0{,}0003*D_1 + 0{,}116*E - 0{,}0604*A^2 + 0{,}0438*C^2 - 0{,}0355*E^2 + 0{,}0231*AC + 0{,}0122*AE - 0{,}0694*CE - 0{,}0043*B_1D_1 - 0{,}0914*B_2D_1 + 0{,}0322*AB_1 - 0{,}0105*CB_1 - 0{,}0641*EB_1 + 0{,}0856*A^2B_1 + 0{,}0518*C^2B_1 + 0{,}0812*E^2B_1 - 0{,}0036*ACB_1 + 0{,}0375*CEB_1 - 0{,}0239*AB_2 + 0{,}0614*CB_2 + 0{,}0231*EB_2 - 0{,}0397*C^2B_2 - 0{,}0625*AEB_2 + 0{,}0394*CEB_2 + 0{,}0220*AD_1 + 0{,}0431*CD_1 - 0{,}0165*ED_1 + 0{,}0453*A^2D_1 - 0{,}0847*C^2D_1 - 0{,}0512*ACD_1 + 0{,}0144*AED_1 + 0{,}102*CED_1 - 0{,}0007*AB_1D_1 + 0{,}0407*EB_1D_1 + 0{,}0799*ACB_1D_1 - 0{,}106*CEB_1D_1 + 0{,}0002*AB_2D_1 - 0{,}102*CB_2D_1 - 0{,}0617*EB_2D_1 + 0{,}105*C^2B_2D_1 + 0{,}121*AEB_2D_1 - 0{,}116*CEB_2D_1 \quad (6.16)$$

Table 6.24 ANOVA for the significance of the best regression model developed for the transformed mean impact resistance based on the full factorial design

Source	df	Sum of Squares	Mean Squares	F	P
Regression	46	6,35346	0,13812	5,30	0,000
Residual Error	439	11,43026	0,02604		
Total	485	17,78372			

$R^2 = 35.7\%$ $R^2_{(adj)} = 29.0\%$ $S = 0.1614$

Durbin-Watson statistic = 2.05

A major improvement can not be achieved by this best model. The $R^2_{(adj)}$ value is increased from 27.8% to 29.0% which is not enough to explain the impact resistance of SFRHSC. The Durbin-Watson statistic is slightly better, 2.05, still indicating uncorrelated residuals. Figures 6.35 and 6.36 show the residual plots and Table 6.25 shows the β significance test. In Appendix D.12, the MINITAB output with the sequential sum of squares can be found.

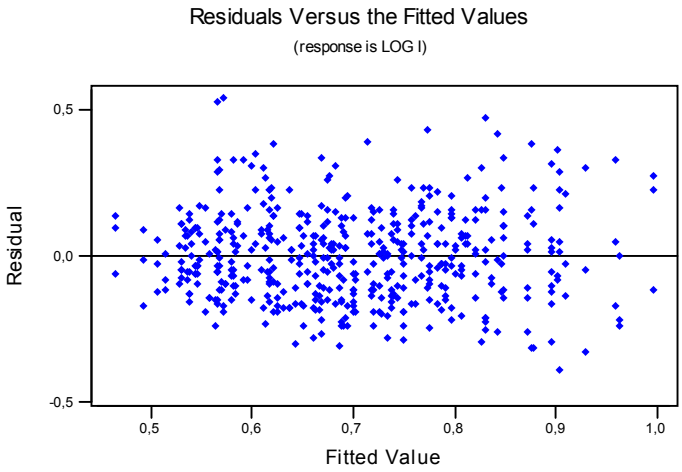

Figure 6.35 Residuals versus fitted values plot of the best regression model in Eqn.6.16

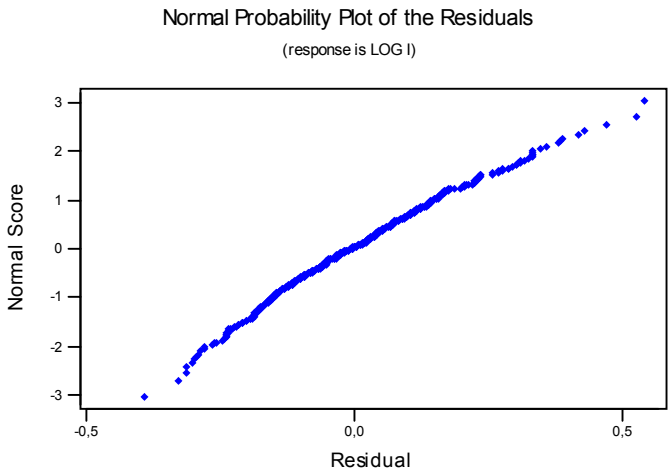

Figure 6.36 Residual normal probability plot of the best regression model in Eqn.6.16

Both residual plots show no indication of violation of the assumptions of the error. The β significance test of the parameters show that most of the terms are significant on the mean impact resistance with p(0.05) confidence.

Table 6.25 Significance of β terms of the best regression model in Eqn.6.16

Predictor	β Estimate	Standard Error	T	P
Constant	0,76674	0,03510	21,84	0,000
A	0,03685	0,02196	1,68	0,094
B_1	-0,19568	0,04744	-4,13	0,000
B_2	0,02460	0,04205	0,59	0,559
C	-0,03588	0,01902	-1,89	0,060
D_1	-0,00027	0,04140	-0,01	0,995
E	0,11630	0,02196	5,30	0,000
A^2	-0,06039	0,02455	-2,46	0,014
C^2	0,04375	0,03294	1,33	0,185
E^2	-0,03551	0,01902	-1,87	0,063
AC	0,02306	0,01902	1,21	0,226
AE	0,01222	0,01902	0,64	0,521
CE	-0,06944	0,02689	-2,58	0,010
B_1D_1	-0,00432	0,03586	-0,12	0,904
B_2D_1	-0,09142	0,05670	-1,61	0,108
AB_1	0,03222	0,03105	1,04	0,300
CB_1	-0,01046	0,02196	-0,48	0,634
EB_1	-0,06407	0,03105	-2,06	0,040
A^2B_1	0,08560	0,03294	2,60	0,010
C^2B_1	0,05176	0,03803	1,36	0,174
E^2B_1	0,08116	0,03294	2,46	0,014
ACB_1	-0,00361	0,03294	-0,11	0,913
CEB_1	0,03750	0,03803	0,99	0,325
AB_2	-0,02389	0,03105	-0,77	0,442
CB_2	0,06144	0,02905	2,11	0,035
EB_2	0,02315	0,03105	0,75	0,456
C^2B_2	-0,03968	0,05031	-0,79	0,431
AEB_2	-0,06250	0,03294	-1,90	0,058
CEB_2	0,03944	0,03803	1,04	0,300
AD_1	0,02204	0,03105	0,71	0,478
CD_1	0,04306	0,02196	1,96	0,051
ED_1	-0,01648	0,03105	-0,53	0,596
A^2D_1	0,04531	0,03105	1,46	0,145
C^2D_1	-0,08472	0,03803	-2,23	0,026
ACD_1	-0,05125	0,02689	-1,91	0,057
AED_1	0,01444	0,02689	0,54	0,591
CED_1	0,10222	0,03803	2,69	0,007
AB_1D_1	-0,00074	0,04392	-0,02	0,987

Table 6.25 Continued

Predictor	β Estimate	Standard Error	T	P
EB_1D_1	0,04074	0,04392	0,93	0,354
ACB_1D_1	0,07986	0,04658	1,71	0,087
CEB_1D_1	-0,10639	0,05379	-1,98	0,049
AB_2D_1	0,00019	0,04392	0,00	0,997
CB_2D_1	-0,10194	0,03803	-2,68	0,008
EB_2D_1	-0,06167	0,04392	-1,40	0,161
$C^2B_2D_1$	0,10509	0,06587	1,60	0,111
AEB_2D_1	0,12083	0,04658	2,59	0,010
CEB_2D_1	-0,11556	0,05379	-2,15	0,032

As a result, the mean impact resistance of SFRHSC can be modeled, but this model is not so adequate to explain the mean impact resistance since, the best regression model can only explain the 30% of the response. The best model fitted is given in Eqn.6.16.

6.2.3 Response Surface Optimization of Mean Impact Resistance Based on the Full Factorial Design

For the MINITAB response optimization the best regression model found in Eqn.6.16 in the previous section for the mean impact resistance will be used. Again as in Taguchi Design, the minimum and target values are set to 5.0 kgf.m and 10.0 kgf.m respectively. The same fourteen starting points are tried again. The results of the optimizer can be seen in Table 6.26. The starting points and the optimum points found by MINITAB response optimizer is shown in Table 6.27.

Table 6.26 The optimum response, its desirability, the confidence and prediction intervals computed by MINITAB Response Optimizer for the mean impact resistance based on the full factorial design

Optimum Points	log μ	Desirability	95% Conf. Int.	95% Pred. Int.	Mean Impact
1	0,9622	0,88582	(0,8896; 1,0755)	(0,6255; 1,2990)	9,1671
2	0,7053	0,15613	(0,5903; 0,8202)	(0,3680; 1,0426)	5,0729
3	0,8485	0,54979	(0,7353; 0,9618)	(0,5118; 1,1853)	7,0554
4	0,9599	0,86095	(0,8380; 1,0817)	(0,6201; 1,2996)	9,1170
5	0,8606	0,61361	(0,7701; 0,9511)	(0,5308; 1,1904)	7,2539
6	0,9599	0,86095	(0,8380; 1,0817)	(0,6201; 1,2996)	9,1170
7	0,5707	0,00000	(0,4773; 0,6640)	(02401; 0,9013)	3,7211
8	0,8203	0,48792	(0,6984; 0,9421)	(0,4805; 1,1600)	6,6109
9	0,9622	0,88582	(0,8896; 1,0755)	(0,6255; 1,2990)	9,1671
10	0,9599	0,86095	(0,8380; 1,0817)	(0,6201; 1,2996)	9,1170
11	0,9622	0,88582	(0,8896; 1,0755)	(0,6255; 1,2990)	9,1671
12	0,9599	0,86095	(0,8380; 1,0817)	(0,6201; 1,2996)	9,1170
13	0,8922	0,71892	(0,8027; 0,9817)	(0,5627; 1,2217)	7,8019
14	0,7830	0,38225	(0,6612; 0,9049)	(0,4433; 1,1228)	6,0678

Table 6.27 The starting and optimum points for MINITAB response optimizer developed for the mean impact resistance based on the full factorial design

	Starting Points					Optimum Points				
Points	**Age (days)**	**B. Type**	**B. Amount (%)**	**Cure**	**Steel (% vol.)**	**Age (days)**	**B. Type**	**B. Amount (%)**	**Cure**	**Steel (% vol.)**
1	90	SF	20	water	1,0	90	SF	20	water	1,0
2	No starting point					82	GGBFS	60	water	0,0
3	90	SF	20	steam	0,5	90	SF	20	steam	1,0
4	90	GGBFS	20	water	0,5	90	GGBFS	20	steam	1,0
5	90	SF	10	water	1,0	90	SF	16,5	water	1,0
6	28	FA	40	steam	0,5	90	GGBFS	20	steam	1,0
7	7	SF	20	water	0,0	11	SF	19	steam	0,0
8	90	GGBFS	60	water	1,0	90	GGBFS	60	water	1,0
9	90	FA	10	water	1,0	90	SF	20	water	1,0
10	28	GGBFS	20	steam	1,0	90	GGBFS	20	steam	1,0
11	90	SF	15	water	1,0	90	SF	20	water	1,0
12	90	GGBFS	20	steam	1,0	90	GGBFS	20	steam	1,0
13	90	SF	20	water	0,0	90	SF	20	water	0,8
14	90	SF	20	steam	1,0	90	GGBFS	20	water	1,0

The starting points 1, 9 and 11 resulted in the same parameter level combination with the highest impact resistance, 9.17 kgf.m, which is close to the desired impact resistance of 10.0 kgf.m. Points 4, 6, 10 and 12 are the second best with 9.12 kgf.m impact resistance. Although their intervals are the widest, it is worth to do the confirmation runs for these points. Point 13 gave 7.80 kgf.m impact resistance and its intervals are narrow and therefore, it is worth to try it. Since points 5 and 3 resulted in around 7.0 kgf.m impact resistance, they can be tried also. The remaining points resulted in relatively lower impact resistance values and therefore they are not taken into consideration for the confirmation experiments. Each experiment is repeated three times for convenience.

Optimum points 1, 9 and 11:

For these points the 3rd level for Age (90 days), 1st level for Binder Amount (Silica Fume), 1st level for Binder Amount (20% for silica fume), 1st level for Curing Type (ordinary water curing) and the 3rd level for Steel Fiber Volume Fraction (1.0%) are assigned to the associated main factors. The results of the experiments correspond to experiment 111 and are 9.20 kgf.m, 5.30 kgf.m and 5.50 kgf.m and their logarithmic transformed values are 0.96, 0.72 and 0.74. All of these transformed values are in the prediction interval and only 0.96 is in the confidence interval. The two results, 5.30 kgf.m and 5.50 kgf.m, are far from the optimum fitted value of 9.17 kgf.m found by the regression model. As a result, it can be said that this point is not well modeled by the regression model in Eqn.6.16.

Optimum points 4, 6, 10 and 12:

For this experiment age, binder type, binder amount, curing type and steel fiber volume fraction are set to 90 days, Ground Granulated Blast Furnace Slag, 20% for GGBFS, steam curing and 1.0% respectively. These combination of the main factor levels corresponds to experiment 150. The results of the experiment are 6.20 kgf.m, 10.30 kgf.m and 19.40 kgf.m with the transformed values of

0.79, 1.01 and 1.29. The difference between the three values is very wide resulting in a high variation. 0.79 is below the lower limit and 1.29 is above the upper limit of the confidence interval. Therefore, it can be concluded that this point has not been modeled well by the regression model formulated for the impact resistance of SFRHSC.

Optimum point 13:

For this experiment age, binder type, binder amount, curing type and steel fiber volume fraction are set to 90 days, Silica Fume, 20% for SF, ordinary water curing and 0.5% respectively. This factor level combination corresponds to experiment 1110. The results of the experiment are 6.60 kgf.m, 6.80 kgf.m and 5.50 kgf.m with the transformed values of 0.82, 0.83, and 0.74. All of them are in the prediction interval with 95%. But 0.74 is below the lower boundary of the confidence interval. But they can be accepted as they are close to the fitted value of 0.89. Although this point is overestimated by the chosen regression model, it can be said that it is somewhat modeled.

Optimum point 5:

For this point the 3rd level for Age (90 days), 1st level for Binder Type (Silica Fume), 2nd level for Binder Amount (15% for SF), 1st level for Curing Type (ordinary water curing) and the 3rd level for Steel Fiber Volume Fraction (1.0%) are assigned to the associated main factors. This combination of the main factor levels corresponds to experiment 117. The results of the experiment are 5.50 kgf.m, 5.70 kgf.m, and 7.70 kgf.m with the transformed values of 0.74, 0.76, and 0.89 and all are in the prediction interval. But 7.70 kgf.m is a little far from the remaining two results. 5.50 kgf.m and 5.70 kgf.m are outside the lower limit of the confidence interval. Although all the confirmation run results are in the prediction interval, it is concluded that this point is not very well modeled by the regression equation. Because it seems that the impact resistance for this combination is around 5.50 kgf.m.

Optimum point 2:

For this experiment age, binder type, binder amount, curing type and steel fiber volume fraction are set to 90 days, Silica Fume, 20% for SF, steam curing and 1.0% respectively. These combination of the main factor levels corresponds to experiment 114. The results of the experiment are 7.10 kgf.m, 8.90 kgf.m and 9.00 kgf.m with the transformed values of 0.85, 0.95 and 0.95. All results are in the prediction interval but closer to the upper side and all are outside the upper boundary of the confidence interval. Also they are above to the fitted value of 0.71. So it can be said that this point is underestimated by the chosen best regression model.

Although point 1 gives the maximum impact resistance, the best point chosen for the result of the regression analysis is the optimum point 2 because, the confirmation run results are the highest ones among the others, with an average of 8.33 kgf.m, and they are very consistent with each other. Besides, its interval limits are one of the narrowest one. Although this point is underestimated by the chosen regression model, the best combination for the impact resistance of SFRHSC is $A_1B_{-1}C_{-1}D_1E_1$.

CHAPTER 7

CONCLUSIONS AND SUGGESTIONS FOR FUTURE WORK

7.1 Conclusions

Two statistical experimental designs and two analysis techniques are employed to maximize process parameters of the compressive strength, flexural strength and impact resistance of steel fiber reinforced high strength concrete. The first applied model was the Taguchi model. This model employs ANOVA optimization algorithm for both the mean and S/N value of the response. By S/N transformation it is aimed to select the optimum level based on least variation around the maximum and also on the average value closest to the maximum. Then regression modeling was applied to the mean of the responses. The best fitting regression model to the response data was searched by trying various regression models. Among all, the one satisfying all the residual assumptions with a high value of adjusted multiple coefficient of determination, $R^2_{(adj)}$, was chosen as the best regression model explaining the response. These are all quadratic for compressive strength, flexural strength and impact resistance. These best chosen regression models are shown in Eqn.4.12 and 4.19 for compressive strength based on Taguchi and full factorial experimental designs respectively, Eqn.5.7 and 5.14 for flexural strength based on Taguchi and full factorial experimental designs respectively, and Eqn.6.8 and 6.16 for impact resistance based on Taguchi and full factorial experimental designs respectively. Finally MINITAB Response Optimizer is used for maximizing the response based on the selected regression model. Same procedure is applied for all the responses for both of the experimental designs separately. However, the

standard deviation of the responses was not modeled by regression methodology and was not compared with the results of Taguchi's S/N analysis. Table 7.1 shows all analysis results including offered best parameter level combinations, expected mean response values, 95% confidence intervals, R^2, adjusted R^2 and Durbin Watson statistic values of the regression models, and standard deviation of the error estimates of the models.

Table 7.1 Results of the statistical experimental design and analysis techniques

Exp. Design	Analysis Method	Response	R^2 (%)	R^2_{adj} (%)	S_{error}	D-W statistic	Best Levels					Expected Response	95% C.I.
							A	B	C	D	E		
$L_{27}(3^{13})$ Taguchi Design	Taguchi's Method	Compressive Strength	-	-	9,38	-	1	-1	-1	-1	1	124,04 MPa	(106,93; 141,15)
		Flexural Strength	-	-	1,52	-	1	-1	-1	-1	0	14,44 MPa	(11,75; 17,13)
		Impact Resistance	-	-	1,31	-	1	1	-1	-1	1	8,53 kgf.m	(6,49; 10,57)
	Regression Analysis	Compressive Strength	97,3	91,1	7,46	1,84	1	-1	-1	-1	1	129,34 MPa	(109,26; 147,45)
		Flexural Strength	97,0	87,2	1,05	2,15	1	-1	1	-1	1	15,39 MPa	(11,60; 19,21)
		Impact Resistance	96,8	88,0	1,12	2,05	1	-1	-1	-1	1	6,52 kgf.m	(4,37; 9,73)
Full Factorial Design	Taguchi's Method	Compressive Strength	-	-	4,90	-	1	-1	-1	-1	1	128,24 MPa	(125,22; 131,26)
		Flexural Strength	-	-	0,77	-	1	-1	-1	-1	1	14,91 MPa	(14,41; 15,41)
		Impact Resistance	-	-	2,52	-	1	-1	-1	1	1	8,77 kgf.m	(7,63; 9,91)
	Regression Analysis	Compressive Strength	92,1	91,2	6,80	2,14	1	-1	-1	-1	1	126,84 MPa	(121,97; 131,71)
		Flexural Strength	86,7	85,2	1,10	2,15	1	-1	1	-1	1	13,97 MPa	(13,18; 14,76)
		Impact Resistance	35,7	29,0	1,45	2,05	1	-1	-1	1	1	5,07 kgf.m	(3,89; 6,61)

Nearly the same results are obtained from both experimental designs and both analysis techniques. Also the best parameter combinations maximizing the compressive strength of SFRHSC are resulted in the same combination for all analysis and design techniques. However, three different combinations are obtained for flexural strength and for impact resistance.

The standard deviations of the error term for compressive strength and flexural strength are closer in regression analysis for both of the experimental design techniques. On the other hand, in Taguchi analysis, there is a wide gap in between what is determined for Taguchi experimental design and full factorial design. In Taguchi design the standard deviation of the error almost doubled when compared with the standard deviation of the error in full factorial design. As a result it can be concluded that when more data points and more interaction terms are included in the model, Taguchi analysis improves itself, but there occurs no significant difference in regression analysis. Also, the confidence intervals for compressive strength, flexural strength and impact resistance became significantly narrow in full factorial experimental design when compared with Taguchi design. This is again due to the inclusion of all possible factor combinations into the model in full factorial design. The confidence intervals are larger in Taguchi design because, it can only account for limited number of two-way interaction terms and does not consider the significance of the remaining two-way interaction and higher ordered factors.

When the design type is full factorial, the residuals are uncorrelated in the regression analysis of all responses, namely, compressive strength, flexural strength and impact resistance. Whereas, when the experimental design type is Taguchi, the Durbin-Watson statistics of compressive strength and flexural strength remain in between the tabulated lower and upper limits, but very close to the upper limit of 1.86. As a result, the residuals can be accepted as independent instead of saying that there is not enough information to conclude whether they are correlated or not. The residuals of impact resistance are independent also in Taguchi experimental design.

In both design methodologies, for compressive strength and for flexural strength the R^2 and $R^2_{(adj)}$ values are nearly the same meaning that the regression models explain the responses approximately to the same extent. However, due to the increased number of data points in full factorial experimental design, it becomes harder to fit the model to these increased number of data points and even though the adjusted multiple coefficient of determination, $R^2_{(adj)}$, is the same with that of Taguchi experimental design's, full factorial design reflects the reality more because of the huge number of experiments conducted. For example, when the response is compressive strength, Taguchi design explains 91% of 27 data points, but full factorial design explains 91% of 162 data points. On the other hand, when the response is impact resistance, the regression model of Taguchi design is more explanatory when compared with the regression model of the full factorial design. This may again be attributable to the increased data points in full factorial design and unconsidered factor interaction effects in Taguchi design. As a result it can be concluded that for impact resistance by full factorial design, we were able to deduct the variations that we could not see in Taguchi experimental design since there are considerably less number of experiments conducted.

The best combination of parameter levels for compressive strength was determined as $A_1B_{-1}C_{-1}D_{-1}E_1$ by all the analysis techniques for all experimental design methodologies. In full factorial design for flexural strength the Taguchi analysis has obtained again the same parameter level combination determined for the compressive strength which is $A_1B_{-1}C_{-1}D_{-1}E_1$. On the contrary, in Taguchi experimental design Taguchi analysis has found a different combination as optimal, $A_1B_{-1}C_{-1}D_{-1}E_0$, and for both design methodologies regression analysis has obtained $A_1B_{-1}C_1D_{-1}E_1$ combination as the best one. The $A_1B_{-1}C_{-1}D_{-1}E_0$ combination seems a little unreasonable because, we know from the previous researches that the addition of steel fibers to SFRHSC significantly improves the flexural strength. This difference may be attributable to the unconsidered remaining two-way factor interaction effects on the response.

The maximum obtained compressive strength is 129.34 MPa from the regression analysis of Taguchi experimental design and the maximum flexural strength is obtained as 15.39 MPa from regression analysis of Taguchi experimental design. However all of the predicted compressive and flexural strength values of all the analysis methods are nearly the same, around 127.0 MPa and 14.50 MPa respectively. The narrowest confidence intervals for these two responses are obtained from Taguchi's method in full factorial design with 128.24 MPa compressive strength and 14.91 MPa flexural strength.

The confirmation runs that were conducted for $A_1B_{-1}C_1D_{-1}E_1$ combination could not reach to the predicted value obtained by the regression model. However, as stated earlier in Chapter 5, Section 5.1.1, the $A_1B_{-1}C_{-1}D_{-1}E_1$ combination can also be selected as the optimum parameter level combination in Taguchi design, Taguchi analysis for flexural strength, since the confirmation runs for this combination gave better results than the confirmation trials performed for $A_1B_{-1}C_{-1}D_{-1}E_0$. Moreover, the $A_1B_{-1}C_{-1}D_{-1}E_1$ combination can also be selected as the optimum parameter level combination in regression analysis of Taguchi design also, because the confirmation runs are very close to the results of $A_1B_{-1}C_1D_{-1}E_1$ combination and even a little higher. Although the points that correspond to $A_1B_{-1}C_{-1}D_{-1}E_1$ combination were underestimated by the regression model in full factorial design, the confirmation experiments resulted in the highest mean flexural strength, even higher than the chosen point having the $A_1B_{-1}C_1D_{-1}E_1$ combination. As a result, the regression models in both designs have underestimated the $A_1B_{-1}C_{-1}D_{-1}E_1$ combination but the confirmation trials have given the largest flexural strengths. Consequently, the $A_1B_{-1}C_{-1}D_{-1}E_1$ can also be selected as the optimal parameter level combination.

The impact resistance of steel fiber reinforced high strength concrete could not be modeled as well as the other two responses. The variation in the results of the impact test was very large. This may be due to the unavoided noise factors. Since this kind of impact test is applied for the first time, the experimenter was inexperienced and the environmental conditions may not have been set properly.

Also the chosen main factors may not reflect impact resistance properly since Charpy Impact Test is used in mainly metallurgical engineering. Although after variance stabilizing data transformation the residuals confirm the assumptions of constant variance and natural distribution, the regression model of full factorial design can only explain about 30% of the variation in the response. In other words the model fits only 30% of the response data. Also the predicted values that are obtained from the regression analysis of both experimental design methodologies are extremely lower than the desired value of 10.0 kgf.m. Besides, the lower and upper boundaries of the confirmation interval of the regression analysis of full factorial design are very low, the lower boundary being 3.89 kgf.m and upper being 6.61 kgf.m which are undesirable. However the upper boundary of the confidence interval of the other regression model is reasonable, 9.73 kgf.m, but this is due to the wideness of the confidence interval since, the lower value is again very low, 4.37 kgf.m. Impact resistance may be better modeled by Taguchi analysis in both experimental designs. Except the regression models, the predicted values for impact resistance in all models are very close to each other, near 8.50 kgf.m. In both analysis techniques of Taguchi design a different parameter level combination is found to be optimal for impact resistance, $A_1B_1C_{-1}D_{-1}E_1$ for Taguchi analysis and $A_1B_{-1}C_{-1}D_{-1}E_1$ for regression analysis and $A_1B_{-1}C_{-1}D_1E_1$ is the best parameter level combination obtained by both analysis methods of full factorial design. However, the most reasonable parameter level combination seems $A_1B_{-1}C_{-1}D_1E_1$ combination because, the confirmation run results are the highest ones among the others, with an average of 8.33 kgf.m, and they are very consistent with each other yet, this parameter level combination is underestimated by both regression models.

This study shows that, both models and both analysis techniques have their own advantages and disadvantages. For example Taguchi design can not account for three-way and higher order interaction terms which turned out to be significant on the responses in full factorial experimental design. However, since there are much more data points in full factorial design, it becomes harder to fit the model

to the most of the data points. Nevertheless, all the models led to nearly the same results with the same optimal parameter level combinations.

By this study it is concluded that the settings of the process parameters should be $A_1B_{-1}C_{-1}D_{-1}E_1$ as 90 days, silica fume, 20%, ordinary water curing and 1.0% by volume for testing age, binder type, binder amount, curing type and steel fiber volume fraction respectively in order to maximize the compressive strength and flexural strength of steel fiber reinforced high strength concrete. Since the impact resistance can not be eliminated from the other two responses, it will also be subjected to this combination.

7.2 Further Studies

It is possible to model the standard deviations by using regression analysis techniques in order to make a robust design of the compressive strength, flexural strength and impact resistance of steel fiber reinforced concrete and to find optimal settings of parameters that produce the maximum response with minimum variation around these maximums for all of the responses in the future. These results may be compared with the results of Taguchi's signal to noise method. Also by expanding the design of the experiment to include noise factors in a controlled manner, optimum conditions insensitive to the influence of the noise factors can be found. After determining the noise factors and their levels, outer orthogonal arrays can be used to design the conditions of the noise factors which dictate the number of repetitions for the trial runs.

A single regression equation can be searched for the two response variables namely the compressive strength and flexural strength of steel fiber reinforced high strength concrete and they can be optimized together as a future study. Another important research that could follow this study could be to optimize the regression models by multi-objective non linear programming, mainly the ones containing higher order terms that are obtained for the maximization of the impact resistance.

For future study a detailed cost analysis of this research can be performed and this can be a constraint on the maximization of compressive strength, flexural strength and impact resistance, since, the fiber reinforced high strength concrete production is an expensive process. Also by conducting a cost analysis, it can easily be seen that employing a full factorial design is extremely costly and time consuming when compared with Taguchi experimental design because Taguchi experimental design decreases 162 experiments to only 27.

Another future research should be to conduct a different kind of impact test since the Charpy Method could not yield good results and it could not be modeled properly. A freely falling ball method or armor penetration kinds of impact test (high velocity impact) should be performed and their mean and standard deviations should be modeled in order to reduce the variations. Also to test SFRHSC's dynamic strength, its fatigue performance should be known and therefore fatigue test should be conducted and analyzed in the future.

Also all the responses discussed could be studied by different combinations of process parameters. For example temperature, different types of steel fibers, different kinds of binder types such as metakaolin, loading rate, different curing combinations could be new main factors and their levels may be varied and a different experimental design can be conducted.

REFERENCES

[1] Nataraja M.C., Dhang N., Gupta A.P., Statistical variations in impact resistance of steel fiber-reinforced concrete subjected to drop weight test, Cement and Concrete Research 29, 1999, p.989-995.

[2] Balendran R.V., Zhou F.P., Nadeem A., Leung A.Y.T., Influence of steel fibers on strength and ductility of normal and lightweight high strength concrete, Building and Environment 37, 2002, p.1361-1367.

[3] Beshr H., Almusallam A.A., Maslehuddin M., Effect of coarse aggregate quality on the mechanical properties of high strength concrete, Construction and Building Materials 17, 2003, p.97-103.

[4] Shannag M.J., High strength concrete containing natural pozzolan and silica fume, Cement and Concrete Composites 22, 2000, p.399-406.

[5] Mindess S., Young F.J., "Concrete", Prentice-Hall Inc., 1981, p.1, 6-7, 119-137, 184-185, 600, 603, 628-634.

[6] Jan G.M. Van Mier, "Fracture Processes of Concrete: Assessment of Material Parameters for Fracture Models", CRC Press, 1997, p.17-19, 27, 33-37.

[7] Neville A.M., "Properties of Concrete", Longman Scientific and Technical, 1981, p.128.

[8] http://www.norchem.com/products.html

[9] Erdoğan T.Y., "Beton", ODTÜ Geliştirme Vakfı Yayıncılık ve İletişim A.Ş., 2003, p.183, 192, 200.

[10] Balaguru P.N., Shah S.P., “Fiber Reinforced Cement Composites”, McGraw-Hill Inc., 1992, p. 105-107.

[11] http://www.sefagroup.com/flyash.htm

[12] http://www.suvino.com/ggbfs.htm

[13] http://www.fhwa.dot.gov/infrastructure/materialsgrp/admixture.html

[14] Wu Ke-Ru, Chen B., Yao W., Zhang D., Effect of coarse aggregate type on mechanical properties of high-performance concrete, Cement and Concrete Research 31, 2001, p.1421-1425.

[15] Donza H., Cabrera O., Irassar E.F., High-strength concrete with different fine aggregate, Cement and Concrete Research 32, 2002, p.1755-1761.

[16] Roumaldi J.P., Batson G.P., Mechanics of crack arrest in concrete, J Eng Mech ASCE 1963, p.89.

[17] Bentur A., Mindess S., “Fiber Reinforced Cementitious Composites”, Elsevier Applied Science, London, UK, 1990, p. 3-4, 6-7.

[18] ITT Total Quality Management Group, “Taguchi Methods”, (2 Volumes), 1992, p.3-1, 3-60, 3-97.

[19] Montgomery D.C., “Design and Analysis of Experiments”, John Wiley & Sons Inc., Fourth Edition, 1997, p.2-3, 82-85, 228, 234.

[20] Roy R.K., “A Primer on the Taguchi Method”, Van Nostrand Reinhold, 1990, p.4-5, 17, 145.

[21] Mendenhall W., Sincich T., “A Second Course in Statistics: Regression Analysis”, Prentice Hall Inc., 1996, p.96, 191, 396, 430-435.

[22] Tanigawa Y., Hatanaka S., Stress-strain relations of steel fiber reinforced concrete under repeated compressive load, Cement and Concrete Research 13, 1983, p.801-808.

[23] Hashemi H.N., Cohen M.D., Ertürk T., Evaluation of fatigue damage on the mechanical properties of fiber reinforced cement pastes, Cement and Concrete Research 15, 1985, p.879-888.

[24] Issa M.A., Shafiq A.B., Hammad A.M., Crack arrest in mortar matrix reinforced with unidirectionally aligned fibers, Cement and Concrete Research 26, 1996, p.1245-1256.

[25] Toutanji H., Bayasi Z., Effects of manufacturing techniques on the flexural behavior of steel fiber-reinforced concrete, Cement and Concrete Research 28, 1998, p.115-124.

[26] Yan, H., Sun W., Chen H., The effect of silica fume and steel fiber on the dynamic mechanical performance of high-strength concrete, Cement and Concrete Research 29, 1999, p.423-426.

[27] Yang Q., Zhang S., Huang S., He Y., Effect of ground quartz sand on properties of high-strength concrete in the steam-autoclaved curing, Cement and Concrete Research 30, 2000, p.1993-1998.

[28] Luo X., Sun W., Chan S.Y.N., Steel fiber reinforced high-performance concrete: a study on the mechanical properties and resistance against impact, Materials and Structures 34, 2001, p.144-149.

[29] Memon A.H., Radin S.S., Zain M.F.M., Trottier J.F., Effects of mineral and chemical admixtures on high-strength concrete in seawater, Cement and Concrete Research 32, 2002, p.373-377.

[30] Srinivasan C.B., Narasimhan N.L., Ilango S.V., Development of rapid-set high-strength cement using statistical experimental design, Cement and Concrete Research 2311, 2003, p.1-6.

[31] Li G., Zhao X., Properties of concrete incorporating fly ash and ground granulated blast furnace slag, Cement and Concrete Composites 25, 2003, p.293-299.

[32] Marzouk H., Langdon S., The effect of alkali-aggregate reactivity on the mechanical properties of high and normal strength concrete, Cement & Concrete Composites 25, 2003, in press.

[33] Padmarajaiah S.K., Ramaswamy A., Flexural strength predictions of steel fiber reinforced high-strength concrete in fully/partially prestressed beam specimens, Cement and Concrete Composites 25, 2003, in press.

[34] Pan L.K., Chang B.D., Chou D.S., Optimization for solidification of low-level-radioactive resin using Taguchi analysis, Waste Management 21, 2001, p.767-772.

[35] Sonebi M., Experimental design to optimize high-volume of fly ash grout in the presence of welan gum and superplasticizer, Materials and Structures 35, 2002, p.373-380.

[36] ACI Committee 544, State of the art report on fiber reinforced concrete, ACI 544, 1R-82, Concrete International, 1982, p.5.

[37] Mu B., Li Z., Peng J., Short fiber-reinforced cementitious extruded plates with high percentage of slag and different fibers, Cement and Concrete Research 30, 2000, p.1277-1282.

[38] Qian C.X., Stroeven P., Development of hybrid polypropylene-steel fiber-reinforced concrete, Cement and Concrete Research 30, 2000, p.63-69.

[39] Kayalı O., Haque M.N., Zhu B., Some characteristics of high strength fiber reinforced lightweight aggregate concrete, Cement and Concrete Composites 25, 2003, P.207-213.

[40] Luo X., Sun W., Chan Y.N., Characteristics of high-performance steel fiber-reinforced concrete subject to high velocity impact, Cement and Concrete Research 30, 2000, p.907-914.

[41] Pigeon M., Cantin R., Flexural properties of steel fiber-reinforced concretes at low temperatures, Cement and Concrete Composites 20, 1998, p.365-375.

[42] Nataraja M.C., Dhang N., Gupta A.P., Stress-strain curves for steel fiber reinforced concrete under compression, Cement and Concrete Composites 21, 1999, p.383-390.

[43] Chang D.I., Chai W.K., Flexural fracture and fatigue behavior of steel-fiber reinforced concrete structures, Nuclear Engineering and Design 156, 1995, p.201-207.

[44] Wu D.S., Peng Y.N., The macro- and microproperties of cement pastes with silica-rich materials cured by wet –mixed steaming injection, Cement and Concrete Research 2320, 2003, p.1-15.

[45] Bushlaibi A.H., Alshamsi A.M., Efficiency of curing on partially exposed high-strength concrete in hot climate, Cement and Concrete Research 32, 2002, p.949-953.

[46] Türkmen İ., Gavgalı M., Gül R., Influence of mineral admixtures on the mechanical properties and corrosion of steel embedded in high strength concrete, Materials Letters 4110, 2002, in press.

[47] Loukili A., Khelidj A., Richard P., Hydration kinetics, change of relative humidity, and autogeneous shrinkage of ultra-high-strength concrete, Cement and Concrete Research 29, 1999, p.577-584.

[48] Marzouk H., Langdon S., The effect of alkali-aggregate reactivity on the mechanical properties of high and normal strength concrete, Cement & Concrete Composites 25, 2003, in press.

[49] Sun M., Liu Q., Li Z., Hu Y., A study of piezoelectric properties of carbon fiber reinforced concrete and plain cement paste during dynamic loading, Cement and Concrete Research 30, 2000, p.1593-1595.

[50] ASTM Committee C-9, Standard practice for making and curing concrete test specimens in the laboratory, ASTM C 192 – 90a, 1990, p.117-123.

[51] Orchard D.F., "Concrete Technology", John Wiley & Sons Inc., 1964, Vol.2, p.259.

[52] ASTM Committee C-1, Standard test method for compressive strength of hydraulic cement mortars, ASTM C 109 – 92, 1992, p.64-68.

[53] ASTM Committee C-9, Standard test method for compressive strength of cylindrical concrete specimens, ASTM C 39 – 86, 1986, p.20-23.

[54] ASTM Committee C-9, Standard test method for flexural strength of concrete (using simple beam with center-point loading), ASTM C 293 – 79, 1979, p.172-173.

[55] Esin A., "Properties of Materials for Mechanical Design", METU Faculty of Engineering Publications, No: 69, 1981, p.435, 439.

APPENDIX A

Appendix A.1 The concrete mixes for all of the combinations of the factors

10% Silica Fume 0.0% Steel Fiber

Material Type	Amount
Silica Fume (kg/m^3)	69,00
Portland Cement (kg/m^3)	621,00
Graded Standard Sand (kg/m^3)	412,00
Fine Aggregate (kg/m^3)	206,00
Coarse Aggregate (kg/m^3)	1442,00
Water (kg/m^3)	186,00
w/c	0,27
Superplasticizer (kg/m^3)	17,25
Steel Fiber (kg/m^3)	0,00

10% Silica Fume 0.5% Steel Fiber

Material Type	Amount
Silica Fume (kg/m^3)	69,00
Portland Cement (kg/m^3)	621,00
Graded Standard Sand (kg/m^3)	412,00
Fine Aggregate (kg/m^3)	206,00
Coarse Aggregate (kg/m^3)	1442,00
Water (kg/m^3)	186,00
w/c	0,27
Superplasticizer (kg/m^3)	17,25
Steel Fiber (kg/m^3)	48,00

10% Silica Fume 1.0% Steel Fiber

Material Type	Amount
Silica Fume (kg/m^3)	69,00
Portland Cement (kg/m^3)	621,00
Graded Standard Sand (kg/m^3)	412,00
Fine Aggregate (kg/m^3)	206,00
Coarse Aggregate (kg/m^3)	1442,00
Water (kg/m^3)	186,00
w/c	0,27
Superplasticizer (kg/m^3)	17,25
Steel Fiber (kg/m^3)	96,00

Appendix A.1 Continued

15% Silica Fume 0.0% Steel Fiber

Material Type	Amount
Silica Fume (kg/m^3)	103,50
Portland Cement (kg/m^3)	586,50
Graded Standard Sand (kg/m^3)	412,00
Fine Aggregate (kg/m^3)	206,00
Coarse Aggregate (kg/m^3)	1442,0
Water (kg/m^3)	186,00
w/c	0,27
Superplasticizer (kg/m^3)	17,25
Steel Fiber (kg/m^3)	0,00

15% Silica Fume 0.5% Steel Fiber

Material Type	Amount
Silica Fume (kg/m^3)	103,50
Portland Cement (kg/m^3)	586,50
Graded Standard Sand (kg/m^3)	412,00
Fine Aggregate (kg/m^3)	206,00
Coarse Aggregate (kg/m^3)	1442,00
Water (kg/m^3)	186,00
w/c	0,27
Superplasticizer (kg/m^3)	17,25
Steel Fiber (kg/m^3)	48,00

15% Silica Fume 1.0% Steel Fiber

Material Type	Amount
Silica Fume (kg/m^3)	103,50
Portland Cement (kg/m^3)	586,50
Graded Standard Sand (kg/m^3)	412,00
Fine Aggregate (kg/m^3)	206,00
Coarse Aggregate (kg/m^3)	1442,00
Water (kg/m^3)	186,00
w/c	0,27
Superplasticizer (kg/m^3)	17,25
Steel Fiber (kg/m^3)	96,00

Appendix A.1 Continued

20% Silica Fume 0.0% Steel Fiber

Material Type	Amount
Silica Fume (kg/m^3)	138,00
Portland Cement (kg/m^3)	552,00
Graded Standard Sand (kg/m^3)	412,00
Fine Aggregate (kg/m^3)	206,00
Coarse Aggregate (kg/m^3)	1442,00
Water (kg/m^3)	186,00
w/c	0,27
Superplasticizer (kg/m^3)	17,25
Steel Fiber (kg/m^3)	0,00

20% Silica Fume 0.5% Steel Fiber

Material Type	Amount
Silica Fume (kg/m^3)	138,00
Portland Cement (kg/m^3)	552,00
Graded Standard Sand (kg/m^3)	412,00
Fine Aggregate (kg/m^3)	206,00
Coarse Aggregate (kg/m^3)	1442,00
Water (kg/m^3)	186,00
w/c	0,27
Superplasticizer (kg/m^3)	17,25
Steel Fiber (kg/m^3)	48,00

20% Silica Fume 1.0% Steel Fiber

Material Type	Amount
Silica Fume (kg/m^3)	138,00
Portland Cement (kg/m^3)	552,00
Graded Standard Sand (kg/m^3)	412,00
Fine Aggregate (kg/m^3)	206,00
Coarse Aggregate (kg/m^3)	1442,00
Water (kg/m^3)	186,00
w/c	0,27
Superplasticizer (kg/m^3)	17,25
Steel Fiber (kg/m^3)	96,00

Appendix A.1 Continued

15% Silica Fume 10% Fly Ash 0.0% Steel Fiber

Material Type	Amount
Silica Fume (kg/m^3)	103,50
Fly Ash (kg/m^3)	69,00
Portland Cement (kg/m^3)	517,50
Graded Standard Sand (kg/m^3)	412,00
Fine Aggregate (kg/m^3)	206,00
Coarse Aggregate (kg/m^3)	1442,00
Water (kg/m^3)	186,00
w/c	0,27
Superplasticizer (kg/m^3)	17,25
Steel Fiber (kg/m^3)	0,00

15% Silica Fume 10% Fly Ash 0.5% Steel Fiber

Material Type	Amount
Silica Fume (kg/m^3)	103,50
Fly Ash (kg/m^3)	69,00
Portland Cement (kg/m^3)	517,50
Graded Standard Sand (kg/m^3)	412,00
Fine Aggregate (kg/m^3)	206,00
Coarse Aggregate (kg/m^3)	1442,00
Water (kg/m^3)	186,00
w/c	0,27
Superplasticizer (kg/m^3)	17,25
Steel Fiber (kg/m^3)	48,00

15% Silica Fume 10% Fly Ash 1.0% Steel Fiber

Material Type	Amount
Silica Fume (kg/m^3)	103,50
Fly Ash (kg/m^3)	69,00
Portland Cement (kg/m^3)	517,50
Graded Standard Sand (kg/m^3)	412,00
Fine Aggregate (kg/m^3)	206,00
Coarse Aggregate (kg/m^3)	1442,00
Water (kg/m^3)	186,00
w/c	0,27
Superplasticizer (kg/m^3)	17,25
Steel Fiber (kg/m^3)	96,00

Appendix A.1 Continued

15% Silica Fume 20% Fly Ash 0.0% Steel Fiber

Material Type	Amount
Silica Fume (kg/m^3)	103,50
Fly Ash (kg/m^3)	138,00
Portland Cement (kg/m^3)	448,50
Graded Standard Sand (kg/m^3)	412,00
Fine Aggregate (kg/m^3)	206,00
Coarse Aggregate (kg/m^3)	1442,00
Water (kg/m^3)	186,00
w/c	0,27
Superplasticizer (kg/m^3)	17,25
Steel Fiber (kg/m^3)	0,00

15% Silica Fume 20% Fly Ash 0.5% Steel Fiber

Material Type	Amount
Silica Fume (kg/m^3)	103,50
Fly Ash (kg/m^3)	138,00
Portland Cement (kg/m^3)	448,50
Graded Standard Sand (kg/m^3)	412,00
Fine Aggregate (kg/m^3)	206,00
Coarse Aggregate (kg/m^3)	1442,00
Water (kg/m^3)	186,00
w/c	0,27
Superplasticizer (kg/m^3)	17,25
Steel Fiber (kg/m^3)	48,00

15% Silica Fume 20% Fly Ash 1.0% Steel Fiber

Material Type	Amount
Silica Fume (kg/m^3)	103,50
Fly Ash (kg/m^3)	138,00
Portland Cement (kg/m^3)	448,50
Graded Standard Sand (kg/m^3)	412,00
Fine Aggregate (kg/m^3)	206,00
Coarse Aggregate (kg/m^3)	1442,00
Water (kg/m^3)	186,00
w/c	0,27
Superplasticizer (kg/m^3)	17,25
Steel Fiber (kg/m^3)	96,00

Appendix A.1 Continued

15% Silica Fume 30% Fly Ash 0.0% Steel Fiber

Material Type	Amount
Silica Fume (kg/m^3)	103,50
Fly Ash (kg/m^3)	207,00
Portland Cement (kg/m^3)	379,50
Graded Standard Sand (kg/m^3)	412,00
Fine Aggregate (kg/m^3)	206,00
Coarse Aggregate (kg/m^3)	1442,00
Water (kg/m^3)	186,00
w/c	0,27
Superplasticizer (kg/m^3)	17,25
Steel Fiber (kg/m^3)	0,00

15% Silica Fume 30% Fly Ash 0.5% Steel Fiber

Material Type	Amount
Silica Fume (kg/m^3)	103,50
Fly Ash (kg/m^3)	207,00
Portland Cement (kg/m^3)	379,50
Graded Standard Sand (kg/m^3)	412,00
Fine Aggregate (kg/m^3)	206,00
Coarse Aggregate (kg/m^3)	1442,00
Water (kg/m^3)	186,00
w/c	0,27
Superplasticizer (kg/m^3)	17,25
Steel Fiber (kg/m^3)	48,00

15% Silica Fume 30% Fly Ash 1.0% Steel Fiber

Material Type	Amount
Silica Fume (kg/m^3)	103,50
Fly Ash (kg/m^3)	207,00
Portland Cement (kg/m^3)	379,50
Graded Standard Sand (kg/m^3)	412,00
Fine Aggregate (kg/m^3)	206,00
Coarse Aggregate (kg/m^3)	1442,00
Water (kg/m^3)	186,00
w/c	0,27
Superplasticizer (kg/m^3)	17,25
Steel Fiber (kg/m^3)	96,00

Appendix A.1 Continued

15% Silica Fume 20% GGBFS 0.0% Steel Fiber

Material Type	Amount
Silica Fume (kg/m^3)	103,50
GGBFS (kg/m^3)	138,00
Portland Cement (kg/m^3)	448,50
Graded Standard Sand (kg/m^3)	412,00
Fine Aggregate (kg/m^3)	206,00
Coarse Aggregate (kg/m^3)	1442,00
Water (kg/m^3)	186,00
w/c	0,27
Superplasticizer (kg/m^3)	17,25
Steel Fiber (kg/m^3)	0,00

15% Silica Fume 20% GGBFS 0.5% Steel Fiber

Material Type	Amount
Silica Fume (kg/m^3)	103,50
GGBFS (kg/m^3)	138,00
Portland Cement (kg/m^3)	448,50
Graded Standard Sand (kg/m^3)	412,00
Fine Aggregate (kg/m^3)	206,00
Coarse Aggregate (kg/m^3)	1442,00
Water (kg/m^3)	186,00
w/c	0,27
Superplasticizer (kg/m^3)	17,25
Steel Fiber (kg/m^3)	48,00

15% Silica Fume 20% GGBFS 1.0% Steel Fiber

Material Type	Amount
Silica Fume (kg/m^3)	103,50
GGBFS (kg/m^3)	138,00
Portland Cement (kg/m^3)	448,50
Graded Standard Sand (kg/m^3)	412,00
Fine Aggregate (kg/m^3)	206,00
Coarse Aggregate (kg/m^3)	1442,00
Water (kg/m^3)	186,00
w/c	0,27
Superplasticizer (kg/m^3)	17,25
Steel Fiber (kg/m^3)	96,00

Appendix A.1 Continued

15% Silica Fume 40% GGBFS 0.0% Steel Fiber

Material Type	Amount
Silica Fume (kg/m^3)	103,50
GGBFS (kg/m^3)	276,00
Portland Cement (kg/m^3)	310,50
Graded Standard Sand (kg/m^3)	412,00
Fine Aggregate (kg/m^3)	206,00
Coarse Aggregate (kg/m^3)	1442,00
Water (kg/m^3)	186,00
w/c	0,27
Superplasticizer (kg/m^3)	17,25
Steel Fiber (kg/m^3)	0,00

15% Silica Fume 40% GGBFS 0.5% Steel Fiber

Material Type	Amount
Silica Fume (kg/m^3)	103,50
GGBFS (kg/m^3)	276,00
Portland Cement (kg/m^3)	310,50
Graded Standard Sand (kg/m^3)	412,00
Fine Aggregate (kg/m^3)	206,00
Coarse Aggregate (kg/m^3)	1442,00
Water (kg/m^3)	186,00
w/c	0,27
Superplasticizer (kg/m^3)	17,25
Steel Fiber (kg/m^3)	48,00

15% Silica Fume 40% GGBFS 1.0% Steel Fiber

Material Type	Amount
Silica Fume (kg/m^3)	103,50
GGBFS (kg/m^3)	276,00
Portland Cement (kg/m^3)	310,50
Graded Standard Sand (kg/m^3)	412,00
Fine Aggregate (kg/m^3)	206,00
Coarse Aggregate (kg/m^3)	1442,00
Water (kg/m^3)	186,00
w/c	0,27
Superplasticizer (kg/m^3)	17,25
Steel Fiber (kg/m^3)	96,00

Appendix A.1 Continued

15% Silica Fume 60% GGBFS 0.0% Steel Fiber

Material Type	Amount
Silica Fume (kg/m^3)	103,50
GGBFS (kg/m^3)	414,00
Portland Cement (kg/m^3)	172,50
Graded Standard Sand (kg/m^3)	412,00
Fine Aggregate (kg/m^3)	206,00
Coarse Aggregate (kg/m^3)	1442,00
Water (kg/m^3)	186,00
w/c	0,27
Superplasticizer (kg/m^3)	17,25
Steel Fiber (kg/m^3)	0,00

15% Silica Fume 60% GGBFS 0.5% Steel Fiber

Material Type	Amount
Silica Fume (kg/m^3)	103,50
GGBFS (kg/m^3)	414,00
Portland Cement (kg/m^3)	172,50
Graded Standard Sand (kg/m^3)	412,00
Fine Aggregate (kg/m^3)	206,00
Coarse Aggregate (kg/m^3)	1442,00
Water (kg/m^3)	186,00
w/c	0,27
Superplasticizer (kg/m^3)	17,25
Steel Fiber (kg/m^3)	48,00

15% Silica Fume 60% GGBFS 1.0% Steel Fiber

Material Type	Amount
Silica Fume (kg/m^3)	103,50
GGBFS (kg/m^3)	414,00
Portland Cement (kg/m^3)	172,50
Graded Standard Sand (kg/m^3)	412,00
Fine Aggregate (kg/m^3)	206,00
Coarse Aggregate (kg/m^3)	1442,00
Water (kg/m^3)	186,00
w/c	0,27
Superplasticizer (kg/m^3)	17,25
Steel Fiber (kg/m^3)	96,00

APPENDIX B

Appendix B.1 L_{27} (3^{13}) orthogonal array

	Columns												
Run	**1**	**2**	**3**	**4**	**5**	**6**	**7**	**8**	**9**	**10**	**11**	**12**	**13**
1	1	1	1	1	1	1	1	1	1	1	1	1	1
2	1	1	1	1	2	2	2	2	2	2	2	2	2
3	1	1	1	1	3	3	3	3	3	3	3	3	3
4	1	2	2	2	1	1	1	2	2	2	3	3	3
5	1	2	2	2	2	2	2	3	3	3	1	1	1
6	1	2	2	2	3	3	3	1	1	1	2	2	2
7	1	3	3	3	1	1	1	3	3	3	2	2	2
8	1	3	3	3	2	2	2	1	1	1	3	3	3
9	1	3	3	3	3	3	3	2	2	2	1	1	1
10	2	1	2	3	1	2	3	1	2	3	1	2	3
11	2	1	2	3	2	3	1	2	3	1	2	3	1
12	2	1	2	3	3	1	2	3	1	2	3	1	2
13	2	2	3	1	1	2	3	2	3	1	3	1	2
14	2	2	3	1	2	3	1	3	1	2	1	2	3
15	2	2	3	1	3	1	2	1	2	3	2	3	1
16	2	3	1	2	1	2	3	3	1	2	2	3	1
17	2	3	1	2	2	3	1	1	2	3	3	1	2
18	2	3	1	2	3	1	2	2	3	1	1	2	3
19	3	1	3	2	1	3	2	1	3	2	1	3	2
20	3	1	3	2	2	1	3	2	1	3	2	1	3
21	3	1	3	2	3	2	1	3	2	1	3	2	1
22	3	2	1	3	1	3	2	2	1	3	3	2	1
23	3	2	1	3	2	1	3	3	2	1	1	3	2
24	3	2	1	3	3	2	1	1	3	2	2	1	3
25	3	3	2	1	1	3	2	3	2	1	2	1	3
26	3	3	2	1	2	1	3	1	3	2	3	2	1
27	3	3	2	1	3	2	1	2	1	3	1	3	2

Appendix B.2 Interaction table for L_{27} (3^{13})

Columns	Columns												
	1	**2**	**3**	**4**	**5**	**6**	**7**	**8**	**9**	**10**	**11**	**12**	**13**
	(1)	3	2	2	6	5	5	9	8	8	12	11	11
		4	4	3	7	7	6	10	10	9	13	13	12
		(2)	1	1	8	9	10	5	6	7	5	6	7
			4	3	11	12	13	11	12	13	8	9	10
			(3)	1	9	10	8	7	5	6	6	7	5
				2	13	11	12	12	13	11	10	8	9
				(4)	10	8	9	6	7	5	7	5	6
					12	13	11	13	11	12	9	10	8
					(5)	1	1	2	3	4	2	4	3
						7	6	11	13	12	8	10	9
						(6)	1	4	2	3	3	2	4
							5	13	12	11	10	9	8
							(7)	3	4	2	4	3	2
								12	11	13	9	8	10
								(8)	1	1	2	3	4
									10	9	5	7	6
									(9)	1	4	2	3
										8	7	6	5
										(10)	3	4	2
											6	5	7
											(11)	1	1
												13	12
												(12)	1
													11

Appendix B.3 The regression model developed for the mean compressive strength based on the L_{27} (3^{13}) design with only main factors

The regression equation is

y = 90,4 + 18,6 A - 25,7 B1 - 18,2 B2 - 9,98 C - 14,4 D1 + 3,03 E

Predictor	Coef	SE Coef	T	P
Constant	90,442	4,837	18,70	0,000
A	18,632	3,168	5,88	0,000
B1	-25,678	6,336	-4,05	0,001
B2	-18,226	6,336	-2,88	0,009
C	-9,983	3,168	-3,15	0,005
D1	-14,381	5,490	-2,62	0,016
E	3,033	3,283	0,92	0,367

S = 13,42 R-Sq = 77,9% R-Sq(adj) = 71,2%

Analysis of Variance

Source	DF	SS	MS	F	P
Regression	6	12663,6	2110,6	11,72	0,000
Residual Error	20	3601,0	180,1		
Total	26	16264,7			

Source	DF	Seq SS
A	1	6361,9
B1	1	1680,0
B2	1	1550,6
C	1	1734,0
D1	1	1183,5
E	1	153,6

Unusual Observations

Obs	A	MEAN1	Fit	SE Fit	Residual	St Resid
22	1,00	54,40	83,42	8,11	-29,02	-2,71R

R denotes an observation with a large standardized residual

Durbin-Watson statistic = 2,07

Appendix B.4 The regression model developed for the mean compressive strength based on the L_{27} (3^{13}) design with main and interaction factors

The regression equation is

y = 98,5 + 17,2 A - 36,6 B1 - 17,6 B2 - 9,33 C - 29,7 D1 + 5,47 E + 6,2 AC - 13,1 AE - 15,6 CE + 23,9 B1D1 - 10,6 B2D1 + 2,94 AB1 - 12,4 CB1 - 11,1 EB1 - 8,2 ACB1 + 17,8 AEB1 + 15,7 CEB1 + 1,94 AB2 + 4,7 CB2 + 16,4 EB2 - 33,3 ACB2 + 20,4 AEB2 + 7,8 CEB2

Predictor	Coef	SE Coef	T	P
Constant	98,467	7,760	12,69	0,001
A	17,167	6,053	2,84	0,066
B1	-36,566	9,046	-4,04	0,027
B2	-17,62	10,97	-1,61	0,207
C	-9,330	7,381	-1,26	0,296
D1	-29,70	16,04	-1,85	0,161
E	5,470	7,381	0,74	0,512
AC	6,20	14,04	0,44	0,689
AE	-13,07	15,22	-0,86	0,454
CE	-15,63	10,81	-1,45	0,244
B1D1	23,91	18,21	1,31	0,281
B2D1	-10,57	26,06	-0,41	0,712
AB1	2,944	7,531	0,39	0,722
CB1	-12,448	8,635	-1,44	0,245
EB1	-11,092	8,635	-1,28	0,289
ACB1	-8,24	15,61	-0,53	0,634
AEB1	17,85	16,67	1,07	0,363
CEB1	15,72	12,78	1,23	0,306
AB2	1,944	9,546	0,20	0,852
CB2	4,66	10,44	0,45	0,685
EB2	16,35	11,61	1,41	0,254
ACB2	-33,26	20,93	-1,59	0,210
AEB2	20,41	19,22	1,06	0,366
CEB2	7,77	15,96	0,49	0,660

S = 10,97 R-Sq = 97,8% R-Sq(adj) = 80,7%

Analysis of Variance

Source	DF	SS	MS	F	P
Regression	23	15903,3	691,4	5,74	0,087
Residual Error	3	361,3	120,4		
Total	26	16264,7			

Source	DF	Seq SS
A	1	6361,9
B1	1	1680,0
B2	1	1550,6
C	1	1734,0
D1	1	1183,5
E	1	153,6
AC	1	19,9
AE	1	80,7
CE	1	186,2
B1D1	1	197,7
B2D1	1	25,5
AB1	1	17,6
CB1	1	1279,6
EB1	1	657,0
ACB1	1	37,2

Appendix B.4 Continued

```
AEB1           1          0,2
CEB1           1         89,1
AB2            1         19,7
CB2            1         18,6
EB2            1        255,6
ACB2           1        136,7
AEB2           1        189,7
CEB2           1         28,5

Unusual Observations
Obs      A      MEAN1         Fit      SE Fit    Residual      St Resid
  2  -1,00      51,60       51,60       10,97       -0,00           * X
  4  -1,00      55,73       55,73       10,97       -0,00           * X
  9  -1,00      43,87       43,87       10,97       -0,00           * X
 11   0,00      62,40       62,40       10,97       -0,00           * X
 13   0,00      99,20       99,20       10,97       -0,00           * X
 18   0,00      28,80       28,80       10,97       -0,00           * X
 20   1,00      77,07       77,07       10,97       -0,00           * X
 22   1,00      54,40       54,40       10,97       -0,00           * X
 27   1,00      82,80       82,80       10,97       -0,00           * X

X denotes an observation whose X value gives it large influence.

Durbin-Watson statistic = 2,11
```

Appendix B.5 The best regression model developed for the mean compressive strength based on the L_{27} (3^{13}) design

The regression equation is

y = 94,5 + 19,6 A - 32,6 B1 - 14,6 B2 - 6,99 C - 20,8 D1 + 2,87 E - 1,01 AC - 7,08 AE - 10,4 CE + 14,8 B1D1 - 16,7 B2D1 - 14,8 CB1 - 8,49 EB1 + 12,2 AEB1 + 10,2 CEB1 + 19,0 EB2 - 26,1 ACB2 + 17,5 AEB2

Predictor	Coef	SE Coef	T	P
Constant	94,529	3,723	25,39	0,000
A	19,613	1,828	10,73	0,000
B1	-32,559	4,799	-6,78	0,000
B2	-14,624	6,345	-2,30	0,050
C	-6,988	2,792	-2,50	0,037
D1	-20,756	6,835	-3,04	0,016
E	2,871	3,948	0,73	0,488
AC	-1,009	4,044	-0,25	0,809
AE	-7,076	6,125	-1,16	0,281
CE	-10,420	3,568	-2,92	0,019
B1D1	14,758	8,665	1,70	0,127
B2D1	-16,69	14,73	-1,13	0,290
CB1	-14,790	4,131	-3,58	0,007
EB1	-8,493	4,986	-1,70	0,127
AEB1	12,162	8,162	1,49	0,175
CEB1	10,201	5,658	1,80	0,109
EB2	18,951	7,257	2,61	0,031
ACB2	-26,06	11,30	-2,31	0,050
AEB2	17,493	9,001	1,94	0,088

S = 7,457 R-Sq = 97,3% R-Sq(adj) = 91,1%

Analysis of Variance

Source	DF	SS	MS	F	P
Regression	18	15819,75	878,88	15,80	0,000
Residual Error	8	444,90	55,61		
Total	26	16264,65			

Source	DF	Seq SS
A	1	6361,92
B1	1	1680,03
B2	1	1550,63
C	1	1733,95
D1	1	1183,48
E	1	153,64
AC	1	19,95
AE	1	80,73
CE	1	186,21
B1D1	1	197,71
B2D1	1	25,51
CB1	1	1282,27
EB1	1	648,03
AEB1	1	0,67
CEB1	1	114,80
EB2	1	168,44
ACB2	1	221,74
AEB2	1	210,07

Appendix B.5 Continued

```
Unusual Observations
Obs        A      MEAN1         Fit      SE Fit    Residual     St Resid
 10    0,00      74,13       86,89        5,29      -12,76       -2,43R
 23    1,00     111,33       99,52        5,07       11,82        2,16R

R denotes an observation with a large standardized residual

Durbin-Watson statistic = 1,84
```

Appendix B.6 $3^4 2^1$ full factorial design and its results when the response variable is the compressive strength

$3^4 2^1$ Full Factorial Design for Compressive Strength										
Exp. Run No	Processing Parameters					Results				
	A	B	C	D	E	Run #1	Run #2	Run #3	μ (Mpa)	S/N ratio
1	-1	-1	-1	-1	-1	61,2	62,8	62,4	62,13	35,86
2	-1	-1	-1	-1	0	70,4	64,0	71,6	68,67	36,70
3	-1	-1	-1	-1	1	71,2	73,2	70,0	71,47	37,08
4	-1	-1	-1	1	-1	48,4	50,0	48,0	48,80	33,76
5	-1	-1	-1	1	0	56,0	60,6	59,6	58,73	35,36
6	-1	-1	-1	1	1	72,4	72,0	68,0	70,80	36,99
7	-1	-1	0	-1	-1	48,4	50,8	58,8	52,67	34,34
8	-1	-1	0	-1	0	66,8	75,2	61,2	67,73	36,52
9	-1	-1	0	-1	1	74,0	72,4	71,6	72,67	37,22
10	-1	-1	0	1	-1	45,6	46,8	49,2	47,20	33,47
11	-1	-1	0	1	0	49,2	50,8	54,8	51,60	34,23
12	-1	-1	0	1	1	59,6	59,6	68,0	62,40	35,85
13	-1	-1	1	-1	-1	54,0	58,4	56,8	56,40	35,01
14	-1	-1	1	-1	0	57,6	67,2	60,4	61,73	35,76
15	-1	-1	1	-1	1	67,2	69,6	70,8	69,20	36,80
16	-1	-1	1	1	-1	60,0	61,0	60,8	60,60	35,65
17	-1	-1	1	1	0	62,4	59,2	60,4	60,67	35,65
18	-1	-1	1	1	1	60,0	60,0	61,6	60,53	35,64
19	-1	0	-1	-1	-1	68,8	74,0	70,0	70,93	37,00
20	-1	0	-1	-1	0	56,0	54,4	55,2	55,20	34,84
21	-1	0	-1	-1	1	66,0	68,8	64,8	66,53	36,45
22	-1	0	-1	1	-1	52,0	48,0	48,8	49,60	33,89
23	-1	0	-1	1	0	57,2	53,2	56,8	55,73	34,91
24	-1	0	-1	1	1	59,6	64,8	58,4	60,93	35,67
25	-1	0	0	-1	-1	52,0	50,8	44,4	49,07	33,75
26	-1	0	0	-1	0	40,4	38,0	39,2	39,20	31,86
27	-1	0	0	-1	1	26,4	32,0	33,6	30,67	29,59
28	-1	0	0	1	-1	29,6	44,0	42,0	38,53	31,30
29	-1	0	0	1	0	42,0	40,8	38,8	40,53	32,14
30	-1	0	0	1	1	41,6	38,8	35,2	38,53	31,66
31	-1	0	1	-1	-1	32,4	34,4	29,2	32,00	30,04
32	-1	0	1	-1	0	27,6	31,6	30,8	30,00	29,50
33	-1	0	1	-1	1	23,2	20,0	24,0	22,40	26,92
34	-1	0	1	1	-1	35,2	32,0	32,8	33,33	30,44
35	-1	0	1	1	0	19,6	24,4	25,2	23,07	27,09
36	-1	0	1	1	1	17,2	17,2	16,0	16,80	24,49
37	-1	1	-1	-1	-1	40,0	34,8	44,0	39,60	31,83

Appendix B.6 Continued

$3^4 2^1$ Full Factorial Design for Compressive Strength										
Exp. Run No	Processing Parameters					Results				
	A	B	C	D	E	Run #1	Run #2	Run #3	μ (Mpa)	S/N ratio
38	-1	1	-1	-1	0	60,4	62,8	63,2	62,13	35,86
39	-1	1	-1	-1	1	67,6	61,2	64,8	64,53	36,17
40	-1	1	-1	1	-1	34,8	32,4	33,6	33,60	30,52
41	-1	1	-1	1	0	50,0	47,2	49,2	48,80	33,76
42	-1	1	-1	1	1	52,4	50,4	49,6	50,80	34,11
43	-1	1	0	-1	-1	54,0	53,6	51,2	52,93	34,47
44	-1	1	0	-1	0	58,8	58,0	56,0	57,60	35,20
45	-1	1	0	-1	1	55,6	57,6	43,2	52,13	34,12
46	-1	1	0	1	-1	46,0	46,0	46,4	46,13	33,28
47	-1	1	0	1	0	46,8	47,6	48,0	47,47	33,53
48	-1	1	0	1	1	34,0	32,0	34,4	33,47	30,48
49	-1	1	1	-1	-1	53,6	54,8	54,0	54,13	34,67
50	-1	1	1	-1	0	39,2	40,8	40,0	40,00	32,04
51	-1	1	1	-1	1	53,2	54,8	49,2	52,40	34,36
52	-1	1	1	1	-1	43,6	44,0	41,6	43,07	32,67
53	-1	1	1	1	0	41,6	40,0	50,0	43,87	32,72
54	-1	1	1	1	1	38,4	40,0	40,8	39,73	31,97
55	0	-1	-1	-1	-1	100,8	102,4	68,8	90,67	38,70
56	0	-1	-1	-1	0	110,0	100,0	105,2	105,07	40,41
57	0	-1	-1	-1	1	116,8	114,0	116,4	115,73	41,27
58	0	-1	-1	1	-1	74,8	73,2	72,0	73,33	37,30
59	0	-1	-1	1	0	90,4	102,8	94,0	95,73	39,58
60	0	-1	-1	1	1	96,0	102,0	99,6	99,20	39,92
61	0	-1	0	-1	-1	84,0	99,6	101,6	95,07	39,46
62	0	-1	0	-1	0	90,8	89,6	102,4	94,27	39,44
63	0	-1	0	-1	1	96,0	97,2	97,6	96,93	39,73
64	0	-1	0	1	-1	99,6	94,4	94,4	96,13	39,65
65	0	-1	0	1	0	82,4	88,4	84,0	84,93	38,57
66	0	-1	0	1	1	100,8	96,8	92,4	96,67	39,69
67	0	-1	1	-1	-1	75,6	88,4	88,4	84,13	38,43
68	0	-1	1	-1	0	84,8	90,0	86,4	87,07	38,79
69	0	-1	1	-1	1	84,4	82,4	80,0	82,27	38,30
70	0	-1	1	1	-1	83,2	80,0	76,4	79,87	38,03
71	0	-1	1	1	0	84,0	82,0	88,0	84,67	38,54
72	0	-1	1	1	1	81,6	78,8	80,4	80,27	38,09
73	0	0	-1	-1	-1	88,0	92,0	86,0	88,67	38,95
74	0	0	-1	-1	0	90,0	81,6	78,4	83,33	38,37
75	0	0	-1	-1	1	92,0	93,2	77,2	87,47	38,74

Appendix B.6 Continued

$3^4 2^1$ Full Factorial Design for Compressive Strength										
Exp. Run No	Processing Parameters					Results				
	A	B	C	D	E	Run #1	Run #2	Run #3	μ (Mpa)	S/N ratio
76	0	0	-1	1	-1	78,0	72,0	78,4	76,13	37,61
77	0	0	-1	1	0	76,4	74,0	77,6	76,00	37,61
78	0	0	-1	1	1	83,2	84,0	86,8	84,67	38,55
79	0	0	0	-1	-1	75,2	70,0	75,2	73,47	37,31
80	0	0	0	-1	0	62,0	66,0	66,4	64,80	36,22
81	0	0	0	-1	1	46,0	46,4	49,6	47,33	33,49
82	0	0	0	1	-1	58,0	60,4	66,8	61,73	35,76
83	0	0	0	1	0	50,0	52,4	52,4	51,60	34,25
84	0	0	0	1	1	54,4	49,2	53,2	52,27	34,34
85	0	0	1	-1	-1	55,6	52,0	52,0	53,20	34,51
86	0	0	1	-1	0	59,2	52,8	56,0	56,00	34,94
87	0	0	1	-1	1	46,0	43,2	41,6	43,60	32,77
88	0	0	1	1	-1	42,4	42,0	43,6	42,67	32,60
89	0	0	1	1	0	38,8	39,2	38,0	38,67	31,74
90	0	0	1	1	1	31,6	30,0	24,8	28,80	29,04
91	0	1	-1	-1	-1	62,4	56,8	55,6	58,27	35,28
92	0	1	-1	-1	0	92,0	84,4	90,0	88,80	38,95
93	0	1	-1	-1	1	96,0	101,6	94,0	97,20	39,74
94	0	1	-1	1	-1	48,0	49,6	46,0	47,87	33,59
95	0	1	-1	1	0	76,8	77,6	68,0	74,13	37,35
96	0	1	-1	1	1	78,4	79,2	78,0	78,53	37,90
97	0	1	0	-1	-1	66,0	66,8	69,2	67,33	36,56
98	0	1	0	-1	0	82,8	78,0	76,0	78,93	37,93
99	0	1	0	-1	1	86,0	97,2	90,8	91,33	39,18
100	0	1	0	1	-1	52,8	61,6	73,6	62,67	35,70
101	0	1	0	1	0	74,8	74,4	74,8	74,67	37,46
102	0	1	0	1	1	61,2	60,0	66,0	62,40	35,88
103	0	1	1	-1	-1	57,6	56,8	55,2	56,53	35,04
104	0	1	1	-1	0	71,2	60,0	60,4	63,87	36,03
105	0	1	1	-1	1	62,4	68,8	69,2	66,80	36,47
106	0	1	1	1	-1	43,6	44,0	50,0	45,87	33,18
107	0	1	1	1	0	52,0	44,0	42,0	46,00	33,15
108	0	1	1	1	1	44,0	46,8	43,6	44,80	33,01
109	1	-1	-1	-1	-1	88,0	94,0	90,4	90,80	39,15
110	1	-1	-1	-1	0	118,8	112,0	122,4	117,73	41,40
111	1	-1	-1	-1	1	136,0	128,0	121,6	128,53	42,15
112	1	-1	-1	1	-1	104,0	86,4	103,2	97,87	39,72
113	1	-1	-1	1	0	100,0	110,0	108,0	106,00	40,48

Appendix B.6 Continued

$3^4 2^1$ Full Factorial Design for Compressive Strength										
Exp. Run No	Processing Parameters					Results				
	A	B	C	D	E	Run #1	Run #2	Run #3	μ (Mpa)	S/N ratio
114	1	-1	-1	1	1	110,0	108,4	104,4	107,60	40,63
115	1	-1	0	-1	-1	94,0	96,0	96,4	95,47	39,60
116	1	-1	0	-1	0	110,0	121,6	89,6	107,07	40,38
117	1	-1	0	-1	1	110,0	113,2	104,0	109,07	40,74
118	1	-1	0	1	-1	100,0	97,2	99,2	98,80	39,89
119	1	-1	0	1	0	77,6	94,4	88,0	86,67	38,67
120	1	-1	0	1	1	96,4	98,4	95,6	96,80	39,72
121	1	-1	1	-1	-1	91,6	88,0	83,6	87,73	38,85
122	1	-1	1	-1	0	95,2	84,8	84,4	88,13	38,86
123	1	-1	1	-1	1	93,6	90,0	92,8	92,13	39,28
124	1	-1	1	1	-1	76,4	90,0	82,0	82,80	38,30
125	1	-1	1	1	0	89,2	80,8	84,8	84,93	38,56
126	1	-1	1	1	1	82,0	80,0	84,8	82,27	38,30
127	1	0	-1	-1	-1	110,8	103,2	98,4	104,13	40,32
128	1	0	-1	-1	0	101,6	85,6	76,8	88,00	38,72
129	1	0	-1	-1	1	97,6	98,0	118	104,53	40,29
130	1	0	-1	1	-1	82,4	74,0	73,2	76,53	37,64
131	1	0	-1	1	0	88,4	86,4	86,0	86,93	38,78
132	1	0	-1	1	1	98,0	94,0	107,2	99,73	39,94
133	1	0	0	-1	-1	91,6	86,8	84,4	87,60	38,84
134	1	0	0	-1	0	82,4	69,2	78,4	76,67	37,62
135	1	0	0	-1	1	70,0	49,6	48,4	56,00	34,61
136	1	0	0	1	-1	82,0	74,4	74,8	77,07	37,71
137	1	0	0	1	0	66,0	64,8	64,0	64,93	36,25
138	1	0	0	1	1	87,2	65,6	61,6	71,47	36,80
139	1	0	1	-1	-1	73,2	70,8	64,0	69,33	36,78
140	1	0	1	-1	0	58,4	59,2	54,8	57,47	35,17
141	1	0	1	-1	1	42,8	38,8	40,4	40,67	32,16
142	1	0	1	1	-1	59,2	62,8	61,2	61,07	35,71
143	1	0	1	1	0	48,0	46,4	45,6	46,67	33,37
144	1	0	1	1	1	38,4	42,0	44,4	41,60	32,34
145	1	1	-1	-1	-1	83,2	79,6	76,8	79,87	38,03
146	1	1	-1	-1	0	88,0	88,0	111,6	95,87	39,47
147	1	1	-1	-1	1	109,6	100,0	90,4	100,00	39,92
148	1	1	-1	1	-1	51,2	54,8	57,2	54,40	34,68
149	1	1	-1	1	0	78,4	90,4	92,8	87,20	38,74
150	1	1	-1	1	1	81,2	82,8	80,8	81,60	38,23
151	1	1	0	-1	-1	92,8	80,0	82,8	85,20	38,56

Appendix B.6 Continued

$3^4 2^1$ Full Factorial Design for Compressive Strength										
Exp. Run No	Processing Parameters					Results				
	A	B	C	D	E	Run #1	Run #2	Run #3	μ (Mpa)	S/N ratio
152	1	1	0	-1	0	114,4	113,6	106,0	111,33	40,92
153	1	1	0	-1	1	98,0	96,0	96,0	96,67	39,70
154	1	1	0	1	-1	82,4	74,4	82,0	79,60	37,99
155	1	1	0	1	0	91,6	94,4	97,6	94,53	39,50
156	1	1	0	1	1	83,6	86,0	80,8	83,47	38,42
157	1	1	1	-1	-1	78,0	73,2	68,0	73,07	37,23
158	1	1	1	-1	0	84,0	88,0	91,6	87,87	38,86
159	1	1	1	-1	1	86,0	84,8	89,2	86,67	38,75
160	1	1	1	1	-1	58,8	58,8	61,6	59,73	35,52
161	1	1	1	1	0	61,6	63,6	60,0	61,73	35,80
162	1	1	1	1	1	61,6	54,8	63,2	59,87	35,49

Appendix B.7 $3^4 2^1$ full factorial design and its results when the response variable is the flexural strength

$3^4 2^1$ Full Factorial Design for Flexural Strength										
Exp. Run No	Processing Parameters					Results				
	A	B	C	D	E	Run #1	Run #2	Run #3	μ (Mpa)	S/N ratio
1	-1	-1	-1	-1	-1	10,14	9,91	9,22	9,76	19,76
2	-1	-1	-1	-1	0	9,91	9,91	8,41	9,41	19,39
3	-1	-1	-1	-1	1	10,02	9,45	9,22	9,56	19,60
4	-1	-1	-1	1	-1	5,41	6,11	6,91	6,14	15,64
5	-1	-1	-1	1	0	7,14	6,80	4,95	6,30	15,63
6	-1	-1	-1	1	1	8,06	9,91	8,06	8,68	18,65
7	-1	-1	0	-1	-1	9,56	8,29	9,45	9,10	19,13
8	-1	-1	0	-1	0	9,91	9,45	8,29	9,22	19,22
9	-1	-1	0	-1	1	10,71	10,37	8,76	9,95	19,85
10	-1	-1	0	1	-1	9,22	8,76	9,45	9,14	19,21
11	-1	-1	0	1	0	8,06	8,53	7,49	8,03	18,05
12	-1	-1	0	1	1	8,29	7,14	5,88	7,10	16,77
13	-1	-1	1	-1	-1	8,64	8,87	8,29	8,6	18,68
14	-1	-1	1	-1	0	9,45	8,64	8,99	9,03	19,09
15	-1	-1	1	-1	1	8,29	10,25	9,33	9,29	19,26
16	-1	-1	1	1	-1	8,06	7,14	7,26	7,49	17,45
17	-1	-1	1	1	0	8,41	9,45	8,29	8,72	18,76
18	-1	-1	1	1	1	7,60	9,68	8,87	8,72	18,68
19	-1	0	-1	-1	-1	9,68	8,29	9,45	9,14	19,16
20	-1	0	-1	-1	0	6,91	5,53	5,30	5,91	15,27
21	-1	0	-1	-1	1	8,76	6,68	8,29	7,91	17,78
22	-1	0	-1	1	-1	6,22	7,60	7,37	7,06	16,88
23	-1	0	-1	1	0	6,45	5,99	5,99	6,14	15,75
24	-1	0	-1	1	1	5,07	6,91	6,11	6,03	15,39
25	-1	0	0	-1	-1	6,91	8,18	8,06	7,72	17,67
26	-1	0	0	-1	0	5,88	5,30	6,11	5,76	15,17
27	-1	0	0	-1	1	4,61	4,15	4,72	4,49	13,01
28	-1	0	0	1	-1	6,80	7,37	5,99	6,72	16,45
29	-1	0	0	1	0	4,72	4,84	5,41	4,99	13,92
30	-1	0	0	1	1	3,23	3,80	3,34	3,46	10,71
31	-1	0	1	-1	-1	4,72	5,41	4,84	4,99	13,92
32	-1	0	1	-1	0	4,38	3,00	3,34	3,57	10,74
33	-1	0	1	-1	1	4,15	3,69	3,34	3,73	11,32
34	-1	0	1	1	-1	4,72	4,84	5,07	4,88	13,75
35	-1	0	1	1	0	4,84	4,49	3,57	4,30	12,45
36	-1	0	1	1	1	3,69	3,46	3,00	3,38	10,49
37	-1	1	-1	-1	-1	5,65	5,76	5,53	5,65	15,03
38	-1	1	-1	-1	0	7,83	7,60	6,45	7,29	17,16

Appendix B.7 Continued

$3^4 2^1$ Full Factorial Design for Flexural Strength										
Exp. Run No	Processing Parameters					Results				
	A	B	C	D	E	Run #1	Run #2	Run #3	μ (Mpa)	S/N ratio
39	-1	1	-1	-1	1	8,41	9,79	10,02	9,41	19,39
40	-1	1	-1	1	-1	6,11	5,53	5,76	5,80	15,25
41	-1	1	-1	1	0	6,80	6,34	6,57	6,57	16,34
42	-1	1	-1	1	1	6,80	7,37	7,14	7,10	17,01
43	-1	1	0	-1	-1	4,61	6,91	3,69	5,07	13,27
44	-1	1	0	-1	0	6,45	6,57	6,11	6,38	16,08
45	-1	1	0	-1	1	6,57	7,72	7,37	7,22	17,11
46	-1	1	0	1	-1	4,15	5,88	6,45	5,49	14,32
47	-1	1	0	1	0	3,46	6,45	5,18	5,03	13,16
48	-1	1	0	1	1	5,41	4,38	4,03	4,61	13,07
49	-1	1	1	-1	-1	6,11	5,53	5,88	5,84	15,31
50	-1	1	1	-1	0	9,56	9,22	9,79	9,52	19,57
51	-1	1	1	-1	1	7,95	6,91	6,57	7,14	16,99
52	-1	1	1	1	-1	6,45	6,91	5,18	6,18	15,62
53	-1	1	1	1	0	6,45	5,99	6,45	6,30	15,97
54	-1	1	1	1	1	6,11	4,61	5,18	5,30	14,31
55	0	-1	-1	-1	-1	12,21	12,21	12,56	12,33	21,81
56	0	-1	-1	-1	0	11,98	12,21	12,44	12,21	21,73
57	0	-1	-1	-1	1	13,36	13,59	13,02	13,32	22,49
58	0	-1	-1	1	-1	10,37	10,71	9,79	10,29	20,23
59	0	-1	-1	1	0	10,25	10,37	11,06	10,56	20,46
60	0	-1	-1	1	1	10,25	10,14	10,71	10,37	20,31
61	0	-1	0	-1	-1	11,98	12,44	12,10	12,17	21,70
62	0	-1	0	-1	0	12,79	14,05	13,82	13,55	22,62
63	0	-1	0	-1	1	11,87	11,98	13,02	12,29	21,77
64	0	-1	0	1	-1	10,71	9,91	9,56	10,06	20,02
65	0	-1	0	1	0	13,02	12,44	12,44	12,63	22,02
66	0	-1	0	1	1	12,44	11,75	12,10	12,10	21,65
67	0	-1	1	-1	-1	12,90	12,44	12,90	12,75	22,10
68	0	-1	1	-1	0	13,48	13,71	13,25	13,48	22,59
69	0	-1	1	-1	1	12,10	13,48	12,90	12,83	22,14
70	0	-1	1	1	-1	11,75	11,29	11,06	11,37	21,10
71	0	-1	1	1	0	12,21	11,98	11,98	12,06	21,62
72	0	-1	1	1	1	11,06	11,75	11,29	11,37	21,10
73	0	0	-1	-1	-1	11,52	11,52	11,75	11,60	21,29
74	0	0	-1	-1	0	7,83	7,83	7,72	7,79	17,83
75	0	0	-1	-1	1	8,41	10,02	10,14	9,52	19,48
76	0	0	-1	1	-1	9,68	10,02	9,68	9,79	19,82

Appendix B.7 Continued

$3^4 2^1$ Full Factorial Design for Flexural Strength										
Exp. Run No	Processing Parameters					Results				
	A	B	C	D	E	Run #1	Run #2	Run #3	μ (Mpa)	S/N ratio
77	0	0	-1	1	0	7,26	7,72	7,83	7,60	17,61
78	0	0	-1	1	1	9,79	10,14	9,91	9,95	19,95
79	0	0	0	-1	-1	10,14	12,67	11,52	11,44	21,06
80	0	0	0	-1	0	8,29	7,60	8,06	7,98	18,03
81	0	0	0	-1	1	4,72	5,30	5,53	5,18	14,23
82	0	0	0	1	-1	10,37	10,48	9,45	10,10	20,06
83	0	0	0	1	0	6,22	7,03	7,37	6,87	16,68
84	0	0	0	1	1	5,41	5,65	5,30	5,45	14,72
85	0	0	1	-1	-1	5,99	5,76	5,07	5,61	14,91
86	0	0	1	-1	0	7,14	6,22	6,91	6,76	16,55
87	0	0	1	-1	1	5,88	5,65	5,76	5,76	15,21
88	0	0	1	1	-1	6,45	6,45	6,11	6,34	16,03
89	0	0	1	1	0	4,84	4,61	5,07	4,84	13,68
90	0	0	1	1	1	5,07	5,18	5,76	5,34	14,51
91	0	1	-1	-1	-1	7,26	6,80	8,64	7,57	17,45
92	0	1	-1	-1	0	7,03	7,37	8,06	7,49	17,44
93	0	1	-1	-1	1	12,9	11,75	11,64	12,10	21,63
94	0	1	-1	1	-1	8,53	8,06	7,95	8,18	18,24
95	0	1	-1	1	0	9,10	8,76	8,64	8,83	18,92
96	0	1	-1	1	1	8,64	8,41	7,37	8,14	18,15
97	0	1	0	-1	-1	11,06	9,68	11,98	10,91	20,65
98	0	1	0	-1	0	10,94	10,14	10,60	10,56	20,46
99	0	1	0	-1	1	11,06	10,14	9,22	10,14	20,05
100	0	1	0	1	-1	7,72	9,33	7,26	8,10	18,03
101	0	1	0	1	0	8,87	7,37	7,83	8,02	18,01
102	0	1	0	1	1	9,10	9,68	8,18	8,99	19,01
103	0	1	1	-1	-1	9,68	10,02	10,60	10,10	20,07
104	0	1	1	-1	0	10,83	10,37	10,02	10,41	20,33
105	0	1	1	-1	1	10,71	11,52	11,06	11,10	20,89
106	0	1	1	1	-1	9,68	8,18	8,18	8,68	18,69
107	0	1	1	1	0	8,18	7,50	8,41	8,03	18,06
108	0	1	1	1	1	8,53	6,91	7,49	7,64	17,57
109	1	-1	-1	-1	-1	14,63	13,13	12,33	13,36	22,45
110	1	-1	-1	-1	0	14,28	13,48	13,36	13,71	22,73
111	1	-1	-1	-1	1	14,05	15,09	13,71	14,28	23,08
112	1	-1	-1	1	-1	9,79	10,83	10,25	10,29	20,23
113	1	-1	-1	1	0	11,52	10,48	10,60	10,87	20,70
114	1	-1	-1	1	1	11,98	11,17	13,36	12,17	21,64

Appendix B.7 Continued

$3^4 2^1$ Full Factorial Design for Flexural Strength										
Exp. Run No	Processing Parameters					Results				
	A	B	C	D	E	Run #1	Run #2	Run #3	μ (Mpa)	S/N ratio
115	1	-1	0	-1	-1	14,28	14,40	13,82	14,17	23,02
116	1	-1	0	-1	0	12,79	13,25	14,75	13,60	22,62
117	1	-1	0	-1	1	14,63	12,79	13,59	13,67	22,68
118	1	-1	0	1	-1	11,40	11,17	10,83	11,13	20,93
119	1	-1	0	1	0	14,17	13,36	12,67	13,40	22,51
120	1	-1	0	1	1	13,02	12,79	11,64	12,48	21,89
121	1	-1	1	-1	-1	13,94	13,82	12,33	13,36	22,48
122	1	-1	1	-1	0	14,40	13,82	13,36	13,86	22,82
123	1	-1	1	-1	1	14,40	14,05	13,59	14,01	22,92
124	1	-1	1	1	-1	11,40	11,75	11,52	11,56	21,25
125	1	-1	1	1	0	13,82	13,25	12,10	13,06	22,28
126	1	-1	1	1	1	11,17	11,40	12,10	11,56	21,24
127	1	0	-1	-1	-1	10,48	11,17	13,48	11,71	21,23
128	1	0	-1	-1	0	11,40	9,56	9,22	10,06	19,94
129	1	0	-1	-1	1	10,83	10,14	8,87	9,95	19,86
130	1	0	-1	1	-1	10,14	9,68	11,87	10,56	20,38
131	1	0	-1	1	0	9,22	8,87	8,29	8,79	18,86
132	1	0	-1	1	1	12,10	12,33	11,4	11,94	21,53
133	1	0	0	-1	-1	11,98	11,29	11,17	11,48	21,19
134	1	0	0	-1	0	9,22	9,68	8,76	9,22	19,27
135	1	0	0	-1	1	5,76	4,61	5,88	5,42	14,51
136	1	0	0	1	-1	9,91	10,83	10,48	10,41	20,33
137	1	0	0	1	0	7,72	7,49	7,03	7,41	17,38
138	1	0	0	1	1	8,18	7,49	5,76	7,14	16,78
139	1	0	1	-1	-1	7,37	6,45	6,91	6,91	16,75
140	1	0	1	-1	0	6,45	5,76	9,10	7,10	16,56
141	1	0	1	-1	1	6,45	6,91	4,95	6,10	15,44
142	1	0	1	1	-1	6,91	7,03	7,03	6,99	16,89
143	1	0	1	1	0	4,61	4,61	5,53	4,92	13,74
144	1	0	1	1	1	6,45	5,99	6,34	6,26	15,92
145	1	1	-1	-1	-1	7,95	7,95	9,91	8,60	18,56
146	1	1	-1	-1	0	12,33	13,25	9,22	11,60	20,96
147	1	1	-1	-1	1	12,33	11,98	12,90	12,40	21,86
148	1	1	-1	1	-1	8,53	8,41	7,72	8,22	18,27
149	1	1	-1	1	0	9,22	8,64	8,76	8,87	18,95
150	1	1	-1	1	1	10,14	9,22	8,76	9,37	19,39
151	1	1	0	-1	-1	11,98	10,25	10,60	10,94	20,73
152	1	1	0	-1	0	15,21	14,28	13,82	14,44	23,17

Appendix B.7 Continued

$3^4 2^1$ Full Factorial Design for Flexural Strength										
Exp. Run No	Processing Parameters					Results				
	A	B	C	D	E	Run #1	Run #2	Run #3	μ (Mpa)	S/N ratio
153	1	1	0	-1	1	14,86	10,02	8,76	11,21	20,37
154	1	1	0	1	-1	11,06	9,68	8,87	9,87	19,78
155	1	1	0	1	0	8,18	8,76	8,53	8,49	18,57
156	1	1	0	1	1	13,82	14,28	11,87	13,32	22,41
157	1	1	1	-1	-1	13,82	14,28	11,87	13,32	22,41
158	1	1	1	-1	0	12,90	10,25	10,60	11,25	20,89
159	1	1	1	-1	1	11,98	13,48	12,44	12,63	22,00
160	1	1	1	1	-1	8,87	9,10	9,22	9,06	19,14
161	1	1	1	1	0	9,91	8,76	10,14	9,60	19,59
162	1	1	1	1	1	9,22	9,56	8,76	9,18	19,24

Appendix B.8 $3^4 2^1$ full factorial design and its results when the response variable is the impact resistance

$3^4 2^1$ Full Factorial Design for Impact Resistance										
Exp. Run No	Processing Parameters					Results				
	A	B	C	D	E	Run #1	Run #2	Run #3	μ (Mpa)	S/N ratio
1	-1	-1	-1	-1	-1	3,8	2,1	2,6	2,83	8,30
2	-1	-1	-1	-1	0	15,8	6,9	4,6	9,10	16,18
3	-1	-1	-1	-1	1	5,9	13,3	7,6	8,93	17,64
4	-1	-1	-1	1	-1	3,5	3,8	4,2	3,83	11,60
5	-1	-1	-1	1	0	4,9	4,8	5,2	4,97	13,91
6	-1	-1	-1	1	1	2,7	5,7	5,7	4,70	11,79
7	-1	-1	0	-1	-1	3,2	4,4	3,0	3,53	10,61
8	-1	-1	0	-1	0	4,2	5,1	4,6	4,63	13,24
9	-1	-1	0	-1	1	4,8	4,2	4,0	4,33	12,66
10	-1	-1	0	1	-1	2,8	3,0	4,0	3,27	9,98
11	-1	-1	0	1	0	5,2	5,7	7,8	6,23	15,52
12	-1	-1	0	1	1	5,5	5,2	5,7	5,47	14,74
13	-1	-1	1	-1	-1	4,2	4,9	5,0	4,70	13,36
14	-1	-1	1	-1	0	4,0	5,9	3,6	4,50	12,51
15	-1	-1	1	-1	1	4,6	3,6	6,2	4,80	13,00
16	-1	-1	1	1	-1	3,0	3,2	2,8	3,00	9,50
17	-1	-1	1	1	0	4,2	3,8	4,6	4,20	12,39
18	-1	-1	1	1	1	3,9	6,8	9,8	6,83	14,87
19	-1	0	-1	-1	-1	3,9	3,4	5,4	4,23	12,06
20	-1	0	-1	-1	0	3,5	2,8	6,2	4,17	11,06
21	-1	0	-1	-1	1	5,9	5,8	7,4	6,37	15,92
22	-1	0	-1	1	-1	2,8	3,0	5,1	3,63	10,34
23	-1	0	-1	1	0	4,8	5,0	3,6	4,47	12,71
24	-1	0	-1	1	1	4,0	7,0	8,0	6,33	14,84
25	-1	0	0	-1	-1	3,6	4,2	4,0	3,93	11,84
26	-1	0	0	-1	0	2,7	3,6	4,9	3,73	10,69
27	-1	0	0	-1	1	4,4	2,4	7,6	4,80	10,92
28	-1	0	0	1	-1	3,2	4,4	3,0	3,53	10,61
29	-1	0	0	1	0	5,2	3,4	4,2	4,27	12,21
30	-1	0	0	1	1	3,0	3,4	2,2	2,87	8,70
31	-1	0	1	-1	-1	5,8	3,2	3,6	4,20	11,66
32	-1	0	1	-1	0	3,6	2,6	2,6	2,93	9,05
33	-1	0	1	-1	1	2,7	6,2	8,2	5,70	12,27
34	-1	0	1	1	-1	4,8	2,4	3,0	3,40	9,61
35	-1	0	1	1	0	2,4	3,6	3,0	3,00	9,19
36	-1	0	1	1	1	7,8	3,2	4,8	5,27	12,80
37	-1	1	-1	-1	-1	4,0	3,6	2,5	3,37	10,00

Appendix B.8 Continued

$3^4 2^1$ Full Factorial Design for Impact Resistance										
Exp. Run No	Processing Parameters					Results				
	A	B	C	D	E	Run #1	Run #2	Run #3	μ (Mpa)	S/N ratio
38	-1	1	-1	-1	0	3,0	7,4	4,2	4,87	12,07
39	-1	1	-1	-1	1	15,6	11,8	3,2	10,20	14,40
40	-1	1	-1	1	-1	6,1	2,8	2,7	3,87	10,12
41	-1	1	-1	1	0	4,5	5,0	5,2	4,90	13,75
42	-1	1	-1	1	1	3,2	4,4	3,0	3,53	10,61
43	-1	1	0	-1	-1	3,8	2,1	3,0	2,97	8,67
44	-1	1	0	-1	0	5,8	6,9	4,0	5,57	14,23
45	-1	1	0	-1	1	4,1	7,7	5,8	5,87	14,51
46	-1	1	0	1	-1	4,2	4,6	4,6	4,47	12,98
47	-1	1	0	1	0	3,0	5,3	2,6	3,63	10,08
48	-1	1	0	1	1	4,6	8,4	3,2	5,40	12,75
49	-1	1	1	-1	-1	2,8	3,0	4,4	3,40	10,14
50	-1	1	1	-1	0	5,9	4,2	7,6	5,90	14,65
51	-1	1	1	-1	1	15,0	8,9	5,4	9,77	17,66
52	-1	1	1	1	-1	4,8	4,4	3,7	4,30	12,52
53	-1	1	1	1	0	6,9	5,2	10,0	7,37	16,45
54	-1	1	1	1	1	3,6	2,8	3,4	3,27	10,13
55	0	-1	-1	-1	-1	4,7	3,0	3,4	3,70	10,92
56	0	-1	-1	-1	0	6,6	5,2	11,9	7,90	16,51
57	0	-1	-1	-1	1	7,6	18,6	16,6	14,27	21,00
58	0	-1	-1	1	-1	5,9	2,9	3,6	4,13	11,25
59	0	-1	-1	1	0	7,6	3,8	6,2	5,87	14,26
60	0	-1	-1	1	1	3,6	3,6	3,2	3,47	10,76
61	0	-1	0	-1	-1	3,6	5,0	3,0	3,87	11,19
62	0	-1	0	-1	0	5,0	8,8	8,6	7,47	16,55
63	0	-1	0	-1	1	5,0	8,2	10,0	7,73	16,65
64	0	-1	0	1	-1	3,2	4,9	2,8	3,63	10,51
65	0	-1	0	1	0	6,4	9,0	5,7	7,03	16,48
66	0	-1	0	1	1	4,2	9,8	4,2	6,07	13,84
67	0	-1	1	-1	-1	5,2	3,0	6,6	4,93	12,44
68	0	-1	1	-1	0	4,9	5,2	4,2	4,77	13,46
69	0	-1	1	-1	1	4,8	4,0	7,6	5,47	13,86
70	0	-1	1	1	-1	12,2	3,8	3,8	6,60	13,15
71	0	-1	1	1	0	4,7	5,5	3,4	4,53	12,60
72	0	-1	1	1	1	10,7	4,0	7,0	7,23	15,15
73	0	0	-1	-1	-1	4,7	4,2	6,1	5,00	13,67
74	0	0	-1	-1	0	12,6	4,6	6,1	7,77	15,72
75	0	0	-1	-1	1	6,8	3,8	18,0	9,53	15,04

Appendix B.8 Continued

$3^4 2^1$ Full Factorial Design for Impact Resistance										
Exp. Run No	Processing Parameters					Results				
	A	B	C	D	E	Run #1	Run #2	Run #3	μ (Mpa)	S/N ratio
76	0	0	-1	1	-1	2,7	2,5	3,3	2,83	8,87
77	0	0	-1	1	0	3,2	8,1	3,4	4,90	11,77
78	0	0	-1	1	1	7,6	4,1	6,2	5,97	14,65
79	0	0	0	-1	-1	3,2	2,6	7,0	4,27	10,52
80	0	0	0	-1	0	13,0	2,5	2,4	5,97	9,46
81	0	0	0	-1	1	2,5	3,2	2,8	2,83	8,91
82	0	0	0	1	-1	4,0	2,8	3,0	3,27	9,98
83	0	0	0	1	0	4,2	7,3	4,2	5,23	13,56
84	0	0	0	1	1	3,4	2,9	6,6	4,30	11,18
85	0	0	1	-1	-1	4,2	4,4	3,8	4,13	12,28
86	0	0	1	-1	0	3,4	10,1	3,8	5,77	12,58
87	0	0	1	-1	1	2,4	4,8	5,2	4,13	10,72
88	0	0	1	1	-1	3,2	3,4	5,2	3,93	11,32
89	0	0	1	1	0	4,6	3,0	3,0	3,53	10,47
90	0	0	1	1	1	4,8	3,0	4,6	4,13	11,72
91	0	1	-1	-1	-1	2,5	3,4	3,2	3,03	9,40
92	0	1	-1	-1	0	7,6	6,1	9,9	7,87	17,42
93	0	1	-1	-1	1	13,4	9,0	8,3	10,23	19,66
94	0	1	-1	1	-1	6,9	3,5	4,0	4,80	12,59
95	0	1	-1	1	0	7,3	7,6	5,7	6,87	16,52
96	0	1	-1	1	1	3,4	9,6	13,4	8,80	14,65
97	0	1	0	-1	-1	3,3	3,4	6,9	4,53	11,78
98	0	1	0	-1	0	4,8	5,7	4,4	4,97	13,77
99	0	1	0	-1	1	16,2	4,0	8,1	9,43	15,66
100	0	1	0	1	-1	4,4	6,8	9,0	6,73	15,45
101	0	1	0	1	0	3,8	6,7	3,4	4,63	12,27
102	0	1	0	1	1	3,4	5,4	5,4	4,73	12,87
103	0	1	1	-1	-1	5,0	8,9	3,6	5,83	13,64
104	0	1	1	-1	0	4,8	6,7	6,9	6,13	15,39
105	0	1	1	-1	1	6,9	6,2	5,9	6,33	15,98
106	0	1	1	1	-1	2,9	2,9	7,2	4,33	10,67
107	0	1	1	1	0	5,9	2,8	4,1	4,27	11,43
108	0	1	1	1	1	6,7	3,3	8,6	6,20	13,71
109	1	-1	-1	-1	-1	4,4	6,2	4,9	5,17	14,00
110	1	-1	-1	-1	0	6,6	6,8	5,5	6,30	15,87
111	1	-1	-1	-1	1	9,2	5,3	5,5	6,67	15,71
112	1	-1	-1	1	-1	5,0	2,4	5,4	4,27	10,83
113	1	-1	-1	1	0	6,8	4,5	5,5	5,60	14,60

Appendix B.8 Continued

$3^4 2^1$ Full Factorial Design for Impact Resistance										
Exp. Run No	Processing Parameters					Results				
	A	B	C	D	E	Run #1	Run #2	Run #3	μ (Mpa)	S/N ratio
114	1	-1	-1	1	1	7,1	8,9	9,0	8,33	18,26
115	1	-1	0	-1	-1	3,6	2,7	4,6	3,63	10,59
116	1	-1	0	-1	0	6,2	4,0	7,0	5,73	14,40
117	1	-1	0	-1	1	5,5	5,7	7,7	6,30	15,7
118	1	-1	0	1	-1	3,0	6,2	4,8	4,67	12,21
119	1	-1	0	1	0	7,0	8,6	7,6	7,73	17,68
120	1	-1	0	1	1	6,8	6,6	18,2	10,53	18,00
121	1	-1	1	-1	-1	4,4	5,0	5,2	4,87	13,68
122	1	-1	1	-1	0	3,4	4,8	7,7	5,30	13,10
123	1	-1	1	-1	1	9,9	8,8	8,6	9,10	19,13
124	1	-1	1	1	-1	2,3	4,0	5,2	3,83	10,17
125	1	-1	1	1	0	5,2	4,8	5,8	5,27	14,35
126	1	-1	1	1	1	5,4	10,2	8,2	7,93	17,08
127	1	0	-1	-1	-1	3,8	3,6	6,4	4,60	12,45
128	1	0	-1	-1	0	5,8	5,8	5,8	5,80	15,27
129	1	0	-1	-1	1	16,8	4,0	7,6	9,47	15,56
130	1	0	-1	1	-1	4,2	2,8	8,2	5,07	11,78
131	1	0	-1	1	0	2,8	3,3	7,9	4,67	11,05
132	1	0	-1	1	1	12,8	3,6	9,7	8,70	15,04
133	1	0	0	-1	-1	5,5	6,2	5,5	5,73	15,13
134	1	0	0	-1	0	3,0	3,6	3,4	3,33	10,38
135	1	0	0	-1	1	9,6	5,5	10,3	8,47	17,50
136	1	0	0	1	-1	3,6	5,9	5,4	4,97	13,30
137	1	0	0	1	0	3,4	3,8	6,6	4,60	12,25
138	1	0	0	1	1	10,6	3,6	18,2	10,8	15,27
139	1	0	1	-1	-1	5,5	6,2	5,9	5,87	15,34
140	1	0	1	-1	0	4,6	5,4	2,8	4,27	11,57
141	1	0	1	-1	1	12,0	7,1	7,6	8,90	18,33
142	1	0	1	1	-1	4,0	4,8	8,0	5,60	13,92
143	1	0	1	1	0	8,6	6,6	6,6	7,27	17,03
144	1	0	1	1	1	8,9	5,4	8,3	7,53	16,89
145	1	1	-1	-1	-1	4,4	3,2	3,2	3,60	10,84
146	1	1	-1	-1	0	3,5	3,2	3,8	3,50	10,82
147	1	1	-1	-1	1	4,2	5,5	10,1	6,60	14,79
148	1	1	-1	1	-1	4,4	3,0	4,2	3,87	11,36
149	1	1	-1	1	0	7,6	5,5	4,0	5,70	14,25
150	1	1	-1	1	1	6,2	10,3	19,4	11,97	18,96
151	1	1	0	-1	-1	7,1	4,7	6,6	6,13	15,32

Appendix B.8 Continued

$3^4 2^1$ Full Factorial Design for Impact Resistance										
Exp. Run No	Processing Parameters					Results				
	A	B	C	D	E	Run #1	Run #2	Run #3	μ (Mpa)	S/N ratio
152	1	1	0	-1	0	9,9	4,4	6,7	7,00	15,52
153	1	1	0	-1	1	3,8	6,2	8,6	6,20	14,41
154	1	1	0	1	-1	2,6	4,6	2,6	3,27	9,42
155	1	1	0	1	0	4,9	3,4	4,0	4,10	11,97
156	1	1	0	1	1	19,8	3,8	6,4	10,00	14,94
157	1	1	1	-1	-1	4,2	3,2	4,4	3,93	11,63
158	1	1	1	-1	0	4,2	5,8	9,0	6,33	14,83
159	1	1	1	-1	1	9,6	5,8	8,8	8,07	17,49
160	1	1	1	1	-1	3,0	4,4	3,2	3,53	10,61
161	1	1	1	1	0	9,7	3,3	6,7	6,57	13,81
162	1	1	1	1	1	4,4	6,1	2,9	4,47	11,82

Appendix B.9 The regression model developed for the mean compressive strength based on the full factorial design with only main factors

The regression equation is

y = 88,1 + 16,9 A - 24,7 B1 - 17,8 B2 - 10,4 C - 9,29 D1 + 2,27 E

Predictor	Coef	SE Coef	T	P
Constant	88,096	1,042	84,52	0,000
A	16,9444	0,6383	26,55	0,000
B1	-24,677	1,277	-19,33	0,000
B2	-17,765	1,277	-13,92	0,000
C	-10,3556	0,6383	-16,22	0,000
D1	-9,289	1,042	-8,91	0,000
E	2,2735	0,6383	3,56	0,000

S = 11,49 R-Sq = 75,3% R-Sq(adj) = 75,0%

Analysis of Variance

Source	DF	SS	MS	F	P
Regression	6	192433	32072	242,99	0,000
Residual Error	479	63223	132		
Total	485	255656			

Source	DF	Seq SS
A	1	93025
B1	1	26940
B2	1	25564
C	1	34745
D1	1	10483
E	1	1675

Unusual Observations

Obs	A	Comp	Fit	SE Fit	Residual	St Resid
64	0,00	99,600	76,534	1,222	23,066	2,02R
109	1,00	88,000	113,123	1,519	-25,123	-2,21R
141	1,00	42,800	72,282	1,519	-29,482	-2,59R
144	1,00	38,400	62,993	1,519	-24,593	-2,16R
148	1,00	51,200	86,069	1,519	-34,869	-3,06R
152	1,00	114,400	87,275	1,222	27,125	2,37R
199	-1,00	34,800	61,469	1,519	-26,669	-2,34R
261	0,00	97,200	72,604	1,222	24,596	2,15R
297	1,00	49,600	82,638	1,379	-33,038	-2,90R
303	1,00	38,800	72,282	1,519	-33,482	-2,94R
310	1,00	54,800	86,069	1,519	-31,269	-2,75R
314	1,00	113,600	87,275	1,222	26,325	2,30R
379	0,00	68,800	96,178	1,379	-27,378	-2,40R
415	0,00	55,600	78,413	1,379	-22,813	-2,00R
418	0,00	46,000	69,124	1,379	-23,124	-2,03R
453	1,00	118,000	92,993	1,519	25,007	2,20R
456	1,00	107,200	83,704	1,519	23,496	2,06R
459	1,00	48,400	82,638	1,379	-34,238	-3,00R
465	1,00	40,400	72,282	1,519	-31,882	-2,80R
472	1,00	57,200	86,069	1,519	-28,869	-2,54R

R denotes an observation with a large standardized residual

Durbin-Watson statistic = 1,43

Appendix B.10 The regression model developed for the mean compressive strength based on the full factorial design with main, interaction and squared factors

The regression equation is

y = 97,0 + 18,6 A - 35,3 B1 - 14,6 B2 - 7,89 C - 9,32 D1 + 6,83 E - 11,3 AA - 1,24 CC - 2,33 EE - 4,51 AC + 1,13 AE - 4,73 CE + 2,85 B1D1 - 1,70 B2D1 - 2,53 AB1 - 11,2 CB1 - 14,0 EB1 + 4,87 AAB1 + 7,01 CCB1 + 3,79 EEB1 + 2,77 ACB1 - 3,42 AEB1 + 1,18 CEB1 + 0,39 AB2 + 2,06 CB2 + 0,99 EB2 + 8,72 AAB2 - 5,39 CCB2 - 3,13 EEB2 + 3,81 ACB2 + 0,77 AEB2 - 0,42 CEB2 - 0,64 AD1 + 3,36 CD1 - 2,88 ED1 - 0,75 AAD1 + 0,81 CCD1 + 3,11 EED1 - 0,90 ACD1 - 3,63 AED1 - 0,08 CED1 - 0,44 AB1D1 - 2,78 CB1D1 + 8,84 EB1D1 + 4,82 AAB1D1 - 6,27 CCB1D1 - 2,17 EEB1D1 + 0,91 ACB1D1 + 6,19 AEB1D1 - 4,11 CEB1D1 - 3,01 AB2D1 - 3,77 CB2D1 - 1,51 EB2D1 + 1,93 AAB2D1 - 3,47 CCB2D1 - 5,94 EEB2D1 - 1,34 ACB2D1 + 4,23 AEB2D1 - 1,37 CEB2D1

Predictor	Coef	SE Coef	T	P
Constant	96,953	2,007	48,30	0,000
A	18,5556	0,9292	19,97	0,000
B1	-35,343	2,839	-12,45	0,000
B2	-14,558	2,839	-5,13	0,000
C	-7,8889	0,9292	-8,49	0,000
D1	-9,321	2,839	-3,28	0,001
E	6,8296	0,9292	7,35	0,000
AA	-11,281	1,609	-7,01	0,000
CC	-1,237	1,609	-0,77	0,443
EE	-2,326	1,609	-1,45	0,149
AC	-4,511	1,138	-3,96	0,000
AE	1,133	1,138	1,00	0,320
CE	-4,733	1,138	-4,16	0,000
B1D1	2,852	4,015	0,71	0,478
B2D1	-1,696	4,015	-0,42	0,673
AB1	-2,533	1,314	-1,93	0,055
CB1	-11,230	1,314	-8,55	0,000
EB1	-14,007	1,314	-10,66	0,000
AAB1	4,874	2,276	2,14	0,033
CCB1	7,007	2,276	3,08	0,002
EEB1	3,785	2,276	1,66	0,097
ACB1	2,767	1,609	1,72	0,086
AEB1	-3,422	1,609	-2,13	0,034
CEB1	1,178	1,609	0,73	0,465
AB2	0,393	1,314	0,30	0,765
CB2	2,059	1,314	1,57	0,118
EB2	0,993	1,314	0,76	0,450
AAB2	8,719	2,276	3,83	0,000
CCB2	-5,393	2,276	-2,37	0,018
EEB2	-3,126	2,276	-1,37	0,170
ACB2	3,811	1,609	2,37	0,018
AEB2	0,767	1,609	0,48	0,634
CEB2	-0,422	1,609	-0,26	0,793
AD1	-0,644	1,314	-0,49	0,624
CD1	3,363	1,314	2,56	0,011
ED1	-2,878	1,314	-2,19	0,029
AAD1	-0,748	2,276	-0,33	0,743
CCD1	0,807	2,276	0,35	0,723
EED1	3,107	2,276	1,37	0,173
ACD1	-0,900	1,609	-0,56	0,576
AED1	-3,628	1,609	-2,25	0,025

Appendix B.10 Continued

CED1	-0,083	1,609	-0,05	0,959
AB1D1	-0,437	1,858	-0,24	0,814
CB1D1	-2,778	1,858	-1,49	0,136
EB1D1	8,841	1,858	4,76	0,000
AAB1D1	4,822	3,219	1,50	0,135
CCB1D1	-6,267	3,219	-1,95	0,052
EEB1D1	-2,167	3,219	-0,67	0,501
ACB1D1	0,911	2,276	0,40	0,689
AEB1D1	6,194	2,276	2,72	0,007
CEB1D1	-4,106	2,276	-1,80	0,072
AB2D1	-3,015	1,858	-1,62	0,105
CB2D1	-3,770	1,858	-2,03	0,043
EB2D1	-1,515	1,858	-0,82	0,415
AAB2D1	1,933	3,219	0,60	0,548
CCB2D1	-3,467	3,219	-1,08	0,282
EEB2D1	-5,944	3,219	-1,85	0,065
ACB2D1	-1,344	2,276	-0,59	0,555
AEB2D1	4,228	2,276	1,86	0,064
CEB2D1	-1,372	2,276	-0,60	0,547

S = 6,828 R-Sq = 92,2% R-Sq(adj) = 91,2%

Analysis of Variance

Source	DF	SS	MS	F	P
Regression	59	235794,3	3996,5	85,72	0,000
Residual Error	426	19861,4	46,6		
Total	485	255655,7			

Source	DF	Seq SS
A	1	93025,0
B1	1	26940,1
B2	1	25564,5
C	1	34745,0
D1	1	10483,4
E	1	1674,6
AA	1	3886,4
CC	1	397,0
EE	1	391,7
AC	1	1743,1
AE	1	6,3
CE	1	6383,1
B1D1	1	386,8
B2D1	1	904,0
AB1	1	346,7
CB1	1	11623,0
EB1	1	6780,9
AAB1	1	143,2
CCB1	1	1327,4
EEB1	1	793,8
ACB1	1	131,1
AEB1	1	149,6
CEB1	1	4,9
AB2	1	67,1
CB2	1	1,6
EB2	1	3,0
AAB2	1	1688,5
CCB2	1	914,0
EEB2	1	669,4
ACB2	1	354,7

Appendix B.10 Continued

AEB2	1	298,7
CEB2	1	44,2
AD1	1	261,0
CD1	1	112,8
ED1	1	15,4
AAD1	1	61,1
CCD1	1	160,4
EED1	1	4,4
ACD1	1	58,9
AED1	1	1,3
CED1	1	196,8
AB1D1	1	20,6
CB1D1	1	14,3
EB1D1	1	1658,2
AAB1D1	1	89,2
CCB1D1	1	123,3
EEB1D1	1	3,9
ACB1D1	1	30,1
AEB1D1	1	199,8
CEB1D1	1	140,3
AB2D1	1	122,7
CB2D1	1	191,9
EB2D1	1	31,0
AAB2D1	1	16,8
CCB2D1	1	54,1
EEB2D1	1	159,0
ACB2D1	1	16,3
AEB2D1	1	160,9
CEB2D1	1	16,9

Unusual Observations

Obs	A	Comp	Fit	SE Fit	Residual	St Resid
48	-1,00	34,000	47,352	2,307	-13,352	-2,08R
64	0,00	99,600	84,462	2,007	15,138	2,32R
119	1,00	77,600	93,514	2,007	-15,914	-2,44R
138	1,00	87,200	69,211	2,307	17,989	2,80R
148	1,00	51,200	64,352	2,813	-13,152	-2,11R
152	1,00	114,400	98,780	2,007	15,620	2,39R
210	-1,00	32,000	47,352	2,307	-15,352	-2,39R
278	1,00	121,600	104,227	2,007	17,373	2,66R
297	1,00	49,600	63,217	2,307	-13,617	-2,12R
314	1,00	113,600	98,780	2,007	14,820	2,27R
369	-1,00	43,200	61,354	2,307	-18,154	-2,82R
372	-1,00	34,400	47,352	2,307	-12,952	-2,02R
378	-1,00	40,800	28,159	2,813	12,641	2,03R
379	0,00	68,800	89,716	2,307	-20,916	-3,25R
385	0,00	101,600	87,798	2,007	13,802	2,11R
424	0,00	73,600	59,659	2,007	13,941	2,14R
431	0,00	42,000	55,852	2,007	-13,852	-2,12R
440	1,00	89,600	104,227	2,007	-14,627	-2,24R
452	1,00	76,800	97,858	2,307	-21,058	-3,28R
453	1,00	118,000	93,406	2,813	24,594	3,95R
459	1,00	48,400	63,217	2,307	-14,817	-2,31R
470	1,00	111,600	98,680	2,307	12,920	2,01R
471	1,00	90,400	108,106	2,813	-17,706	-2,85R

R denotes an observation with a large standardized residual

Durbin-Watson statistic = 2,17

Appendix B.11 The best regression model developed for the mean compressive strength based on the full factorial design

The regression equation is

y = 96,3 + 18,7 A - 34,4 B1 - 13,7 B2 - 7,89 C - 8,09 D1 + 6,83 E - 11,8 AA - 0,37 CC - 1,78 EE - 4,96 AC + 1,13 AE - 4,94 CE + 0,90 B1D1 - 3,44 B2D1 - 2,75 AB1 - 11,2 CB1 - 14,0 EB1 + 5,36 AAB1 + 6,14 CCB1 + 2,70 EEB1 + 3,22 ACB1 - 3,42 AEB1 + 1,39 CEB1 + 0,28 AB2 + 2,06 CB2 + 0,99 EB2 + 9,69 AAB2 - 7,13 CCB2 - 3,67 EEB2 + 3,14 ACB2 + 0,77 AEB2 - 0,863 AD1 + 3,36 CD1 - 2,88 ED1 + 0,22 AAD1 - 0,93 CCD1 + 2,02 EED1 - 3,63 AED1 - 0,77 CED1 - 2,78 CB1D1 + 8,84 EB1D1 + 3,86 AAB1D1 - 4,53 CCB1D1 + 6,19 AEB1D1 - 3,42 CEB1D1 - 2,80 AB2D1 - 3,77 CB2D1 - 1,51 EB2D1 - 4,86 EEB2D1 + 4,23 AEB2D1

Predictor	Coef	SE Coef	T	P
Constant	96,336	1,772	54,36	0,000
A	18,6648	0,8015	23,29	0,000
B1	-34,365	2,506	-13,71	0,000
B2	-13,686	2,329	-5,88	0,000
C	-7,8889	0,9255	-8,52	0,000
D1	-8,088	2,137	-3,78	0,000
E	6,8296	0,9255	7,38	0,000
AA	-11,765	1,388	-8,47	0,000
CC	-0,370	1,388	-0,27	0,790
EE	-1,784	1,388	-1,29	0,199
AC	-4,9611	0,8015	-6,19	0,000
AE	1,133	1,134	1,00	0,318
CE	-4,9444	0,8015	-6,17	0,000
B1D1	0,896	3,023	0,30	0,767
B2D1	-3,441	2,390	-1,44	0,151
AB1	-2,7519	0,9255	-2,97	0,003
CB1	-11,230	1,309	-8,58	0,000
EB1	-14,007	1,309	-10,70	0,000
AAB1	5,357	2,121	2,53	0,012
CCB1	6,141	2,121	2,90	0,004
EEB1	2,702	1,603	1,69	0,093
ACB1	3,222	1,134	2,84	0,005
AEB1	-3,422	1,603	-2,13	0,033
CEB1	1,389	1,388	1,00	0,318
AB2	0,283	1,224	0,23	0,817
CB2	2,059	1,309	1,57	0,116
EB2	0,993	1,309	0,76	0,449
AAB2	9,685	1,603	6,04	0,000
CCB2	-7,126	1,603	-4,45	0,000
EEB2	-3,668	2,121	-1,73	0,084
ACB2	3,139	1,134	2,77	0,006
AEB2	0,767	1,603	0,48	0,633
AD1	-0,8630	0,9255	-0,93	0,352
CD1	3,363	1,309	2,57	0,011
ED1	-2,878	1,309	-2,20	0,028
AAD1	0,219	1,603	0,14	0,892
CCD1	-0,926	1,603	-0,58	0,564
EED1	2,024	1,603	1,26	0,207
AED1	-3,628	1,603	-2,26	0,024
CED1	-0,769	1,134	-0,68	0,498
CB1D1	-2,778	1,851	-1,50	0,134
EB1D1	8,841	1,851	4,78	0,000
AAB1D1	3,856	2,777	1,39	0,166
CCB1D1	-4,533	2,777	-1,63	0,103

Appendix B.11 Continued

AEB1D1	6,194	2,267	2,73	0,007
CEB1D1	-3,419	1,963	-1,74	0,082
AB2D1	-2,796	1,603	-1,74	0,082
CB2D1	-3,770	1,851	-2,04	0,042
EB2D1	-1,515	1,851	-0,82	0,414
EEB2D1	-4,861	2,777	-1,75	0,081
AEB2D1	4,228	2,267	1,86	0,063

S = 6,801 R-Sq = 92,1% R-Sq(adj) = 91,2%

Analysis of Variance

Source	DF	SS	MS	F	P
Regression	50	235533,3	4710,7	101,83	0,000
Residual Error	435	20122,4	46,3		
Total	485	255655,7			

Source	DF	Seq SS
A	1	93025,0
B1	1	26940,1
B2	1	25564,5
C	1	34745,0
D1	1	10483,4
E	1	1674,6
AA	1	3886,4
CC	1	397,0
EE	1	391,7
AC	1	1743,1
AE	1	6,3
CE	1	6383,1
B1D1	1	386,8
B2D1	1	904,0
AB1	1	346,7
CB1	1	11623,0
EB1	1	6780,9
AAB1	1	143,2
CCB1	1	1327,4
EEB1	1	793,8
ACB1	1	131,1
AEB1	1	149,6
CEB1	1	4,9
AB2	1	67,1
CB2	1	1,6
EB2	1	3,0
AAB2	1	1688,5
CCB2	1	914,0
EEB2	1	669,4
ACB2	1	354,7
AEB2	1	298,7
AD1	1	261,0
CD1	1	112,8
ED1	1	15,4
AAD1	1	61,1
CCD1	1	160,4
EED1	1	4,4
AED1	1	1,3
CED1	1	196,8
CB1D1	1	14,3
EB1D1	1	1658,2
AAB1D1	1	89,2

Appendix B.11 Continued

```
CCB1D1        1       123,3
AEB1D1        1       199,8
CEB1D1        1       140,3
AB2D1         1       140,7
CB2D1         1       191,9
EB2D1         1        31,0
EEB2D1        1       141,8
AEB2D1        1       160,9

Unusual Observations
Obs        A       Comp          Fit      SE Fit    Residual      St Resid
 64     0,00     99,600       84,537       1,832      15,063        2,30R
109     1,00     88,000      101,024       2,478     -13,024       -2,06R
119     1,00     77,600       94,504       1,772     -16,904       -2,57R
138     1,00     87,200       69,501       2,235      17,699        2,76R
148     1,00     51,200       64,255       2,535     -13,055       -2,07R
152     1,00    114,400       99,519       1,908      14,881        2,28R
210    -1,00     32,000       46,613       2,219     -14,613       -2,27R
255     0,00    101,600       88,299       2,070      13,301        2,05R
278     1,00    121,600      103,236       1,772      18,364        2,80R
297     1,00     49,600       62,927       2,235     -13,327       -2,07R
314     1,00    113,600       99,519       1,908      14,081        2,16R
369    -1,00     43,200       62,093       2,219     -18,893       -2,94R
378    -1,00     40,800       28,062       2,535      12,738        2,02R
379     0,00     68,800       90,297       2,052     -21,497       -3,32R
385     0,00    101,600       87,723       1,832      13,877        2,12R
424     0,00     73,600       59,404       1,851      14,196        2,17R
431     0,00     42,000       56,463       1,908     -14,463       -2,22R
440     1,00     89,600      103,236       1,772     -13,636       -2,08R
452     1,00     76,800       98,104       2,035     -21,304       -3,28R
453     1,00    118,000       93,111       2,631      24,889        3,97R
459     1,00     48,400       62,927       2,235     -14,527       -2,26R
471     1,00     90,400      108,890       2,535     -18,490       -2,93R

R denotes an observation with a large standardized residual

Durbin-Watson statistic = 2,14
```

APPENDIX C

Appendix C.1 The regression model developed for the mean flexural strength based on the L_{27} (3^{13}) design with only main factors

The regression equation is

y = 11,8 + 2,12 A - 3,78 B1 - 2,16 B2 - 0,323 C - 1,48 D1 - 0,019 E

Predictor	Coef	SE Coef	T	P
Constant	11,8309	0,6337	18,67	0,000
A	2,1239	0,4150	5,12	0,000
B1	-3,7825	0,8301	-4,56	0,000
B2	-2,1570	0,8301	-2,60	0,017
C	-0,3234	0,4150	-0,78	0,445
D1	-1,4786	0,7192	-2,06	0,053
E	-0,0194	0,4301	-0,05	0,965

S = 1,758 R-Sq = 72,2% R-Sq(adj) = 63,9%

Analysis of Variance

Source	DF	SS	MS	F	P
Regression	6	160,899	26,816	8,68	0,000
Residual Error	20	61,803	3,090		
Total	26	222,702			

Source	DF	Seq SS
A	1	81,111
B1	1	43,836
B2	1	20,895
C	1	1,895
D1	1	13,156
E	1	0,006

Unusual Observations

Obs	A	MEAN2	Fit	SE Fit	Residual	St Resid
16	0,00	11,597	8,391	0,851	3,205	2,08R

R denotes an observation with a large standardized residual

Durbin-Watson statistic = 2,18

Appendix C.2 The regression model developed for the mean flexural strength based on the L_{27} (3^{13}) design with main and interaction factors

The regression equation is

y = 12,8 + 1,97 A - 5,09 B1 - 3,42 B2 + 0,006 C - 3,74 D1 + 0,175 E + 1,21 AC - 0,96 AE - 1,32 CE + 3,23 B1D1 + 3,10 B2D1 + 0,304 AB1 - 1,66 CB1 - 1,63 EB1 - 2,38 ACB1 + 0,40 AEB1 + 2,15 CEB1 + 1,61 AB2 + 0,63 CB2 + 0,24 EB2 - 1,11 AD1 + 0,40 CD1

Predictor	Coef	SE Coef	T	P
Constant	12,8153	0,6130	20,91	0,000
A	1,970	1,340	1,47	0,215
B1	-5,0929	0,8064	-6,32	0,003
B2	-3,4240	0,9730	-3,52	0,024
C	0,0056	0,8045	0,01	0,995
D1	-3,736	1,308	-2,86	0,046
E	0,1752	0,9115	0,19	0,857
AC	1,210	1,518	0,80	0,470
AE	-0,961	1,253	-0,77	0,486
CE	-1,322	1,196	-1,11	0,331
B1D1	3,235	1,628	1,99	0,118
B2D1	3,105	2,318	1,34	0,251
AB1	0,3042	0,9178	0,33	0,757
CB1	-1,6630	0,9448	-1,76	0,153
EB1	-1,628	1,212	-1,34	0,250
ACB1	-2,381	2,746	-0,87	0,435
AEB1	0,398	1,157	0,34	0,748
CEB1	2,151	1,251	1,72	0,161
AB2	1,611	1,848	0,87	0,432
CB2	0,627	1,098	0,57	0,598
EB2	0,243	1,726	0,14	0,895
AD1	-1,106	1,839	-0,60	0,580
CD1	0,397	1,464	0,27	0,800

S = 1,237 R-Sq = 97,3% R-Sq(adj) = 82,1%

Analysis of Variance

Source	DF	SS	MS	F	P
Regression	22	216,584	9,845	6,44	0,041
Residual Error	4	6,117	1,529		
Total	26	222,702			

Source	DF	Seq SS
A	1	81,111
B1	1	43,836
B2	1	20,895
C	1	1,895
D1	1	13,156
E	1	0,006
AC	1	1,458
AE	1	0,765
CE	1	0,069
B1D1	1	2,661
B2D1	1	0,387
AB1	1	0,300
CB1	1	18,248
EB1	1	11,533
ACB1	1	3,265
AEB1	1	0,071

Appendix C.2 Continued

```
CEB1           1       5,816
AB2            1       6,630
CB2            1       1,512
EB2            1       1,912
AD1            1       0,946
CD1            1       0,112

Unusual Observations
Obs       A      MEAN2          Fit      SE Fit    Residual      St Resid
  4  -1,00      6,143       6,143       1,237      -0,000           * X
 18   0,00      5,337       5,337       1,237      -0,000           * X
 20   1,00     10,407      10,407       1,237      -0,000           * X
 22   1,00      8,217       8,217       1,237      -0,000           * X
 27   1,00     11,557      11,557       1,237      -0,000           * X

X denotes an observation whose X value gives it large influence.

Durbin-Watson statistic = 2,22
```

Appendix C.3 The best regression model developed for the mean flexural strength based on the L_{27} (3^{13}) design

```
The regression equation is

y = 12,8 + 2,58 A - 5,07 B1 - 3,31 B2 + 0,375 C - 3,90 D1 + 0,048 E +
     1,73 AC - 1,30 AE - 0,83 CE + 3,41 B1D1 + 2,98 B2D1 + 0,171 AB1 -
     1,86 CB1 - 1,80 EB1 - 3,53 ACB1 + 1,54 CEB1 + 1,03 AB2 - 0,39 ACB2
     - 2,00 AD1 + 0,65 ED1

Predictor        Coef     SE Coef          T        P
Constant      12,7944      0,5026      25,46    0,000
A              2,5760      0,9152       2,81    0,031
B1            -5,0743      0,6664      -7,61    0,000
B2            -3,3080      0,8443      -3,92    0,008
C              0,3751      0,3160       1,19    0,280
D1            -3,8992      0,9838      -3,96    0,007
E              0,0485      0,5957       0,08    0,938
AC             1,7290      0,8888       1,95    0,100
AE            -1,3020      0,9337      -1,39    0,213
CE             -0,829       1,016      -0,82    0,445
B1D1            3,405       1,274       2,67    0,037
B2D1            2,983       1,775       1,68    0,144
AB1            0,1710      0,7135       0,24    0,819
CB1            -1,8603      0,5831      -3,19    0,019
EB1            -1,8024      0,6871      -2,62    0,039
ACB1            -3,534       1,425      -2,48    0,048
CEB1             1,540       1,629       0,95    0,381
AB2              1,034       1,059       0,98    0,367
ACB2            -0,387       1,566      -0,25    0,813
AD1             -1,999       1,063      -1,88    0,109
ED1              0,654       1,234       0,53    0,615

S = 1,048       R-Sq = 97,0%     R-Sq(adj) = 87,2%

Analysis of Variance

Source            DF          SS          MS         F        P
Regression        20     216,116      10,806      9,84    0,005
Residual Error     6       6,586       1,098
Total             26     222,702

Source       DF      Seq SS
A             1      81,111
B1            1      43,836
B2            1      20,895
C             1       1,895
D1            1      13,156
E             1       0,006
AC            1       1,458
AE            1       0,765
CE            1       0,069
B1D1          1       2,661
B2D1          1       0,387
AB1           1       0,300
CB1           1      18,248
EB1           1      11,533
ACB1          1       3,265
```

Appendix C.3 Continued

```
CEB1           1       5,471
AB2            1       7,007
ACB2           1       0,064
AD1            1       3,679
ED1            1       0,309

Unusual Observations
Obs        A      MEAN2         Fit      SE Fit    Residual     St Resid
 10    0,00       7,487       9,111       0,752      -1,625       -2,23R
 23    1,00      14,437      13,096       0,815       1,341        2,04R

R denotes an observation with a large standardized residual

Durbin-Watson statistic = 2,15
```

Appendix C.4 The regression model developed for the mean flexural strength based on the full factorial design with only main factors

The regression equation is

y = 11,8 + 1,90 A - 3,89 B1 - 2,36 B2 - 0,427 C - 1,33 D1 - 0,0586 E

Predictor	Coef	SE Coef	T	P
Constant	11,7848	0,1487	79,23	0,000
A	1,89824	0,09109	20,84	0,000
B1	-3,8885	0,1822	-21,34	0,000
B2	-2,3556	0,1822	-12,93	0,000
C	-0,42704	0,09109	-4,69	0,000
D1	-1,3294	0,1487	-8,94	0,000
E	-0,05858	0,09109	-0,64	0,520

S = 1,640 R-Sq = 67,6% R-Sq(adj) = 67,2%

Analysis of Variance

Source	DF	SS	MS	F	P
Regression	6	2685,44	447,57	166,49	0,000
Residual Error	479	1287,67	2,69		
Total	485	3973,11			

Source	DF	Seq SS
A	1	1167,48
B1	1	793,60
B2	1	449,44
C	1	59,08
D1	1	214,74
E	1	1,11

Unusual Observations

Obs	A	Flex	Fit	SE Fit	Residual	St Resid
4	-1,00	5,4100	9,0427	0,2168	-3,6327	-2,24R
82	0,00	10,3700	6,6254	0,1744	3,7446	2,30R
132	1,00	12,1000	8,8335	0,2168	3,2665	2,01R
135	1,00	5,7600	9,7359	0,1968	-3,9759	-2,44R
143	1,00	4,6100	8,0380	0,1968	-3,4280	-2,11R
145	1,00	7,9500	11,8131	0,2168	-3,8631	-2,38R
152	1,00	15,2100	11,3275	0,1744	3,8825	2,38R
153	1,00	14,8600	11,2689	0,1968	3,5911	2,21R
156	1,00	13,8200	9,9395	0,1968	3,8805	2,38R
241	0,00	12,6700	7,9548	0,1744	4,7152	2,89R
244	0,00	10,4800	6,6254	0,1744	3,8546	2,36R
294	1,00	12,3300	8,8335	0,2168	3,4965	2,15R
297	1,00	4,6100	9,7359	0,1968	-5,1259	-3,15R
302	1,00	5,7600	9,3675	0,1968	-3,6075	-2,22R
305	1,00	4,6100	8,0380	0,1968	-3,4280	-2,11R
307	1,00	7,9500	11,8131	0,2168	-3,8631	-2,38R
318	1,00	14,2800	9,9395	0,1968	4,3405	2,67R
319	1,00	14,2800	10,9590	0,2168	3,3210	2,04R
329	-1,00	4,9500	8,9841	0,1968	-4,0341	-2,48R
367	-1,00	3,6900	7,5896	0,1968	-3,8996	-2,40R
397	0,00	11,7500	8,3819	0,1968	3,3681	2,07R
403	0,00	11,5200	7,9548	0,1744	3,5652	2,19R
459	1,00	5,8800	9,7359	0,1968	-3,8559	-2,37R
465	1,00	4,9500	9,3089	0,2168	-4,3589	-2,68R

R denotes an observation with a large standardized residual

Durbin-Watson statistic = 1,45

Appendix C.5 The regression model developed for the mean flexural strength based on the full factorial design with main, interaction and squared factors

The regression equation is

y = 12,8 + 2,23 A - 5,13 B1 - 2,54 B2 - 0,041 C - 0,895 D1 + 0,201 E - 1,22 AA - 0,015 CC - 0,073 EE + 0,141 AC - 0,022 AE - 0,025 CE - 0,184 B1D1 - 1,14 B2D1 - 0,855 AB1 - 1,80 CB1 - 1,45 EB1 + 0,545 AAB1 - 0,166 CCB1 + 0,647 EEB1 - 0,219 ACB1 - 0,221 AEB1 + 0,288 CEB1 + 0,154 AB2 + 0,553 CB2 + 0,652 EB2 + 0,619 AAB2 - 0,002 CCB2 - 0,289 EEB2 + 0,229 ACB2 - 0,297 AEB2 - 0,848 CEB2 - 0,217 AD1 + 0,609 CD1 + 0,192 ED1 - 0,158 AAD1 - 0,575 CCD1 - 0,439 EED1 - 0,221 ACD1 + 0,148 AED1 - 0,246 CED1 + 0,370 AB1D1 - 0,474 CB1D1 + 0,287 EB1D1 + 0,211 AAB1D1 + 0,757 CCB1D1 + 0,980 EEB1D1 - 0,239 ACB1D1 + 0,360 AEB1D1 - 0,327 CEB1D1 - 0,298 AB2D1 - 1,18 CB2D1 - 0,819 EB2D1 + 0,154 AAB2D1 + 0,437 CCB2D1 + 1,01 EEB2D1 + 0,108 ACB2D1 + 0,604 AEB2D1 + 0,768 CEB2D1

Predictor	Coef	SE Coef	T	P
Constant	12,8290	0,3257	39,39	0,000
A	2,2285	0,1508	14,78	0,000
B1	-5,1291	0,4606	-11,14	0,000
B2	-2,5362	0,4606	-5,51	0,000
C	-0,0409	0,1508	-0,27	0,786
D1	-0,8946	0,4606	-1,94	0,053
E	0,2006	0,1508	1,33	0,184
AA	-1,2181	0,2611	-4,66	0,000
CC	-0,0154	0,2611	-0,06	0,953
EE	-0,0731	0,2611	-0,28	0,780
AC	0,1414	0,1847	0,77	0,444
AE	-0,0225	0,1847	-0,12	0,903
CE	-0,0253	0,1847	-0,14	0,891
B1D1	-0,1836	0,6514	-0,28	0,778
B2D1	-1,1428	0,6514	-1,75	0,080
AB1	-0,8550	0,2132	-4,01	0,000
CB1	-1,7957	0,2132	-8,42	0,000
EB1	-1,4520	0,2132	-6,81	0,000
AAB1	0,5446	0,3693	1,47	0,141
CCB1	-0,1665	0,3693	-0,45	0,652
EEB1	0,6469	0,3693	1,75	0,081
ACB1	-0,2186	0,2611	-0,84	0,403
AEB1	-0,2206	0,2611	-0,84	0,399
CEB1	0,2881	0,2611	1,10	0,271
AB2	0,1541	0,2132	0,72	0,470
CB2	0,5528	0,2132	2,59	0,010
EB2	0,6524	0,2132	3,06	0,002
AAB2	0,6185	0,3693	1,67	0,095
CCB2	-0,0020	0,3693	-0,01	0,996
EEB2	-0,2887	0,3693	-0,78	0,435
ACB2	0,2286	0,2611	0,88	0,382
AEB2	-0,2969	0,2611	-1,14	0,256
CEB2	-0,8481	0,2611	-3,25	0,001
AD1	-0,2172	0,2132	-1,02	0,309
CD1	0,6087	0,2132	2,85	0,005
ED1	0,1920	0,2132	0,90	0,368
AAD1	-0,1580	0,3693	-0,43	0,669
CCD1	-0,5746	0,3693	-1,56	0,120
EED1	-0,4391	0,3693	-1,19	0,235
ACD1	-0,2214	0,2611	-0,85	0,397
AED1	0,1481	0,2611	0,57	0,571
CED1	-0,2464	0,2611	-0,94	0,346

Appendix C.5 Continued

AB1D1	0,3696	0,3015	1,23	0,221
CB1D1	-0,4743	0,3015	-1,57	0,117
EB1D1	0,2874	0,3015	0,95	0,341
AAB1D1	0,2107	0,5223	0,40	0,687
CCB1D1	0,7569	0,5223	1,45	0,148
EEB1D1	0,9796	0,5223	1,88	0,061
ACB1D1	-0,2394	0,3693	-0,65	0,517
AEB1D1	0,3597	0,3693	0,97	0,331
CEB1D1	-0,3267	0,3693	-0,88	0,377
AB2D1	-0,2978	0,3015	-0,99	0,324
CB2D1	-1,1826	0,3015	-3,92	0,000
EB2D1	-0,8191	0,3015	-2,72	0,007
AAB2D1	0,1541	0,5223	0,29	0,768
CCB2D1	0,4374	0,5223	0,84	0,403
EEB2D1	1,0091	0,5223	1,93	0,054
ACB2D1	0,1078	0,3693	0,29	0,771
AEB2D1	0,6036	0,3693	1,63	0,103
CEB2D1	0,7683	0,3693	2,08	0,038

S = 1,108 R-Sq = 86,8% R-Sq(adj) = 85,0%

Analysis of Variance

Source	DF	SS	MS	F	P
Regression	59	3450,165	58,477	47,64	0,000
Residual Error	426	522,946	1,228		
Total	485	3973,111			

Source	DF	Seq SS
A	1	1167,475
B1	1	793,596
B2	1	449,440
C	1	59,085
D1	1	214,735
E	1	1,112
AA	1	77,775
CC	1	2,758
EE	1	2,701
AC	1	0,032
AE	1	0,338
CE	1	14,774
B1D1	1	35,861
B2D1	1	0,116
AB1	1	32,589
CB1	1	291,933
EB1	1	147,185
AAB1	1	2,192
CCB1	1	0,258
EEB1	1	25,400
ACB1	1	11,040
AEB1	1	0,089
CEB1	1	6,106
AB2	1	0,001
CB2	1	0,080
EB2	1	3,185
AAB2	1	8,708
CCB2	1	0,845
EEB2	1	0,839
ACB2	1	2,873
AEB2	1	0,001

Appendix C.5 Continued

```
CEB2          1       7,747
AD1           1       3,026
CD1           1       0,258
ED1           1       0,018
AAD1          1       0,036
CCD1          1       0,842
EED1          1       1,353
ACD1          1       3,800
AED1          1      11,886
CED1          1       0,531
AB1D1         1       4,840
CB1D1         1       0,247
EB1D1         1       8,743
AAB1D1        1       0,107
CCB1D1        1       1,738
EEB1D1        1       1,354
ACB1D1        1       1,033
AEB1D1        1       0,040
CEB1D1        1       6,063
AB2D1         1       1,197
CB2D1         1      18,880
EB2D1         1       9,057
AAB2D1        1       0,107
CCB2D1        1       0,861
EEB2D1        1       4,582
ACB2D1        1       0,105
AEB2D1        1       3,279
CEB2D1        1       5,313

Unusual Observations
Obs      A       Flex         Fit       SE Fit    Residual     St Resid
 21   -1,00     8,7600      6,5329      0,4565      2,2271        2,21R
 47   -1,00     3,4600      5,7843      0,3257     -2,3243       -2,19R
 50   -1,00     9,5600      7,4351      0,3744      2,1249        2,04R
 81    0,00     4,7200      7,0221      0,3257     -2,3021       -2,17R
 92    0,00     7,0300      9,7636      0,3257     -2,7336       -2,58R
152    1,00    15,2100     12,0758      0,3257      3,1342        2,96R
153    1,00    14,8600     12,2475      0,3744      2,6125        2,51R
156    1,00    13,8200     10,3858      0,3744      3,4342        3,29R
168   -1,00     9,9100      7,3357      0,4565      2,5743        2,55R
241    0,00    12,6700      9,5251      0,3257      3,1449        2,97R
254    0,00     7,3700      9,7636      0,3257     -2,3936       -2,26R
297    1,00     4,6100      7,4790      0,3744     -2,8690       -2,75R
314    1,00    14,2800     12,0758      0,3257      2,2042        2,08R
315    1,00    10,0200     12,2475      0,3744     -2,2275       -2,14R
318    1,00    14,2800     10,3858      0,3744      3,8942        3,73R
320    1,00    10,2500     12,9402      0,3744     -2,6902       -2,58R
329   -1,00     4,9500      7,3093      0,3744     -2,3593       -2,26R
336   -1,00     5,8800      8,3019      0,3744     -2,4219       -2,32R
367   -1,00     3,6900      5,7764      0,3744     -2,0864       -2,00R
374   -1,00     9,7900      7,4351      0,3744      2,3549        2,26R
409    0,00     5,0700      7,2438      0,3744     -2,1738       -2,08R
421    0,00    11,9800      9,0780      0,3257      2,9020        2,74R
462    1,00     5,7600      8,1339      0,3744     -2,3739       -2,28R
464    1,00     9,1000      6,3041      0,3744      2,7959        2,68R
477    1,00     8,7600     12,2475      0,3744     -3,4875       -3,34R
482    1,00    10,6000     12,9402      0,3744     -2,3402       -2,24R

R denotes an observation with a large standardized residual

Durbin-Watson statistic = 2,18
```

Appendix C.6 The best regression model developed for the mean flexural strength based on the full factorial design

The regression equation is

y = 12,9 + 2,23 A - 5,20 B1 - 2,59 B2 - 0,041 C - 1,15 D1 + 0,201 E - 1,30 AA - 0,016 CC - 0,073 EE + 0,163 AC - 0,133 AE + 0,056 CE + 0,103 B1D1 - 0,749 B2D1 - 0,855 AB1 - 1,80 CB1 - 1,45 EB1 + 0,650 AAB1 - 0,165 CCB1 + 0,647 EEB1 - 0,338 ACB1 + 0,125 CEB1 + 0,154 AB2 + 0,553 CB2 + 0,652 EB2 + 0,696 AAB2 - 0,289 EEB2 + 0,282 ACB2 - 0,187 AEB2 - 0,930 CEB2 - 0,217 AD1 + 0,609 CD1 + 0,192 ED1 - 0,356 CCD1 - 0,439 EED1 - 0,265 ACD1 + 0,328 AED1 - 0,410 CED1 + 0,370 AB1D1 - 0,474 CB1D1 + 0,287 EB1D1 + 0,538 CCB1D1 + 0,980 EEB1D1 - 0,298 AB2D1 - 1,18 CB2D1 - 0,819 EB2D1 + 1,01 EEB2D1 + 0,424 AEB2D1 + 0,932 CEB2D1

Predictor	Coef	SE Coef	T	P
Constant	12,8823	0,2735	47,11	0,000
A	2,2285	0,1498	14,88	0,000
B1	-5,2001	0,4056	-12,82	0,000
B2	-2,5889	0,3459	-7,48	0,000
C	-0,0409	0,1498	-0,27	0,785
D1	-1,1457	0,3459	-3,31	0,001
E	0,2006	0,1498	1,34	0,181
AA	-1,2971	0,1834	-7,07	0,000
CC	-0,0164	0,1834	-0,09	0,929
EE	-0,0731	0,2594	-0,28	0,778
AC	0,1633	0,1498	1,09	0,276
AE	-0,1328	0,1297	-1,02	0,307
CE	0,0564	0,1589	0,35	0,723
B1D1	0,1027	0,5189	0,20	0,843
B2D1	-0,7485	0,4237	-1,77	0,078
AB1	-0,8550	0,2118	-4,04	0,000
CB1	-1,7957	0,2118	-8,48	0,000
EB1	-1,4520	0,2118	-6,85	0,000
AAB1	0,6500	0,2594	2,51	0,013
CCB1	-0,1655	0,3177	-0,52	0,603
EEB1	0,6469	0,3669	1,76	0,079
ACB1	-0,3383	0,1834	-1,84	0,066
CEB1	0,1247	0,1834	0,68	0,497
AB2	0,1541	0,2118	0,73	0,467
CB2	0,5528	0,2118	2,61	0,009
EB2	0,6524	0,2118	3,08	0,002
AAB2	0,6956	0,2594	2,68	0,008
EEB2	-0,2887	0,3669	-0,79	0,432
ACB2	0,2825	0,1834	1,54	0,124
AEB2	-0,1867	0,2247	-0,83	0,407
CEB2	-0,9297	0,2427	-3,83	0,000
AD1	-0,2172	0,2118	-1,03	0,306
CD1	0,6087	0,2118	2,87	0,004
ED1	0,1920	0,2118	0,91	0,365
CCD1	-0,3559	0,2594	-1,37	0,171
EED1	-0,4391	0,3669	-1,20	0,232
ACD1	-0,2653	0,1498	-1,77	0,077
AED1	0,3279	0,1834	1,79	0,075
CED1	-0,4097	0,1834	-2,23	0,026
AB1D1	0,3696	0,2996	1,23	0,218
CB1D1	-0,4743	0,2996	-1,58	0,114
EB1D1	0,2874	0,2996	0,96	0,338
CCB1D1	0,5381	0,4494	1,20	0,232
EEB1D1	0,9796	0,5189	1,89	0,060

Appendix C.6 Continued

AB2D1	-0,2978	0,2996	-0,99	0,321
CB2D1	-1,1826	0,2996	-3,95	0,000
EB2D1	-0,8191	0,2996	-2,73	0,007
EEB2D1	1,0091	0,5189	1,94	0,052
AEB2D1	0,4237	0,3177	1,33	0,183
CEB2D1	0,9317	0,3177	2,93	0,004

S = 1,101 R-Sq = 86,7% R-Sq(adj) = 85,2%

Analysis of Variance

Source	DF	SS	MS	F	P
Regression	49	3444,888	70,304	58,03	0,000
Residual Error	436	528,223	1,212		
Total	485	3973,111			

Source	DF	Seq SS
A	1	1167,475
B1	1	793,596
B2	1	449,440
C	1	59,085
D1	1	214,735
E	1	1,112
AA	1	77,775
CC	1	2,758
EE	1	2,701
AC	1	0,032
AE	1	0,338
CE	1	14,774
B1D1	1	35,861
B2D1	1	0,116
AB1	1	32,589
CB1	1	291,933
EB1	1	147,185
AAB1	1	2,192
CCB1	1	0,258
EEB1	1	25,400
ACB1	1	11,040
CEB1	1	6,106
AB2	1	0,001
CB2	1	0,080
EB2	1	3,185
AAB2	1	8,708
EEB2	1	0,839
ACB2	1	2,873
AEB2	1	0,031
CEB2	1	7,747
AD1	1	3,026
CD1	1	0,258
ED1	1	0,018
CCD1	1	0,842
EED1	1	1,353
ACD1	1	3,800
AED1	1	11,886
CED1	1	0,531
AB1D1	1	4,840
CB1D1	1	0,247
EB1D1	1	8,743
CCB1D1	1	1,738
EEB1D1	1	1,354

Appendix C.6 Continued

```
AB2D1          1       1,197
CB2D1          1      18,880
EB2D1          1       9,057
EEB2D1         1       4,582
AEB2D1         1       2,155
CEB2D1         1      10,416

Unusual Observations
Obs        A        Flex         Fit      SE Fit    Residual     St Resid
 21    -1,00      8,7600      6,4153      0,4068      2,3447        2,29R
 46    -1,00      4,1500      6,3445      0,3459     -2,1945       -2,10R
 47    -1,00      3,4600      5,9301      0,2933     -2,4701       -2,33R
 50    -1,00      9,5600      7,3589      0,3459      2,2011        2,11R
 81     0,00      4,7200      7,0045      0,2996     -2,2845       -2,16R
 92     0,00      7,0300      9,7652      0,2933     -2,7352       -2,58R
152     1,00     15,2100     12,0745      0,2933      3,1355        2,96R
153     1,00     14,8600     12,2461      0,3459      2,6139        2,50R
156     1,00     13,8200     10,5316      0,3459      3,2884        3,15R
168    -1,00      9,9100      7,4248      0,4021      2,4852        2,43R
241     0,00     12,6700      9,5075      0,2996      3,1625        2,99R
254     0,00      7,3700      9,7652      0,2933     -2,3952       -2,26R
297     1,00      4,6100      7,5981      0,3432     -2,9881       -2,86R
308     1,00     13,2500     11,1004      0,3459      2,1496        2,06R
314     1,00     14,2800     12,0745      0,2933      2,2055        2,08R
315     1,00     10,0200     12,2461      0,3459     -2,2261       -2,13R
318     1,00     14,2800     10,5316      0,3459      3,7484        3,59R
320     1,00     10,2500     13,0158      0,3459     -2,7658       -2,65R
329    -1,00      4,9500      7,3862      0,3459     -2,4362       -2,33R
336    -1,00      5,8800      8,1135      0,3207     -2,2335       -2,12R
374    -1,00      9,7900      7,3589      0,3459      2,4311        2,33R
409     0,00      5,0700      7,3078      0,3391     -2,2378       -2,14R
421     0,00     11,9800      9,0786      0,2735      2,9014        2,72R
462     1,00      5,7600      8,0555      0,3432     -2,2955       -2,19R
464     1,00      9,1000      6,2152      0,3513      2,8848        2,77R
477     1,00      8,7600     12,2461      0,3459     -3,4861       -3,34R
482     1,00     10,6000     13,0158      0,3459     -2,4158       -2,31R

R denotes an observation with a large standardized residual

Durbin-Watson statistic = 2,15
```

APPENDIX D

Appendix D.1 The regression model developed for the mean impact resistance based on the L_{27} (3^{13}) design with only main factors

The regression equation is

y = 4,97 + 0,283 A + 0,663 B1 + 1,84 B2 - 0,406 C - 1,14 D1 + 1,10 E

Predictor	Coef	SE Coef	T	P
Constant	4,9696	0,5566	8,93	0,000
A	0,2832	0,3645	0,78	0,446
B1	0,6632	0,7290	0,91	0,374
B2	1,8446	0,7290	2,53	0,020
C	-0,4056	0,3645	-1,11	0,279
D1	-1,1428	0,6317	-1,81	0,085
E	1,1017	0,3777	2,92	0,009

S = 1,544 R-Sq = 48,4% R-Sq(adj) = 32,9%

Analysis of Variance

Source	DF	SS	MS	F	P
Regression	6	44,755	7,459	3,13	0,025
Residual Error	20	47,670	2,384		
Total	26	92,426			

Source	DF	Seq SS
A	1	2,136
B1	1	0,616
B2	1	13,347
C	1	2,136
D1	1	6,247
E	1	20,274

Unusual Observations

Obs	A	MEAN3	Fit	SE Fit	Residual	St Resid
2	-1,00	6,233	3,544	0,759	2,690	2,00R

R denotes an observation with a large standardized residual

Durbin-Watson statistic = 2,67

Appendix D.2 The regression model developed for the mean impact resistance based on the L_{27} (3^{13}) design with main and interaction factors

The regression equation is

y = 3,23 + 0,198 A + 2,13 B1 + 5,65 B2 + 1,38 C + 3,20 D1 - 0,794 E - 4,18 AC + 3,75 AE + 0,787 CE - 3,52 B1D1 - 10,5 B2D1 + 0,674 AB1 - 2,44 CB1 + 1,50 EB1 + 3,42 ACB1 - 3,51 AEB1 - 1,34 CEB1 - 1,40 AB2 + 0,301 CB2 + 3,98 EB2 + 1,25 ACB2 - 7,34 AEB2 + 1,09 CEB2

Predictor	Coef	SE Coef	T	P
Constant	3,2278	0,5329	6,06	0,009
A	0,1981	0,4157	0,48	0,666
B1	2,1303	0,6212	3,43	0,042
B2	5,6500	0,7536	7,50	0,005
C	1,3833	0,5069	2,73	0,072
D1	3,204	1,102	2,91	0,062
E	-0,7944	0,5069	-1,57	0,215
AC	-4,1796	0,9644	-4,33	0,023
AE	3,746	1,045	3,58	0,037
CE	0,7870	0,7426	1,06	0,367
B1D1	-3,523	1,250	-2,82	0,067
B2D1	-10,537	1,789	-5,89	0,010
AB1	0,6741	0,5172	1,30	0,283
CB1	-2,4389	0,5929	-4,11	0,026
EB1	1,5000	0,5929	2,53	0,085
ACB1	3,424	1,072	3,19	0,050
AEB1	-3,507	1,145	-3,06	0,055
CEB1	-1,3430	0,8774	-1,53	0,223
AB2	-1,4029	0,6555	-2,14	0,122
CB2	0,3008	0,7168	0,42	0,703
EB2	3,9833	0,7972	5,00	0,015
ACB2	1,246	1,437	0,87	0,450
AEB2	-7,337	1,320	-5,56	0,011
CEB2	1,089	1,096	0,99	0,393

S = 0,7536 R-Sq = 98,2% R-Sq(adj) = 84,0%

Analysis of Variance

Source	DF	SS	MS	F	P
Regression	23	90,7217	3,9444	6,95	0,068
Residual Error	3	1,7039	0,5680		
Total	26	92,4255			

Source	DF	Seq SS
A	1	2,1356
B1	1	0,6158
B2	1	13,3472
C	1	2,1356
D1	1	6,2469
E	1	20,2740
AC	1	0,9882
AE	1	0,0285
CE	1	4,4847
B1D1	1	0,5164
B2D1	1	0,6291
AB1	1	2,7263
CB1	1	4,2745
EB1	1	1,1841
ACB1	1	1,5566

Appendix D.2 Continued

```
AEB1          1      1,2951
CEB1          1      0,0664
AB2           1      0,4647
CB2           1      1,5880
EB2           1      5,9897
ACB2          1      2,3907
AEB2          1     17,2222
CEB2          1      0,5612

Unusual Observations
Obs      A      MEAN3         Fit      SE Fit    Residual      St Resid
  2  -1,00      6,233       6,233       0,754       0,000           * X
  4  -1,00      4,467       4,467       0,754      -0,000           * X
  9  -1,00      7,367       7,367       0,754      -0,000           * X
 11   0,00      4,733       4,733       0,754      -0,000           * X
 13   0,00      3,467       3,467       0,754      -0,000           * X
 18   0,00      4,133       4,133       0,754      -0,000           * X
 20   1,00      4,967       4,967       0,754      -0,000           * X
 22   1,00      3,867       3,867       0,754      -0,000           * X
 27   1,00      3,833       3,833       0,754       0,000           * X

X denotes an observation whose X value gives it large influence.

Durbin-Watson statistic = 2,19
```

Appendix D.3 The best regression model developed for the mean impact resistance based on the L_{27} (3^{13}) design

The regression equation is

y = 4,93 + 2,95 A + 0,432 B1 + 2,28 B2 - 0,160 C - 0,757 D1 + 0,857 E
+ 1,95 AC - 2,30 AE + 1,78 CE + 0,438 B1D1 - 1,56 B2D1 - 0,388 AB1
- 0,052 CB1 - 0,996 EB1 - 5,24 ACB1 - 2,33 CEB1 - 2,42 AB2 - 0,953
EB2 - 1,12 AEB2 - 5,07 AD1

Predictor	Coef	SE Coef	T	P
Constant	4,9261	0,3335	14,77	0,000
A	2,9491	0,5300	5,56	0,001
B1	0,4323	0,3981	1,09	0,319
B2	2,2791	0,6055	3,76	0,009
C	-0,1596	0,2610	-0,61	0,563
D1	-0,7573	0,7305	-1,04	0,340
E	0,8569	0,3995	2,14	0,076
AC	1,9477	0,9110	2,14	0,076
AE	-2,2971	0,7165	-3,21	0,018
CE	1,7776	0,4039	4,40	0,005
B1D1	0,4378	0,8182	0,54	0,612
B2D1	-1,558	1,536	-1,01	0,350
AB1	-0,3881	0,3717	-1,04	0,337
CB1	-0,0515	0,4489	-0,11	0,912
EB1	-0,9957	0,5610	-1,77	0,126
ACB1	-5,238	1,467	-3,57	0,012
CEB1	-2,3345	0,5408	-4,32	0,005
AB2	-2,4158	0,4957	-4,87	0,003
EB2	-0,9529	0,9587	-0,99	0,359
AEB2	-1,1183	0,6828	-1,64	0,153
AD1	-5,0663	0,9732	-5,21	0,002

S = 0,5538 R-Sq = 98,0% R-Sq(adj) = 91,4%

Analysis of Variance

Source	DF	SS	MS	F	P
Regression	20	90,5852	4,5293	14,77	0,002
Residual Error	6	1,8404	0,3067		
Total	26	92,4255			

Source	DF	Seq SS
A	1	2,1356
B1	1	0,6158
B2	1	13,3472
C	1	2,1356
D1	1	6,2469
E	1	20,2740
AC	1	0,9882
AE	1	0,0285
CE	1	4,4847
B1D1	1	0,5164
B2D1	1	0,6291
AB1	1	2,7263
CB1	1	4,2745
EB1	1	1,1841
ACB1	1	1,5566
CEB1	1	0,1886
AB2	1	0,2373
EB2	1	7,9047

Appendix D.3 Continued

```
AEB2           1     12,7981
AD1            1      8,3126

Unusual Observations
Obs       A      MEAN3         Fit      SE Fit    Residual      St Resid
  4  -1,00      4,467       4,465       0,553       0,001        0,05 X
 18   0,00      4,133       4,132       0,553       0,001        0,05 X
 20   1,00      4,967       4,969       0,551      -0,003       -0,05 X

X denotes an observation whose X value gives it large influence.

Durbin-Watson statistic = 2,26
```

Appendix D.4 The y* = log y variance stabilizing data transformation of the mean impact resistance based on the L_{27} (3^{13}) design

Run No	y1	y2	y3	μ	log μ
1	3,8	2,1	2,6	2,8333	0,45229
2	5,2	5,7	7,8	6,2333	0,79472
3	4,6	3,6	6,2	4,8000	0,68124
4	4,8	5,0	3,6	4,4667	0,64999
5	4,4	2,4	7,6	4,8000	0,68124
6	5,8	3,2	3,6	4,2000	0,62325
7	15,6	11,8	3,2	10,2000	1,00860
8	3,8	2,1	3,0	2,9667	0,47227
9	6,9	5,2	10,0	7,3667	0,86727
10	7,6	6,1	9,9	7,8667	0,89579
11	3,4	5,4	5,4	4,7333	0,67516
12	5,0	8,9	3,6	5,8333	0,76591
13	3,6	3,6	3,2	3,4667	0,53992
14	3,6	5,0	3,0	3,8667	0,58734
15	4,9	5,2	4,2	4,7667	0,67822
16	4,7	4,2	6,1	5,0000	0,69897
17	13,0	2,5	2,4	5,9667	0,77573
18	4,8	3,0	4,6	4,1333	0,61630
19	16,8	4,0	7,6	9,4667	0,97620
20	3,6	5,9	5,4	4,9667	0,69607
21	4,6	5,4	2,8	4,2667	0,63009
22	4,4	3,0	4,2	3,8667	0,58734
23	9,9	4,4	6,7	7,0000	0,84510
24	9,6	5,8	8,8	8,0667	0,90670
25	6,6	6,8	5,5	6,3000	0,79934
26	5,5	5,7	7,7	6,3000	0,79934
27	2,3	4,0	5,2	3,8333	0,58357

Appendix D.5 The best quadratic regression model developed for the log transformed mean impact resistance based on the L_{27} (3^{13}) design

The regression equation is

log μ = 0,707 + 0,105 A + 0,0091 B1 + 0,101 B2 - 0,0288 C - 0,0802 D1 + 0,0959 E + 0,0558 AC - 0,104 AE - 0,0381 CE + 0,0492 B1D1 - 0,0001 AB1 - 0,0055 CB1 - 0,0583 EB1 - 0,197 ACB1 + 0,0566 AEB1 + 0,0398 CEB1 - 259 AD1 + 0,0831 CD1 - 0,156 ED1

Predictor	Coef	SE Coef	T	P
Constant	0,70658	0,01931	36,60	0,000
A	0,10464	0,02232	4,69	0,002
B1	0,00907	0,02853	0,32	0,760
B2	0,10061	0,02404	4,19	0,004
C	-0,02882	0,01807	-1,59	0,155
D1	-0,08019	0,02752	-2,91	0,023
E	0,09594	0,02231	4,30	0,004
AC	0,05585	0,02442	2,29	0,056
AE	-0,10411	0,03125	-3,33	0,013
CE	-0,03810	0,02547	-1,50	0,178
B1D1	0,04918	0,04765	1,03	0,336
AB1	-0,00010	0,02627	-0,00	0,997
CB1	-0,00549	0,02767	-0,20	0,848
EB1	-0,05831	0,02675	-2,18	0,066
ACB1	-0,19661	0,05588	-3,52	0,010
AEB1	0,05658	0,04009	1,41	0,201
CEB1	0,03975	0,05774	0,69	0,513
AD1	-0,25942	0,04213	-6,16	0,000
CD1	0,08309	0,03285	2,53	0,039
ED1	-0,15640	0,04875	-3,21	0,015

S = 0,04959 R-Sq = 96,8% R-Sq(adj) = 88,0%

Analysis of Variance

Source	DF	SS	MS	F	P
Regression	19	0,517495	0,027237	11,08	0,002
Residual Error	7	0,017212	0,002459		
Total	26	0,534707			

Source	DF	Seq SS
A	1	0,019528
B1	1	0,001107
B2	1	0,068225
C	1	0,003638
D1	1	0,029258
E	1	0,112651
AC	1	0,012448
AE	1	0,002321
CE	1	0,021915
B1D1	1	0,003116
AB1	1	0,005980
CB1	1	0,033629
EB1	1	0,012182
ACB1	1	0,003747
AEB1	1	0,003804
CEB1	1	0,000060
AD1	1	0,136639
CD1	1	0,021941
ED1	1	0,025306

Appendix D.5 Continued

Unusual Observations

Obs	A	LOG I	Fit	SE Fit	Residual	St Resid
4	-1,00	0,64999	0,64999	0,04959	-0,00000	* X
18	0,00	0,61630	0,61630	0,04959	-0,00000	* X
20	1,00	0,69607	0,69607	0,04959	-0,00000	* X

X denotes an observation whose X value gives it large influence.

Durbin-Watson statistic = 2,05

Appendix D.6 The regression model developed for the mean impact resistance based on the full factorial design with only main factors

The regression equation is

y = 5,98 + 0,670 A - 0,552 B1 - 0,048 B2 - 0,312 C - 0,484 D1 + 1,36 E

Predictor	Coef	SE Coef	T	P
Constant	5,9784	0,2373	25,19	0,000
A	0,6701	0,1453	4,61	0,000
B1	-0,5519	0,2906	-1,90	0,058
B2	-0,0475	0,2906	-0,16	0,870
C	-0,3117	0,1453	-2,15	0,032
D1	-0,4840	0,2373	-2,04	0,042
E	1,3583	0,1453	9,35	0,000

S = 2,616 R-Sq = 20,3% R-Sq(adj) = 19,3%

Analysis of Variance

Source	DF	SS	MS	F	P
Regression	6	833,52	138,92	20,30	0,000
Residual Error	479	3277,59	6,84		
Total	485	4111,11			

Source	DF	Seq SS
A	1	145,47
B1	1	30,12
B2	1	0,18
C	1	31,48
D1	1	28,46
E	1	597,80

Unusual Observations

Obs	A	Impact	Fit	SE Fit	Residual	St Resid
2	-1,00	15,800	5,620	0,314	10,180	3,92R
39	-1,00	15,600	6,931	0,346	8,669	3,34R
51	-1,00	15,000	6,307	0,346	8,693	3,35R
70	0,00	12,200	3,824	0,314	8,376	3,23R
74	0,00	12,600	5,738	0,278	6,862	2,64R
80	0,00	13,000	5,427	0,237	7,573	2,91R
93	0,00	13,400	7,601	0,314	5,799	2,23R
99	0,00	16,200	7,289	0,278	8,911	3,43R
129	1,00	16,800	7,767	0,346	9,033	3,48R
132	1,00	12,800	7,283	0,346	5,517	2,13R
156	1,00	19,800	7,475	0,314	12,325	4,75R
165	-1,00	13,300	6,978	0,346	6,322	2,44R
219	0,00	18,600	7,648	0,314	10,952	4,22R
377	-1,00	10,000	4,465	0,314	5,535	2,13R
380	0,00	11,900	6,290	0,278	5,610	2,16R
381	0,00	16,600	7,648	0,314	8,952	3,45R
399	0,00	18,000	7,097	0,314	10,903	4,20R
420	0,00	13,400	7,117	0,314	6,283	2,42R
444	1,00	18,200	7,523	0,314	10,677	4,11R
462	1,00	18,200	6,971	0,314	11,229	4,32R
474	1,00	19,400	7,787	0,346	11,613	4,48R

R denotes an observation with a large standardized residual

Durbin-Watson statistic = 1,94

Appendix D.7 The regression model developed for the mean impact resistance based on the full factorial design with main, interaction and squared factors

The regression equation is

y = 6,22 + 0,317 A - 1,90 B1 - 0,07 B2 - 0,913 C - 0,10 D1 + 1,69 E - 1,10 AA + 1,05 CC - 0,365 EE + 0,667 AC + 0,117 AE - 1,11 CE - 0,40 B1D1 - 0,58 B2D1 + 0,593 AB1 + 0,300 CB1 - 0,674 EB1 + 0,970 AAB1 - 0,119 CCB1 + 1,18 EEB1 - 0,575 ACB1 + 0,394 AEB1 + 0,525 CEB1 - 0,346 AB2 + 1,05 CB2 + 0,307 EB2 + 0,350 AAB2 - 0,844 CCB2 + 0,656 EEB2 - 0,333 ACB2 - 0,858 AEB2 + 0,606 CEB2 + 0,554 AD1 + 1,15 CD1 - 0,391 ED1 + 1,29 AAD1 - 1,86 CCD1 + 0,083 EED1 - 0,808 ACD1 + 0,478 AED1 + 1,47 CED1 - 0,217 AB1D1 - 0,698 CB1D1 + 0,470 EB1D1 - 0,07 AAB1D1 + 1,08 CCB1D1 - 0,44 EEB1D1 + 1,11 ACB1D1 - 0,364 AEB1D1 - 1,34 CEB1D1 + 0,183 AB2D1 - 1,84 CB2D1 - 0,537 EB2D1 - 1,02 AAB2D1 + 1,92 CCB2D1 - 0,29 EEB2D1 - 0,325 ACB2D1 + 1,61 AEB2D1 - 1,80 CEB2D1

Predictor	Coef	SE Coef	T	P
Constant	6,2235	0,7426	8,38	0,000
A	0,3167	0,3437	0,92	0,357
B1	-1,898	1,050	-1,81	0,071
B2	-0,067	1,050	-0,06	0,949
C	-0,9130	0,3437	-2,66	0,008
D1	-0,096	1,050	-0,09	0,927
E	1,6870	0,3437	4,91	0,000
AA	-1,0981	0,5954	-1,84	0,066
CC	1,0463	0,5954	1,76	0,080
EE	-0,3648	0,5954	-0,61	0,540
AC	0,6667	0,4210	1,58	0,114
AE	0,1167	0,4210	0,28	0,782
CE	-1,1083	0,4210	-2,63	0,009
B1D1	-0,398	1,485	-0,27	0,789
B2D1	-0,580	1,485	-0,39	0,696
AB1	0,5926	0,4861	1,22	0,224
CB1	0,3000	0,4861	0,62	0,537
EB1	-0,6741	0,4861	-1,39	0,166
AAB1	0,9704	0,8420	1,15	0,250
CCB1	-0,1185	0,8420	-0,14	0,888
EEB1	1,1815	0,8420	1,40	0,161
ACB1	-0,5750	0,5954	-0,97	0,335
AEB1	0,3944	0,5954	0,66	0,508
CEB1	0,5250	0,5954	0,88	0,378
AB2	-0,3463	0,4861	-0,71	0,477
CB2	1,0481	0,4861	2,16	0,032
EB2	0,3074	0,4861	0,63	0,527
AAB2	0,3500	0,8420	0,42	0,678
CCB2	-0,8444	0,8420	-1,00	0,316
EEB2	0,6556	0,8420	0,78	0,437
ACB2	-0,3333	0,5954	-0,56	0,576
AEB2	-0,8583	0,5954	-1,44	0,150
CEB2	0,6056	0,5954	1,02	0,310
AD1	0,5537	0,4861	1,14	0,255
CD1	1,1500	0,4861	2,37	0,018
ED1	-0,3907	0,4861	-0,80	0,422
AAD1	1,2944	0,8420	1,54	0,125
CCD1	-1,8611	0,8420	-2,21	0,028
EED1	0,0833	0,8420	0,10	0,921
ACD1	-0,8083	0,5954	-1,36	0,175
AED1	0,4778	0,5954	0,80	0,423
CED1	1,4667	0,5954	2,46	0,014

Appendix D.7 Continued

```
AB1D1         -0,2167      0,6875      -0,32    0,753
CB1D1         -0,6981      0,6875      -1,02    0,310
EB1D1          0,4704      0,6875       0,68    0,494
AAB1D1         -0,069       1,191      -0,06    0,954
CCB1D1          1,076       1,191       0,90    0,367
EEB1D1         -0,441       1,191      -0,37    0,711
ACB1D1         1,1111      0,8420       1,32    0,188
AEB1D1        -0,3639      0,8420      -0,43    0,666
CEB1D1        -1,3389      0,8420      -1,59    0,113
AB2D1          0,1833      0,6875       0,27    0,790
CB2D1         -1,8407      0,6875      -2,68    0,008
EB2D1         -0,5370      0,6875      -0,78    0,435
AAB2D1         -1,020       1,191      -0,86    0,392
CCB2D1          1,919       1,191       1,61    0,108
EEB2D1         -0,293       1,191      -0,25    0,806
ACB2D1        -0,3250      0,8420      -0,39    0,700
AEB2D1         1,6139      0,8420       1,92    0,056
CEB2D1        -1,7972      0,8420      -2,13    0,033

S = 2,526       R-Sq = 33,9%     R-Sq(adj) = 24,7%

Analysis of Variance

Source            DF          SS          MS         F        P
Regression        59    1393,028      23,611     3,70    0,000
Residual Error   426    2718,080       6,380
Total            485    4111,108

Source       DF      Seq SS
A             1     145,470
B1            1      30,119
B2            1       0,183
C             1      31,485
D1            1      28,456
E             1     597,802
AA            1       3,993
CC            1       9,324
EE            1       3,011
AC            1       1,779
AE            1      36,179
CE            1      58,594
B1D1          1       0,127
B2D1          1       0,631
AB1           1      26,930
CB1           1       0,919
EB1           1      15,125
AAB1          1      24,784
CCB1          1       3,146
EEB1          1      11,979
ACB1          1       2,506
AEB1          1       2,723
CEB1          1       0,000
AB2           1       3,501
CB2           1       0,882
EB2           1       0,082
AAB2          1       0,462
CCB2          1       0,237
EEB2          1       4,668
ACB2          1       8,851
AEB2          1       0,095
```

Appendix D.7 Continued

CEB2	1	3,092
AD1	1	23,847
CD1	1	7,471
ED1	1	13,814
AAD1	1	23,427
CCD1	1	20,107
EED1	1	0,701
ACD1	1	16,116
AED1	1	43,202
CED1	1	9,584
AB1D1	1	1,711
CB1D1	1	0,889
EB1D1	1	9,827
AAB1D1	1	1,170
CCB1D1	1	0,082
EEB1D1	1	0,520
ACB1D1	1	19,465
AEB1D1	1	16,450
CEB1D1	1	2,326
AB2D1	1	0,454
CB2D1	1	45,742
EB2D1	1	3,894
AAB2D1	1	4,685
CCB2D1	1	16,563
EEB2D1	1	0,385
ACB2D1	1	0,951
AEB2D1	1	23,442
CEB2D1	1	29,070

Unusual Observations

Obs	A	Impact	Fit	SE Fit	Residual	St Resid
2	-1,00	15,800	7,435	0,854	8,365	3,52R
39	-1,00	15,600	9,368	1,041	6,232	2,71R
51	-1,00	15,000	7,966	1,041	7,034	3,06R
70	0,00	12,200	3,613	0,854	8,587	3,61R
74	0,00	12,600	5,867	0,743	6,733	2,79R
80	0,00	13,000	4,326	0,743	8,674	3,59R
96	0,00	3,400	8,277	0,854	-4,877	-2,05R
99	0,00	16,200	8,442	0,743	7,758	3,21R
129	1,00	16,800	9,481	1,041	7,319	3,18R
141	1,00	12,000	7,271	1,041	4,729	2,05R
156	1,00	19,800	8,212	0,854	11,588	4,87R
161	1,00	9,700	4,617	0,854	5,083	2,14R
219	0,00	18,600	10,613	0,854	7,987	3,36R
248	0,00	10,100	4,641	0,743	5,459	2,26R
291	1,00	4,000	9,481	1,041	-5,481	-2,38R
294	1,00	3,600	8,718	1,041	-5,118	-2,22R
363	-1,00	3,200	9,368	1,041	-6,168	-2,68R
377	-1,00	10,000	4,802	0,854	5,198	2,19R
381	0,00	16,600	10,613	0,854	5,987	2,52R
399	0,00	18,000	8,280	0,854	9,720	4,09R
420	0,00	13,400	8,277	0,854	5,123	2,16R
444	1,00	18,200	8,803	0,854	9,397	3,95R
462	1,00	18,200	8,353	0,854	9,847	4,14R
474	1,00	19,400	10,660	1,041	8,740	3,80R

R denotes an observation with a large standardized residual

Durbin-Watson statistic = 2,08

Appendix D.8 The best regression model developed for the mean impact resistance based on the full factorial design

The regression equation is

y = 6,00 + 0,317 A - 1,69 B1 + 0,564 B2 - 0,913 C - 0,157 D1 + 1,69 E - 0,997 AA + 0,987 CC - 0,069 EE + 0,500 AC + 0,314 AE - 1,11 CE - 0,020 B1D1 - 1,10 B2D1 + 0,593 AB1 + 0,300 CB1 - 0,674 EB1 + 1,02 AAB1 + 0,706 EEB1 - 0,408 ACB1 + 0,525 CEB1 - 0,346 AB2 + 1,05 CB2 + 0,307 EB2 - 0,785 CCB2 - 1,06 AEB2 + 0,606 CEB2 + 0,554 AD1 + 1,15 CD1 - 0,391 ED1 + 0,931 AAD1 - 1,32 CCD1 - 0,971 ACD1 + 0,296 AED1 + 1,47 CED1 - 0,217 AB1D1 - 0,698 CB1D1 + 0,470 EB1D1 + 1,27 ACB1D1 - 1,34 CEB1D1 + 0,183 AB2D1 - 1,84 CB2D1 - 0,537 EB2D1 + 1,38 CCB2D1 + 1,80 AEB2D1 - 1,80 CEB2D1

Predictor	Coef	SE Coef	T	P
Constant	5,9978	0,5079	11,81	0,000
A	0,3167	0,3407	0,93	0,353
B1	-1,6904	0,6220	-2,72	0,007
B2	0,5642	0,6220	0,91	0,365
C	-0,9130	0,3407	-2,68	0,008
D1	-0,1574	0,6424	-0,25	0,807
E	1,6870	0,3407	4,95	0,000
AA	-0,9968	0,3809	-2,62	0,009
CC	0,9870	0,4173	2,37	0,018
EE	-0,0685	0,2951	-0,23	0,816
AC	0,5000	0,2951	1,69	0,091
AE	0,3139	0,2951	1,06	0,288
CE	-1,1083	0,4173	-2,66	0,008
B1D1	-0,0198	0,5564	-0,04	0,972
B2D1	-1,0969	0,8797	-1,25	0,213
AB1	0,5926	0,4818	1,23	0,219
CB1	0,3000	0,4818	0,62	0,534
EB1	-0,6741	0,4818	-1,40	0,163
AAB1	1,0162	0,5110	1,99	0,047
EEB1	0,7065	0,5110	1,38	0,168
ACB1	-0,4083	0,5110	-0,80	0,425
CEB1	0,5250	0,5901	0,89	0,374
AB2	-0,3463	0,4818	-0,72	0,473
CB2	1,0481	0,4818	2,18	0,030
EB2	0,3074	0,4818	0,64	0,524
CCB2	-0,7852	0,7227	-1,09	0,278
AEB2	-1,0556	0,5110	-2,07	0,039
CEB2	0,6056	0,5901	1,03	0,305
AD1	0,5537	0,4818	1,15	0,251
CD1	1,1500	0,4818	2,39	0,017
ED1	-0,3907	0,4818	-0,81	0,418
AAD1	0,9315	0,4818	1,93	0,054
CCD1	-1,3231	0,5901	-2,24	0,025
ACD1	-0,9708	0,4173	-2,33	0,020
AED1	0,2958	0,4173	0,71	0,479
CED1	1,4667	0,5901	2,49	0,013
AB1D1	-0,2167	0,6814	-0,32	0,751
CB1D1	-0,6981	0,6814	-1,02	0,306
EB1D1	0,4704	0,6814	0,69	0,490
ACB1D1	1,2736	0,7227	1,76	0,079
CEB1D1	-1,3389	0,8345	-1,60	0,109
AB2D1	0,1833	0,6814	0,27	0,788
CB2D1	-1,8407	0,6814	-2,70	0,007
EB2D1	-0,5370	0,6814	-0,79	0,431
CCB2D1	1,381	1,022	1,35	0,177

Appendix D.8 Continued

```
AEB2D1         1,7958      0,7227       2,48    0,013
CEB2D1        -1,7972      0,8345      -2,15    0,032

S = 2,504       R-Sq = 33,1%     R-Sq(adj) = 26,1%

Analysis of Variance

Source            DF          SS          MS         F        P
Regression        46    1359,441      29,553      4,71    0,000
Residual Error   439    2751,667       6,268
Total            485    4111,108

Source       DF      Seq SS
A             1     145,470
B1            1      30,119
B2            1       0,183
C             1      31,485
D1            1      28,456
E             1     597,802
AA            1       3,993
CC            1       9,324
EE            1       3,011
AC            1       1,779
AE            1      36,179
CE            1      58,594
B1D1          1       0,127
B2D1          1       0,631
AB1           1      26,930
CB1           1       0,919
EB1           1      15,125
AAB1          1      24,784
EEB1          1      11,979
ACB1          1       2,506
CEB1          1       0,000
AB2           1       3,501
CB2           1       0,882
EB2           1       0,082
CCB2          1       0,216
AEB2          1       1,193
CEB2          1       3,092
AD1           1      23,847
CD1           1       7,471
ED1           1      13,814
AAD1          1      23,427
CCD1          1      20,107
ACD1          1      16,116
AED1          1      43,202
CED1          1       9,584
AB1D1         1       1,711
CB1D1         1       0,889
EB1D1         1       9,827
ACB1D1        1      19,465
CEB1D1        1       2,326
AB2D1         1       0,454
CB2D1         1      45,742
EB2D1         1       3,894
CCB2D1        1      11,436
AEB2D1        1      38,700
CEB2D1        1      29,070
```

Appendix D.8 Continued

Unusual Observations

Obs	A	Impact	Fit	SE Fit	Residual	St Resid
2	-1,00	15,800	7,084	0,686	8,716	3,62R
39	-1,00	15,600	9,332	0,962	6,268	2,71R
51	-1,00	15,000	7,597	0,962	7,403	3,20R
70	0,00	12,200	4,018	0,760	8,182	3,43R
74	0,00	12,600	5,907	0,627	6,693	2,76R
80	0,00	13,000	4,307	0,579	8,693	3,57R
99	0,00	16,200	8,488	0,650	7,712	3,19R
129	1,00	16,800	9,293	0,962	7,507	3,25R
141	1,00	12,000	7,083	0,962	4,917	2,13R
156	1,00	19,800	8,298	0,815	11,502	4,86R
219	0,00	18,600	10,625	0,760	7,975	3,34R
248	0,00	10,100	4,681	0,627	5,419	2,24R
291	1,00	4,000	9,293	0,962	-5,293	-2,29R
294	1,00	3,600	8,554	0,962	-4,954	-2,14R
300	1,00	3,600	8,668	0,720	-5,068	-2,11R
363	-1,00	3,200	9,332	0,962	-6,132	-2,65R
377	-1,00	10,000	4,710	0,700	5,290	2,20R
381	0,00	16,600	10,625	0,760	5,975	2,50R
399	0,00	18,000	8,142	0,791	9,858	4,15R
420	0,00	13,400	7,954	0,772	5,446	2,29R
444	1,00	18,200	8,483	0,707	9,717	4,05R
462	1,00	18,200	8,668	0,720	9,532	3,98R
474	1,00	19,400	10,417	0,962	8,983	3,89R

R denotes an observation with a large standardized residual

Durbin-Watson statistic = 2,06

Appendix D.9 Residual plots of the best regression model including main, two-way interaction and squared terms for the mean impact resistance based on the full factorial design

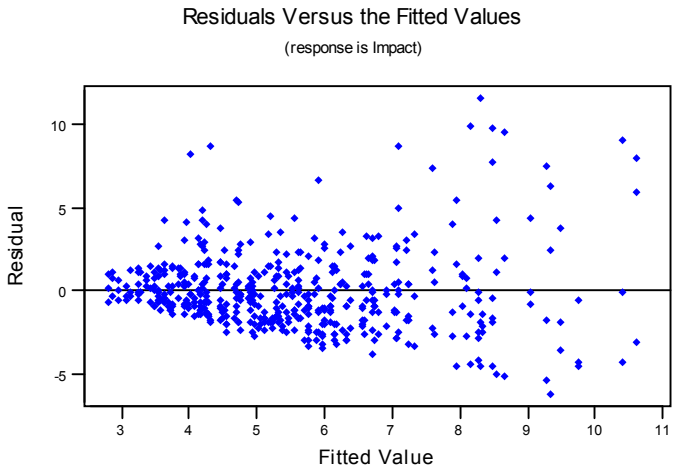

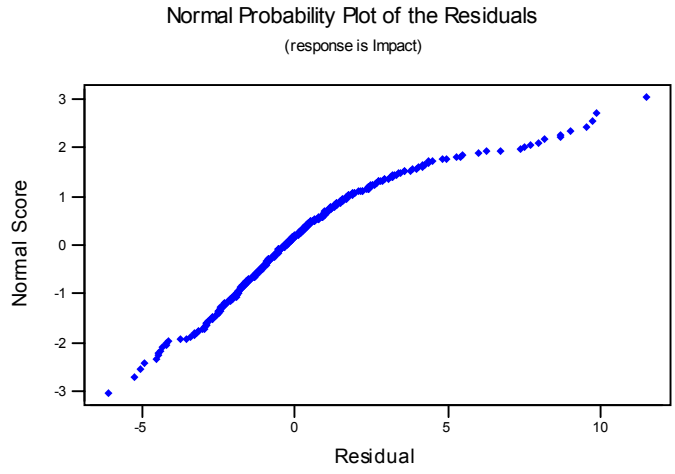

Appendix D.10 The y* = log y variance stabilizing data transformation of the mean impact resistance based on the full factorial design

Run No	y1	y2	y3	log y1	log y2	log y3
1	3,80	2,10	2,60	0,58	0,32	0,41
2	15,80	6,90	4,60	1,20	0,84	0,66
3	5,90	13,30	7,60	0,77	1,12	0,88
4	3,50	3,80	4,20	0,54	0,58	0,62
5	4,90	4,80	5,20	0,69	0,68	0,72
6	2,70	5,70	5,70	0,43	0,76	0,76
7	3,20	4,40	3,00	0,51	0,64	0,48
8	4,20	5,10	4,60	0,62	0,71	0,66
9	4,80	4,20	4,00	0,68	0,62	0,60
10	2,80	3,00	4,00	0,45	0,48	0,60
11	5,20	5,70	7,80	0,72	0,76	0,89
12	5,50	5,20	5,70	0,74	0,72	0,76
13	4,20	4,90	5,00	0,62	0,69	0,70
14	4,00	5,90	3,60	0,60	0,77	0,56
15	4,60	3,60	6,20	0,66	0,56	0,79
16	3,00	3,20	2,80	0,48	0,51	0,45
17	4,20	3,80	4,60	0,62	0,58	0,66
18	3,90	6,80	9,80	0,59	0,83	0,99
19	3,90	3,40	5,40	0,59	0,53	0,73
20	3,50	2,80	6,20	0,54	0,45	0,79
21	5,90	5,80	7,40	0,77	0,76	0,87
22	2,80	3,00	5,10	0,45	0,48	0,71
23	4,80	5,00	3,60	0,68	0,70	0,56
24	4,00	7,00	8,00	0,60	0,85	0,90
25	3,60	4,20	4,00	0,56	0,62	0,60
26	2,70	3,60	4,90	0,43	0,56	0,69
27	4,40	2,40	7,60	0,64	0,38	0,88
28	3,20	4,40	3,00	0,51	0,64	0,48
29	5,20	3,40	4,20	0,72	0,53	0,62
30	3,00	3,40	2,20	0,48	0,53	0,34
31	5,80	3,20	3,60	0,76	0,51	0,56
32	3,60	2,60	2,60	0,56	0,41	0,41
33	2,70	6,20	8,20	0,43	0,79	0,91
34	4,80	2,40	3,00	0,68	0,38	0,48
35	2,40	3,60	3,00	0,38	0,56	0,48
36	7,80	3,20	4,80	0,89	0,51	0,68
37	4,00	3,60	2,50	0,60	0,56	0,40
38	3,00	7,40	4,20	0,48	0,87	0,62
39	15,60	11,80	3,20	1,19	1,07	0,51
40	6,10	2,80	2,70	0,79	0,45	0,43
41	4,50	5,00	5,20	0,65	0,70	0,72
42	3,20	4,40	3,00	0,51	0,64	0,48
43	3,80	2,10	3,00	0,58	0,32	0,48

Appendix D.10 Continued

Run No	y1	y2	y3	log y1	log y2	log y3
44	5,80	6,90	4,00	0,76	0,84	0,60
45	4,10	7,70	5,80	0,61	0,89	0,76
46	4,20	4,60	4,60	0,62	0,66	0,66
47	3,00	5,30	2,60	0,48	0,72	0,41
48	4,60	8,40	3,20	0,66	0,92	0,51
49	2,80	3,00	4,40	0,45	0,48	0,64
50	5,90	4,20	7,60	0,77	0,62	0,88
51	15,00	8,90	5,40	1,18	0,95	0,73
52	4,80	4,40	3,70	0,68	0,64	0,57
53	6,90	5,20	10,00	0,84	0,72	1,00
54	3,60	2,80	3,40	0,56	0,45	0,53
55	4,70	3,00	3,40	0,67	0,48	0,53
56	6,60	5,20	11,90	0,82	0,72	1,08
57	7,60	18,60	16,60	0,88	1,27	1,22
58	5,90	2,90	3,60	0,77	0,46	0,56
59	7,60	3,80	6,20	0,88	0,58	0,79
60	3,60	3,60	3,20	0,56	0,56	0,51
61	3,60	5,00	3,00	0,56	0,70	0,48
62	5,00	8,80	8,60	0,70	0,94	0,93
63	5,00	8,20	10,00	0,70	0,91	1,00
64	3,20	4,90	2,80	0,51	0,69	0,45
65	6,40	9,00	5,70	0,81	0,95	0,76
66	4,20	9,80	4,20	0,62	0,99	0,62
67	5,20	3,00	6,60	0,72	0,48	0,82
68	4,90	5,20	4,20	0,69	0,72	0,62
69	4,80	4,00	7,60	0,68	0,60	0,88
70	12,20	3,80	3,80	1,09	0,58	0,58
71	4,70	5,50	3,40	0,67	0,74	0,53
72	10,70	4,00	7,00	1,03	0,60	0,85
73	4,70	4,20	6,10	0,67	0,62	0,79
74	12,60	4,60	6,10	1,10	0,66	0,79
75	6,80	3,80	18,00	0,83	0,58	1,26
76	2,70	2,50	3,30	0,43	0,40	0,52
77	3,20	8,10	3,40	0,51	0,91	0,53
78	7,60	4,10	6,20	0,88	0,61	0,79
79	3,20	2,60	7,00	0,51	0,41	0,85
80	13,00	2,50	2,40	1,11	0,40	0,38
81	2,50	3,20	2,80	0,40	0,51	0,45
82	4,00	2,80	3,00	0,60	0,45	0,48
83	4,20	7,30	4,20	0,62	0,86	0,62
84	3,40	2,90	6,60	0,53	0,46	0,82
85	4,20	4,40	3,80	0,62	0,64	0,58
86	3,40	10,10	3,80	0,53	1,00	0,58
87	2,40	4,80	5,20	0,38	0,68	0,72
88	3,20	3,40	5,20	0,51	0,53	0,72

Appendix D.10 Continued

Run No	y1	y2	y3	log y1	log y2	log y3
89	4,60	3,00	3,00	0,66	0,48	0,48
90	4,80	3,00	4,60	0,68	0,48	0,66
91	2,50	3,40	3,20	0,40	0,53	0,51
92	7,60	6,10	9,90	0,88	0,79	1,00
93	13,40	9,00	8,30	1,13	0,95	0,92
94	6,90	3,50	4,00	0,84	0,54	0,60
95	7,30	7,60	5,70	0,86	0,88	0,76
96	3,40	9,60	13,40	0,53	0,98	1,13
97	3,30	3,40	6,90	0,52	0,53	0,84
98	4,80	5,70	4,40	0,68	0,76	0,64
99	16,20	4,00	8,10	1,21	0,60	0,91
100	4,40	6,80	9,00	0,64	0,83	0,95
101	3,80	6,70	3,40	0,58	0,83	0,53
102	3,40	5,40	5,40	0,53	0,73	0,73
103	5,00	8,90	3,60	0,70	0,95	0,56
104	4,80	6,70	6,90	0,68	0,83	0,84
105	6,90	6,20	5,90	0,84	0,79	0,77
106	2,90	2,90	7,20	0,46	0,46	0,86
107	5,90	2,80	4,10	0,77	0,45	0,61
108	6,70	3,30	8,60	0,83	0,52	0,93
109	4,40	6,20	4,90	0,64	0,79	0,69
110	6,60	6,80	5,50	0,82	0,83	0,74
111	9,20	5,30	5,50	0,96	0,72	0,74
112	5,00	2,40	5,40	0,70	0,38	0,73
113	6,80	4,50	5,50	0,83	0,65	0,74
114	7,10	8,90	9,00	0,85	0,95	0,95
115	3,60	2,70	4,60	0,56	0,43	0,66
116	6,20	4,00	7,00	0,79	0,60	0,85
117	5,50	5,70	7,70	0,74	0,76	0,89
118	3,00	6,20	4,80	0,48	0,79	0,68
119	7,00	8,60	7,60	0,85	0,93	0,88
120	6,80	6,60	18,20	0,83	0,82	1,26
121	4,40	5,00	5,20	0,64	0,70	0,72
122	3,40	4,80	7,70	0,53	0,68	0,89
123	9,90	8,80	8,60	1,00	0,94	0,93
124	2,30	4,00	5,20	0,36	0,60	0,72
125	5,20	4,80	5,80	0,72	0,68	0,76
126	5,40	10,20	8,20	0,73	1,01	0,91
127	3,80	3,60	6,40	0,58	0,56	0,81
128	5,80	5,80	5,80	0,76	0,76	0,76
129	16,80	4,00	7,60	1,23	0,60	0,88
130	4,20	2,80	8,20	0,62	0,45	0,91
131	2,80	3,30	7,90	0,45	0,52	0,90
132	12,80	3,60	9,70	1,11	0,56	0,99
133	5,50	6,20	5,50	0,74	0,79	0,74

Appendix D.10 Continued

Run No	y1	y2	y3	log y1	log y2	log y3
134	3,00	3,60	3,40	0,48	0,56	0,53
135	9,60	5,50	10,30	0,98	0,74	1,01
136	3,60	5,90	5,40	0,56	0,77	0,73
137	3,40	3,80	6,60	0,53	0,58	0,82
138	10,60	3,60	18,20	1,03	0,56	1,26
139	5,50	6,20	5,90	0,74	0,79	0,77
140	4,60	5,40	2,80	0,66	0,73	0,45
141	12,00	7,10	7,60	1,08	0,85	0,88
142	4,00	4,80	8,00	0,60	0,68	0,90
143	8,60	6,60	6,60	0,93	0,82	0,82
144	8,90	5,40	8,30	0,95	0,73	0,92
145	4,40	3,20	3,20	0,64	0,51	0,51
146	3,50	3,20	3,80	0,54	0,51	0,58
147	4,20	5,50	10,10	0,62	0,74	1,00
148	4,40	3,00	4,20	0,64	0,48	0,62
149	7,60	5,50	4,00	0,88	0,74	0,60
150	6,20	10,30	19,40	0,79	1,01	1,29
151	7,10	4,70	6,60	0,85	0,67	0,82
152	9,90	4,40	6,70	1,00	0,64	0,83
153	3,80	6,20	8,60	0,58	0,79	0,93
154	2,60	4,60	2,60	0,41	0,66	0,41
155	4,90	3,40	4,00	0,69	0,53	0,60
156	19,80	3,80	6,40	1,30	0,58	0,81
157	4,20	3,20	4,40	0,62	0,51	0,64
158	4,20	5,80	9,00	0,62	0,76	0,95
159	9,60	5,80	8,80	0,98	0,76	0,94
160	3,00	4,40	3,20	0,48	0,64	0,51
161	9,70	3,30	6,70	0,99	0,52	0,83
162	4,40	6,10	2,90	0,64	0,79	0,46

Appendix D.11 The quadratic regression model developed for the log transformed mean impact resistance based on the full factorial design with main, interaction and squared factors

The regression equation is

log μ = 0,762 + 0,0369 A - 0,197 B1 + 0,0141 B2 - 0,0406 C + 0,0072 D1 + 0,116 E - 0,0576 AA + 0,0580 CC - 0,0448 EE + 0,0258 AC + 0,0033 AE - 0,0694 CE + 0,0005 B1D1 - 0,0647 B2D1 + 0,0322 AB1 - 0,0011 CB1 - 0,0641 EB1 + 0,0778 AAB1 + 0,0233 CCB1 + 0,119 EEB1 - 0,0064 ACB1 + 0,0178 AEB1 + 0,0375 CEB1 - 0,0239 AB2 + 0,0661 CB2 + 0,0231 EB2 - 0,0006 AAB2 - 0,0539 CCB2 + 0,0306 EEB2 - 0,0056 ACB2 - 0,0536 AEB2 + 0,0394 CEB2 + 0,0220 AD1 + 0,0524 CD1 - 0,0165 ED1 + 0,0746 AAD1 - 0,113 CCD1 - 0,0120 EED1 - 0,0319 ACD1 + 0,0244 AED1 + 0,102 CED1 - 0,0007 AB1D1 - 0,0187 CB1D1 + 0,0407 EB1D1 - 0,0193 AAB1D1 + 0,0569 CCB1D1 - 0,0448 EEB1D1 + 0,0606 ACB1D1 - 0,0200 AEB1D1 - 0,106 CEB1D1 + 0,0002 AB2D1 - 0,111 CB2D1 - 0,0617 EB2D1 - 0,0687 AAB2D1 + 0,134 CCB2D1 + 0,0002 EEB2D1 - 0,0386 ACB2D1 + 0,111 AEB2D1 - 0,116 CEB2D1

Predictor	Coef	SE Coef	T	P
Constant	0,76160	0,04783	15,92	0,000
A	0,03685	0,02214	1,66	0,097
B1	-0,19667	0,06764	-2,91	0,004
B2	0,01407	0,06764	0,21	0,835
C	-0,04056	0,02214	-1,83	0,068
D1	0,00716	0,06764	0,11	0,916
E	0,11630	0,02214	5,25	0,000
AA	-0,05759	0,03835	-1,50	0,134
CC	0,05796	0,03835	1,51	0,131
EE	-0,04481	0,03835	-1,17	0,243
AC	0,02583	0,02712	0,95	0,341
AE	0,00333	0,02712	0,12	0,902
CE	-0,06944	0,02712	-2,56	0,011
B1D1	0,00049	0,09566	0,01	0,996
B2D1	-0,06469	0,09566	-0,68	0,499
AB1	0,03222	0,03131	1,03	0,304
CB1	-0,00111	0,03131	-0,04	0,972
EB1	-0,06407	0,03131	-2,05	0,041
AAB1	0,07778	0,05423	1,43	0,152
CCB1	0,02333	0,05423	0,43	0,667
EEB1	0,11889	0,05423	2,19	0,029
ACB1	-0,00639	0,03835	-0,17	0,868
AEB1	0,01778	0,03835	0,46	0,643
CEB1	0,03750	0,03835	0,98	0,329
AB2	-0,02389	0,03131	-0,76	0,446
CB2	0,06611	0,03131	2,11	0,035
EB2	0,02315	0,03131	0,74	0,460
AAB2	-0,00056	0,05423	-0,01	0,992
CCB2	-0,05389	0,05423	-0,99	0,321
EEB2	0,03056	0,05423	0,56	0,573
ACB2	-0,00556	0,03835	-0,14	0,885
AEB2	-0,05361	0,03835	-1,40	0,163
CEB2	0,03944	0,03835	1,03	0,304
AD1	0,02204	0,03131	0,70	0,482
CD1	0,05241	0,03131	1,67	0,095
ED1	-0,01648	0,03131	-0,53	0,599
AAD1	0,07463	0,05423	1,38	0,170
CCD1	-0,11315	0,05423	-2,09	0,038

Appendix D.11 Continued

EED1	-0,01204	0,05423	-0,22	0,824
ACD1	-0,03194	0,03835	-0,83	0,405
AED1	0,02444	0,03835	0,64	0,524
CED1	0,10222	0,03835	2,67	0,008
AB1D1	-0,00074	0,04428	-0,02	0,987
CB1D1	-0,01870	0,04428	-0,42	0,673
EB1D1	0,04074	0,04428	0,92	0,358
AAB1D1	-0,01926	0,07670	-0,25	0,802
CCB1D1	0,05685	0,07670	0,74	0,459
EEB1D1	-0,04481	0,07670	-0,58	0,559
ACB1D1	0,06056	0,05423	1,12	0,265
AEB1D1	-0,02000	0,05423	-0,37	0,712
CEB1D1	-0,10639	0,05423	-1,96	0,050
AB2D1	0,00019	0,04428	0,00	0,997
CB2D1	-0,11130	0,04428	-2,51	0,012
EB2D1	-0,06167	0,04428	-1,39	0,164
AAB2D1	-0,06870	0,07670	-0,90	0,371
CCB2D1	0,13352	0,07670	1,74	0,082
EEB2D1	0,00019	0,07670	0,00	0,998
ACB2D1	-0,03861	0,05423	-0,71	0,477
AEB2D1	0,11083	0,05423	2,04	0,042
CEB2D1	-0,11556	0,05423	-2,13	0,034

S = 0,1627 R-Sq = 36,6% R-Sq(adj) = 27,8%

Analysis of Variance

Source	DF	SS	MS	F	P
Regression	59	6,50728	0,11029	4,17	0,000
Residual Error	426	11,27645	0,02647		
Total	485	17,78372			

Source	DF	Seq SS
A	1	0,82810
B1	1	0,22749
B2	1	0,01272
C	1	0,06674
D1	1	0,14971
E	1	2,67868
AA	1	0,00914
CC	1	0,05680
EE	1	0,00772
AC	1	0,01965
AE	1	0,07594
CE	1	0,19022
B1D1	1	0,00109
B2D1	1	0,00924
AB1	1	0,13781
CB1	1	0,01773
EB1	1	0,11440
AAB1	1	0,17586
CCB1	1	0,04930
EEB1	1	0,15808
ACB1	1	0,06332
AEB1	1	0,00227
CEB1	1	0,00205
AB2	1	0,03058
CB2	1	0,00591
EB2	1	0,00319
AAB2	1	0,02193

Appendix D.11 Continued

CCB2	1	0,00298
EEB2	1	0,01691
ACB2	1	0,02225
AEB2	1	0,00012
CEB2	1	0,01210
AD1	1	0,03868
CD1	1	0,00667
ED1	1	0,04457
AAD1	1	0,05543
CCD1	1	0,06667
EED1	1	0,01956
ACD1	1	0,03276
AED1	1	0,16170
CED1	1	0,04307
AB1D1	1	0,00001
CB1D1	1	0,02457
EB1D1	1	0,09221
AAB1D1	1	0,00137
CCB1D1	1	0,00059
EEB1D1	1	0,01210
ACB1D1	1	0,07653
AEB1D1	1	0,06825
CEB1D1	1	0,02836
AB2D1	1	0,00000
CB2D1	1	0,16722
EB2D1	1	0,05134
AAB2D1	1	0,02124
CCB2D1	1	0,08022
EEB2D1	1	0,00000
ACB2D1	1	0,01342
AEB2D1	1	0,11056
CEB2D1	1	0,12018

Unusual Observations

Obs	A	LOG I	Fit	SE Fit	Residual	St Resid
2	-1,00	1,20000	0,79151	0,05498	0,40849	2,67R
36	-1,00	0,89000	0,55880	0,06703	0,33120	2,23R
51	-1,00	1,18000	0,85938	0,06703	0,32062	2,16R
70	0,00	1,09000	0,53599	0,05498	0,55401	3,62R
74	0,00	1,10000	0,68790	0,04783	0,41210	2,65R
80	0,00	1,11000	0,56494	0,04783	0,54506	3,51R
87	0,00	0,38000	0,69892	0,05498	-0,31892	-2,08R
96	0,00	0,53000	0,85444	0,05498	-0,32444	-2,12R
156	1,00	1,30000	0,82130	0,05498	0,47870	3,13R
161	1,00	0,99000	0,64194	0,05498	0,34806	2,27R
210	-1,00	0,92000	0,58093	0,05498	0,33907	2,21R
248	0,00	1,00000	0,60457	0,04783	0,39543	2,54R
291	1,00	0,60000	0,93707	0,06703	-0,33707	-2,27R
294	1,00	0,56000	0,87880	0,06703	-0,31880	-2,15R
357	-1,00	0,91000	0,60948	0,06703	0,30052	2,03R
363	-1,00	0,51000	0,90883	0,06703	-0,39883	-2,69R
377	-1,00	1,00000	0,67213	0,05498	0,32787	2,14R
399	0,00	1,26000	0,84614	0,05498	0,41386	2,70R
424	0,00	0,95000	0,63074	0,04783	0,31926	2,05R
444	1,00	1,26000	0,91543	0,05498	0,34457	2,25R
454	1,00	0,91000	0,60250	0,06703	0,30750	2,07R
462	1,00	1,26000	0,85778	0,05498	0,40222	2,63R
474	1,00	1,29000	0,97269	0,06703	0,31731	2,14R

R denotes an observation with a large standardized residual

Durbin-Watson statistic = 2,06

Appendix D.12 The best regression model developed for the log transformed mean impact resistance based on the full factorial design

The regression equation is

log μ = 0,767 + 0,0369 A - 0,196 B1 + 0,0246 B2 - 0,0359 C - 0,0003 D1 + 0,116 E - 0,0604 AA + 0,0438 CC - 0,0355 EE + 0,0231 AC + 0,0122 AE - 0,0694 CE - 0,0043 B1D1 - 0,0914 B2D1 + 0,0322 AB1 - 0,0105 CB1 - 0,0641 EB1 + 0,0856 AAB1 + 0,0518 CCB1 + 0,0812 EEB1 - 0,0036 ACB1 + 0,0375 CEB1 - 0,0239 AB2 + 0,0614 CB2 + 0,0231 EB2 - 0,0397 CCB2 - 0,0625 AEB2 + 0,0394 CEB2 + 0,0220 AD1 + 0,0431 CD1 - 0,0165 ED1 + 0,0453 AAD1 - 0,0847 CCD1 - 0,0512 ACD1 + 0,0144 AED1 + 0,102 CED1 - 0,0007 AB1D1 + 0,0407 EB1D1 + 0,0799 ACB1D1 - 0,106 CEB1D1 + 0,0002 AB2D1 - 0,102 CB2D1 - 0,0617 EB2D1 + 0,105 CCB2D1 + 0,121 AEB2D1 - 0,116 CEB2D1

Predictor	Coef	SE Coef	T	P
Constant	0,76674	0,03510	21,84	0,000
A	0,03685	0,02196	1,68	0,094
B1	-0,19568	0,04744	-4,13	0,000
B2	0,02460	0,04205	0,59	0,559
C	-0,03588	0,01902	-1,89	0,060
D1	-0,00027	0,04140	-0,01	0,995
E	0,11630	0,02196	5,30	0,000
AA	-0,06039	0,02455	-2,46	0,014
CC	0,04375	0,03294	1,33	0,185
EE	-0,03551	0,01902	-1,87	0,063
AC	0,02306	0,01902	1,21	0,226
AE	0,01222	0,01902	0,64	0,521
CE	-0,06944	0,02689	-2,58	0,010
B1D1	-0,00432	0,03586	-0,12	0,904
B2D1	-0,09142	0,05670	-1,61	0,108
AB1	0,03222	0,03105	1,04	0,300
CB1	-0,01046	0,02196	-0,48	0,634
EB1	-0,06407	0,03105	-2,06	0,040
AAB1	0,08560	0,03294	2,60	0,010
CCB1	0,05176	0,03803	1,36	0,174
EEB1	0,08116	0,03294	2,46	0,014
ACB1	-0,00361	0,03294	-0,11	0,913
CEB1	0,03750	0,03803	0,99	0,325
AB2	-0,02389	0,03105	-0,77	0,442
CB2	0,06144	0,02905	2,11	0,035
EB2	0,02315	0,03105	0,75	0,456
CCB2	-0,03968	0,05031	-0,79	0,431
AEB2	-0,06250	0,03294	-1,90	0,058
CEB2	0,03944	0,03803	1,04	0,300
AD1	0,02204	0,03105	0,71	0,478
CD1	0,04306	0,02196	1,96	0,051
ED1	-0,01648	0,03105	-0,53	0,596
AAD1	0,04531	0,03105	1,46	0,145
CCD1	-0,08472	0,03803	-2,23	0,026
ACD1	-0,05125	0,02689	-1,91	0,057
AED1	0,01444	0,02689	0,54	0,591
CED1	0,10222	0,03803	2,69	0,007
AB1D1	-0,00074	0,04392	-0,02	0,987
EB1D1	0,04074	0,04392	0,93	0,354
ACB1D1	0,07986	0,04658	1,71	0,087
CEB1D1	-0,10639	0,05379	-1,98	0,049
AB2D1	0,00019	0,04392	0,00	0,997
CB2D1	-0,10194	0,03803	-2,68	0,008

Appendix D.12 Continued

EB2D1	-0,06167	0,04392	-1,40	0,161
CCB2D1	0,10509	0,06587	1,60	0,111
AEB2D1	0,12083	0,04658	2,59	0,010
CEB2D1	-0,11556	0,05379	-2,15	0,032

S = 0,1614 R-Sq = 35,7% R-Sq(adj) = 29,0%

Analysis of Variance

Source	DF	SS	MS	F	P
Regression	46	6,35346	0,13812	5,30	0,000
Residual Error	439	11,43026	0,02604		
Total	485	17,78372			

Source	DF	Seq SS
A	1	0,82810
B1	1	0,22749
B2	1	0,01272
C	1	0,06674
D1	1	0,14971
E	1	2,67868
AA	1	0,00914
CC	1	0,05680
EE	1	0,00772
AC	1	0,01965
AE	1	0,07594
CE	1	0,19022
B1D1	1	0,00109
B2D1	1	0,00924
AB1	1	0,13781
CB1	1	0,01773
EB1	1	0,11440
AAB1	1	0,17586
CCB1	1	0,04930
EEB1	1	0,15808
ACB1	1	0,06332
CEB1	1	0,00205
AB2	1	0,03058
CB2	1	0,00591
EB2	1	0,00319
CCB2	1	0,00298
AEB2	1	0,00021
CEB2	1	0,01210
AD1	1	0,03868
CD1	1	0,00667
ED1	1	0,04457
AAD1	1	0,05543
CCD1	1	0,06667
ACD1	1	0,03276
AED1	1	0,16170
CED1	1	0,04307
AB1D1	1	0,00001
EB1D1	1	0,09221
ACB1D1	1	0,07653
CEB1D1	1	0,02836
AB2D1	1	0,00000
CB2D1	1	0,18707
EB2D1	1	0,05134
CCB2D1	1	0,06627
AEB2D1	1	0,17521
CEB2D1	1	0,12018

Appendix D.12 Continued

Unusual Observations

Obs	A	LOG I	Fit	SE Fit	Residual	St Resid
2	-1,00	1,20000	0,77219	0,04330	0,42781	2,75R
36	-1,00	0,89000	0,56542	0,06135	0,32458	2,17R
51	-1,00	1,18000	0,84878	0,06200	0,33122	2,22R
70	0,00	1,09000	0,56457	0,04814	0,52543	3,41R
74	0,00	1,10000	0,71291	0,03942	0,38709	2,47R
80	0,00	1,11000	0,57106	0,03942	0,53894	3,44R
99	0,00	1,21000	0,89527	0,04189	0,31473	2,02R
129	1,00	1,23000	0,92979	0,06135	0,30021	2,01R
156	1,00	1,30000	0,83055	0,05253	0,46945	3,08R
210	-1,00	0,92000	0,59017	0,05253	0,32983	2,16R
239	0,00	0,91000	0,58055	0,03942	0,32945	2,11R
248	0,00	1,00000	0,62023	0,03942	0,37977	2,43R
291	1,00	0,60000	0,92979	0,06135	-0,32979	-2,21R
294	1,00	0,56000	0,87829	0,06135	-0,31829	-2,13R
300	1,00	0,56000	0,87616	0,04814	-0,31616	-2,05R
357	-1,00	0,91000	0,61063	0,06135	0,29937	2,01R
363	-1,00	0,51000	0,90378	0,06200	-0,39378	-2,64R
377	-1,00	1,00000	0,66869	0,04512	0,33131	2,14R
399	0,00	1,26000	0,84273	0,05018	0,41727	2,72R
424	0,00	0,95000	0,60284	0,04189	0,34716	2,23R
444	1,00	1,26000	0,90126	0,04729	0,35874	2,33R
454	1,00	0,91000	0,59977	0,06135	0,31023	2,08R
462	1,00	1,26000	0,87616	0,04814	0,38384	2,49R
474	1,00	1,29000	0,95985	0,06200	0,33015	2,22R

R denotes an observation with a large standardized residual

Durbin-Watson statistic = 2,05